

# Benthic Foraminifera as Proxies in Contourite Drift Systems

Inaugural-Dissertation  
zur  
Erlangung des Doktorgrades  
der Mathematisch-Naturwissenschaftlichen Fakultät  
der Universität zu Köln



vorgelegt von

**Anna Saupe**  
geboren in Rostock

2023



Erstgutachter:  
Zweitgutachter:

Prof. Dr. Patrick Grunert  
Prof. Dr. Gerhard Schmiedl

Vorsitzender der Prüfungskommission:  
Beisitzender:

Prof. Dr. Hartmut Arndt  
Dr. Jassin Petersen

Tag der mündlichen Prüfung:

25.Mai.2023

---



Benthic Foraminifera as Proxies  
in Contourite Drift Systems

vorgelegt von  
Anna Saupe  
geboren in Rostock

2023



*La mer est tout!*

*Elle couvre les sept dixièmes du globe terrestre. Son souffle est pur et sain.  
C'est l'immense désert où l'homme n'est jamais seul, car il sent frémir la vie  
à ses côtés. La mer n'est que le véhicule d'une surnaturelle et prodigieuse  
existence; elle n'est que mouvement et amour; c'est l'infini vivant.*

*- Jules Verne*





## Abstract

Benthic foraminifera are highly adaptable to a wide range of environments, which makes them excellent tools for the reconstruction of palaeoenvironments. Certain species prefer regions with significantly increased current velocities, such as present in contourite drift systems (CDS). Contourites form elongated sedimentary bodies that are deposited under persistent, contour-parallel bottom currents and cover extensive areas of the Atlantic Ocean. An increased current activity substantially affects the composition of the associated epibenthic community, and some benthic foraminiferal species preferably settle on elevated substrates, summarised as elevated epifauna (EEF). EEF species optimise the acquisition of food particles carried by strong bottom currents, giving them a competitive advantage over other epibenthic microorganisms. The EEF was established at the Iberian Margin (Northeast Atlantic Basin) within the Mediterranean Outflow Water (MOW) and evaluated for its suitability as a bottom current indicator (Schönfeld, 1997).

In this thesis, biogeographic distribution patterns of benthic foraminifera in sediment surface samples from CDSs beyond the Northeast Atlantic Basin, within the low and high latitudes of the Atlantic Ocean, are evaluated. Investigations along the Brazilian continental margin (Campos and Brazil basins, 11-22°S, 36-40°W) reveal a diverse foraminiferal community, although with a rather poor EEF, that is almost exclusively represented by *Cibicoides wuellerstorfi*. Samples from the North Atlantic Iceland (Björn and Gardar Drift, 55-62°N, 23-28°W) and Irminger basins (Eirik Drift, 57-59°N, 45-49°W) also reveal lacking or sparse EEF occurrences. Instead, tubular agglutinated suspension feeders, such as *Rhabdammina abyssorum* or *Saccorhiza ramosa*, preferably colonise the weak to moderate current regime in the Björn and Gardar drifts. In the slightly enhanced currents of the Eirik Drift, abundances of EEF taxon *Cibicoides wuellerstorfi* are recorded.

The integration of the new data sets with previous studies, primarily from the Iberian Margin, reveal that temperature variations, substrate properties, hydrodynamic conditions at the sediment-water interface, and suspended organic matter crucially contribute to the assemblage composition in CDSs. The hydrodynamic properties of the warm (13°C) and saline (38.4) MOW, its strongly increased current velocities (up to 100 cm/s) and its Mediterranean origin create a unique environment that seems to be highly beneficial for EEF species. This contrasts with an environment that is largely controlled by the Atlantic Meridional Overturning Circulation (AMOC) comprising major cold (> 4°C) and comparatively less saline (34.2-34.9) deep water masses with weak to moderate bottom current intensities (max. 30 cm/s). In this oligotrophic deep-sea environment, agglutinated tubular suspension feeders may serve as indicators for the reconstruction of weaker bottom currents at the high latitudes. However, further studies will be necessary to understand a potential taphonomic bias on their abundance in the fossil record.



## Kurzfassung

Benthische Foraminiferen sind äußerst gut an ein breites Spektrum unterschiedlicher Lebensräume angepasst, wodurch sie sich hervorragend für die Rekonstruktion von Paläoumweltbedingungen eignen. Bestimmte Arten bevorzugen Regionen mit deutlich erhöhten Strömungsgeschwindigkeiten, wie sie in Konturit-Driftsystemen (CDS) vorkommen. Konturite bilden langgestreckte Sedimentkörper, die unter anhaltenden, konturparallelen Bodenströmungen abgelagert werden und weite Bereiche des Atlantischen Ozeans bedecken. Die dort herrschende erhöhte Strömungsaktivität wirkt sich auch erheblich auf die Zusammensetzung der zugehörigen epibenthischen Fauna aus. Einige benthische Foraminiferenarten siedeln sich z.B. bevorzugt auf erhöhten Substraten an, und werden daher als "elevated epifauna" (EEF) bezeichnet. EEF-Arten optimieren durch ihre erhöhte Position die Aufnahme von suspendierten Nahrungspartikeln in der Strömung, und verschaffen sich so einen Wettbewerbsvorteil gegenüber der übrigen epibenthischen Mikrofauna. Die EEF wurde entlang der Iberischen Halbinsel (nordöstliches Atlantikbecken) im Mittelmeerausstromwassers (Mediterranean Outflow Water, MOW) etabliert und dort bereits hinsichtlich ihrer Eignung zur Rekonstruktion von Bodenströmungen untersucht (Schönfeld, 1997).

Erstmals werden in der vorliegenden Arbeit die biogeographischen Verbreitungsmuster benthischer Foraminiferen in CDS über das nordostatlantische Becken hinaus in den niedrigen und hohen Breiten des Atlantischen Ozeans ausgewertet. Untersuchungen entlang des brasilianischen Kontinentalrandes (Campos- und Brasilienbecken, 11-22°S, 36-40°W) ergeben eine artenreiche Foraminiferen-Gemeinschaft, in der EEF-Taxa jedoch nur vereinzelt und relativ homogen vorkommen (vor allem *Cibicidoides wuellerstorfi*). Proben aus den nordatlantischen Island (Björn und Gardar Drift, 55-62°N, 23-28°W) und Irminger Becken (Eirik Drift, 57-59°N, 45-49°W) enthalten ebenfalls nur wenige bis gänzlich fehlende EEF-Vorkommen. Dagegen besiedeln röhrenförmige agglutinierte Suspensionsfiltrierer, wie z.B. *Rhabdammina abyssorum* oder *Saccorhiza ramosa*, bevorzugt die schwachen bis mäßigen Strömungen in der Björn- und Gardar-Drift. Aus den mäßig starken Strömungen der Eirik-Drift werden Vorkommen des EEF-Taxons *Cibicidoides wuellerstorfi* verzeichnet.

Die Auswertung der neuen Datensätze in Verbindung mit früheren Studien, insbesondere von der Iberischen Halbinsel, zeigt, dass Temperaturunterschiede, Substratzusammensetzung, hydrodynamische Bedingungen an der Sediment-Wasser-Grenzfläche und suspendierte organische Partikel entscheidend zur Zusammensetzung der Faunenvergesellschaftung in CDS beitragen. Die hydrodynamischen Eigenschaften des warmen (13°C) und salzigen (38.4) MOW, seine vergleichsweise hohen Fließgeschwindigkeiten (bis zu 100 cm/s) und sein Ursprung im Mittelmeer erschaffen einen einzigartigen Lebensraum, der für EEF-Arten äußerst günstig zu sein scheint. Dem entgegen steht ein Lebensraum, der maßgeblich von der atlantischen meridionalen Umwälzirkulation (Atlantic Meridional Overturning Circulation, AMOC) gesteuert wird. Die AMOC ist der Treiber von Tiefenwassermassen mit niedrigeren Temperaturen (> 4°C), vergleichsweise geringeren Salinitäten (34,2-34,9) und mit schwacher bis mäßiger Bodenströmungsintensität (max. 30 cm/s). In dieser oligotrophen Tiefseeumgebung könnten agglutinierte röhrenförmige Suspensionsfiltrierer als Indikatoren für die Rekonstruktion schwächerer Bodenströmungen in den hohen Breitengraden dienen. Um einen möglichen taphonomischen Bias hinsichtlich ihres Vorkommens im Fossilbericht besser zu verstehen werden in Zukunft weitere Studien erforderlich sein.



## Contents

1. Introduction .....	15
1.1. Oceanographic Setting .....	17
2. Sample Material and Processing of Benthic Foraminifera .....	19
3. Results & Discussion .....	21
3.1. The Brazilian Continental Margin (Saupe et al. 2022, <i>Frontiers in Marine Science</i> ) .....	23
3.2. High Latitude Contourite Drift Systems (Saupe et al. 2023, <i>Palaeogeography Palaeoclimatology Palaeoecology</i> ) .....	57
3.3. Biogeographic Patterns in the Atlantic Ocean (Saupe et al. in prep.) .....	101
4. Summary & Conclusions .....	137
5. References .....	139
6. Acknowledgements .....	147

Three sub-chapters were already published (3.1, 3.2) or prepared (3.3) as separate research papers. Therefore, each of these sub-chapters has its own headline numbering, figure captions, table descriptions and reference lists. Repetitions could not be avoided. All other citations mentioned in the scope of this thesis can be found in chapter 5.



## 1. Introduction

The Atlantic Ocean is largely controlled by a complex system of current patterns linked to the thermohaline circulation. Oceanic circulation causes the movement of water masses and decisively shapes the seafloor. Sustained contour-parallel and along-slope bottom currents control much of the deep-sea sedimentation and cause the deposition of extensive contourite drift systems (CDS) (Rebesco et al., 2014). The exceptionally high sedimentation rates of contourite drifts make them ideal study areas for the understanding of ocean-climate dynamics and the contribution of intermediate and deep-water masses (Knutz, 2008). These extensive sedimentary bodies represent fundamental archives for paleoclimatology and palaeoceanography. Their wide distribution makes the Atlantic Ocean of key importance for the investigation of past and future bottom current patterns (e.g., Faugères et al., 1999; Hodell et al., 2009; Faugères and Mulder, 2011; Hernández-Molina et al., 2014; Müller-Michaelis and Uenzelmann-Neben, 2014).

As the interplay of bottom currents and deep-sea sedimentation has been increasingly studied in recent decades, reliable current speed proxy methods became crucial (e.g., McCave et al., 1995; Bianchi et al., 1999; McCave and Hall, 2006; Bahr et al., 2014). Although physical processes in CDS, such as hydrodynamics or sediment transport, are increasingly well understood, biological and ecological factors, such as the associated benthic fauna, were considered less (Rebesco et al., 2014). For palaeoceanographic and paleoclimatic interpretations, however, actuopalaeontological and palaeobiological approaches are indispensable (Rebesco et al., 2014).

The potential for the use of fossils as biogenic proxies has already been demonstrated for benthic foraminifera. Since they are highly adapted to a wide range of environments, benthic foraminifera provide a suitable tool for the reconstruction of palaeoenvironments (e.g., van der Zwaan et al., 1999; Murray, 2001; Gooday, 2003; Jorissen et al., 2007; Gooday and Jorissen, 2012). Hydrological parameters such as oxygen, temperature and salinity, or sedimentological parameters such as substrate composition and grain size generally function as limiting abiotic factors that determine the distribution of benthic foraminifera (Murray, 2006). Their high abundance and diversity make benthic foraminifera important organisms within deep-sea communities, where they can rely on a wide range of trophic mechanisms, including suspension or detritus feeding (Gooday, 2003, 2014; Gooday and Jorissen, 2012). A highly functional pseudopodial network enables suspension feeding species to capture and ingest suspended matter such as bacteria, organic detritus, microalgae, or sediment particles (Wildish and Kristmanson, 1997). Flux rates of particulate organic matter are considered as a direct controlling factor for the abundances of certain foraminiferal species and their preferred microhabitats (Altenbach, 1988; Jorissen et al., 1995; Mackensen et al., 1995; Harloff and Mackensen, 1997; Morigi et al., 2001). Some studies report that an increased bottom current activity can substantially influence the composition of the epibenthic community, and several well-adapted species can be assessed as bottom current indicators, summarized here as the bottom current fauna (BCF, [Table 1](#)) (Lutze and Coulbourn, 1984; Lutze and Altenbach, 1988; Lutze and Thiel, 1989; Linke

and Lutze, 1993; Schönfeld, 1997, 2002a, 2002b). Schönfeld (1997) noted that a number of these well-adapted BCF species prefer to settle on elevated substrates within the current, and he introduced the elevated epibenthos group or elevated epifauna (hereafter abbreviated as EEF, [Table 1](#), e.g., García-Gallardo et al., 2016). Elevated microhabitats include biogenic objects such as hydroids, sponges, erect

**Table 1** | Species related to increased current regimes.

BCF and *EEF species	Reference
* <i>Ammodiscus anguillae</i> Höglund, 1947	Schönfeld (2002a)
* <i>Cibicides lobatulus</i> (Walker & Jacob, 1798)	Schönfeld (1997, 2002a)
* <i>Cibicides refulgens</i> Montfort, 1808	Schönfeld (2002a)
* <i>Cibicides</i> sp.	Schönfeld (2002a)
* <i>Cibicidoides pachyderma</i> (Rzehak, 1886)	Reported as <i>Cibicidoides</i> sp. in Schönfeld (2002a) and as <i>C. pseudoungerianus</i> in Altenbach et al. (1987).  Note: According to Schönfeld (2002a) his species <i>Cibicidoides</i> sp. was determined by several authors as <i>Cibicidoides pseudoungerianus</i> (Cushman, 1922), but in Schönfeld's opinion with a more broadly rounded periphery. We group Schönfeld's <i>Cibicidoides</i> sp. and <i>C. pseudoungerianus</i> because of their joint EEF behaviour (Altenbach et al. 1987). <i>Cibicidoides pseudoungerianus</i> is a junior synonym of <i>Cibicidoides pachyderma</i> (Schönfeld, 2002b).
* <i>Cibicidoides wuellerstorfi</i> (Schwager, 1866)	Lutze & Thiel (1989), Linke & Lutze (1993)
* <i>Deuterammia ochracea</i> (Williamson, 1858)	Schönfeld (2002a)
* <i>Discanomalina coronata</i> (Parker & Jones, 1865)	Schönfeld (1997, 2002a)
* <i>Discanomalina semipunctata</i> (Bailey, 1851)	Schönfeld (2002a)
* <i>Epistominella rugosa</i> (Phleger & Parker, 1951)	Schönfeld (2002a)
* <i>Eponides repandus</i> (Fichtel & Moll, 1798)	Schönfeld (2002a)
* <i>Gavelinopsis translucens</i> (Phleger & Parker, 1951)	Schönfeld (2002a)
<i>Globocassidulina subglobosa</i> (Brady, 1881)	Mackensen et al. (1995), Rasmussen et al. (2002)
* <i>Guttulina</i> sp.	Schönfeld (2002a), fistulous variety of the species
* <i>Hanzawaia concentrica</i> (Cushman, 1918)	Schönfeld (1997, 2002a)
* <i>Hanzawaia rhodiensis</i> (Terquem, 1878)	Schönfeld (2002a)
* <i>Hanzawaia strattoni</i> (Applin, 1925)	Schönfeld (2002a)
<i>Miliolinella subrotunda</i> (Montagu, 1803)	Altenbach et al. (1993), Linke & Lutze (1993)
* <i>Placopsilina confusa</i> Cushman, 1920	Schönfeld (2002a)
* <i>Planulina ariminensis</i> d'Orbigny, 1826	Schönfeld (1997, 2002a)
<i>Psammosphaera fusca</i> Schulze, 1875	Harloff and Mackensen (1997)
<i>Psammosphaera parva</i> Flint, 1899	Kuhnt et al. (2000)
* <i>Rosalina anomala</i> Terquem, 1875	Schönfeld (2002a)
* <i>Rupertina stabilis</i> (Wallich, 1877)	Lutze & Altenbach (1988), Linke & Lutze (1993)
* <i>Saccammia sphaerica</i> Brady, 1871	Schönfeld (2002a)
* <i>Spiroplectinella saggitula</i> (Defrance, 1824)	Schönfeld (2002a)
* <i>Textularia pseudogramen</i> Chapman & Parr, 1937	Schönfeld (2002a)
<i>Trifarina angulosa</i> (Williamson, 1858)	Sejrup et al. (1981), Mackensen et al. (1995), Rasmussen et al. (2002)
* <i>Tritaxis fusca</i> (Williamson, 1858)	Schönfeld (2002a)
* <i>Trochammina squamata</i> Jones & Parker, 1860	Schönfeld (2002a)
* <i>Vulvulina pennatula</i> (Batsch, 1791)	Schönfeld (1997, 2002a)

Listed are benthic foraminiferal species associated with increased bottom current intensities, summarised as bottom current fauna (BCF). Asterisks indicate species that additionally prefer to settle on elevated substrates referred to as the elevated epifauna (EEF).

tubular foraminiferal tests (e.g., *Rhabdammina* tubes), or terrigenous particles such as pebbles and gravels (Jorissen et al., 2007). Through their elevated microhabitat, EEF species optimize the acquisition of food particles carried by strong bottom currents, providing them with a competitive advantage over other epibenthic microfauna (Schönfeld, 1997, 2002a, 2002b). The Iberian Margin



serves as a crucial region for the development of a potential EEf bottom current proxy, as the Mediterranean Outflow Water (MOW) forms extensive CDSs through its persistent interaction with the seafloor (Faugères et al., 1984; Mulder et al., 2003; de Castro et al., 2021). The EEf has been tested and applied as a proxy for bottom currents by a few studies in the Gulf of Cadiz (Schönfeld and Zahn, 2000; Singh et al., 2015; García-Gallardo et al., 2017), and occasionally at the western European continental margin (Diz et al., 2004; Rüggeberg et al., 2007). However, all this research focuses on MOW-related areas, while studies beyond the Northeast Atlantic basin and under the influence of major Atlantic water masses, are largely lacking.

This thesis aims to analyse recent biogeographic patterns of benthic foraminifera in increased current regimes of selected Atlantic CDSs. Its objective is to evaluate the distribution of BCF and EEf taxa in the low and high latitudes of the Atlantic Ocean from surface sediment samples. The effects of bottom current strength and nutrient loads on the benthic community is evaluated via multivariate statistical analyses. Key parameters such as quantity and quality of organic matter flux as well as substrate properties and hydrodynamic conditions at the sediment-water interface are thoroughly assessed as determinants of the local assemblage distribution.

## 1.1 Oceanographic Setting

The Atlantic Ocean encompasses a vast and complex system of surface, intermediate and deep-water masses driven by the Atlantic Meridional Overturning Circulation (AMOC). The main drivers of this system include upwelling processes, surface currents, deep-water formation and deep currents that span the Atlantic in both hemispheres and create a complex, extensive circulation pattern (Kuhlbrodt et al., 2007). This makes the AMOC an important player in global ocean-climate dynamics (Kuhlbrodt et al., 2007; Eldevik and Nilsen, 2013). This extensive circulation system leads to deep-water formation in the Nordic Seas and the Labrador Sea of the northern high latitudes, as well as in the Weddel Sea in the southern high latitudes, generating intense near-bottom currents (Kuhlbrodt et al., 2007; Faugères and Mulder, 2011). This network of deep currents and water masses significantly shapes the ocean floor and favours contourite deposition at the continental slopes of the Atlantic Ocean (Faugères et al., 1999; Stramma and England, 1999; Uenzelmann-Neben and Gruetzner, 2018). The deep currents transport sediments from nearby land masses, causing e.g., the formation of the Björn and Gardar drifts in the Iceland Basin or the Eirik Drift in the Irminger Basin (Bianchi and McCave, 2000; Hunter et al., 2007b).

One of the Atlantic's most important and widely spread deep water masses is the North Atlantic Deep Water (NADW), which is formed by downwelling of highly saline surface waters in the Greenland and Iceland seas and the Arctic Ocean (Dickson and Brown, 1994; Sarthein et al., 1994). NADW is transported southwards from the high northern latitudes, largely driven by the Deep Western Boundary Current (DWBC; Stramma and England, 1999). While a large part of NADW (reaching depths of 4000 m, e.g., Schott et al., 2005) moves southwards, a smaller part mixes with shallower and saline waters when crossing the Iceland-Scotland Ridge and forms homogeneous Iceland Scotland Overflow Water (ISOW, 1.7 °C, 35 psu; van Aken and de Boer, 1995; Bianchi and McCave, 2000). Along with

Labrador Sea Water (LSW, 3.4, 34.88 psu), circulating anti-clockwise from the Labrador Sea via Hatton and Rockall Banks to the Reykjanes Ridge, the ISOW interacts with the massive sedimentary Björn and Gardar drift bodies at maximum flow velocities of 10 cm/s (Bianchi and McCave, 2000). The NADW, however, impinges on the Eirik Drift, located on the divide of Labrador Sea and Atlantic Ocean, with current velocities of 12-22 cm/s (Hunter et al., 2007a, 2007b).

Along its path to the Southern Hemisphere, comparatively warmer ( $\sim 3^{\circ}\text{C}$ ) and more saline (34.88-34.98) northern NADW (Stramma and England, 1999; Hunter et al., 2007a) transforms into cooled ( $\sim 1.9^{\circ}\text{C}$ ) and less saline (34.6-34.9) southern NADW (de Madron and Weatherly, 1994; Yamashita et al., 2018). When it reaches the South Atlantic, NADW influences the Brazilian continental margin and shapes the ocean floor with current velocities of up to 20 cm/s (da Silveira et al., 2020). Deep water masses also form in the southern Hemisphere, such as warm South Atlantic Central Water (SACW, up to 500 m,  $10-17^{\circ}\text{C}$ ) and the Antarctic Intermediate Water (AAIW, up to 1100 m,  $4^{\circ}\text{C}$ ). They are transported northwards by the North Brazilian Undercurrent (NBU) with flow velocities of 80 and 30 cm/s, respectively (Table 2, Peterson and Stramma, 1991; Stramma and England, 1999; da Silveira et al., 2020).

**Table 2** | Investigated regions with increased current regimes and/or CDS occurrences.

	Greenland Margin	Eirik Drift	Björn Drift	Gardar Drift	Gulf of Cadiz	Portugese Margin	Porcupine Seabight	Brazil & Campos basins		
<b>Range (Lat)</b>	60°N	57-59°N	60-62°N	55-60°N	36-37°N	37-38°N	51-52°N	11-22°S		
<b>Range (Long)</b>	43°W	45-49°W	24-25°W	23-28°W	7-8°W	9-10°W	12-13°W	36-40°W		
<b>Water depth (m)</b>	800	2000-3500	1500-2000	2200-3000	100-2000	250-3500	700-1000	400-2000		
<b>Water mass</b>	EGC	N NADW	LSW	ISOW	MOW	MOW	MOW	SACW	AAIW	S NADW
<b>Temperature (°C)</b>	6-9	3	3.4	1.7-2.5	13	11	10	10-17	4	1.9
<b>Salinity</b>	34.95-35.05	34.88-34.98	34.88	34.98-35.0	38.4	36.6	35.48	34.3-35.8	34.2-34.8	34.6-34.9
<b>Flow Speed (cm/s)</b>	40	12-22	3.1	10	10-100 max. 300	12 max. 20-30	5-20 max. 40	50-80	30	20
<b>published in</b>		Saupe et al., 2023			Schönfeld, 2002a	Schönfeld, 1997	Fentimen et al., 2018; Schönfeld et al., 2011	Saupe et al., 2022		

Hydrographic and sedimentological parameters are compiled from de Madron and Weatherly (1994), Dickson and Brown (1994), van Aken and de Boer (1995), Stramma and England (1999), Bianchi and McCave (2000), Viana (2001), Holliday et al. (2007), Hunter et al. (2007a), Fraile-Nuez et al. (2010), Sánchez-Leal et al. (2017), Lim et al. (2018), da Silveira et al. (2020) and Sierro et al. (2020), and the respective publications of the analysed sample sites. Abbreviations mean AAIW: Antarctic Intermediate Water, EGC: East Greenland Current, ISOW: Iceland-Scotland Overflow Water, LSW: Labrador Sea Water, MOW: Mediterranean Outflow Water, NADW: North Atlantic Deep Water, SACW: South Atlantic Central Water. Grey shaded are all sample areas in AMOC-driven water masses that have been studied in this thesis.

The Northeast Atlantic Basin contrasts distinctly with regions affected by AMOC-driven water masses. It is largely shaped by the high-density and saline current of the Mediterranean Outflow Water (MOW, e.g., Hernández-Molina et al., 2014; Sierro et al., 2020). As the MOW exits the Mediterranean Sea at

the narrowing of the Strait of Gibraltar, it develops extremely high current velocities of up to 300 cm/s and passes the Gulf of Cadiz at about 100 cm/s (Schönfeld, 2002a; Sierro et al., 2020). This leads to the formation of various sedimentary drift bodies, such as the Faro Drift in the Gulf of Cadiz (Faugères et al., 1984, 1993; Mulder et al., 2003). On its northward path, the velocity of the MOW decreases continuously, and its rather high salinity reduces from 38.4 to 34-35 (Table 2, Toucanne et al., 2007; Sierro et al., 2020). The MOW thus comprises an important component in the hydrodynamic system along the European continental margin, and vertical density gradients of AMOC and MOW are critical players within Atlantic water mass dynamics (Sierro et al., 2020).

## 2. Sample Material and Processing of Benthic Foraminifera

Fifteen surface samples were examined from the high latitudes of the North Atlantic, taken during cruises 88 (NEAPACC) and 159 (RAPID) with the research vessel *Charles Darwin* (McCave, 1994, 2005). Targeted localities were the Björn and Gardar drifts southeast of Reykjanes Ridge in the Iceland Basin, and the Eirik Drift and adjacent Greenland continental margin in the Labrador Sea and Irminger Basin (Figure 1, Table 2). The top 2 cm of sediment has been recovered from box and kasten cores for analysis of the benthic fauna.



**Figure 1** | Geographical positions of the study areas. Circles denote the areas processed in this study, squares refer to datasets previously studied for benthic foraminifera in increased current regimes or CDS (Schönfeld, 1997, 2002a; Schönfeld et al., 2011; Fentimen et al., 2018). Blue indicates the high latitude data set (Saupe et al., 2023), green the low latitude data set (Saupe et al., 2022). Abbreviations mean GCM: Greenland Continental Margin, ED: Eirik Drift, BD: Björn Drift, GD: Gardar Drift, PS: Porcupine Seabight, IM: Iberian Margin, GoC: Gulf of Cadiz, BB: Brazil Basin, CB: Campos Basin.

The material for the analysis of the Brazilian continental margin was obtained during the R/V Meteor expedition M125 SAMBA (Bahr et al., 2016). Samples were collected from three different transects, including one in the Campos Basin (22°S, 40°W) and two in the Brazil Basin (11-14°S, 36-39°W; Figure 1, Table 2). The top 0.5-1 cm of sediment were removed from 13 multi- and box cores for foraminiferal analysis. The sediment samples were stored between April 2016 and March 2017 in buffered 4% formaldehyde solution with a Rose Bengal concentration of 1g/L to distinguish live (stained) from dead (unstained) specimens.

All sediment samples were wet sieved, separated into three fractions (250  $\mu\text{m}$ , 125  $\mu\text{m}$  and 63  $\mu\text{m}$ ) and then dried at 30°C. If the sample quantity appeared too large, a dry splitter has been used for sample partitioning. For a detailed assessment of the composition of the benthic community, all grain size fractions were analysed. However, only the > 250  $\mu\text{m}$  fraction was considered for an overarching biogeographical evaluation of all datasets to ensure comparability with previously published datasets from the NE Atlantic Basin. This minimises a potential bias caused by remobilised foraminifera (Lohmann, 1978; Lutze and Coulbourn, 1984; Schönfeld, 1997), since even in the Iceland Basin drift system (with comparatively lowest current velocities, [Table 2](#)) particles < 200  $\mu\text{m}$  are actively resuspended in the strong current (Bianchi and McCave, 2000).

Taxonomic identification of the foraminiferal species is primarily based on the work of Loeblich and Tappan (1988), Cimerman and Langer (1991), Jones (1994), Schönfeld (2006), Kaminski et al. (2008) and Milker and Schmiedl (2012), and was performed by using a ZEISS SteREO Discovery.V12 light microscope. Selected specimens were photographed for documentation and detailed morphological analyses using the Zeiss Sigma 300-VP scanning electron microscope (SEM) at the Institute of Geology and Mineralogy of the University of Cologne.

The software PAST, version 4.02 (Hammer et al., 2001) was applied to the taxonomic data sets for evaluation and interpretation via multivariate statistics. The applied statistical methods include hierarchical cluster analyses (HCA), similarity percentage analyses (SIMPER analysis) and canonical correspondence analyses (CCA).

### 3. Results and Discussion



## 3.1 The Brazilian Continental Margin

this chapter was published by  
Saupe et al. (2022) in *Frontiers in Marine Sciences*





## Controlling Parameters of Benthic Deep-Sea Foraminiferal Biogeography at the Brazilian Continental Margin (11-22°S)

Anna Saupe <sup>1\*</sup>, Johanna Schmidt <sup>1</sup>, Jassin Petersen <sup>1</sup>, André Bahr <sup>2</sup>, Bruna Borba Dias <sup>3</sup>, Ana Luiza Spadano Albuquerque <sup>4</sup>, Rut Amelia Díaz Ramos <sup>4</sup> and Patrick Grunert <sup>1</sup>

<sup>1</sup> Institute of Geology and Mineralogy, University of Cologne, Cologne, Germany, <sup>2</sup> Institute of Earth Sciences, Heidelberg University, Heidelberg, Germany, <sup>3</sup> School of Arts, Sciences and Humanities, University of São Paulo, São Paulo, Brazil, <sup>4</sup> Departamento de Geoquímica, University Federal Fluminense, Niterói, Brazil

\*Correspondence: Anna Saupe ([anna.saupe@uni-koeln.de](mailto:anna.saupe@uni-koeln.de))

### Abstract

This study presents new quantitative data on benthic foraminifera from three bathymetric transects of the Brazil (11-14°S, 420-1900 m) and Campos (22°S, 430-2000 m) basins. The quantity and quality of organic matter flux as well as substrate properties and hydrodynamic conditions at the sediment-water interface are identified as key parameters controlling assemblage distribution. Based on the total (stained and unstained) fauna, a distinct biogeographic divide between a *Globocassidulina subglobosa/crassa* assemblage in the Campos Basin and a rosalinid/bolivinid assemblage in the Brazil Basin occurs across the bifurcation of the South Atlantic Central Water into its southward subtropical and northward tropical branches. In the Campos Basin, coarser sediments, increased bottom current activity, and variable nutrient supply favor an assemblage of *Globocassidulina subglobosa/crassa*, *Nuttallides umbonifer* and *Alabaminella weddellensis*. Occurrences of cold-water coral mounds in 870 m provide an ecological niche favoring species such as *Alabaminella weddellensis* which benefit from trapped nutrients. The Brazil Basin is characterized by increased abundances of *Rosalina* and *Bolivina*, while *Globocassidulina subglobosa/crassa* is comparatively less frequent. Assemblages with *G. subglobosa/crassa*, *Rosalina* spp., *Bolivina variabilis* and *Bolivina subreticulata* are favored by a relatively high nutrient input at 14°S. Further north, assemblages with *Bolivina subreticulata*, *Bolivina variabilis*, *Epistominella exigua*, *G. subglobosa/crassa* are located beneath the velocity core of the North Brazil Undercurrent (NBUC), coinciding with more clayey sediments rich in TOC. Occurrences of delicate branching forms such as *Saccorhiza ramosa* indicate a more stable setting, distal to the main current. Rose Bengal stained (living) specimens are scarce in all three regions, as is typical for deep-sea foraminiferal faunas. Their patterns of species distribution largely reflect those observed for the total fauna.

**Keywords:** benthic foraminifera, Brazilian margin, continental slope, deep-sea, South Atlantic

## 1. Introduction

Benthic deep-sea foraminifera are a diverse group of shell-bearing unicellular eukaryotes adapted to a wide range of marine microhabitats (e.g., Sen Gupta, 2002). Their distribution is largely determined by the interplay of organic carbon influx, physical and chemical properties of major water masses, and the hydrodynamic regime at the sediment-water interface (Mackensen et al., 1995; Schmiedl et al., 1997; Gooday and Jorissen, 2012). At the extensive Brazilian continental margin, the impact of such environmental factors on the benthic foraminiferal fauna is poorly understood as previous studies have mainly focused on shelf areas south of 20°S (Oliveira-Silva et al., 2005; de Mello e Sousa et al., 2006; Eichler et al., 2008; Burone et al., 2011; Eichler et al., 2012; Vieira et al., 2015; Yamashita et al., 2018; Yamashita et al., 2020). Studies on benthic foraminiferal assemblages on the continental slope are particularly rare and limited to the Campos Basin (~22°S; de Mello e Sousa et al., 2006; Yamashita et al., 2018; de Almeida et al., 2022). Analyses of modern deep-sea foraminifera from the continental shelf and slope north of 20°S off Eastern Brazil are lacking (Murray, 2006). Environmental conditions vary greatly along the Brazilian continental slope due to a complex water mass system and varied local seafloor topographies. Diverse microhabitats occupied by a wide range of different foraminiferal associations are thus to be expected to the North of the Campos Basin. Filling this gap in biogeographic documentation is essential to fully understand the controls on foraminiferal distribution off Brazil.

During R/V METEOR expedition M125, the Brazilian continental shelf and slope were sampled between 10°S and 23°S (Bahr et al., 2016), offering a unique opportunity to document benthic foraminiferal distribution patterns north of 20°S. Here we investigate recent benthic foraminiferal assemblages from three bathymetric transects in the Brazil (11°S, 14°S) and Campos (22°S) basins. Through integration of the observed faunal patterns with environmental parameters we gain new insights into the drivers of diversity and biogeographic patterns of deep-sea benthic foraminifera along the Brazilian continental margin. This study will serve as a baseline for future biogeographic and palaeoceanographic investigations on benthic foraminiferal faunas in the area.

## 2. Study Area

The Brazilian margin, with a length of 7400 km, can be divided into different physiographical provinces (Martins and Coutinho, 1981). The north-eastern part stretches from Cabo Sao Roque to Belmonte and includes the Brazil Basin (5-16°S; [Figure 1](#); Martins and Coutinho, 1981; da Silveira et al., 2020). Reduced continental erosion and low marine sedimentation rates result in a very narrow continental shelf ([Figures 2A, B](#)) less than 10 km in width (Summerhayes et al., 1976; Knoppers et al., 1999; Bahr et al., 2016). Extensive canyon systems are common and determine seafloor topography along the continental slope (Bahr et al., 2016). Further south (16-23°S), the east coast extends to Cabo Frio including the Campos Basin. The shelf area is considerably wider compared to the north and may reach a width of up to 90 km ([Figure 2C](#); Martins and Coutinho, 1981; Knoppers et al., 1999). The upper slope is characterized by bottom current-induced and contour-parallel erosional ridges (Viana et al., 2002;

Bahr et al., 2016). Contouritic deposits shaped by bottom currents characterize the middle and lower slope of the Campos Basin (Viana, 2001).

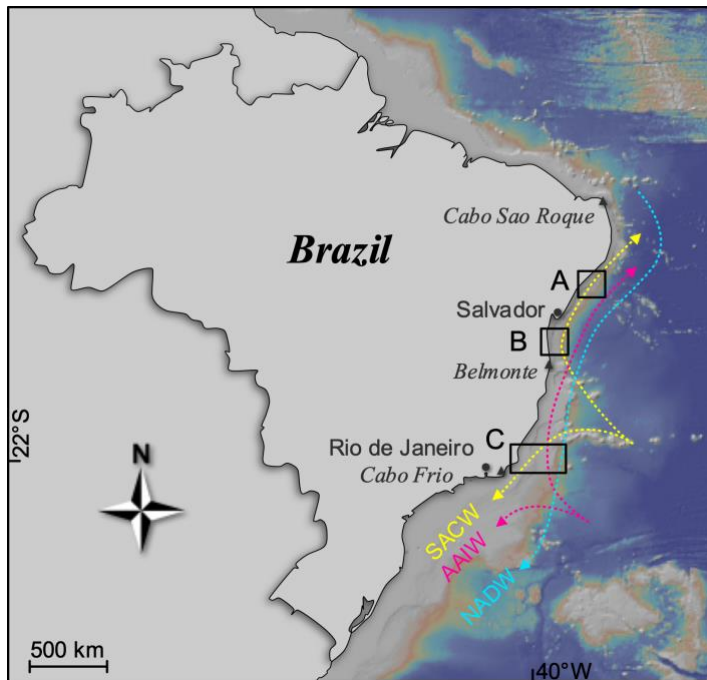


**Figure 1** | General map of the study area along the Brazilian continental margin. A, B, and C indicate the three investigated areas at 11°S, 14°S, and 22°S, respectively. South Atlantic Central Water (SACW), Antarctic Intermediate Water (AAIW) and North Atlantic Deep Water (NADW) are the major water masses. The map was created with GeoMapApp ([www.geomapapp.org](http://www.geomapapp.org)), using the base map of Ryan et al. (2009).

Four major water masses strongly affect the Brazilian continental margin to a water depth of 3500 m: the Tropical Water (TW), the South Atlantic Central Water (SACW), the Antarctic Intermediate Water (AAIW) and the North Atlantic Deep Water (NADW; [Figure 1](#); Stramma and England, 1999; da Silveira et al., 2020). The warm and saline TW represents the uppermost layer and extends to a depth of 150 m. Beneath the TW, the nutrient-rich SACW with salinities around 35.8 prevails to a depth of 500 m.

Sediments transported from the shelf, facilitated by the complex channel system, are considered a major source of organic matter input to the continental margin and contribute to an enhanced nutrient availability within the SACW (Braga et al., 2008). SACW is generated in the South Atlantic at about 40°S by the Brazil- and Falkland Currents (Stramma and England, 1999). It circulates as subtropical SACW within the Southern Subtropical Gyre and is largely driven by the Brazil Current (BC) (Peterson and Stramma, 1991; Stramma and England, 1999). The BC reaches current velocities between 50-80  $\text{s}^{-1}$  in the subtropical SACW at the Campos Basin (de Mello e Sousa et al., 2006). At about 20°S, part of the SACW is deflected northwards (Stramma and England, 1999; da Silveira et al., 2020). Slightly lower salinities distinguish it from the subtropical SACW (Stramma and England, 1999). The tropical branch of the SACW, as well as the underlying AAIW, are controlled by the North Brazil Undercurrent (NBUC), which is formed mainly in the northern Drake Passage and the Falkland Current Loop at about 40°S and flows towards the north along the eastern continental margin of South America (Stramma and England, 1999). The AAIW, present at water depths between 500 and 1100 m, is distinguishable from SACW by lower salinities of about 34.2 (Mémery et al., 2000; da Silveira et al., 2020; Raddatz et al., 2020). The equatorward flowing NBUC reaches current velocities of up to

80 cm s<sup>-1</sup> in the tropical SACW (da Silveira et al., 2020) and up to 30 cm s<sup>-1</sup> in the underlying AAIW (Viana, 2001). The layer of the AAIW at the Brazilian continental slope provides an ideal habitat for cold water coral (CWC) mounds which are mainly known from the Campos Basin at depths of 800-900 m (Viana et al., 1998; Bahr et al., 2016; Raddatz et al., 2020). Below the AAIW lies the upper North Atlantic Deep Water (UNADW), which is carried by the Deep Western Boundary Current (DWBC) from the Northern Hemisphere into the South Atlantic (Stramma and England, 1999; da Silveira et al., 2020). It achieves current speeds up to 20 cm s<sup>-1</sup> in the study area (De Madron and Weatherly, 1994) and is characterized by lower nutrient levels compared to its overlying water mass layers (da Silveira et al., 2020; Raddatz et al., 2020).

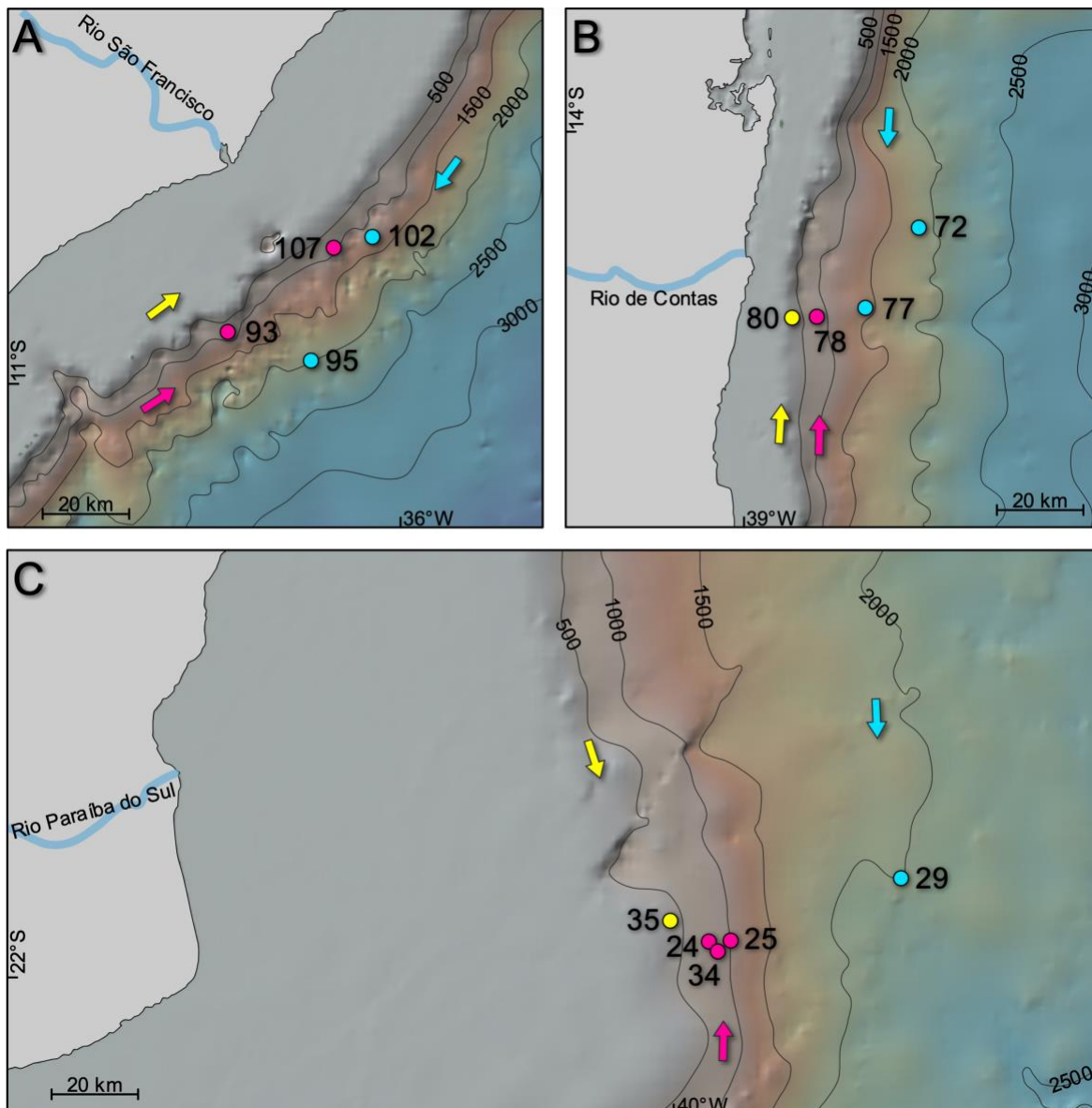


**Figure 2** | Sample sites of the studied transects of R/V Meteor cruise M125: (A) Transect 7 off Rio São Francisco at 11°S; (B) Transect 6 off Rio de Contas at 14°S; (C) Transect 2 off Rio Paraíba do Sul at 22°S. Arrows indicate direction of South Atlantic Central Water (SACW; yellow), Antarctic Intermediate Water (AAIW; pink), and North Atlantic Deep Water (NADW; blue), respectively. Maps were created with GeoMapApp ([www.geomapapp.org](http://www.geomapapp.org)), using the base map of Ryan et al. (2009).

### 3. Material & Methods

#### 3.1 Stations and Sample Material

All samples used in this study were obtained during R/V METEOR expedition M125 'SAMBA' along the Brazilian Margin (Bahr et al., 2016). They were taken as multicores or box cores, from which the upper 0.5 cm or 1 cm of sediment were used for foraminiferal analysis, respectively. The internal diameter of the multicore tubes was 10 cm. For the box corer samples, ~78.5 cm<sup>3</sup> of surface sediment (1cm depth) was removed using the MUC tube. Samples were partitioned for the measurement of various parameters (e.g., benthic foraminifera, grain size, bulk geochemistry). For calculating the benthic foraminiferal density, the analyzed 'real' sediment volume was calculated based on sediment density and analyzed dry weight. A total of 13 surface samples, stained with Rose Bengal, were selected from bathymetric transects 2, 6 and 7 of the cruise. They range from the upper to lower slope between 400 and 2000 m water depth. Transect 2 represents the southernmost transect at approximately 22°S, consisting of 5 stations (24, 25, 29, 34, 35) in water depths ranging from 430 to 2019 m. Transects 6 and 7 are located about 800 km and 1100 km further north, respectively. At 14°S, transect 6 spans four stations (72, 77, 78, 80) at water depths between 420 and 1738 m. Four stations from transect 7 (93, 95, 102, 107) are located at 11°S between 924 and 1900 m ([Table 1](#)).

**Table 1** | Position and hydrological parameters of the selected transects and sample sites of Meteor cruise M125.

Station ID	Sample #	Lat. S°	Long. W°	Watermass	Water depth (mbsl)	Temp. (C°)	Salinity	O <sub>2</sub> (ml/l)	Density kg/m <sup>3</sup>
<b>Transect 2</b>									
M125-24-2	24	21° 55,924'	39° 54,122'	AAIW	872	4.66	34.36	4.55	1027.206
M125-25-2	25	21° 55,924'	39° 51,508'	AAIW	960	4.15	34.35	4.53	1027.254
M125-29-9	29	21° 48,732'	39° 32,031'	NADW	2019	3.49	34.95	5.42	1027.799
M125-34-1	34	21° 56,960'	39° 53,112'	AAIW	876	4.65	34.35	4.56	1027.202
M125-35-2	35	21° 53,607'	40° 00,282'	SACW	430	12.53	35.14	4.56	1026.596
<b>Transect 6</b>									
M125-72-2	72	14° 12,774'	38° 36,528'	NADW	1738	4.15	34.95	5.06	1027.727
M125-77-2	77	14° 23,200'	38° 43,551'	NADW	1394	4.18	34.73	4.04	1027.551
M125-78-2	78	14° 24,356'	38° 50,070'	AAIW	845	5.31	34.40	4.29	1027.166
M125-80-3	80	14° 24,559'	38° 53,307'	SACW	422	11.22	34.97	4.24	1026.713
<b>Transect 7</b>									
M125-93-2	93	10° 24,285'	36° 23,840'	AAIW	955	4.04	34.44	4.05	1027.337
M125-95-2	95	10° 56,728'	36° 12,348'	NADW	1901	3.92	34.96	5.31	1027.763
M125-102-2	102	10° 40,032'	36° 03,953'	NADW	1256	4.14	34.71	4.06	1027.539
M125-107-1	107	10° 41,489'	36° 09,142'	AAIW	924	4.00	34.40	4.00	1027.309

AAIW, Antarctic Intermediate Water; NADW, North Atlantic Deep Water; SACW, South Atlantic Central Water.

#### 3.2 Sedimentological Parameters

Grain size analysis ([Table 2](#); [Figure 3](#)) was performed with a particle analyzer via laser diffraction (CILAS 1064) at the Institute of Chemistry, Department of Geochemistry, Universidade Federal Fluminense (UFF), Brazil. The analysis was conducted with decarbonized samples free of organic matter by adding 1M HCl and 30 % hydrogen peroxide. For particle dispersion sodium hexametaphosphate solution (4 %) was added before the laser analysis.

**Table 2** | Sediment analyses of surface samples.

Sample #	Device	Interval	TOC wt.%	TN wt.%	C:N (bulk)	$\delta^{15}\text{N}$ bulk (per mil)	$\delta^{13}\text{C}$ bulk (per mil VPDB)	clay %	silt %	sand %	mean grain size ( $\mu\text{m}$ )	median grain size ( $\mu\text{m}$ )
<b>Transect 2</b>												
24	BC/VV	0-1	0.64	0.08	8.0	6.39	-22.24	11.7	88.3	-	8.6	7.4
25	MUC	0-0.5	0.40	0.04	10.0	6.25	-22.42	22.0	78.0	-	6.3	4.8
29	MUC	0-1	1.69	0.21	8.0	7.06	-21.01	36.4	63.7	-	4.3	3.2
34	BC/VV	0-1	0.49	0.06	8.2	7.29	-21.64	12.0	75.5	12.5	19.5	10.8
35	MUC	0-0.5	0.23	0.03	7.7	4.65	-22.19	33.9	66.1	-	4.4	3.5
<b>Transect 6</b>												
72	MUC	0-0.5	2.96	0.25	11.8	6.26	-21.56	23.8	76.2	-	6.5	5.3
77	MUC	0-0.5	1.86	0.23	8.1	6.73	-20.71	23.2	76.8	-	7.5	5.9
78	MUC	0-0.5	1.46	0.19	7.7	4.82	-20.73	14.9	73.6	11.5	21.0	11.5
80	MUC	0-0.5	1.28	0.13	9.8	4.94	-22.07	13.8	56.3	29.9	30.5	14.4
<b>Transect 7</b>												
93	MUC	0-0.5	1.40	0.18	7.8	4.80	-21.04	37.4	62.7	-	3.8	2.9
95	MUC	0-0.5	1.42	0.16	8.9	5.41	-22.23	33.7	66.3	-	4.2	3.0
102	MUC	0-0.5	1.00	0.13	7.7	5.40	-20.86	28.4	71.6	-	5.1	3.7
107	BC	0-0.5	1.15	0.16	7.2	5.56	-20.79	26.3	73.7	-	7.0	5.2

BC, Boxcorer; VV, Van Veen Grab; MUC for Multicorer.

Total organic carbon (TOC) and total nitrogen (TN) contents, and their stable carbon ( $\delta^{13}\text{C}_{\text{org}}$ ) and nitrogen ( $\delta^{15}\text{N}$ ) isotopes were measured in approximately 60 mg of decarbonized, macerated sediment samples. They were analyzed in the PDZ Europa ANCA-GSL elemental analyzer at the UFF, coupled to a 20-20 PDZ Europa isotope ratio mass spectrometer (SERCON Ltd. Cheshire UK). Isotope ratios were reported relative to the Vienna Pee Dee Belemnite (V-PDB) international standard for carbon and atmospheric N<sub>2</sub> for nitrogen. The analytical precision for standards was within  $\pm 0.14$  ‰ for  $\delta^{13}\text{C}_{\text{org}}$  and  $\pm 0.13$  ‰ for  $\delta^{15}\text{N}$ .

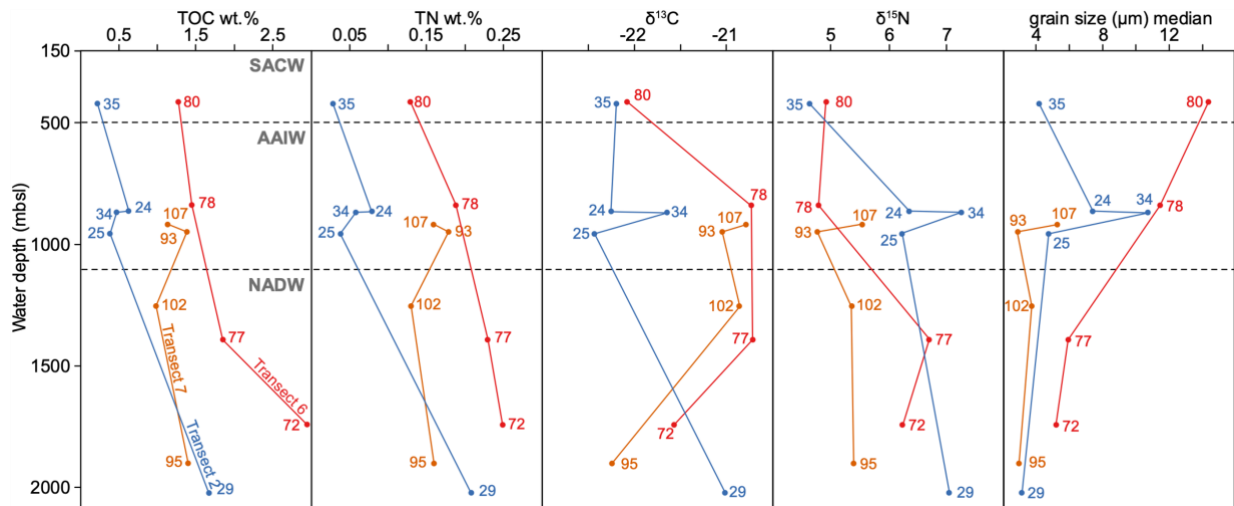


**Figure 3** | Main sedimentological properties of transects 2, 6 and 7 plotted with increasing water depth. The numbers refer to the samples of the respective transect. Transect 2 is shown in blue, transect 6 in red and transect 7 in orange.

### 3.3 Benthic Foraminifera

All samples were stored between April 2016 to March 2017 in buffered 4 % formaldehyde solution to which had been added Rose Bengal with a concentration of 1g/L. The samples were wet sieved with water over a 63  $\mu\text{m}$  sieve and then dried at 30°C. A dry splitter was used for sample partitioning. All benthic foraminiferal tests > 63  $\mu\text{m}$  of the whole sample or split were counted, yielding at least 400 individuals per sample. Stained (Rose Bengal) and unstained specimens were counted separately, allowing to differentiate the living and dead assemblages in the total faunas (see Bernhard, 2000 for review). Only brightly stained specimens were counted as living. For porcelaneous tests, pale pink-stained specimens were distinguished from white ones. Due to very low amounts of stained foraminifera, their evaluation is approached with caution.

Epi- and infaunal microhabitats were assigned according to Schönfeld (1997); Sen Gupta (2002); Murray (2006); Jorissen et al. (2007) and Rasmussen and Thomsen (2017).

**Table 3** | Diversity of benthic foraminifera > 63  $\mu\text{m}$  concerning the total, living and dead fauna.

Sample #		t	s	s/10 ccm	% of total	hya. %	agg. %	porc. %	epif. %	inf. %	epi-to inf. %	*transp. sp. %	*tub. fr. %	H	Fisher's $\alpha$
<b>Transect 2</b>															
<b>24</b>	<b>total</b>	<b>130</b>	<b>2576</b>	<b>82106</b>		<b>86.9</b>	<b>10.6</b>	<b>2.5</b>	<b>32.3</b>	<b>54.8</b>	<b>3.3</b>	<b>1.3</b>	<b>0.1</b>	<b>2.8</b>	<b>12.2</b>
AAIW	living	21	46	914	1.1	49.7	49.8	0.5	66.6	0.4	33.0				
	dead	130	2530	81192	98.9	87.3	10.2	2.5	31.9	55.4	3.0				
<b>25</b>	<b>total</b>	<b>97</b>	<b>604</b>	<b>43587</b>		<b>86.0</b>	<b>12.6</b>	<b>1.4</b>	<b>28.6</b>	<b>61.8</b>	<b>1.9</b>	<b>1.8</b>	<b>0.4</b>	<b>2.9</b>	<b>11.7</b>
AAIW	living	41	108	2461	5.6	72.9	26.7	0.4	74.6	15.8	4.8				
	dead	86	496	41126	94.4	86.8	11.7	1.4	25.8	64.6	1.7				
<b>29</b>	<b>total</b>	<b>89</b>	<b>626</b>	<b>57454</b>		<b>77.7</b>	<b>15.8</b>	<b>6.5</b>	<b>39.4</b>	<b>49.3</b>	<b>4.5</b>	<b>3.7</b>	<b>1.0</b>	<b>3.1</b>	<b>8.3</b>
NADW	living	26	40	2741	4.8	41.1	52.7	6.2	64.9	29.1	6.0				
	dead	87	586	54713	95.2	79.5	14.0	6.5	38.2	50.3	4.5				
<b>34</b>	<b>total</b>	<b>117</b>	<b>1123</b>	<b>165232</b>		<b>87.4</b>	<b>10.5</b>	<b>2.1</b>	<b>34.5</b>	<b>49.2</b>	<b>1.4</b>	<b>3.8</b>	<b>0.0</b>	<b>2.7</b>	<b>10.6</b>
AAIW	living	12	22	502	0.3	0.7	93.1	6.1	98.6	1.4	0.0				
	dead	113	1101	164730	99.7	87.7	10.3	2.1	34.3	49.3	1.4				
<b>35</b>	<b>total</b>	<b>67</b>	<b>621</b>	<b>320694</b>		<b>86.5</b>	<b>5.7</b>	<b>7.8</b>	<b>31.9</b>	<b>55.6</b>	<b>0.2</b>	<b>1.8</b>	<b>0.0</b>	<b>2.6</b>	<b>6.0</b>
subtropical	living	22	58	7242	2.3	72.6	27.4	0.0	36.6	63.4	0.0				
	dead	65	563	313452	97.7	86.8	5.2	7.9	31.8	55.4	0.2				
<b>Transect 6</b>															
<b>72</b>	<b>total</b>	<b>86</b>	<b>530</b>	<b>54496</b>		<b>75.5</b>	<b>14.3</b>	<b>10.2</b>	<b>37.5</b>	<b>45.6</b>	<b>3.2</b>	<b>5.0</b>	<b>0.0</b>	<b>3.2</b>	<b>10.2</b>
NADW	living	32	57	3184	5.8	81.1	18.6	0.3	63.6	36.0	0.4				
	dead	83	473	51312	94.2	75.2	14.0	10.8	35.9	46.2	3.4				
<b>77</b>	<b>total</b>	<b>81</b>	<b>429</b>	<b>98955</b>		<b>87.8</b>	<b>5.5</b>	<b>6.7</b>	<b>32.9</b>	<b>52.8</b>	<b>0.5</b>	<b>4.4</b>	<b>0.4</b>	<b>2.8</b>	<b>7.9</b>
NADW	living	22	45	2938	3.0	99.1	0.5	0.3	70.9	28.7	0.4				
	dead	73	384	96017	97.0	87.5	5.6	6.9	31.8	53.6	0.5				
<b>78</b>	<b>total</b>	<b>99</b>	<b>692</b>	<b>358733</b>		<b>83.7</b>	<b>6.0</b>	<b>10.3</b>	<b>40.6</b>	<b>45.7</b>	<b>2.2</b>	<b>4.4</b>	<b>0.0</b>	<b>3.1</b>	<b>9.5</b>
AAIW	living	28	37	11174	3.1	79.7	20.1	0.2	20.5	59.6	0.1				
	dead	92	655	347559	96.9	83.9	5.5	10.6	41.2	45.3	2.2				
<b>80</b>	<b>total</b>	<b>108</b>	<b>1067</b>	<b>798547</b>		<b>80.0</b>	<b>11.9</b>	<b>8.1</b>	<b>29.4</b>	<b>52.9</b>	<b>2.3</b>	<b>4.8</b>	<b>0.0</b>	<b>3.2</b>	<b>9.3</b>
tropical	living	31	52	4918	0.6	65.2	33.5	1.2	3.4	64.1	31.3				
	dead	101	1015	793629	99.4	80.1	11.7	8.2	29.6	52.9	2.2				
<b>Transect 7</b>															
<b>93</b>	<b>total</b>	<b>144</b>	<b>2363</b>	<b>13394</b>		<b>68.2</b>	<b>18.7</b>	<b>13.0</b>	<b>27.8</b>	<b>42.4</b>	<b>1.6</b>	<b>2.6</b>	<b>2.1</b>	<b>4.0</b>	<b>23.3</b>
AAIW	living	48	128	795	5.9	83.3	10.4	6.3	39.7	50.9	3.0				
	dead	141	2235	12599	94.1	67.3	19.3	13.5	27.0	41.9	1.6				
<b>95</b>	<b>total</b>	<b>98</b>	<b>714</b>	<b>5496</b>		<b>65.4</b>	<b>27.7</b>	<b>6.9</b>	<b>23.5</b>	<b>57.2</b>	<b>3.8</b>	<b>1.8</b>	<b>8.8</b>	<b>3.5</b>	<b>18.1</b>
NADW	living	28	53	269	4.9	71.0	19.2	9.8	21.8	45.1	2.1				
	dead	93	661	5227	95.1	65.1	28.1	6.8	23.6	57.9	3.9				
<b>102</b>	<b>total</b>	<b>107</b>	<b>996</b>	<b>7096</b>		<b>76.8</b>	<b>16.7</b>	<b>6.5</b>	<b>22.6</b>	<b>56.2</b>	<b>3.1</b>	<b>1.8</b>	<b>9.0</b>	<b>3.5</b>	<b>16.1</b>
NADW	living	40	114	810	11.4	86.5	10.3	3.2	39.4	48.0	11.4				
	dead	102	882	6286	88.6	75.6	17.5	6.9	20.5	57.2	2.0				
<b>107</b>	<b>total</b>	<b>92</b>	<b>824</b>	<b>5008</b>		<b>66.8</b>	<b>22.4</b>	<b>10.8</b>	<b>27.9</b>	<b>51.5</b>	<b>1.0</b>	<b>2.8</b>	<b>4.0</b>	<b>3.7</b>	<b>13.2</b>
AAIW	living	17	29	196	3.9	78.4	17.6	4.1	24.3	68.9	0.0				
	dead	89	795	4812	96.1	66.3	22.6	11.0	28.0	50.8	1.0				

Values in bold refer to the total fauna used for the analyses. Presented are the absolute number of taxa (t), and analyzed specimens (s); specimens per 10 cubic centimeters (s/10 ccm); proportions of living and dead specimens within the total fauna (% of total); proportions of different test types agglutinated, calcareous hyaline and porcelaneous; epi- and infaunal proportions. Asterisks indicate that the values of transported specimens (transp. sp.) and tubular fragments (tub. fr.) have been calculated with reference to the whole assemblages. Diversity indices are Shannon H and Fisher's alpha ( $\alpha$ ).

The assessment of tubular agglutinated species is challenging as almost all tests are fragmented. Tubular fragments were thus counted individually but excluded from the total species dataset to avoid over-representation (Goineau and Gooday, 2017). Tubular fragments comprise the species *Rhabdammina abyssorum*, *Rhabdamminella cylindrica*, *Rhizammina algaeformis* and *Saccorhiza ramosa*. Likewise, species that were not deposited autochthonously but had clearly been transported were removed, including *Criboelphidium* spp. and *Discorbis williamsoni* (see also [Appendix 2](#)). To document and assess the role of these excluded taxa, they are presented in [Table 3](#), referred to an expanded matrix that includes tubular fragments and transported specimens.

The species *Globocassidulina subglobosa* and *G. crassa* were often not distinguishable from each other. We therefore combined them under the name *G. subglobosa/crassa*.

For diversity analysis, Fisher's  $\alpha$  and Shannon  $H$  indices were calculated (Fisher et al., 1943; Shannon and Weaver, 1949). Due to the very low numbers of stained foraminiferal tests, these calculations were limited to the total assemblages. The dimensionless Fisher's  $\alpha$ , based on logarithmic series, facilitates the comparison of species richness between different habitats as well as samples of different size (Peet, 1974; Murray, 2006). Species diversity, expressed via Shannon  $H$ , incorporates rare species that make a smaller contribution (Peet, 1974; Murray, 2006). To estimate foraminiferal densities, the total absolute number of foraminifera for each sample was normalized to 10 cubic centimeter (ccm).

### 3.4 Multivariate Statistical Analysis

The software package Past 4.02 (Hammer et al., 2001) was used for multivariate statistical analysis. Since abundances of living specimens were very low, statistical analyses were limited to the total fauna (live + dead specimens), as previously implemented by e.g., de Mello e Sousa et al. (2006) for the Campos Basin.

A hierarchical Q-mode cluster analysis (HCA; UPGMA algorithm, Bray-Curtis similarity index) was performed to identify groups of samples based on their similarity and dissimilarity. Based on a similarity percentage analysis (=SIMPER analysis, Bray-Curtis similarity index), the contribution of each species to the dissimilarity of each cluster is obtained for the total fauna ([Table 4](#)).

To contextualize foraminiferal data and environmental parameters, a canonical correspondence analysis (CCA) was conducted. A CCA is based on unimodal relationships between species abundances and site-specific environmental variables via synthetic ordination axes (ter Braak and Verdonschot, 1995; Ramette, 2007; Paliy and Shankar, 2016). Hydrographic properties such as salinity and oxygen are excluded as limiting factors as the faunal composition is unlikely to be affected by the rather uniform and stable values for salinity and relatively high oxygen concentrations ([Table 1](#); de Mello e Sousa et al., 2006). However, parameters reflecting export productivity and sedimentation show considerably greater variability. We therefore included six parameters in the CCA that exhibit the greatest impact on the benthic fauna (TOC, TN,  $\delta^{13}\text{C}_{\text{org}}$ ,  $\delta^{15}\text{N}$ , proportion of silt and clay; [Table 2](#)).



Since rare species tend to be overestimated in a CCA (Legendre and Legendre, 1998; Ramette, 2007), only species that occur to > 3 % in at least one sample were included; indeterminate taxa were removed, tubular fragments and transported specimens were excluded.

## 4. Results

### 4.1 Environmental Characteristics

#### 4.1.1 Grain Size Distribution

In the Campos Basin at transect 2 (22°S), mean grain sizes between 4.3 and 19.5  $\mu\text{m}$  were recorded. A wider range of 6.5 to 30.5  $\mu\text{m}$  is observed in the samples of transect 6 in the Brazil Basin (14°S). Finer sediment was encountered in transect 7 (11°S) with mean grain sizes between 3.8 and 7  $\mu\text{m}$ . Sand contents were only recorded in sample 34 from transect 2 (12.5 %, AAIW in 876 m) as well as samples 78 (11.5 %, AAIW in 845 m) and 80 (29.9 %, SACW in 422 m) from transect 6, while the remainder consist of silt and clay only ([Table 2](#)).

In the Campos Basin, sample 34 was taken within a cold-water coral (CWC) mound sequence, and sample 24 was retrieved from the marginal mound facies, covered with corals only at the surface (Bahr et al., 2016). Both samples contain the highest mean grain sizes within transect 2 of 19.5  $\mu\text{m}$  (sample 34) and 8.6  $\mu\text{m}$  (sample 24), as well as the highest silt contents ranging from 76 to 88 %, and lowest clay contents at about 12 % in each case ([Table 2](#)). Coarsest mean grain sizes within transect 6 are present in SACW sample 80 (422 m) with 30.5  $\mu\text{m}$  and AAIW sample 78 (845 m) with 21  $\mu\text{m}$  on average ([Table 2](#)). In transect 7, mean grain sizes reach their maximum in AAIW sample 107 (924 m) with only 7  $\mu\text{m}$ . Clay contents are highest in this transect and vary between 26 and 37 % ([Table 2](#)).

#### 4.1.2 Total Organic Carbon, Total Nitrogen Contents and Their Stable Isotopes $\delta^{13}\text{C}_{\text{org}}$ and $\delta^{15}\text{N}$

The range of total organic carbon within the sediment is 0.2-3.0 wt. % with the maximum being measured in sample 72 (transect 6, NADW, 1738 m). Total nitrogen contents also reach their maximum of 0.3 wt. % in sample 72. In the Campos Basin (22°S) TN levels are 0.03-0.2, whereas they are 0.1-0.3 wt. % in the Brazil Basin transects (11-14°S). The C:N ratios range from 7 to 12 for the entire data set, with only sample 72 yielding a value exceeding 10 ([Table 2](#)).

The stable carbon isotope  $\delta^{13}\text{C}_{\text{org}}$  within the bulk organic matter spans values between -22.4 and -20.7 ‰ for the entire data set.  $\delta^{15}\text{N}$  content ranges from 4.7 to 7.3 ‰ of the bulk sediment ([Table 2](#)).

### 4.2 Benthic Foraminifera

#### 4.2.1 Total Assemblage Composition

A total of 278 species was identified, of which 139 have hyaline tests, 104 are agglutinated, and 35 have a porcelaneous test.

Densities of benthic foraminifera per 10 ccm are higher in transect 2 and 6 (44 000-800 000 specimens/10 ccm) than in transect 7 (5 000-13 000 specimens/10 ccm). The highest density in transect 2 in the Campos Basin was observed in sample 35 associated with subtropical SACW (321 000 specimens/10 ccm). Population density is even higher in sample 80 associated with tropical SACW in the Brazil Basin (799 000 specimens/10 ccm; [Table 3](#)). A comparison of samples associated with AAIW and NADW reveals that transect 7, with a maximum of 13 000 specimens/10 ccm, has generally reduced population densities than transect 2 (max. 165 000 s/10 ccm for AAIW and NADW) and 6 (max. 359 000 s/10 ccm for AAIW and NADW; [Table 3](#)). However, species richness, indicated by Fisher's  $\alpha$ , is lower in transects 2 and 6 ( $\alpha=6-12$ ) than in the northern transect 7 ( $\alpha=13-23$ ; [Table 3](#)). This is also reflected by the Shannon  $H$  index, where rare species contribute less (Murray, 2006). Smaller values were calculated for transect 2 ( $H=2.6-3.1$ ), they increased slightly in transect 6 ( $H=2.8-3.2$ ) and highest in transect 7 ( $H=3.5-4.0$ ; [Table 3](#); see also [Appendix 1](#)).

**Table 4** | Composition of the total benthic foraminiferal community via SIMPER analysis based on clusters, see [Figure 4](#).

Taxon	Av. dissim	Contrib. %	Cumulative %	CB		BB	
				Tr. 2	Tr. 6	Tr. 7	
<i>Globocassidulina subglobosa/crassa</i>	10.1	-	15.8	<b>32.4</b>	14.9	6.4	
<i>Rosalina</i> spp.	4.9	7.6	23.4	3.3	<b>14.6</b>	1.1	
<i>Bolivina variabilis</i>	4.8	7.5	30.9	0.9	<b>11.5</b>	9.0	
<i>Bolivina subreticulata</i>	4.2	6.5	37.4	0.8	6.3	<b>11.3</b>	
<i>Nuttallides umbonifer</i>	3.2	4.9	42.3	<b>8.0</b>	0.6	0.1	
<i>Alabaminella weddellensis</i>	2.8	4.4	46.7	<b>7.2</b>	2.0	-	
<i>Epistominella exigua</i>	2.5	4.0	50.7	2.9	5.1	<b>7.4</b>	
<i>Bolivina striatula</i>	1.5	2.4	53.0	<b>4.8</b>	1.7	1.7	
<i>Bolivina albatrossi</i>	1.0	1.6	54.6	0.6	0.5	<b>2.7</b>	
<i>Sigmavirgulina tortuosa</i>	0.9	1.4	56.0	0.1	0.8	<b>2.4</b>	
<i>Pyrgoella irregularis</i>	0.9	1.4	57.4	<b>1.7</b>	1.6	0.4	
<i>Cassidulina laevigata</i>	0.8	1.3	58.7	1.1	<b>2.4</b>	0.6	
<i>Trochammina advena</i>	0.8	1.3	59.9	<b>2.1</b>	0.8	0.7	
<i>Miliolinella subrotunda</i>	0.8	1.2	61.2	0.6	<b>2.4</b>	0.7	
<i>Nonionella</i> spp.	0.8	1.2	62.4	1.9	<b>2.5</b>	1.0	
<i>Bolivina spathulata</i>	0.7	1.1	63.5	1.3	<b>1.4</b>	0.6	
<i>Sigmoilopsis schlumbergeri</i>	0.7	1.0	64.6	-	-	<b>1.8</b>	
<i>Gyroidinoides soldanii</i>	0.6	0.9	65.5	<b>1.4</b>	0.9	0.3	
<i>Neoconorbina terquemii</i>	0.6	0.9	66.4	<b>1.4</b>	-	0.1	
<i>Cassidulinoides bradyi</i>	0.6	0.9	67.3	<b>1.5</b>	0.2	-	
<i>Gavelinopsis praegeri</i>	0.6	0.9	68.2	0.4	0.7	<b>1.4</b>	
<i>Glomospira gordialis</i>	0.6	0.9	69.1	0.4	0.7	<b>1.3</b>	
<i>Cibicides/Cibicides</i> sp. juv.	0.5	0.9	69.9	0.3	0.2	<b>1.6</b>	
<i>Cibicides/Cibicides</i> sp. juv.	0.5	0.8	70.7	1.1	<b>1.6</b>	0.3	
<i>Uvigerina peregrina</i>	0.5	0.8	71.5	0.3	0.2	<b>1.3</b>	
<i>Trochammina squamata</i>	0.5	0.7	72.2	<b>1.1</b>	0.6	0.2	
<i>Cibicides</i> <i>wuellerstorfi</i>	0.5	0.7	73.0	0.3	-	<b>1.2</b>	
<i>Valvulineria minuta</i>	0.5	0.7	73.7	<b>0.9</b>	0.3	0.5	
<i>Ioanella tumidula</i>	0.4	0.7	74.4	0.1	<b>1.2</b>	-	
<i>Paratrochammina challengerii</i>	0.4	0.7	75.0	0.1	0.6	<b>0.8</b>	

CB, Campos Basin; and BB, Brazil Basin; Av. dissim= Average dissimilarity. Shown are the first cumulative 75% of all taxa. The Bray-Curtis index was used; the average overall dissimilarity is 64.1. The highest value of a species between the clusters/transects is marked in bold.

Calcareous-hyaline species predominate all investigated transects, with the highest abundances of > 86 % recorded in transect 2 (samples 24, 25, 34, 35) and transect 6 (sample 77; [Table 3](#)). *Globocassidulina subglobosa/crassa* is abundant across all studied transects. However, it is more frequent along the Campos Basin (32 %) than along the Brazil Basin transects (6-15 %; result of the SIMPER analysis see [Table 4](#)). Important hyaline taxa that further define the dataset are *Rosalina* spp.,

*Bolivina variabilis* and *B. subreticulata*, which are more abundant in the Brazil Basin (each taxon occurs at > 11 % in transect 6 or 7) than in the Campos Basin (each taxon occurs < 4 %; according to the SIMPER analysis in [Table 4](#)). Agglutinated tests are more frequent in transect 7 (17-28 %) than in transects 2 and 6 (6-16 %; [Table 3](#)), with a broad range of taxa being responsible (e.g., cribristomoidids, trochamminids; see [Appendix 2](#)). Additionally, the proportion of tubular fragments is increased in transect 7 (2-9 %) compared to the southern sample sites (0-1 %), with *Saccorhiza ramosa* fragments being most abundant ([Table 3](#) and [Figure 5](#)). Frequently occurring porcelaneous taxa include *Pyrgoella irregularis* and *Miliolinella subrotunda* in all transects ([Tables 3, 4](#)).

Infaunal species dominate the data set. In the Campos Basin they make up 49-62 % of the total fauna, while they range between 42 and 57 % in the Brazil Basin ([Table 3](#)).

#### 4.2.2 Total (Live + Dead) Assemblage Distributions

According to the hierarchical cluster analysis (HCA; cophenetic correlation coefficient: 0.88), the data set of the total assemblage can be divided into two major clusters representing the Campos Basin (cluster 'CB') and the Brazil Basin (cluster 'BB'), respectively. Cluster 'CB' comprises all transect 2 samples, while Cluster 'BB' is internally subdivided into two groups of samples corresponding to transects 6 and 7 ([Figure 4](#)). SIMPER analysis reveals that 30 taxa determine 75 % of the cumulative dissimilarity between clusters and groups ([Table 4](#)). Cluster 'CB' is distinguished by increased abundances of *Globocassidulina subglobosa/crassa* associated with *Nuttallides umbonifer* and *Alabaminella weddellensis*. In contrast, Cluster 'BB' is mainly determined by an assemblage comprising various bolivinids and *Rosalina* species ([Table 4](#)).

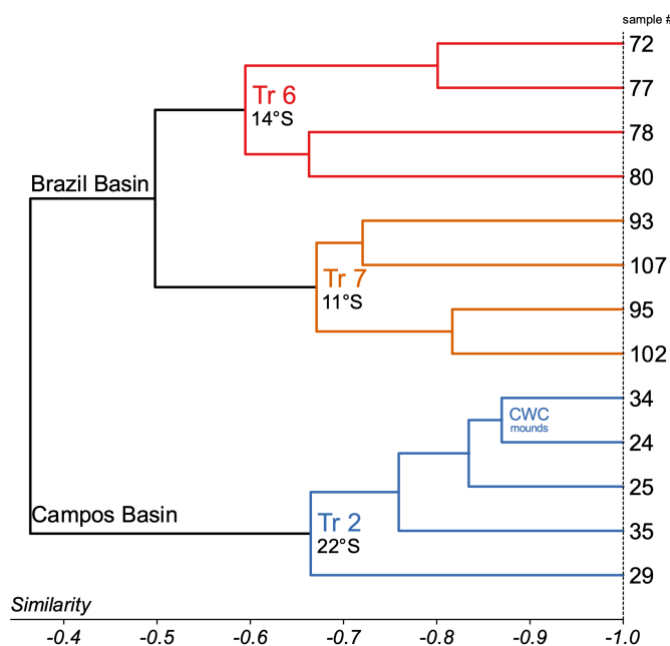


**Figure 4** | Cluster analysis of the total assemblages of benthic foraminifera > 63  $\mu\text{m}$ . The UPGMA algorithm and Bray-Curtis dissimilarity were used, cophenetic correlation is 0.88. Three clusters could be distinguished, reflecting the surveyed transects (Tr. 2, Tr. 6, and Tr. 7).

A *Globocassidulina subglobosa/crassa* assemblage prevails in the Campos Basin. According to the SIMPER analysis the transect is characterized by *G. subglobosa/crassa* (32 %), *Nuttallides umbonifer* (8 %), *Alabaminella weddellensis* (7 %), *Bolivina striatula* (5 %) and *Rosalina* spp. (3 %; [Table 4](#)). *Globocassidulina subglobosa/crassa* and *N. umbonifer* decrease slightly with increasing depth, while *A. weddellensis* increases in the AAIW and NADW samples 24, 25, 29, 34 ([Figure 5](#)). *Epistominella exigua*, *Rosalina* spp. and *Pyrgoella irregularis* are associated taxa in the deeper sample 29 within the NADW ([Figure 5](#)). Within the 'CB' cluster, both CWC mound samples 24 and 34 form a distinct subgroup, plotting closest to cluster 'BB'.

The total assemblage of transect 6 at 14°S is mainly determined by *G. subglobosa/crassa* (15 %), *Rosalina* spp. (15 %), *Bolivina variabilis* (12 %), *Bolivina subreticulata* (6 %) and *Epistominella exigua* (5 %; [Table 4](#)). Occurrences of *G. subglobosa/crassa* are mainly concentrated on the upper slope within SACW (sample 80) and abundances are substantially reduced when compared to the Campos Basin ([Figure 5](#)). With increasing depth, assemblages with various species of *Rosalina* determine the benthic fauna of transect 6. In samples 72 and 77, which are associated with NADW, bolivinids become predominant, with *Bolivina variabilis* being most abundant ([Figure 5](#)).

In transect 7 at 11°S, a *Bolivina* assemblage characterizes the benthic foraminiferal association. The SACW layer was not investigated in this area, so the association only reflects AAIW and NADW samples. The assemblage is composed of *Bolivina subreticulata* (11 %), *Bolivina variabilis* (9 %), *Epistominella exigua* (7 %) and *Globocassidulina subglobosa/crassa* (6 %; [Table 4](#)). Tubular fragments are common in transect 7 and increase with depth ([Table 3](#); [Figure 5](#)). Bolivinids are slightly more common in deeper NADW samples 95 and 102 than in AAIW samples 93 and 107, where they are accompanied by increased occurrences of *Saccorhiza ramosa* fragments. Associated *Epistominella exigua* occurs equally in both water masses ([Figure 5](#)). Thus, the assemblages in the Brazil Basin are strongly determined by rosalinids and bolivinids, contrasting a *Globocassidulina* assemblage in the Campos Basin.

#### 4.2.3 Key Environmental Factors and Total Assemblage Distribution

A canonical correspondence analysis (CCA) based on scale type 1 after Legendre and Legendre (1998) explains the relationship between foraminiferal species, environmental variables, and sample sites ([Figure 6](#)). As a function of distance between the variables TOC, TN,  $\delta^{13}\text{C}_{\text{org}}$ ,  $\delta^{15}\text{N}$ , silt and clay, the canonical axes CCA1 (eigenvalue=0.28, variance=58.4 %) and CCA2 (eigenvalue=0.09, variance=18.1 %) explain > 75 % of the entire data set.

The sample sites are separated along the axes in terms of their assignment to the 'CB' and 'BB' clusters. Cluster 'CB' (transect 2) plots on negative CCA1 together with the  $\delta^{15}\text{N}$  and silt vectors. Sample 35 from the upper slope (SACW) and deepest sample 29 (NADW) plot in the positive range of CCA2, more strongly associated with silt. All AAIW samples (24, 25, 34) plot in the negative range and are more strongly associated with  $\delta^{15}\text{N}$ . All cluster 'BB' samples (transects 6 and 7) plot on positive CCA1 in the range of TOC, TN,  $\delta^{13}\text{C}_{\text{org}}$  and clay vectors. Within cluster 'BB', all transect 6 samples plot on negative

CCA2, where they are associated with TOC. The samples of transect 7 fall in the positive range of CCA2, within the quadrant of TN, clay and  $\delta^{13}\text{C}_{\text{org}}$  vectors ([Figure 6](#)).

The *Globocassidulina subglobosa/crassa* assemblage of the Campos Basin falls within the negative range of CCA1. *Globocassidulina subglobosa/crassa*, and *Alabaminella weddellensis* occur rather close to  $\delta^{15}\text{N}$ , while *Trochammina advena* and *Bolivina striatula* plot between the silt and clay vectors ([Figure 6](#)). *Bolivina spathulata* is the only bolivinid species that contrasts with the clay vector, as it is slightly enhanced in the samples close to the CWC mounds (24, 25). The CCA illustrates that the *G. subglobosa/crassa* assemblage is mainly associated with *Nuttallides umbonifer* at the upper slope (sample 35), while *Alabaminella weddellensis* is predominant in the deeper areas (samples 24, 25, 34; [Figures 5, 6](#)).

The *Rosalina* assemblage of transect 6 plots on positive CCA1 and negative CCA2. *Rosalina* spp., *Miliolinella subrotunda* and *Cassidulina laevigata* are associated with relatively higher organic carbon levels ([Figure 6](#)).

The CCA shows that various infaunal species of the *Bolivina* assemblage, such as *Bolivina subreticulata*, *Sigmavirgulina tortuosa*, *Bolivina albatrossi* and *Sigmoilopsis schlumbergeri* occur preferentially in the clay-rich samples of transect 7, all plotting in the positive range of CCA1 and CCA2. The associated species *Epistominella exigua*, *Pyrgoella irregularis* and *Nonionella* spp. also show good concordance with higher clay contents.

#### 4.2.4 Stained (Living) Assemblage Composition

Between 22 to 128 stained specimens were picked per sample, exceeding 100 specimens in only three samples (25, 93, 102). The contribution of living individuals to the total assemblage ranges from 0.3 % to 11 %, being highest in transect 7 ([Table 3](#)). Similar to the total assemblages, the number of living foraminifera per 10 ccm is the lowest in transect 7 (200-800 specimens/10 ccm); it is slightly increased at transect 2 in the Campos Basin (500-7 000 specimens/10 ccm) and highest in transect 6 in the Brazil Basin (3 000-11 000 specimens/10 ccm; [Table 3](#)).

Stained specimens belong to 147 species (63 hyaline, 61 agglutinated, 23 porcelaneous) all of which are represented among dead tests. The biocoenosis of transect 2 from the Campos Basin consists primarily of *G. subglobosa/crassa*, *Trochammina squamata*, and *Tritaxis fusca*. Stained specimens of *G. subglobosa/crassa* are abundant on the upper slope within the SACW in sample 35, associated with common occurrences of *Spiroplectinella wrighti* ([Figure 5](#)). AAIW samples 34 and 24, which were retrieved directly from, or very close to, a cold-water coral mound, contain mainly stained *Trochammina squamata* with *Epistominella exigua* and *Trochammina advena* ([Figure 5](#)). In adjacent AAIW sample 25, located distal to the coral mounds, *E. exigua*, *Nuttallides umbonifer* and *Tritaxis fusca* occur commonly within the biocoenosis. In sample 29, associated with NADW, *Tritaxis fusca* was the most common species in the live assemblage ([Figure 5](#)).

In the Brazil Basin at transect 6, the living assemblage within SACW (sample 80) consists of abundant *Trifarina bradyi*, *Paratrochammina challengerii* and *Bolivina spathulata*. Stained specimens of

*Epistominella exigua* are common in sample 78 associated with AAIW. With increasing depth, live individuals of *E. exigua* are associated with live *Ioanella tumidula* and *Bolivina variabilis* in the NADW (Figure 5). The biocoenosis of transect 7 is mainly determined by *E. exigua*, *G. subglobosa/crassa*, *Bolivina subreticulata* and *B. variabilis* and shows the highest resemblance to the total assemblage (Figure 5; see also Appendix 2).

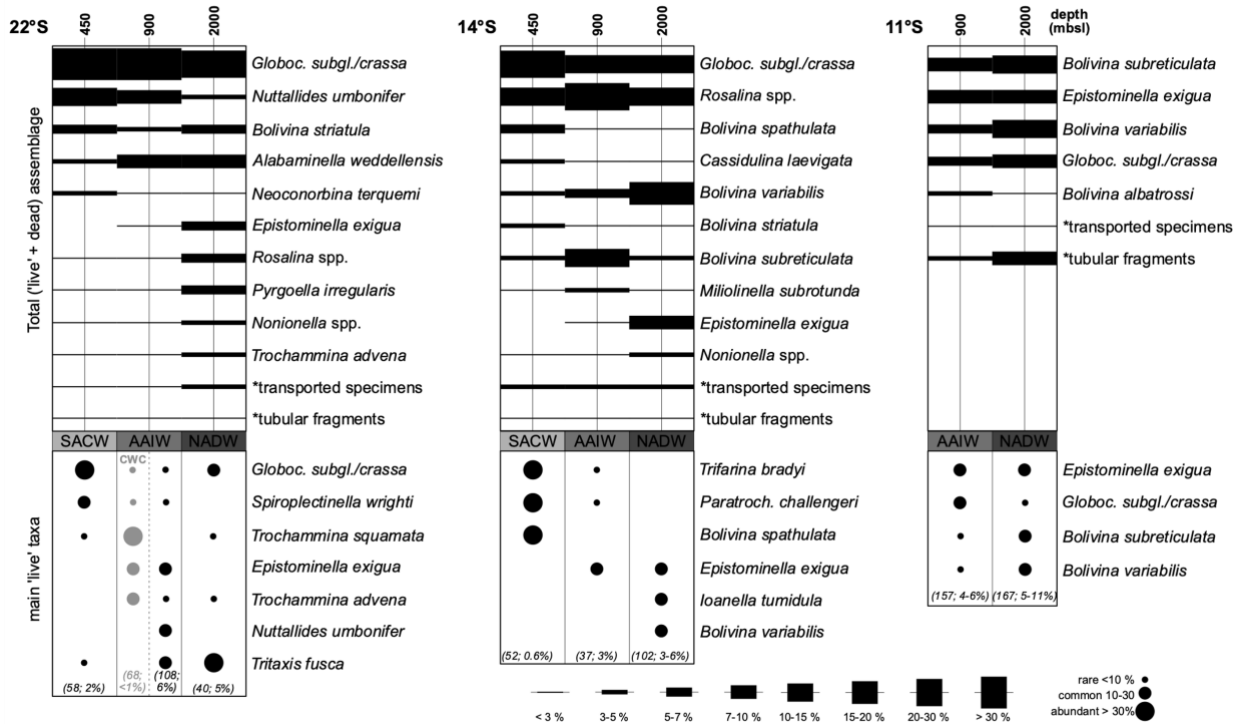


**Figure 5** | Abundances of benthic foraminiferal taxa > 63 μm in the studied areas at 22°S, 14°S and 11°S relative to water masses. Proportions of transported specimens and tubular fragments indicated by asterisks have been calculated with reference to the whole assemblages (Table 3). All taxa that occur with at least 3 % in one water mass are plotted. Bars indicate abundances based on the total (live+dead) assemblage. Stained (living) specimens are indicated by circles and given as rare (< 10 %), common (10-30 %), and abundant (> 30 %). The values in parentheses indicate the absolute analyzed census counts and proportions of living specimens.

## 5. Discussion

### 5.1 Patterns of Foraminiferal Diversity, Density, and Distribution

Diversity analyses indicate that the benthic foraminiferal faunas correspond to typical assemblages from well-oxygenated deep-sea environments (Gooday, 2003; Murray, 2006). Calculated Fisher’s  $\alpha$  and Shannon  $H$  indices are comparable to the species diversity for the South Atlantic (Murray, 2006). Lower diversity indices in transect 2 ( $\alpha=6-12$ ;  $H=2.6-3.1$ ), slightly increased indices in transect 6 ( $\alpha=8-10$ ;  $H=2.8-3.2$ ), followed by higher indices in transect 7 ( $\alpha=13-23$ ;  $H=3.5-4.0$ ) may reflect a general increase in foraminiferal diversity along the Brazilian Margin from South to North (Table 3; Appendix 1). Clearly, more studies with a higher spatial resolution are needed to test the robustness of this pattern.

No direct relation is observed between benthic foraminiferal diversity and density. The latter is substantially lower in transect 7 (5 000-13 000 specimens/10 ccm) than in transects 2 and 6 (44 000-800 000 specimens/10 ccm; [Table 3](#)) for both total and living faunas. Thus, the population density of transect 7 is more similar to the eastern South Atlantic (cf. Schmiedl et al., 1997). The densities of transect 2 agree well with those measured in the Campos Basin by de Mello e Sousa et al. (2006), while transect 6 even exceeds these values.

Lower numbers of foraminiferal tests per 10 cubic centimeter in transect 7 do not result in a lower diversity, as might be expected from other faunal studies, e.g., Jorissen et al. (1995) and Fontanier et al. (2002). A low number of specimens per 10 ccm coupled with a high species heterogeneity could be linked to increased inputs of phytodetritus (Lamshead and Gooday, 1990; Gooday and Rathburn, 1999). This is supported by occurrences of species sometimes associated with phytodetritus such as *Pyrgoella irregularis* in transect 7 ([Figure 6](#) and [Appendix 2](#); Gooday, 1988). A higher sampling resolution would be necessary to gain more detailed insight into the observed patterns of species density and diversity.

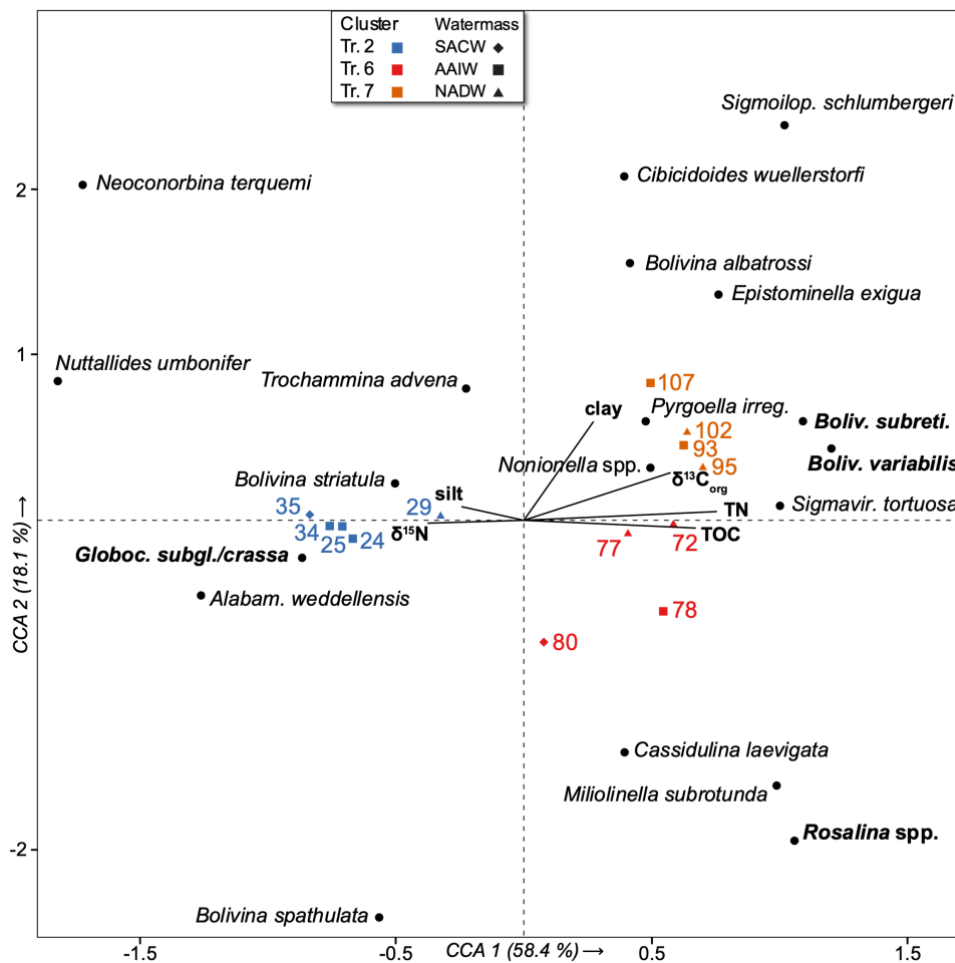


**Figure 6** | Canonical correspondence analysis, scale type 1, with environmental parameters  $\delta^{15}\text{N}$ ,  $\delta^{13}\text{C}_{\text{org}}$ , clay and silt contents, total organic carbon (TOC) and total nitrogen (TN).

Percentages of stained specimens in all transects (0.3-11 %; [Table 3](#)) are consistent with the observations of de Mello e Sousa et al. (2006), who describe similarly low values from the Campos Basin. It is a common observation in deep-sea samples that only a small proportion of benthic foraminiferal specimens consists of living individuals (Murray, 2006). Great variation in the volume of protoplasm (e.g., during periods of low food influx) in certain species further complicates the recognition of stained tests and thus limits the application of Rose Bengal (Linke and Lutze, 1993; Murray, 2006).

Regarding the distribution of different test types, a northward trend can be observed. Agglutinated tests are relatively more abundant in transect 7 (17-28 %) compared to both southern transects (6-16 %; [tab. 3](#)). This is further underlined when comparing the proportions of tubular fragments between transect 7 (2-9 %) and transects 2 and 6 (0-1 %; [Table 3](#)). In transect 7, tubular fragments mainly include *Saccorhiza ramosa* ([Figure 7](#)), which prefers areas with less pronounced bottom current activity (Altenbach et al., 1988; Gooday, 2003). Individual species of each test type will be examined in more detail in the following chapters.

## 5.2 Controlling Factors of Faunistic Differences Between the Campos and Brazil Basins

Multivariate statistical analyses of the total assemblages suggest that the observed patterns of benthic foraminiferal distribution are explained by the quantity and quality of organic matter exported to the seafloor, properties of the substrate and the hydrodynamic regime at the sediment/water interface.  $\delta^{15}\text{N}$  values in the range of 4.7-7.3 ‰, together with  $\delta^{13}\text{C}_{\text{org}}$  between -20 to -22 ‰ indicate a marine origin of the organic matter deposited along the investigated transects in the Campos and Brazil Basins (Nagel et al., 2009; Rumolo et al., 2011; Gaye et al., 2018). This interpretation is further validated by C:N ratios between 4 and 10, indicating that nitrogen is remineralized and nutrients are released ([Table 2](#); Anderson, 1992; Rumolo et al., 2011). The main food source on the continental slope in the Campos Basin was previously reported to be autochthonous organic material derived from primary production (Carreira et al., 2010; Yamashita et al., 2018). Despite the exceedingly narrow shelf at the Rio de Contas and the Rio Sao Francisco (11-14°S), the southward drift of sediments delivered by these rivers prevents their transport to the continental slope (Rebouças et al., 2011; Cavalcante et al., 2020). Terrestrial organic material thus seems to play a minor role in the sediments despite nearby river discharges, implying a predominance of marine organic material (Cordeiro et al., 2018). In addition to primary production, along- and downslope transport due to major current systems and local canyons and channel networks delivers more refractory organic matter to all three study areas (Bahr et al., 2016; da Silveira et al., 2020). The Campos Basin in particular is characterized by contourite deposition and coarser sediments indicating increased bottom currents in this area (Viana, 2001; de Mello e Sousa et al., 2006). Constant bottom flow velocities reflected in increased silt proportions ([Table 2](#)) as well as reworked sediments result in relatively reduced organic matter concentrations in the surface substrates (de Mello e Sousa et al., 2006; Gaye et al., 2018). Towards the north, where the subtropical gyre becomes less vigorous, calmer settings and more clayey sediments predominate ([Table 2](#); Stramma and England, 1999; Mémery et al., 2000; da Silveira et al., 2020).



### 5.2.1 Campos Basin

High abundances of *Globocassidulina subglobosa/crassa* are typical for the shelf and upper slope of the Campos Basin (Lohmann, 1978; de Mello e Sousa et al., 2006; Eichler et al., 2008; Burone et al., 2011; Dias et al., 2018). Their high abundances coincide with increased grain sizes ([Figure 6](#)), suggesting they prefer constant bottom flow velocities, as already suggested in previous studies (e.g., Schmiedl et al., 1997; de Mello e Sousa et al., 2006). Local occurrences of upper slope contourites as well as CWC mounds in the Campos Basin document an increased bottom current activity in this area as well (Viana, 2001; Viana et al., 2002; Bahr et al., 2020; Raddatz et al., 2020). On the upper slope in the subtropical part of the SACW at 430 m (sample 35) a *G. subglobosa/crassa*-*Nuttallides umbonifer* assemblage is adapted to lower nitrogen levels and reduced primary productivity, highlighted in the CCA by TN plotting contrary to it ([Figure 6](#); Gooday, 1994; Gooday, 2003; Margreth et al., 2009; De and Gupta, 2010). The assemblage is complemented by *Alabaminella weddellensis* with increasing depth beyond 850 m in the AAIW. Similar to *G. subglobosa/crassa*, *A. weddellensis* can be considered as an r-strategist that responds opportunistically to the input of organic material (e.g., Gooday, 1988; Gooday, 1993; Dias et al., 2018). Bolivinids contribute less to the Campos Basin than to the Brazil Basin samples, with *Bolivina striatula* and *B. spathulata* being the most prevalent species ([Table 4](#) and [Figure 6](#)). *Bolivina striatula* is mainly recorded from the upper slope (450 m, SACW sample 35; [Figure 5](#)). However, it is well known from the continental shelf down to a depth of 200 m and can serve as an indicator for freshwater input in estuarine areas (Boltovskoy et al., 1980; Eichler et al., 2008; Mendes et al., 2012). Since no stained *B. striatula* were found in sample 35, downslope transport from the shelf, favored by the pronounced canyon system on the slope of the Campos Basin (Bahr et al., 2016), might explain the occurrences of *B. striatula* at greater water depths. Support for downslope transport comes from occurrences of shelf-dwelling *Discorbis williamsoni* as well as some occurrences of elphidiids, mainly represented by *Criboelphidium incertum* ([Figure 7](#); Boltovskoy et al., 1980; Murray, 2006).

The surveyed transect in the Campos Basin (430-2000 m, 22°S) agrees well in its faunal composition with the former study by de Mello e Sousa et al. (2006; 750-2000 m, 22-23°S) near the Sao Tomé and Itapemirim Canyons. The authors describe a *Globocassidulina subglobosa* assemblage, inhabiting sandier sediments and being adapted to oligotrophic conditions and increased bottom currents (de Mello e Sousa et al., 2006). Opportunistic species such as *G. subglobosa*, *Nuttallides umbonifer* and *Alabaminella weddellensis* thrive in more unstable substrates due to local bottom currents and cope with high fluctuations in food availability (Schmiedl et al., 1997; de Mello e Sousa et al., 2006; Fentimen et al., 2018; Fentimen et al., 2020). These species decline northwards and are clearly under-represented in the northern study areas.

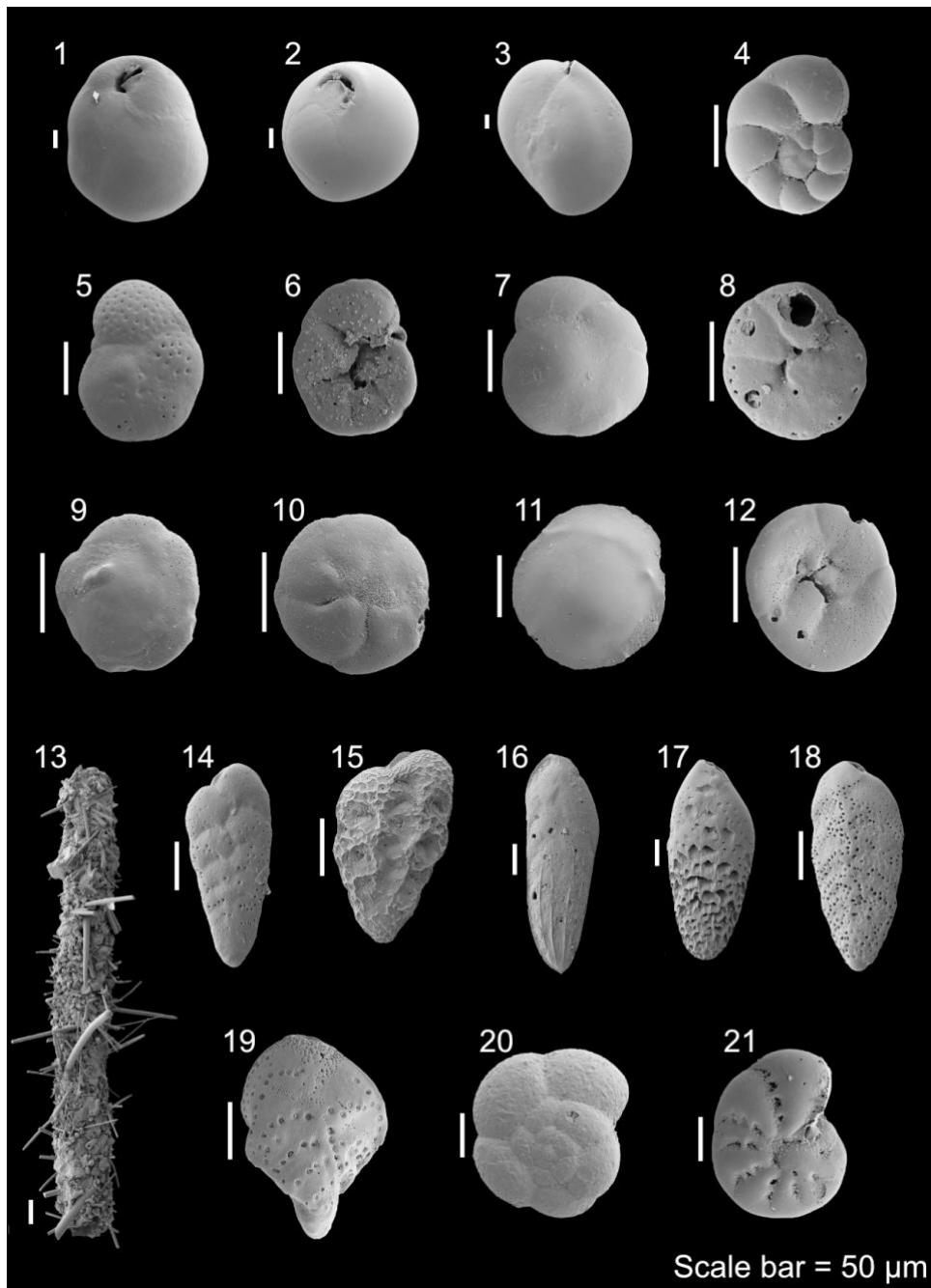


**Figure 7** | The main taxa of the Brasil and Campos basin records: **1** *Globocassidulina subglobosa* (Brady, 1881); **2** *Pyrgoella irregularis* (d'Orbigny, 1839); **3** *Miliolinella subrotunda* (Montagu, 1803); **4** *Nonionella* sp.; **5** *Rosalina globularis* (d'Orbigny, 1826), spiral side; **6** *R. globularis* (d'Orbigny, 1826), umbilical side; **7** *Nuttallides umbonifer* (Cushman, 1933), spiral side; **8** *N. umbonifer* (Cushman, 1933), umbilical side; **9** *Alabaminella weddellensis* (Earland, 1936), spiral side; **10** *A. weddellensis* (Earland, 1936), umbilical side; **11** *Discorbis williamsoni* (Chapman & Parr, 1932), spiral side; **12** *D. williamsoni* (Chapman & Parr, 1932), umbilical side; **13** Fragment of *Saccorhiza ramosa* (Brady, 1879); **14** *Bolivina variabilis* (Williamson, 1858); **15** *Bolivina subreticulata* (Parr, 1932) **16** *Bolivina striatula* (Cushman, 1922) **17** *Bolivina albatrossi* (Cushman, 1922) **18** *Bolivina spathulata* (Williamson, 1858); **19** *Sigmavirgulina tortuosa* (Brady, 1881); **20** *Trochammina advena* Cushman, 1922, spiral side; **21** *Criboelphidium incertum* (Williamson, 1858), side view.

The CWC mounds of the Campos Basin represent a distinct facies not addressed in previous studies and yielding a slightly divergent foraminiferal association. The high abundances of *A. weddellensis* in

the AAIW are mainly linked to the CWC mound samples ([Figure 6](#); [Appendix 2](#)). As coral scaffolds capture phytodetritus, increased *A. weddellensis* occurrences seem to be favored here (Fentimen et al., 2018). Attached species such as *Trochammina advena* use the constant near-bottom current for suspension feeding (Schönfeld, 2002a). It was also noticeable that particularly large specimens of *Cibicidoides wuellerstorfi* occur exclusively in CWC mounds (they occur in samples 24 and 34 almost exclusively in the > 250 µm fraction). Although *C. wuellerstorfi* appears to be more numerous in the samples from the Brazil Basin ([Figure 6](#)), the examined specimens were clearly smaller there. Probably *C. wuellerstorfi* benefits from a better nutrient supply in the increased current regime within the CWC mounds, which is reflected in its size. The increased proportion of attached *Trochammina squamata* in the living stock of the CWC samples, coinciding with the lack of stained globocassidulinids, demonstrates that attached suspension feeders use the elevated substrates of coral reefs as a niche to benefit from trapped suspended nutrients (Lutze and Thiel, 1989; Linke and Lutze, 1993; Schönfeld, 1997). Occurrences of *B. spathulata* close to the CWC mounds (samples 24, 25) imply that this particular bolivinid species prefers to live in silty environments near a coral facies, which has already been shown by Fentimen et al. (2018); Fentimen et al., 2020) for the CWC mounds of the Porcupine Seabight in the northeast Atlantic Ocean. The preference of *B. spathulata* for silty substrates is further reflected in its occurrences within the SACW (sample 35 in transect 2 and sample 80 in transect 6; [Table 2](#) and [Figure 6](#)), which exhibits relatively higher current velocities (de Mello e Sousa et al., 2006; da Silveira et al., 2020).

### 5.2.2 Brazil Basin

The bolivinid-dominated assemblages of transects 6 and 7 coincide with comparably higher total nitrogen and organic carbon contents, as implied in the CCA ([Figure 6](#)). This association suggests an increased nutrient input and thus slightly higher food availability in these areas (Corliss, 1985; Schmiedl et al., 1997; de Mello e Sousa et al., 2006). The consistent presence of *Epistominella exigua* in all samples > 900 m depth ([Figure 5](#)) further indicates increased primary production, as this species is often associated with phytodetrital input (Gooday, 1988; Gooday, 1993; Mackensen et al., 1995; Gooday, 1996; Kurbjeweit et al., 2000; De and Gupta, 2010). Seasonal variability of the NBUC at about 10°S (Stramma et al., 1995) seems to be associated with increased *E. exigua* occurrences, as this species prefers seasonal inputs of phytodetritus (Gooday, 1988; Mackensen et al., 1990; Schmiedl et al., 1997).

In transect 6 increased occurrences of *Cassidulina laevigata*, generally linked to enhanced influx of organic matter (Schmiedl et al., 1997; de Mello e Sousa et al., 2006; De and Gupta, 2010), are mainly observed in SACW sample 80, where it coincides within the same quadrant as the TOC vector in the CCA ([Figure 5](#)). Downslope transport in this region is indicated by occurrences of elphidiids which are present in the total assemblage in all samples of transect 6, extending into the areas of NADW (sample 72, 1700 m; represented as 'transported species' in [Figure 5](#)). The steep slope with deeply incised canyons characterized by a network of meandering and straight channels, together with a very narrow continental shelf, facilitates downslope transport of entrained material (Bahr et al., 2016). Rich

*Rosalina* spp. occurrences are mainly documented from the middle slope (Figure 5). *Rosalina* species favor more distal settings in terms of increased bottom current activity and prefer to inhabit slightly elevated substrates that are exposed to light currents (Corliss, 1985; Schönfeld, 2002b). They can move from their clinging position to a motile situation when food is scarce (DeLaca and Lipps, 1972). *Rosalina* species are thus able to search for areas with an increased nutrient supply, where they can stretch out their pseudopodia to ingest food (DeLaca and Lipps, 1972). A high *Rosalina* density in transect 6 is likely linked to sufficient food availability, as suggested by the correspondence with TOC and TN contents (depicted in the CCA, Figure 6). Slightly increased occurrences of *Miliolinella subrotunda* within the AAIW (sample 78) coincide with the highest occurrences of rosalinids within transect 6 (Figure 5). Suspension-feeding *M. subrotunda* also prefers rather gentle currents as this protist uses flexible agglutinated tubes to support its pseudopodial system that it deploys into the water to feed. These tubes may be distorted or damaged by bottom flow speeds that were too high (Altenbach et al., 1993). Along the slope in NADW samples 72 and 77, the *Rosalina* assemblage is complemented by occurrences of various *Nonionella* species (*N. turgida*, *N. iridea*, *Nonionella* spp. juv.; Figure 5). *Nonionella* is associated in several studies with the input of fresh organic matter and phytodetritus (Mackensen et al., 1990; Gooday and Hughes, 2002; Duffield et al., 2015; Alve et al., 2016). Transect 6 is thus characterized by a comparably higher nutrient input, corroborated by the positive association with TOC and TN contents in the CCA (Figure 6; Gooday, 2003; Alve et al., 2016).

Substrates sampled on the slope along transect 7 at 11°S are much finer compared to the study sites at 22°S and 14°S (Figure 6 and Table 2). The fauna defined by various *Bolivina* species is complemented by occurrences of *Pyrgoella irregularis*, which is sometimes associated with phytodetritus and inhabits more clayey areas (Gooday, 1988; Gooday, 1993). *Saccorhiza ramosa* colonizes the NADW samples 95 and 102 on transect 7 (shown as ‘tubular fragments’ in Figure 5), each of which was collected at elevated positions within the canyon system and thus located distal to the main downslope transport (Figure 5; Bahr et al., 2016). This tubular and fragile suspension feeder requires stable substrates to dwell upright in the sediment and indicates moderate to low current intensities and poor reworking by detritus feeders (Altenbach et al., 1987; Mackensen, 1987; Linke and Lutze, 1993). Occurrences of *S. ramosa* are already known from similar settings in the Gulf of Cadiz where they live distal to the main current of the Mediterranean outflow water (Schönfeld, 1997; Schönfeld, 2002a; Schönfeld 2002b). The coincidence of enhanced silt contents with all samples from transect 7 in the CCA emphasizes a generally calmer setting in this study area (Figure 6). The current velocity of the northward flowing North Brazilian Undercurrent (NBUC) appears to be weaker at 11°S compared to the southern study areas (Stramma et al., 1995). This can be explained by the sampling depth far below the velocity core of the NBUC, which is located at the pycnocline between BC and SACW in this area (150-200 m; Stramma et al., 1995; da Silveira et al., 2020).

De Mello e Sousa et al. (2006) describe a *Bolivina* assemblage with reduced *G. subglobosa* abundances, from the deeper and muddier areas of the Campos Basin, where more stable substrates and reduced bottom currents prevail. In some respects, their *Bolivina* assemblage resembles that found between 11 and 14°S in the present study. However, the abundance of *G. subglobosa/crassa* on transects 6 and

7 is even lower than reported by de Mello e Sousa et al. (2006). The faunal data from 11-14°S suggests that the northward directed branch of tropical SACW, strongly controlled by the NBUC, favors an assemblage that prefers high organic matter fluxes and finer sediments (Stramma and England, 1999; Gooday, 2003; da Silveira et al., 2020). In transect 6, *G. subglobosa/crassa* is still the most common taxon, but accompanied by a rich *Rosalina* association, which is missing at the Campos Basin (de Mello e Sousa et al., 2006). *Globocassidulina subglobosa/crassa* plays a very minor role at 11°S in transect 7 (Table 4). *Alabaminella weddellensis* is much less abundant in the northern sample sites compared to the Campos Basin; in transect 7 it is not recorded at all (Table 4). This could be due to the lack of CWC mounds in the Brazil Basin as well as finer sediments in transect 7 (Fentimen et al., 2018; Fentimen et al., 2020). High organic matter fluxes considerably influence the bolivinid-determined assemblage in these areas (Gooday, 2003). The additional occurrence of the opportunistic species *Epistominella exigua* further distinguishes the northern assemblage from the deeper Campos Basin, where this species is under-represented (de Mello e Sousa et al., 2006).

Regarding the sparse living assemblage, stained specimens such as attached *Tritaxis fusca* and *Trochammina squamata* in transect 2 contrast with the few living foraminifera at transects 6 and 7, some of which are infaunal bolivinids (transect 6) and vulnerable tube-shaped tests of *Saccorhiza ramosa* (transect 7). *Tritaxis fusca* and *Trochammina squamata* have already been mentioned in relation to increased bottom currents, confirming an increased hydrodynamic energy level in the Campos Basin (e.g., Schönfeld, 1997; Schönfeld and Zahn, 2000; Schönfeld 2002a), whereas the biocenosis of the Brazil Basin transects well reflects calmer environments (Figure 5).

## 6. Conclusions and Future Directions

New microfaunal and sedimentological data indicate that the benthic foraminiferal fauna at the Brazilian continental margin between 11 and 22°S is controlled by the quantity and quality of organic matter fluxes as well as substrate properties and hydrodynamic conditions at the sediment water interface. This study reveals that a *Globocassidulina subglobosa/crassa* assemblage in the Campos Basin is contrasted by a rosalinid/bolivinid assemblage in the Brazil Basin. This biogeographic divide occurs across the bifurcation of the SACW into its southward subtropical and northward tropical branches. The subtropical transect at 22°S reveals slightly lower diversity indices but increased population densities compared to the tropical study areas (11-14°S). The proportion of stained (living) specimens is somewhat lower at 22°S compared to 11-14°S. However, typically for deep-sea samples, their proportion is rather small for all three sample areas.

The Campos Basin is characterized by a *Globocassidulina subglobosa/crassa* assemblage, further defined by *Nuttallides umbonifer* and *Alabaminella weddellensis*. This assemblage reflects a variable nutrient supply and coarser substrates due to increased bottom current activity. *Alabaminella weddellensis* occupies an ecological niche in CWC mounds to benefit from trapped phytodetritus. Occurrences of elphidiids and *Bolivina striatula* indicate downslope transport due to the large canyon network on the continental slope of the Campos Basin.

A *Rosalina-Bolivina* assemblage characterizes the continental slope in the Brazil Basin. At 14°S, the assemblage composition is defined by *G. subglobosa/crassa*, *Rosalina* spp., *Bolivina variabilis* and *Bolivina subreticulata*, with a lower proportion of *G. subglobosa* compared to the Campos Basin. Enhanced abundances of *Rosalina* spp. are associated with increased TOC and TN levels. In transect 7, a faunal association of *Bolivina subreticulata*, *Bolivina variabilis*, *Epistominella exigua*, *G. subglobosa/crassa* characterises the upper to lower continental slope, coinciding with more clayey sediments. The bolivinid dominated assemblage is associated with an increased nutrient supply, as reflected by its coincidence with relatively higher TOC values in the CCA. Occurrences of *Saccorhiza ramosa*, especially at the lower slope, are linked to more stable substrates.

The new data set implies distinct contrasts in foraminiferal densities, diversities and assemblage composition between the Campos and Brazil basins. The quantity, quality, and seasonality of organic matter influx together with substrate properties and hydrodynamic conditions are identified as the main drivers of the observed patterns. However, the present study, while presenting the first quantitative data for the Brazilian continental margin 11-14°S, is limited in its ability to predict large-scale biogeographic patterns due to its coarse spatial resolution. It should thus be considered a base line and starting point for further faunistic studies along the Brazilian continental margin in the future. Only a significantly higher spatial resolution will allow a fuller understanding of patterns of foraminiferal densities, diversity, and biogeography in this vast area. Investigations of faunal distributions across the potentially critical water mass divide of the northern and southern SACW branches might prove particularly informative in this endeavor.

## Author Contributions

**Anna Saupe** performed the statistical analyses and wrote the manuscript. **Anna Saupe**, Jassin Petersen and Patrick Grunert drafted the concept of the study and contributed to the evaluation of the statistical analyses. **Anna Saupe** and Johanna Schmidt conducted the taxonomic evaluation. André Bahr and Bruna Borba Dias contributed to the collection of samples and interpretation of sedimentological parameters. Bruna Borba Dias, Ana Luiza S. Albuquerque and Rut Amelia Díaz performed the chemical analyses on the sediment samples.

## Acknowledgments

We acknowledge Hanna Cieszynski (University of Cologne) for her support with the SEM. Marie Scheel (University of Cologne) is thanked for her assistance in washing and picking the samples. We thank Tobias Walla who contributed to the sample preparation. BD acknowledges the financial support from FAPESP (grants 2020/11452-3, 2019/24349-9, and 2018/15123-4). We further thank the three reviewers Andrew John Gooday, Michael Martínez-Colón, and Bryan O'Malley for their helpful comments.

## Funding

This study was financially supported and enabled by the Deutsche Forschungsgemeinschaft (DFG, German Research Foundation) through project GR52851/1-1.

## Supplementary Material

The Supplementary Material for this article can be found online at:

<https://www.frontiersin.org/articles/10.3389/fmars.2022.901224/full#supplementary-material>

## References

- Altenbach A. V., Heeger T., Linke P., Spindler M., Thies A. (1993). *Miliolinella subrotunda* (Montagu), a Miliolid Foraminifer Building Large Detritic Tubes for a Temporary Epibenthic Lifestyle. *Mar. Micropaleontol.* 20, 293–301. [https://doi.org/10.1016/0377-8398\(93\)90038-Y](https://doi.org/10.1016/0377-8398(93)90038-Y)
- Altenbach A. V., Lutze G. F., Weinholz, P. (1987). Beobachtungen an Benthos-Foraminiferen (Teilprojekt A3). *Berichte aus dem Sonderforschungsbereich.* 313 (6), 86.
- Altenbach A. V., Unsöld G., Walger E. (1988). The Hydrodynamic Environment of *Saccorhiza ramosa* (BRADY). *Meyniana* 40, 119–132.
- Alve E., Korsun S., Schönfeld J., Dijkstra N., Golikova E., Hess S., et al. (2016). ForAMBI: A Sensitivity Index Based on Benthic Foraminiferal Faunas From North-East Atlantic and Arctic Fjords, Continental Shelves and Slopes. *Mar. Micropaleontol.* 122, 1–12. <https://doi.org/10.1016/j.marmicro.2015.11.001>
- Anderson T. R. (1992). Modelling the Influence of Food C:N Ratio, and Respiration on Growth and Nitrogen Excretion in Marine Zooplankton and Bacteria. *J. Plankton Res.* 14, 1645–1671. <https://doi.org/10.1093/plankt/14.12.1645>
- Bahr A., Doubrawa M., Titschack J., Austermann G., Koutsodendris A., Nürnberg D., et al. (2020). Monsoonal Forcing of Cold-Water Coral Growth Off Southeastern Brazil During the Past 160,000 Years. *Biogeosciences* 17, 5883–5908. <https://doi.org/10.5194/bg-17-5883-2020>
- Bahr A., Spadano Albuquerque A. L., Ardenghi N., Batenburg S. J., Bayer M., Catunda M. C., et al. (2016). METEOR-Berichte: South American Hydrological Balance and Paleoceanography During the Late Pleistocene and Holocene (SAMBA) Cruise No. M125. (Bremen, Germany: MARUM – Zentrum für Marine Umweltwissenschaften der Universität Bremen) [https://doi.org/10.2312/cr\\_m125](https://doi.org/10.2312/cr_m125)
- Bernhard J. M. (2000). Distinguishing Live From Dead Foraminifera: Methods Review and Proper Applications. *Micropaleontology* 46, 38–46.

- Boltovskoy E., Giussani G., Watanabe S., Wright R. C. (1980). Atlas of Benthic Shelf Foraminifera of the Southwest Atlantic 1st ed. Ed. Junk W. (The Netherlands: bv. publishers, The Hague). [https://doi.org/10.1016/0377-8398\(81\)90028-1](https://doi.org/10.1016/0377-8398(81)90028-1)
- Brady H. B., (1879). Notes on some of the Reticularian Rhizopoda of the "Challenger" Expedition; Part I. On New or Little Known Arenaceous Types. Quarterly Journal of Microscopical Sciences 19, 20–67.
- Brady H. B., (1881). Notes on some of the Reticularian Rhizopoda of the "Challenger" Expedition. Part III. Quarterly Journal of Microscopical Science 21, 31–71.
- Braga E. S., Chiozzini V. C., Berbel G. B. B., Maluf J. C. C., Aguiar V. M. C., Charo M., et al. (2008). Nutrient Distributions Over the Southwestern South Atlantic Continental Shelf From Mar Del Plata (Argentina) to Itajaí (Brazil): Winter-Summer Aspects. Cont. Shelf Res. 28, 1649–1661. <https://doi.org/10.1016/j.csr.2007.06.018>
- Burone L., de e Sousa S. H. M., de Mahiques M. M., Valente P., Ciotti A., Yamashita C. (2011). Benthic Foraminiferal Distribution on the Southeastern Brazilian Shelf and Upper Slope. Mar. Biol. 158, 159–179. <https://doi.org/10.1007/s00227-010-1549-7>
- Carreira R. S., Araújo M. P., Costa T. L. F., Ansari N. R., Pires L. C. M. (2010). Lipid Biomarkers in Deep Sea Sediments From the Campos Basin, SE Brazilian Continental Margin. Org. Geochem. 41, 879–884. <https://doi.org/10.1016/j.orggeochem.2010.04.017>
- Cavalcante G., Vieira F., Campos E., Brandini N., Medeiros P. R. P. (2020). Temporal Streamflow Reduction and Impact on the Salt Dynamics of the São Francisco River Estuary and Adjacent Coastal Zone (NE/Brazil). Reg. Stud. Mar. Sci. 38, 101363. <https://doi.org/10.1016/j.rsma.2020.101363>
- Chapman F., Parr W. J. (1932). Victorian and South Australian Shallow-Water Foraminifera. Part II. Proceedings of the Royal Society of Victoria 44, 218–234.
- Cordeiro L. G. M. S., Wagener A. L. R., Carreira R. S. (2018). Organic Matter in Sediments of a Tropical and Upwelling Influenced Region of the Brazilian Continental Margin (Campos Basin, Rio De Janeiro). Org. Geochem. 120, 86–98. <https://doi.org/10.1016/j.orggeochem.2018.01.005>
- Corliss B. H. (1985). Microhabitats of Benthic Foraminifera Within Deep-Sea Sediments. Nature 314, 435–438. <https://doi.org/10.1038/314435a0>
- Cushman J. A. (1922). Shallow-Water Foraminifera of the Tortugas Region. Publications of the Carnegie Institution of Washington 311. Department of Marine Biology of the Carnegie Institution of Washington 17, 1–85.
- Cushman J. A., (1933). Some New Recent Foraminifera from the Tropical Pacific. Contributions from the Cushman Laboratory for Foraminiferal Research 9(4), 77–95.
- da Silveira I. C. A., Napolitano D. C., Farias I. U. (2020). Water Masses and Oceanic Circulation of the Brazilian Continental Margin and Adjacent Abyssal Plain. In: Sumida P.Y.G., Bernardino A.F., De



- Léo F.C. (eds) Brazilian Deep-Sea Biodiversity. Brazilian Marine Biodiversity. Springer: Cham. 7–36. [https://doi.org/10.1007/978-3-030-53222-2\\_2](https://doi.org/10.1007/978-3-030-53222-2_2)
- de Almeida F. K., de Mello R. M., Rodrigues A. R., Bastos A. C. (2022). Bathymetric and Regional Benthic Foraminiferal Distribution on the Espírito Santo Basin Slope, Brazil (SW Atlantic). Deep. Res. Part I Oceanogr. Res. Pap. 181, 103688. <https://doi.org/10.1016/j.dsr.2022.103688>
- De S., Gupta A. K. (2010). Deep-Sea Faunal Provinces and Their Inferred Environments in the Indian Ocean Based on Distribution of Recent Benthic Foraminifera. Palaeogeogr. Palaeoclimatol. Palaeoecol. 291, 429–442. <https://doi.org/10.1016/j.palaeo.2010.03.012>
- DeLaca T. E., Lipps J. H. (1972). The Mechanism and Adaptive Significance of Attachment and Substrate Pitting in the Foraminiferan *Rosalina* Globularis d'Orbigny. J. Foraminifer. Res. 2, 68–72. <https://doi.org/10.2113/gsjfr.2.2.68>
- De Madron X. D., Weatherly G. (1994). Circulation, Transport and Bottom Boundary Layers of the Deep Currents in the Brazil Basin. J. Mar. Res. 52, 583–638. <https://doi.org/10.1357/0022240943076975>
- de Mello e Sousa S. H., Passos R. F., Fukumoto M., da Silveira I. C. A., Figueira R. C. L., Koutsoukos E. A. M., et al. (2006). Mid-Lower Bathyal Benthic Foraminifera of the Campos Basin, Southeastern Brazilian Margin: Biotopes and Controlling Ecological Factors. Mar. Micropaleontol. 61, 40–57. <https://doi.org/10.1016/j.marmicro.2006.05.003>
- Dias B. B., Barbosa C. F., Faria G. R., Seoane J. C. S., Albuquerque A. L. S. (2018). The Effects of Multidecadal-Scale Phytodetritus Disturbances on the Benthic Foraminiferal Community of a Western Boundary Upwelling System, Brazil. Mar. Micropaleontol. 139, 102–112. <https://doi.org/10.1016/j.marmicro.2017.12.003>
- d'Orbigny A.D., (1826). Tableau méthodique de la classe des Céphalopodes. Annales des Sciences Naturelles 7, 245–314.
- d'Orbigny A. D., (1839). Voyage dans l'Amérique méridionale. Foraminifères Pitoit-Levrault, Paris. 1–86. <https://doi.org/.5962/bhl.title.110540>
- Duffield C. J., Hess S., Norling K., Alve E. (2015). The Response of *Nonionella iridea* and Other Benthic Foraminifera to “Fresh” Organic Matter Enrichment and Physical Disturbance. Mar. Micropaleontol. 120, 20–30. <https://doi.org/10.1016/j.marmicro.2015.08.002>
- Earland A., (1936). Foraminifera, Part IV. Additional Records from the Weddell Sea Sector from Material obtained by the S.Y 'Scotia'. Discovery Reports 13. 1–76.
- Eichler P. P. B., Rodrigues A. R., Eichler B. B., Braga E. S., Campos E. J. D. (2012). Tracing Latitudinal Gradient, River Discharge and Water Masses Along the Subtropical South American Coast Using Benthic Foraminifera Assemblages. Braz. J. Biol. 72, 723–759. <https://doi.org/10.1590/s1519-69842012000400010>

- Eichler P. P. B., Sen Gupta B. K., Eichler B. B., Braga E. S., Campos E. J. (2008). Benthic Foraminiferal Assemblages of the South Brazil: Relationship to Water Masses and Nutrient Distributions. *Cont. Shelf Res.* 28, 1674–1686. <https://doi.org/10.1016/j.csr.2007.10.012>
- Fentimen R., Lim A., Rüggeberg A., Wheeler A. J., Van Rooij D. (2020). Impact of Bottom Water Currents on Benthic Foraminiferal Assemblages in a Cold-Water Coral Environment: The Moira Mounds (NE Atlantic). *Mar. Micropaleontol.* 154, 1–14. <https://doi.org/10.1016/j.marmicro.2019.101799>
- Fentimen R., Rüggeberg A., Lim A., Kateb A., Foubert A., Wheeler A. J., et al. (2018). Benthic Foraminifera in a Deep-Sea High-Energy Environment: The Moira Mounds (Porcupine Seabight, SW of Ireland). *Swiss. J. Geosci.* 111, 533–544. <https://doi.org/10.1007/s00015-018-0317-4>
- Fisher R. A., Corbet A. S., Williams C. B. (1943). The Relation Between the Number of Species and the Number of Individuals in a Random Sample of an Animal Population. *J. Anim. Ecol.* 12, 42. <https://doi.org/10.2307/1411>
- Fontanier C., Jorissen F. J., Licari L., Alexandre A., Anschutz P., Carbonel P. (2002). Live Benthic Foraminiferal Faunas From the Bay of Biscay: Faunal Density, Composition, and Microhabitats. *Deep. Res. Part I Oceanogr. Res. Pap.* 49, 751–785. [https://doi.org/10.1016/S0967-0637\(01\)00078-4](https://doi.org/10.1016/S0967-0637(01)00078-4)
- Gaye B., Böll A., Segschneider J., Burdanowitz N., Emeis K. C., Ramaswamy V., et al. (2018). Glacial-Interglacial Changes and Holocene Variations in Arabian Sea Denitrification. *Biogeosciences* 15, 507–527. <https://doi.org/10.5194/bg-15-507-2018>
- Goineau A., Gooday A. J. (2017). Novel Benthic Foraminifera are Abundant and Diverse in an Area of the Abyssal Equatorial Pacific Licensed for Polymetallic Nodule Exploration. *Sci. Rep.* 7, 1–15. <https://doi.org/10.1038/srep45288>
- Gooday A. J. (1988). A Response by Benthic Foraminifera to the Deposition of Phytodetritus in the Deep Sea. *Nature* 332, 70–73. <https://doi.org/10.1038/332070a0>
- Gooday A. J. (1993). Deep-Sea Benthic Foraminiferal Species Which Exploit Phytodetritus: Characteristic Features and Controls on Distribution. *Mar. Micropaleontol.* 22, 187–205. [https://doi.org/10.1016/0377-8398\(93\)90043-W](https://doi.org/10.1016/0377-8398(93)90043-W)
- Gooday A. J. (1994). The Biology of Deep-Sea Foraminifera: A Review of Some Advances and Their Applications in Paleoceanography. *PALAIOS* 9, 14–31. <https://doi.org/10.2307/3515075>
- Gooday A. J. (1996). Epifaunal and Shallow Infaunal Foraminiferal Communities at Three Abyssal NE Atlantic Sites Subject to Differing Phytodetritus Input Regimes. *Deep. Res. Part I Oceanogr. Res. Pap.* 43, 1395–1421. [https://doi.org/10.1016/S0967-0637\(96\)00072-6](https://doi.org/10.1016/S0967-0637(96)00072-6)
- Gooday A. J. (2003). Benthic Foraminifera (Protista) as Tools in Deep-Water Palaeoceanography: Environmental Influences on Faunal Characteristics. *Adv. Mar. Biol.* 46, 1–90. [https://doi.org/10.1016/S0065-2881\(03\)46002-1](https://doi.org/10.1016/S0065-2881(03)46002-1)

- Gooday A. J., Hughes J. A. (2002). Foraminifera Associated With Phytodetritus Deposits at a Bathyal Site in the Northern Rockall Trough (NE Atlantic): Seasonal Contrasts and a Comparison of Stained and Dead Assemblages. *Mar. Micropaleontol.* 46, 83–110. [https://doi.org/10.1016/S0377-8398\(02\)00050-6](https://doi.org/10.1016/S0377-8398(02)00050-6)
- Gooday A. J., Jorissen F. J. (2012). Benthic Foraminiferal Biogeography: Controls on Global Distribution Patterns in Deep-Water Settings. *Ann. Rev. Mar. Sci.* 4, 237–262. <https://doi.org/10.1146/annurev-marine-120709-142737>
- Gooday A. J., Rathburn A. E. (1999). Temporal Variability in Living Deep-Sea Benthic Foraminifera: A Review. *Earth Sci. Rev.* 46, 187–212. [https://doi.org/10.1016/S0012-8252\(99\)00010-0](https://doi.org/10.1016/S0012-8252(99)00010-0)
- Hammer Ø., Harper D. A. T., Ryan P. D. (2001). Past: Paleontological Statistics Software Package for Education and Data Analysis. *Palaeontol. Electron.* 4, 9. [https://palaeo-electronica.org/2001\\_1/past/issue1\\_01.htm](https://palaeo-electronica.org/2001_1/past/issue1_01.htm)
- Jorissen F. J., de Stigter H. C., Widmark J. G. V. (1995). A Conceptual Model Explaining Benthic Foraminiferal Microhabitats. *Mar. Micropaleontol.* 26, 3–15. [https://doi.org/10.1016/0377-8398\(95\)00047-X](https://doi.org/10.1016/0377-8398(95)00047-X)
- Jorissen F. J., Fontanier C., Thomas E. (2007). “Paleoceanographical Proxies Based on Deep-Sea Benthic Foraminiferal Assemblage Characteristics,” in *Proxies in Late Cenozoic Paleoceanography: Pt. 2: Biological Tracers and Biomarkers*. Eds. Hillaire-Marcel C., de Vernal A., (Amsterdam, The Netherlands: Elsevier) 263–325. [https://doi.org/10.1016/S1572-5480\(07\)01012-3](https://doi.org/10.1016/S1572-5480(07)01012-3)
- Knoppers B., Ekau W., Figueiredo A. G. (1999). The Coast and Shelf of East and Northeast Brazil and Material Transport. *Geo-Marine. Lett.* 19, 171–178. <https://doi.org/10.1007/s003670050106>
- Kurbjewit F., Schmiedl G., Schiebel R., Hemleben C., Pfannkuche O., Wallmann K., et al. (2000). Distribution, Biomass and Diversity of Benthic Foraminifera in Relation to Sediment Geochemistry in the Arabian Sea. *Deep. Res. Part II Top. Stud. Oceanogr.* 47, 2913–2955. [https://doi.org/10.1016/S0967-0645\(00\)00053-9](https://doi.org/10.1016/S0967-0645(00)00053-9)
- Lambshhead P. J. D., Gooday A. J. (1990). The Impact of Seasonally Deposited Phytodetritus on Epifaunal and Shallow Infaunal Benthic Foraminiferal Populations in the Bathyal Northeast Atlantic: The Assemblage Response. *Deep Sea Res. Part A Oceanogr. Res. Pap.* 37:1263-1283. [https://doi.org/10.1016/0198-0149\(90\)90042-T](https://doi.org/10.1016/0198-0149(90)90042-T)
- Legendre L., Legendre P. (1998). *Numerical Ecology 2nd ed Volume 24* (Amsterdam, The Netherlands: Elsevier Science).
- Linke P., Lutze G. F. (1993). Microhabitat Preferences of Benthic Foraminifera – a Static Concept or a Dynamic Adaptation to Optimize Food Acquisition? *Mar. Micropaleontol.* 20, 215–234. [https://doi.org/10.1016/0377-8398\(93\)90034-U](https://doi.org/10.1016/0377-8398(93)90034-U)
- Lohmann G. P. (1978). Abyssal Benthonic Foraminifera as Hydrographic Indicators in the Western South Atlantic Ocean. *J. Foraminifer. Res.* 8, 6–34. <https://doi.org/10.2113/gsfpr.8.1.6>

- Lutze G. F., Thiel H. (1989). Epibenthic Foraminifera From Elevated Microhabitats; *Cibicidoides wuellerstorfi* and *Planulina Ariminensis*. J. Foraminifer. Res. 19, 153–158. <https://doi.org/10.2113/gsjfr.19.2.153>
- Mackensen A. (1987). Benthische Foraminiferen Auf Dem Island-Schottland Rücken: Umwelt-Anzeiger an Der Grenze Zweier Ozeanischer Räume. Paläontologische Zeitschrift 61, 149–179. <https://doi.org/10.1007/BF02985902>
- Mackensen A., Grobe H., Kuhn G., Fütterer D. K. (1990). Benthic Foraminiferal Assemblages From the Eastern Weddell Sea Between 68 and 73°S: Distribution, Ecology and Fossilization Potential. Mar. Micropaleontol. 16, 241–283. [https://doi.org/10.1016/0377-8398\(90\)90006-8](https://doi.org/10.1016/0377-8398(90)90006-8)
- Mackensen A., Schmiedl G., Harloff J., Giese M. (1995). Deep-Sea Foraminifera in the South Atlantic Ocean: Ecology and Assemblage Generation. Micropaleontology 41, 342–358. <https://doi.org/10.2307/1485808>
- Margreth S., Rüggeberg A., Spezzaferri S. (2009). Benthic Foraminifera as Bioindicator for Cold-Water Coral Reef Ecosystems Along the Irish Margin. Deep. Res. Part I Oceanogr. Res. Pap. 56, 2216–2234. <https://doi.org/10.1016/j.dsr.2009.07.009>
- Martins L. R., Coutinho P. N. (1981). The Brazilian Continental Margin. Earth Sci. Rev. 17, 87–107. [https://doi.org/10.1016/0012-8252\(81\)90007-6](https://doi.org/10.1016/0012-8252(81)90007-6)
- Mémery L., Arhan M., Alvarez-Salgado X. A., Messias M. J., Mercier H., Castro C. G., et al. (2000). The Water Masses Along the Western Boundary of the South and Equatorial Atlantic. Prog. Oceanogr. 47, 69–98. [https://doi.org/10.1016/S0079-6611\(00\)00032-X](https://doi.org/10.1016/S0079-6611(00)00032-X)
- Mendes I., Dias J. A., Schönfeld J., Ferreira O. (2012). Distribution of Living Benthic Foraminifera on the Northern Gulf of Cadiz Continental Shelf. J. Foraminifer. Res. 42, 18–38. <https://doi.org/10.2113/gsjfr.42.1.18>
- Montagu G., (1803). Testacea Britannica, or Natural History of British Shells, Marine, Land and Fresh Water, Including the Most Minute: Systematically Arranged and Embellished with Figures. J. White, London, England, 606 pp. <https://doi.org/10.5962/bhl.title.33927>
- Murray J. W. (2006). Ecology and Applications of Benthic Foraminifera. Cambridge University Press, Cambridge. 426 pp.
- Nagel B., Gaye B., Kodina L. A., Lahajnar N. (2009). Stable Carbon and Nitrogen Isotopes as Indicators for Organic Matter Sources in the Kara Sea. Mar. Geol. 266, 42–51. <https://doi.org/10.1016/j.margeo.2009.07.010>
- Oliveira-Silva P., Fernandes Barbosa C., Soares-Gomes A. (2005). Distribution of Macrobenthic Foraminifera on Brazilian Continental Margin Between 18°S – 23°S. Rev. Bras. Geociências. 35, 209–216. <https://doi.org/10.25249/0375-7536.2005352209216>
- Paliy O., Shankar V. (2016). Application of Multivariate Statistical Techniques in Microbial Ecology. Mol. Ecol. 25, 1032–1057. <https://doi.org/10.1111/mec.13536>

- Parr W. J. (1932). Victorian and South Australian Shallow-Water Foraminifera. Part I. Proceedings of the Royal Society of Victoria 44, 1–14.
- Peet R. K. (1974). The Measurement of Species Diversity. *Annu. Rev. Ecol. Syst.* 5, 285–307. <https://doi.org/10.2110/scn.79.06.0003>
- Peterson R. G., Stramma L. (1991). Upper-Level Circulation in the South Atlantic Ocean. *Prog. Oceanogr.* 26, 1–73. [https://doi.org/10.1016/0079-6611\(91\)90006-8](https://doi.org/10.1016/0079-6611(91)90006-8)
- Raddatz J., Titschack J., Frank N., Freiwald A., Conforti A., Osborne A., et al. (2020). *Solenosmilia variabilis*-Bearing Cold-Water Coral Mounds Off Brazil. *Coral. Reefs* 39, 69–83. <https://doi.org/10.1007/s00338-019-01882-w>
- Ramette A. (2007). Multivariate Analyses in Microbial Ecology. *FEMS Microbiol. Ecol.* 62, 142–160. <https://doi.org/10.1111/j.1574-6941.2007.00375.x>
- Rasmussen T. L., Thomsen E. (2017). Ecology of Deep-Sea Benthic Foraminifera in the North Atlantic During the Last Glaciation: Food or Temperature Control. *Palaeogeogr. Palaeoclimatol. Palaeoecol.* 472, 15–32. <https://doi.org/10.1016/j.palaeo.2017.02.012>
- Rebouças R. C., Dominguez J. M. L., da Silva Pinto Bittencourt A. C. (2011). Provenance, Transport and Composition of Dendê Coast Beach Sands in Bahia, Central Coast of Brazil. *Braz. J. Oceanogr.* 59, 339–347. <https://doi.org/10.1590/S1679-87592011000400004>
- Rumolo P., Barra M., Gherardi S., Marsella E., Sprovieri M. (2011). Stable Isotopes and C/N Ratios in Marine Sediments as a Tool for Discriminating Anthropogenic Impact. *J. Environ. Monit.* 13, 3399–3408. <https://doi.org/10.1039/c1em10568j>
- Ryan W.B.F., Carbotte S.M., Coplan J.O., O’Hara S., Melkonian A, Arko R, et al. (2009). Global Multi-Resolution Topography Synthesis. *Geochemistry, Geophys. Geosystems* 10, 1–9. <https://doi.org/10.1029/2008GC002332>
- Schmiedl G., Mackensen A., Müller P. J. (1997). Recent Benthic Foraminifera From the Eastern South Atlantic Ocean: Dependence on Food Supply and Water Masses. *Mar. Micropaleontol.* 32, 249–287. [https://doi.org/10.1016/S0377-8398\(97\)00023-6](https://doi.org/10.1016/S0377-8398(97)00023-6)
- Schönfeld J. (1997). The Impact of the Mediterranean Outflow Water (MOW) on Benthic Foraminiferal Assemblages and Surface Sediments at the Southern Portuguese Continental Margin. *Mar. Micropaleontol.* 29, 21–236. [https://doi.org/10.1016/S0377-8398\(96\)00050-3](https://doi.org/10.1016/S0377-8398(96)00050-3)
- Schönfeld J. (2002a). Recent Benthic Foraminiferal Assemblages in Deep High-Energy Environments From the Gulf of Cadiz (Spain). *Mar. Micropaleontol.* 44, 141–162. [https://doi.org/10.1016/S0377-8398\(01\)00039-1](https://doi.org/10.1016/S0377-8398(01)00039-1)
- Schönfeld J. (2002b). A New Benthic Foraminiferal Proxy for Near-Bottom Current Velocities in the Gulf of Cadiz, Northeastern Atlantic Ocean. *Deep. Res. I* 49, 1853–1875. [https://doi.org/10.1016/S0967-0637\(02\)00088-2](https://doi.org/10.1016/S0967-0637(02)00088-2)

- Schönfeld J., Zahn R. (2000). Late Glacial to Holocene History of the Mediterranean Outflow. Evidence From Benthic Foraminiferal Assemblages and Stable Isotopes at the Portuguese Margin. *Palaeogeogr. Palaeoclimatol. Palaeoecol.* 159, 85–111. [https://doi.org/10.1016/S0031-0182\(00\)00035-3](https://doi.org/10.1016/S0031-0182(00)00035-3)
- Sen Gupta B. K. (Ed.) (2002). *Modern Foraminifera* (Dordrecht, The Netherlands: Kluwer Academic Publishers), 384.
- Shannon C. E, Weaver W. (1949). *The Mathematical Theory of Communication*. University of Illinois Press, Urbana, pp. 144.
- Stramma L., England M. (1999). On the Water Masses and Mean Circulation of the South Atlantic Ocean. *Geophys. Res.* 104, 20,863–20,883. <https://doi.org/10.1029/1999JC900139>
- Stramma L., Fischer J., Reppin J. (1995). The North Brazil Undercurrent. *Deep. Res. Part I* 42, 773–795. [https://doi.org/10.1016/0967-0637\(95\)00014-W](https://doi.org/10.1016/0967-0637(95)00014-W)
- Summerhayes C. P., Fainstein R., Ellis J. P. (1976). Continental Margin Off Sergipe and Alagoas, Northeastern Brazil: A Reconnaissance Geophysical Study of Morphology and Structure. *Mar. Geol.* 20, 345–361. [https://doi.org/10.1016/0025-3227\(76\)90112-2](https://doi.org/10.1016/0025-3227(76)90112-2)
- ter Braak C. J. F., Verdonschot P. F. M. (1995). Canonical Correspondence Analysis and Related Multivariate Methods in Aquatic Ecology. *Aquat. Sci.* 57, 255–289. <https://doi.org/10.1007/BF00877430>
- Viana A. R. (2001). Seismic Expression of Shallow- to Deep-Water Contourites Along the South-Eastern Brazilian Margin. *Mar. Geophys. Res.* 22, 509–521. <https://doi.org/10.1023/A:1016307918182>
- Viana A. R., Almeida W. Jr., Almeida C. W. (2002). Upper Slope Sands: Late Quaternary Shallow-Water Sandy Contourites of Campos Basin, SW Atlantic Margin. *Geol. Soc London. Mem.* 22, 261–270. <https://doi.org/10.1144/GSL.MEM.2002.022.01.19>
- Viana A. R., Faugères J. C., Kowsmann R. O., Lima J. A. M., Caddah L. F. G., Rizzo J. G. (1998). Hydrology, Morphology and Sedimentology of the Campos Continental Margin, Offshore Brazil. *Sediment. Geol.* 115, 133–157. [https://doi.org/10.1016/S0037-0738\(97\)00090-0](https://doi.org/10.1016/S0037-0738(97)00090-0)
- Vieira F. S., Koutsoukos E. A. M., Machado A. J., Dantas M. A. T. (2015). Biofaciological Zonation of Benthic Foraminifera of the Continental Shelf of Campos Basin, SE Brazil. *Quat. Int.* 377, 18–27. <https://doi.org/10.1016/j.quaint.2014.12.020>
- Williamson W.C., (1858). *On the Recent Foraminifera of Great Britain*. The Ray Society, London. 1–107.
- Yamashita C., Mello e Sousa S. H., Vicente T. M., Martins M. V., Nagai R. H., Frontalini F., et al. (2018). Environmental Controls on the Distribution of Living (Stained) Benthic Foraminifera on the Continental Slope in the Campos Basin Area (SW Atlantic). *J. Mar. Syst.* 181, 37–52. <https://doi.org/10.1016/j.imarsys.2018.01.010>

Yamashita C., Omachi C., Santarosa A. C. A., Iwai F. S., Araujo B. D., Disaró S. T., et al. (2020). Living Benthic Foraminifera of Santos Continental Shelf, Southeastern Brazilian Continental Margin (SW Atlantic): Chlorophyll-a and Particulate Organic Matter Approach. *J. Sediment. Environ.* 5, 17–34. <https://doi.org/10.1007/s43217-019-00001-7>

**Citation:** Saupe, A., Schmidt, J., Petersen, J., Bahr, A., Dias, B. B., Albuquerque, A. L. S., Díaz Ramos, R. A., and Grunert, P. (2022): Controlling Parameters of Benthic Deep-Sea Foraminiferal Biogeography at the Brazilian Continental Margin (11-22°S). *Front. Mar. Sci.* 9:901224. doi: [10.3389/fmars.2022.901224](https://doi.org/10.3389/fmars.2022.901224)

**Received:** 21 March 2022; **Accepted:** 01 June 2022.

**Published:** 20 July 2022.

**Edited by:** Jeroen Ingels, Florida State University, United States

**Reviewed by:** Andrew John Gooday, National Oceanography Centre, Southampton, United Kingdom; Michael Martínez-Colón, Florida Agricultural and Mechanical University, United States; Bryan O' Malley, Eckerd College, United States.

**\*Correspondence:** Anna Saupe, [anna.saupe@uni-koeln.de](mailto:anna.saupe@uni-koeln.de)



## 3.2 High Latitude Contourite Drift Systems

this chapter was published by  
Saupe et al. (2023) in *Palaeogeography Palaeoclimatology Palaeoecology*



## Benthic Foraminifera in High Latitude Contourite Drift Systems (North Atlantic: Björn, Gardar and Eirik Drifts)

Anna Saupe <sup>1\*</sup>, Johanna Schmidt <sup>1</sup>, Jassin Petersen <sup>1</sup>, André Bahr <sup>2</sup> and Patrick Grunert <sup>1</sup>

<sup>1</sup> Institute of Geology and Mineralogy, University of Cologne, Cologne, Germany, <sup>2</sup> Institute of Earth Sciences, Heidelberg University, Heidelberg, Germany

\*Correspondence: Anna Saupe ([anna.saupe@uni-koeln.de](mailto:anna.saupe@uni-koeln.de))

### Abstract

Benthic foraminifera colonize a wide range of marine environments including contourite drift systems. Contourites form elongated sedimentary bodies deposited under persistent contour-parallel bottom currents, and certain suspension-feeding foraminifera benefit from the entrained nutrient load. Their distribution patterns have been shown to be highly valuable for reconstructing ocean circulation at mid-latitudes. However, comparable faunal studies from the high-latitude North Atlantic, a crucial region for global ocean circulation and the widespread deposition of contourite drifts, are missing. This study examines foraminiferal faunas > 250 µm from surface samples of the Björn and Gardar drifts in the Iceland Basin and the Eirik Drift south of Greenland. It serves as baseline for understanding the biogeographic patterns of benthic foraminifera from high latitude contourites.

The results show that four types of suspension-feeding species characterize different hydrodynamic environments. Bottom currents < 3 cm s<sup>-1</sup> at the Björn Drift sustain assemblages rich in the finely branching, erect species *Saccorhiza ramosa* and *Rhizammina algaeformis*, which capture food particles with a pseudopodial net. The northern Gardar Drift displays intermediate flow velocities up to 10 cm s<sup>-1</sup> and is determined by tubular branching and facultative suspension-feeding species such as *Rhabdammina abyssorum*. Assemblages with abundant *Rhabdammina abyssorum* and *Hoeglundina elegans* colonize the southern detached and finer grained Gardar Drift. The Eirik Drift of Greenland with flow velocities of 12 to 22 cm s<sup>-1</sup> displays a fauna different from the contourites of the Iceland Basin. Assemblages with attached *Cibicidoides wuellerstorfi* and *Heterolepa broeckhiana* largely determine the benthic community. Also attached species, but composed primarily of *Cibicides lobatulus*, *Cibicides refulgens*, and *Cibicidoides pachyderma*, settle at the Greenland continental margin in high energy areas with velocities up to 40 cm s<sup>-1</sup>.

**Keywords:** Björn Drift, Gardar Drift, Bottom currents, Suspension feeders, Ocean circulation, Distribution patterns

# 1 Introduction

Benthic foraminifera form a diverse group of unicellular, test-bearing protists that colonize a wide range of marine environments (e.g. Murray, 2006). They exhibit various trophic strategies, including epifaunal suspension-feeding (Schönfeld et al., 2012). To ingest nutrients, active and passive suspension feeding foraminifera capture seston, i.e., suspended matter such as bacteria, organic detritus, microalgae, and sediment particles (Wildish and Kristmanson, 1997). The seston load carried by bottom currents is particularly important for passive suspension feeders, including many epifaunal foraminiferal species (Wildish and Kristmanson, 1997; Gili and Coma, 1998). They are trapping seston by using their pseudopodial network, which also helps them to attach to elevated substrates at the sea floor and to stabilize themselves within the current (Murray, 2006). The interplay of bottom current intensity and carried seston load controls abundance, diversity, and morphology of suspension-feeding foraminiferal communities (Gili and Coma, 1998; Jorissen et al., 2007).

The ability of certain epibenthic foraminifera to colonize areas of increased flow velocities make them highly valuable for reconstructing hydrodynamic conditions at the sea floor and thus ocean circulation (Murray, 2006; Gooday and Jorissen, 2012). In contourite drift systems (CDS) – sediments deposited under the influence of sustained bottom currents – suspension-feeding foraminiferal species encounter optimal living conditions (Jorissen et al., 2007; Knutz, 2008). Extensive studies of benthic foraminifera in the CDS along the continental margin of Iberian Peninsula have demonstrated the relationship between discrete faunal distribution patterns, gradients of bottom current strength, and nutrient load (Mackensen, 1987; Lutze and Altenbach, 1988; Lutze and Thiel, 1989; Linke and Lutze, 1993; Schönfeld, 1997, 2002a, 2002b; Rasmussen et al., 2002; Diz et al., 2004; Jorissen et al., 2007; Rogerson et al., 2011). Some researchers have already demonstrated their applicability as a proxy for reconstructing water mass exchange between the Mediterranean and the Atlantic Ocean (Schönfeld and Zahn, 2000; Singh et al., 2015; Guo et al., 2017). Beyond the Iberian Margin, however, foraminifera from contourite deposits have so far remained largely unexplored (Rebesco et al., 2014).

CDS are particularly prevalent in the North Atlantic Ocean north of 50°N as a result of the meridional overturning circulation (e.g., Stow and Holbrook, 1984; Faugères et al., 1993; Rebesco et al., 2014). As warm and saline surface waters cool down in the Nordic Seas and return as deep-water currents into the North Atlantic, they favour the formation of extensive CDSs by contour-parallel bottom currents (Rebesco et al., 2014; Uenzelmann-Neben and Gruetzner, 2018). Enhanced sediment accumulation rates potentially make high-latitude CDSs unique and highly valuable archives to constrain the role of Atlantic meridional overturning circulation (AMOC) in the ocean-climate system (e.g., Faugères et al., 1993; Knutz, 2008; Stow et al., 2013; Müller-Michaelis and Uenzelmann-Neben, 2014; de Castro et al., 2021). However, due to the lack of knowledge on distribution patterns and adaptive strategies of suspension feeding foraminifera in CDSs north of 50°N, the full potential of these palaeoceanographic archives remains untapped (Rebesco et al., 2014).

In this study, distribution patterns of benthic foraminiferal faunas along a hydrodynamic gradient from the Björn and Gardar drifts in the Iceland Basin (52-63 °N) and the Eirik Drift south of Greenland

(57-59 °N) will be documented for the first time. Specific focus is given to the response of suspension-feeding foraminifera to different hydrodynamic regimes.

## 2 Geographic and Oceanographic Setting

Deep-water masses and bottom currents, such as the Iceland Scotland and Denmark Strait Overflow Waters (ISOW; DSOW), the Labrador Sea Water (LSW) and Lower Deep Water (LDW), as well as such as the Deep Western Boundary Current (DWBC), formed by the Atlantic Meridional Overturning Circulation (AMOC), favour contourite deposition in the North Atlantic Ocean (Faugères et al., 1999). Sustained and along-slope contour currents ablate, transport and deposit fine-grained particles, resulting in elongated sediment bodies (Heezen and Hollister, 1964; Knutz, 2008; Rebesco et al., 2014).

The contourite drift system (CDS) of the Iceland Basin is located between the Reykjanes Ridge to the West and the Hatton and Rockall Bank to the East and comprises several drift bodies ([Figure 1](#)). The Björn Drift (60-63°N, 20-25°W) extends over 300 km from northeast to southwest and covers water depths between 1000 and 2000 m. It is separated from the Reykjanes Ridge by a sediment-filled channel (Bianchi and McCave, 2000). To the southwest, the Björnsson Drift represents a former extension of the Björn Drift, presumably separated by turbidity currents (Bianchi and McCave, 2000). An approximately 100 km wide trough separates the Björn Drift on its south-eastern flank from the north-western end of the Gardar Drift (Bianchi and McCave, 2000). The Gardar Drift (52-61°N, 18-32°W) extends over a length of 1100 km southwards close to the Charlie-Gibbs Fracture Zone in water depths between 1400 to 3000 m (Bianchi and McCave, 2000). The elongated drift body is subdivided into an attached northern and a detached southern part. A deep channel delimits the Gardar Drift on its eastern side (Parnell-Turner et al., 2015).

Contourite deposition in the Iceland Basin is linked to the activity of the southward-flowing LSW and underlying ISOW (Bianchi and McCave, 2000). The LSW, being formed in the Labrador and Irminger seas, spreads throughout the northern Atlantic (Hunter et al., 2007a; Parnell-Turner et al., 2015). It reaches the Björn Drift from the Northeast after passing the Rockall Trough and as strongly modified water mass typically showing salinities < 34.9 and temperatures of approx. 3.4 °C (Talley and McCartney, 1982; Schmitz and McCartney, 1993; Van Aken and Becker, 1996; Holliday et al., 2000; Sayago-Gil et al., 2010). In the Iceland Basin, the LSW forms a low-velocity layer at intermediate depths between 700-1500 m with maximum flow speeds of 3.1 cm s<sup>-1</sup> (Van Aken and De Boer, 1995; Hunter et al., 2007a).

In the Norwegian-Greenland Sea, North Atlantic Deep Water (NADW) develops as a result of cooling and sinking of warm saline surface waters (Kuhlbrodt et al., 2007; Müller-Michaelis and Uenzelmann-Neben, 2014; Uenzelmann-Neben and Gruetzner, 2018). As NADW passes the Iceland-Scotland Ridge, it partly mixes with shallower waters and forms the homogeneous ISOW, occurring at depths between 1400-3200 m (Van Aken and De Boer, 1995; Bianchi and McCave, 2000; Hunter et al., 2007a; Kuhlbrodt et al., 2007). Temperatures of 2.5 °C and salinities of 34.98 characterize the ISOW in the Iceland Basin with fastest flow velocities of nearly 10 cm s<sup>-1</sup> (Van Aken and Becker, 1996; Bianchi and McCave, 2000).

A large part of NADW, however, spreads southward crossing the Charlie Gibbs Fracture Zone and gradually passes the Mid-Atlantic Ridge, thus north of the Azores a strong NADW signal is measurable (Sarnthein et al., 1994).

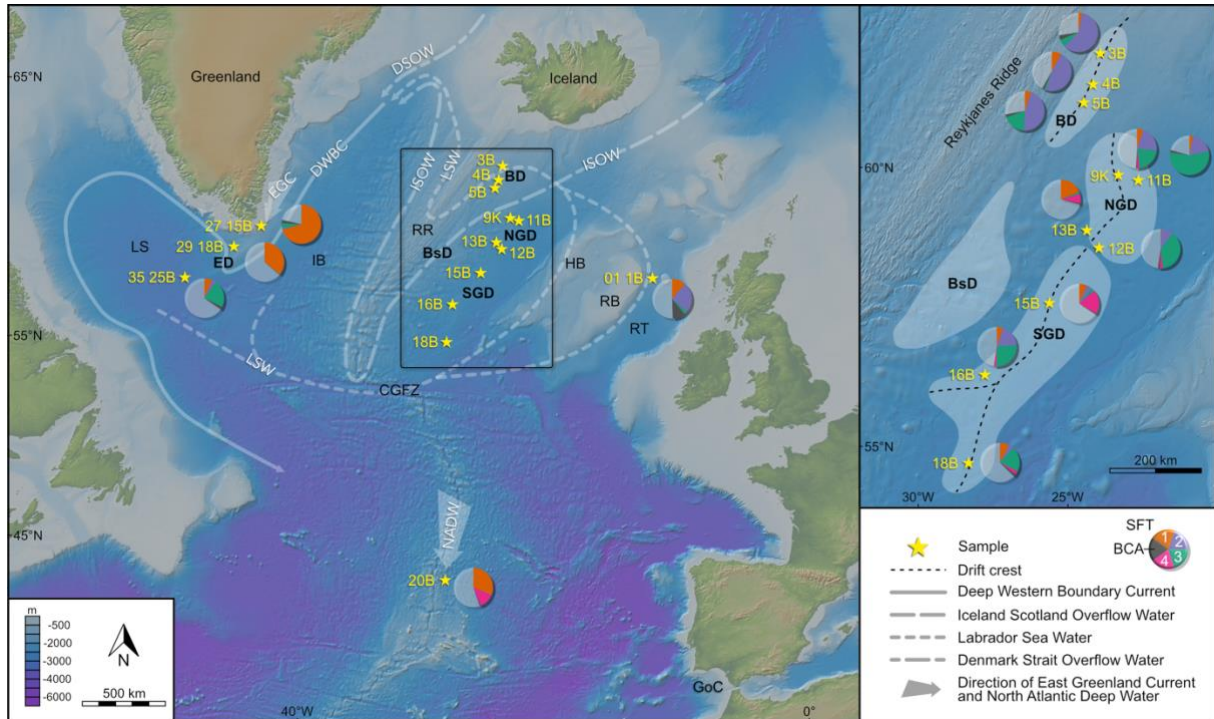


**Figure 1** | General bathymetric map of the Iceland Basin showing locations of the investigated sample sites and contourite drifts. Yellow stars indicate the sample sites. Grey lines represent the water masses, dashed black lines the drift crest. The pie charts show the proportion of the four types of suspension feeding foraminifera (SFT 1-4) and bottom current associated taxa (BCA), within the total benthic foraminiferal assemblage. CGFZ=Charlie Gibbs Fracture Zone, GoC=Gulf of Cadiz, HB=Hatton Bank, IB=Irminger Basin, LS=Labrador Sea, RB=Rockall Bank, RR=Reykjanes Ridge, RT=Rockall Trough, DSOW=Denmark Strait Overflow Water, DWBC=Deep Western Boundary Current, EGC=East Greenland Current, ISOW=Iceland Scotland Overflow Water, LSW=Labrador Sea Water, NADW=North Atlantic Deep Water, BD=Björn Drift, BsD=Björnson Drift, ED=Eirik Drift, NGD=Northern attached Gardar Drift, SGD=Southern detached Gardar Drift. Location and outline of the drifts are based on Bianchi and McCave (2000); direction and paths of the different water masses are used after Hunter et al. (2007b). The map was created with GeoMapApp ([www.geomapp.org](http://www.geomapp.org), using the base map of Ryan et al., 2009).

ISOW and LSW circulate contour-parallel around Reykjanes Ridge into the Irminger Basin (Hunter et al., 2007a), while DSOW enters herein after passing the Denmark Strait west of Iceland. (Hunter et al., 2007a; Parnell-Turner et al., 2015; Uenzelmann-Neben and Gruetzner, 2018). ISOW and DSOW entrain the LSW and LDW to form the Deep Western Boundary Current (DWBC) southeast of Greenland (Hunter et al., 2007a). The DWBC, with its core between 1900-3000 m (Clarke, 1984), significantly influences the Eirik Drift (57-59°N, 43-49°W), which is located south of Greenland on the eastern margin of the Labrador Sea (Clarke, 1984; Hunter et al., 2007b). This 360 km elongated detached sedimentary drift body extends from NE at 1500 m to SW at depths of about 3600 m (Hunter et al., 2007a; Müller-Michaelis et al., 2013). Water temperature, salinity, and current speed vary within the DWBC depending on its different components and their distance above the seafloor (Hunter et al.,

2007a). However, flow velocities are generally higher compared to the deep-water currents of the Iceland Basin, varying between 12 and 22 cm s<sup>-1</sup> (Hunter et al., 2007a).

In the surface to intermediate water depths, the western boundary current system encompasses the East Greenland Current (EGC), which influences the ocean floor to depths of 1000 m reaching velocities of up to 40 cm s<sup>-1</sup> (Holliday et al., 2007).

### 3 Material & Methods

#### 3.1 Stations and Sample Material

The samples of this study were taken during cruises 88 (NEAPACC) and 159 (RAPID) of the research vessel *Charles Darwin* (McCave, 1994, 2005). A total of 15 surface samples obtained from the upper 2 cm of sediment (14 from box cores, 1 from a kasten core) were selected for analysis of foraminiferal faunas. The bulk of the sample material originates from the Iceland Basin. Samples NEAP-3B, N-4B, and N-5B were retrieved along a bathymetric transect forming the Björn Drift between 1502 to 1825 m. Samples NEAP-9K, N-11B, N-12B, N-13B, N-15B, N-16B, and N-18B represent a NE-SW transect along the Gardar Drift at water depths of 2222 to 2879 m. Sample RAPID-27 15B is located on the Greenland Margin at 768 m, samples RAPID-29 18B and R-35 25B from the Eirik Drift cover a water depth range between 2145 and 3486 m (Table 1). Two samples from outside major CDS have also been included to provide references for assemblages outside the influence of major bottom currents. Sample RAPID-01 1B is located at 1805 m water depth in the Rockall Trough, sample NEAP-20B was retrieved north of the Azores at 2878 m water depth along the Mid-Atlantic Ridge. They resemble the depth range of the studied Atlantic fauna but are located outside any drift bodies.

**Table 1** | Position and hydrological parameters of the selected transects and sample sites of Meteor cruise M125.

Cruise	Sample	Drifts/Sites	Lat. N°	Long. W°	Water mass	Water depth (mbsl)	Temp. (°C)	Salinity (g/kg <sup>-1</sup> )	Sedimentation rates
CD 159	01 1B	Rockall Trough	57° 29.15'	12° 14.23'	LSW	1805	3.25	34.9	> 50 cm/ka
RAPID	27 15B	Greenl. cont. margin	59° 36.18'	42° 42.47'	EGC	768	7.25	35.16	> 50 cm/ka
	29 18B	Eirik	58° 48.01'	44° 51.82'	DWBC	2145	3.25	34.98	> 50 cm/ka
	35 25B	Eirik	57° 30.47'	48° 43.40'	DWBC	3486	-	-	> 50 cm/ka
	CD 88	3B	Björn	61° 52.10'	23° 56.48'	LSW	1502	3.2	34.89
NEAPACC	4B	Björn	61° 21.98'	24° 10.27'	LSW	1627	3.2	34.91	16 cm/ka
	5B	Björn	61° 04.50'	24° 31.76'	LSW, ISOW	1826	3.2	34.93	20 cm/ka
	9K	N Gardar	59° 53.19'	23° 19.81'	ISOW	2222	3	34.96	5 cm/ka
	11B	N Gardar	59° 47.49'	22° 39.24'	ISOW	2484	2.9	34.96	4 cm/ka
	12B	N Gardar	58° 38.36'	23° 59.63'	ISOW	2786	2.7	34.96	20 cm/ka
	13B	N Gardar	58° 56.41'	24° 24.02'	ISOW	2546	2.9	34.96	1 (?) cm/ka
	15B	S Gardar	57° 40.53'	25° 38.43'	ISOW	2703	2.7	34.96	7 cm/ka
	16B	S Gardar	56° 21.99'	27° 49.00'	ISOW	2847	2.7	34.96	44 cm/ka
	18B	S Gardar	54° 41.56'	28° 21.02'	ISOW	2879	2.7	34.96	20 cm/ka
	20B	N of Azores	42° 29.31'	28° 24.87'	NADW	2878	2.7	34.96	?

Hydrographical parameters water depth, temperature, salinity, and sedimentation rates were used after McCave (2005, 1994) and Bianchi and McCave (2000). Abbreviations mean LSW: Labrador Sea Water, EGC: East Greenland Current, DWBC: Deep Western Boundary Current, ISOW: Iceland Scotland Overflow Water, NADW: North Atlantic Deep Water.

### 3.2 Sedimentology

Grain size analysis of the siliciclastic fraction (11-27 g) was performed with a laser particle analyser Beckman Coulter LS13320 at the Institute of Geology and Mineralogy, University of Cologne.

The program Gradistat v 8.0 (Blott and Pye, 2001) was used to determine the sediment composition, i.e., mean grain size ( $\mu\text{m}$ ), and sediment description according to Folk and Ward (1957). Sortable silt mean sizes ( $\overline{SS}$ ; 10-63  $\mu\text{m}$ ) and its relative contribution (SS%) were calculated to obtain information about hydrodynamic conditions (McCave et al., 1995). For the Björn and Gardar Drifts, Bianchi and McCave (2000) already determined  $\overline{SS}$ -values using a Sedigraph. To ensure consistency within our data set, we measured all samples with the Coulter Multisizer (Bianchi et al., 1999). Following the concept of McCave and Hall (2006) the  $\overline{SS}$ -to-SS% ratio provides a unified variable for assessing and comparing flow regimes. The total organic carbon content (TOC) was determined with a vario MICRO cube CHNS-analyzer at the University of Cologne ([Table 2](#)).

Averaged Holocene sedimentation rates for each station were adopted from Bianchi and McCave (2000). The authors used records of down-core magnetic susceptibility as well as x-radiographs for detection of coarse, ice-rafted debris to determine sedimentation rates (Bianchi and McCave, 2000).

### 3.3 Benthic Foraminifera

10-20 g of sediment from each sample were wet sieved with demineralised water over a 63- $\mu\text{m}$  sieve and dried at 30°C. Demineralised water has a slightly lower pH than tap water, yet dissolution of foraminiferal tests when using demineralised water for the short duration of the sieving process can be excluded (Petro et al., 2018).

To maintain consistency with previous foraminiferal studies from areas with increased bottom current intensity, quantitative analyses were limited to the size fraction > 250  $\mu\text{m}$  (e.g., Schönfeld, 1997, 2002a, 2002b; Schönfeld and Altenbach, 2005; Schönfeld and Zahn, 2000; Schönfeld et al., 2011). Since smaller tests are more susceptible to current transport, they might be transported away from the study site and thus bias assemblage composition. By performing faunal analysis of the fraction > 250  $\mu\text{m}$ , we minimise a potential bias of remobilised foraminifera in our data set (Lohmann, 1978; Lutze and Coulbourn, 1984; Schönfeld, 1997). Support for this approach is provided by Bianchi and McCave (2000), who point out that even particles exceeding 125  $\mu\text{m}$  in size are actively resuspended within the strong current of the ISOW in the Iceland Basin Drift System. The size fraction 125-250  $\mu\text{m}$  was nonetheless screened to identify predominant species to ensure comparability of the data set to foraminiferal studies from regions north of 50°N outside CDS (e.g., Belanger and Streeter, 1980; Rasmussen et al., 2002; Lukashina and Bashirova, 2015).

Available sample material was limited. Previous studies propose that 300 specimens are needed to ensure statistical significance (e.g., Patterson and Fishbein, 1989; Schönfeld et al., 2012). To obtain census data of about 300 foraminifera, samples were picked completely where necessary or split with a riffle splitter for larger sample volumes. However, some samples did not contain 300 specimens, even after picking the entire sample. Fatela and Taborda (2002) suggest that counts of 100



foraminifera already provide an adequate statistical reliability with the main focus being on changes in more abundant species. This approach is justified when considering taxa occurring with at least 5 % in the assemblage (Fatela and Taborda, 2002). Hence, all statistical analyses were performed with a reduced data set (taxa occurring with > 5 % in a sample).

**Table 2** | Sediment analysis of surface samples (upper 2 cm).

Sample	Drifts/Sites	TOC (wt%)	Sediment description	Mean grain size ( $\mu\text{m}$ )	Sand (%)	Silt (%)	Clay (%)	Mud/sand	SS mean ( $\mu\text{m}$ )	SS%	FSR
01 1B	Rockall Trough	0.3	Medium Silt	21.0	8.2	73.4	18.3	11.2	25.0	39.9	-
27 15B	Greenl. cont. margin	0.6	Very Coarse Silt	79.2	47.3	42.1	10.5	1.1	36.4	51.2	-
29 18B	Eirik	0.3	Very Fine Sand	136.1	75.5	19.6	4.8	0.3	39.2	55.2	-
35 25B	Eirik	0.6	Medium Silt	22.4	8.9	70.2	20.8	10.2	26.6	41.4	-
3B	Björn	0.6	Fine Silt	14.7	2.5	77.6	19.9	38.9	22.8	42.6	2.0
4B	Björn	0.6	Fine Silt	14.6	2.3	78.4	19.3	43.3	22.4	43.8	4.5
5B	Björn	0.7	Fine Silt	13.9	2.0	78.3	19.8	49.5	21.3	42.6	5.0
9K	N Gardar	0.7	Medium Silt	22.7	6.9	76.6	16.5	13.5	26.2	51.4	7.0
11B	N Gardar	0.7	Fine Silt	17.9	4.6	76.1	19.3	20.8	24.2	44.4	7.0
12B	N Gardar	0.4	Medium Silt	16.1	2.7	78.8	18.6	36.4	23.9	46.9	6.0
13B	N Gardar	0.3	Medium Silt	37.2	13.7	69.4	16.9	6.3	24.9	46.7	6.0
15B	S Gardar	0.1	Fine Silt	11.5	1.9	74.5	23.6	51.4	20.0	32.8	-
16B	S Gardar	0.3	Very Fine Silt	6.9	0.8	68.2	31.0	123.0	17.0	16.6	2.0
18B	S Gardar	0.3	Very Fine Silt	7.9	2.4	65.0	32.7	41.4	18.4	13.7	1.5
20B	N of Azores	0.7	Fine Silt	19.2	8.2	67.8	24.0	11.2	26.2	29.8	-

Sediment description and composition were determined with Gradistat v 8.0 classified after Folk and Ward (1957); the flow speed rank (FSR) established by McCave and Tucholke (1986), is used according to measurements of Bianchi and McCave (2000) for the Iceland Basin Drift System.

Tubular and branching agglutinated foraminifera in the samples were almost always broken and their fragments were counted individually. This includes the following genera: *Bathysiphon*, *Hyperammina*, *Rhabdammina*, *Rhabdamminella* and *Saccorhiza*. Due to the richness in fragments, an overestimation of their contribution to the assemblages must be considered. To reduce such overestimation, without completely excluding tubular species, we follow the concept of Kurbjeweit et al. (2000), who propose combining three fragments to define one individual. Hence tubular agglutinated taxa were reduced by a factor of 3 for the analyses.

Abundances are referred to as follows: A taxon contributing < 5 % is rare, at 5-10 % it represents few occurrences, between 10-30 % it is abundant, and > 30 % it is considered dominant.

As samples from both cruises were not stained onboard, dead and living faunas are not distinguished here, and represent the total assemblage of the upper 2 cm of sediment. Many studies, such as Murray (2006) or Schönfeld et al. (2012), recommend the exclusive analysis of stained (live) assemblages to assess biogeographical distribution patterns. However, the examination of total (live and dead) assemblages may provide equally important biogeographic information for palaeoceanographic studies as they resemble fossil, time-averaged assemblages more closely. Based on averaged sedimentation rates after Bianchi and McCave (2000), the herein studied total assemblages probably represent a few decades to 500 years, time spans in which hydrographical conditions did not change significantly in the study area (Bianchi and McCave, 1999; Moffa-Sánchez et al., 2019; [Table 1](#)). Sortable silt records over the past 2000 years along the deep overflow waters passing the Iceland-Scotland Ridge as well as DWBC records show relatively constant flow velocities on centennial scales (Thornalley et al., 2013, 2018; Moffa-Sánchez et al., 2019). Thus, our sub-recent faunas represent a

time-averaged assemblage of putatively constant hydrographic conditions. Our time-averaged samples will allow a direct comparison between sortable silt and foraminiferal data and will facilitate interpretations in the fossil record (e.g., Haunold, 1999; Langer and Lipps, 2003; Fajemila et al., 2015).

Taxonomic identification is based on Cimerman and Langer (1991), Jones (1994), Schönfeld (2006) and Milker and Schmiedl (2012), using a ZEISS SteREO Discovery.V12 light microscope. For documentation and a detailed analysis of morphological features, images of selected specimens were taken with the Zeiss Sigma 300-VP scanning electron microscope at the Institute of Geology and Mineralogy, University of Cologne.

**Table 3** | Diversity of benthic foraminifera.

Sample	t	s	epifauna %	agg. %	hya. %	porc. %	SFT 1 %	SFT 2 %	SFT 3 %	SFT 4 %	BCA %	SFT+BCA total %
01 1B	38	441	51.4	54.5	26.1	19.4	13.9	10.4	1.4	0.0	12.5	38.1
27 15B	49	1819	92.8	5.1	86.8	8.1	72.9	0.4	1.6	0.0	2.8	77.7
29 18B	32	1017	47.7	1.5	95.6	2.9	35.8	0.0	0.1	0.0	0.2	36.1
35 25B	27	142	38.0	47.8	45.7	6.5	7.3	1.9	12.5	0.0	2.4	24.2
3B	26	131	63.7	66.4	21.5	12.1	5.4	35.0	4.5	0.0	6.7	51.6
4B	33	218	50.0	37.8	38.5	23.6	11.5	23.2	1.1	0.0	2.7	38.5
5B	37	308	64.7	68.3	23.9	7.8	8.3	33.4	10.0	0.0	3.6	55.4
9K	40	236	45.1	44.0	50.9	5.0	6.7	15.1	9.3	2.8	1.1	35.1
11B	29	330	69.0	70.1	21.4	8.5	5.6	17.7	34.4	0.6	3.4	61.7
12B	29	203	42.2	53.0	41.2	5.8	0.7	5.1	18.3	3.6	2.2	29.9
13B	37	216	41.4	26.9	58.1	15.0	19.2	0.2	0.5	7.5	0.9	28.3
15B	40	304	37.6	42.1	46.8	11.1	6.6	1.7	0.9	20.8	0.7	30.7
16B	22	101	46.0	44.5	49.8	5.7	7.1	9.0	12.8	2.8	0.0	31.8
18B	22	102	50.8	23.8	59.8	16.4	9.4	1.6	8.2	3.5	2.3	25.0
20B	45	353	75.2	25.6	56.4	17.9	30.5	0.2	0.1	12.8	0.9	44.4

Shown are absolute numbers of taxa (t) and specimens (s); proportion of epifaunal taxa within the total fauna; amount of different test types agglutinated, hyalin and porcelaneous; amount of every single Suspension Feeding Type (SFT 1–4%), the Bottom Current Associated (BCA %) species and the total of all SFT and BCA taxa (SFT + BCA total %).

Epi- and infaunal microhabitats were assigned based on available information from Schönfeld (1997), Kuhnt et al. (2000), Schönfeld and Zahn (2000), Sen Gupta (2002), Murray (2006), and Jorissen et al. (2007). Particular attention was paid to the suspension feeders, as they are potentially associated with bottom currents (e.g., Schönfeld, 1997). The majority of epibenthic species in the studied areas lead a suspension-feeding lifestyle, being beneficial under persistent bottom currents (Altenbach et al., 1987; Lutze and Altenbach, 1988; Linke, 1992; Linke and Lutze, 1993; Schönfeld, 1997, 2002b, 2002a; De Stigter et al., 1998). Herein, four different suspension feeding types (SFT) 1-4 and one bottom current associated (BCA) group were defined. Affiliation of a species with a SFT is based on its way of stabilizing itself on or in the sediment (attached, encrusted, anchored, interlocked with other individuals), and feeding strategy (obligate or facultative suspension feeding; for details on individual SFTs see [Table 3](#) and [Table 4](#)). Bottom current associated (BCA) species lack a rigorous epifaunal suspension-feeding lifestyle but have previously been connected to bottom currents (e.g., *Miliolinella subrotunda*; Altenbach et al., 1993; Linke and Lutze, 1993; Balestra et al., 2017).

**Table 4** | Suspension feeding types (SFT 1–4) and bottom current associated (BCA) taxa.

Suspension Feeding Type	Taxa	Reference
<b>SFT 1:</b> Attached, some on elevated substrates.	<i>Anomalinoidea globulosus</i> (Chapman & Parr, 1937)	Dubicka et al. (2015)
	<i>Cibicides lobatulus</i> (Walker & Jacob, 1798)	Mackensen et al. (1985); Mackensen (1987); Schönfeld (1997, 2002a, 2002b)
	<i>Cibicides mollis</i> Phleger & Parker	Schönfeld (1997); Schönfeld and Zahn (2000)
	<i>Cibicidoides pachyderma</i> (Rzehak, 1886)	Lutze and Thiel (1989); Schmiedl et al. (2000)
	<i>Cibicides refulgens</i> Montfort, 1808	Mackensen (1987); Schönfeld (1997, 2002a, 2002b)
	<i>Cibicidoides wuellerstorfi</i> (Schwager, 1866)	Lutze and Thiel (1989); Linke and Lutze (1993)
	<i>Discanomalina semipunctata</i> (Bailey, 1851)	Mackensen (1987); Schönfeld (1997, 2002a, 2002b)
	<i>Guttulina ovata</i> (d'Orbigny, 1846)	Schönfeld (2002a, 2002b)
	<i>Guttulina yabei</i> Cushman & Ozawa, 1929	Schönfeld (2002a, 2002b)
	<i>Hemisphaerammina bradyi</i> Loeblich & Tappan, 1957	Rodrigues et al. (2010)
	<i>Heterolepa broeckhiana</i> (Karrer, 1878)	Murray (2006)
	<i>Placopsilina confusa</i> Cushman, 1920	Schönfeld (2002a, 2002b)
	<i>Rupertina stabilis</i> (Wallich, 1877)	Altenbach et al. (1987); Mackensen (1987); Lutze and Altenbach (1988); Linke and Lutze (1993)
	<i>Saccamina sphaerica</i> Brady, 1871	Schönfeld (1997, 2002a, 2002b)
	<i>Tritaxis fusca</i> (Williamson, 1858)	Schönfeld (1997, 2002a, 2002b); Schönfeld and Zahn (2000)
<i>Trochammina inflata</i> (Montagu, 1808)	Gooday et al. (1992); Schönfeld (1997, 2002a, 2002b)	
<b>SFT 2:</b> Tubular branching with protoplasm net, sometimes interlocked.	<i>Lituotuba lituiformis</i> (Brady, 1879)	Murray, (2006); Wisshak and Rüggeberg (2006)
	<i>Rhabdammina cylindrica</i> Brady, 1882	Kaminski et al. (2008); Kender and Kaminski (2017)
	<i>Rhizammina algaeformis</i> Brady, 1879	Cartwright et al. (1989)
	<i>Saccorhiza ramosa</i> (Brady, 1879)	Altenbach et al. (1988)
	<i>Tolypammina vagans</i> (Brady, 1879).	Schröder et al. (1988); Kender and Kaminski (2017)
<b>SFT 3:</b> Facultative suspension feeders, also able to feed on detritus/grazing.	<i>Tolypammina vagans</i> (Brady, 1879)	Gooday et al. (1992)
	<i>Bathysiphon</i> sp.	Gooday et al. (1992)
	<i>Hyperammina</i> sp. div.	Linke and Lutze (1993); Gooday (1996); Murray (2006)
	<i>Pelosina arborescens</i> Pearcey, 1914	Cedhagen (1993); Sen Gupta (2002)
	<i>Rhabdammina abyssorum</i> Sars in Carpenter, 1869	Linke (1992); Linke and Lutze (1993)
<b>SFT 4:</b> Tubularly encrusting on hard substrates.	<i>Ammolagena clavata</i> (Jones & Parker, 1860)	Gooday (1986); Schönfeld (2002a)
<b>BCA:</b> Bottom Current Associated; Non-suspension feeders, but connected to increased bottom currents.	<i>Globocassidulina subglobosa</i> (Brady, 1881)	Mackensen et al. (1995); Schmiedl et al. (1997); Rasmussen et al. (2002); Balestra et al. (2017)
	<i>Miliolinella subrotunda</i> (Montagu, 1803)	Altenbach et al. (1993); Linke and Lutze (1993); Balestra et al. (2017)
	<i>Trifarina angulosa</i> (Williamson, 1858)	Sejrup et al. (1981); Mackensen et al. (1985, 1995); Mackensen (1987); Harloff and Mackensen (1997); Rasmussen et al. (2002); Balestra et al. (2017)
	<i>Psammosphaera fusca</i> Schulze, 1875	Kaminski (1985); Schmiedl et al. (1997); Kuhnt et al. (2000); Kender and Kaminski (2017)
	<i>Psammosphaera parva</i> Flint, 1899	Kaminski (1985); Schmiedl et al. (1997); Hayward et al. (2010)

Taxa are sorted by their living position in the sediment (e.g., attached, encrusting, anchored, interlocked with other individuals), and their type of feeding (e.g., obligate or facultative suspension feeding). Taxonomic references are not included in the reference list.

### 3.4 Multivariate Statistical Analysis

Statistical analysis was conducted with the software PAST (version 4.02; Hammer et al., 2001). Hierarchical clustering was performed for faunal analysis, applying the UPGMA algorithm and Bray-Curtis similarity index (Ramette, 2007; Paliy and Shankar, 2016). Indeterminate taxa as well as taxa not exceeding 5% in at least one sample were not included in the statistical analyses, with the remainder representing 60 to 90% of the taxa per sample. A similarity percentage analysis (= SIMPER analysis; Bray-Curtis similarity) provides information on the contribution of each species to the dissimilarity between the identified clusters (Table 5).

A canonical correspondence analysis (CCA) was performed to assess the relationship between foraminiferal taxa and environmental parameters. The following variables were considered as environmental factors: salinity, temperature, TOC contents in the sediments,  $\overline{SS}$  mean size, and water depth. Interpretation of explanatory variables becomes increasingly problematic when they are interrelated or their number increases (Ramette, 2007; Paliy and Shankar, 2016). Therefore, only three independent parameters were chosen, and the number of explanatory variables was kept low. Firstly, TOC values were included as they indicate deposited organic matter and can be linked to bottom nepheloid layers and thus to increased currents (Schönfeld, 1997). Secondly, the  $\overline{SS}$  mean size is used as flow velocity indicator (Manighetti and McCave, 1995; McCave and Hall, 2006; McCave et al., 2017), showing considerable variability over the data set. Water depth, as third parameter, is regarded as representative of different water masses that change with depth due to their different properties (Lee and Ellett, 1967; Pickart, 1992; Van Aken and De Boer, 1995; Hunter et al., 2007a; Uenzelmann-Neben and Gruetzner, 2018). Numerous influencing factors are combined here (e.g., temperature, salinity, oxygen), which individually show very little variability throughout the data set (Table 1). Water depth thus indicates interfaces between different water masses that affect hydrographic parameters. All three environmental parameters are linked directly or implicitly to bottom currents.

**Table 5** | SIMPER analysis (Bray-Curtis similarity index) based on clusters A-D given in Figure 4.

Taxon	Av. dissim	Contrib. %	Cumulative %	Cluster A	Cluster B	Cluster C	Cluster D	
<i>Hoeglundina elegans</i>	7.3	9.8	9.8	<b>19.6</b>	<b>15.5</b>	0.5	-	
<i>Cibicides wuellerstorfi</i>	4.9	6.5	16.3	<b>22.7</b>	5.5	9.3	1.4	
<i>Rhabdammina abyssorum</i>	4.4	5.9	22.3	0.1	<b>11.0</b>	1.3	1.4	
<i>Cibicides refulgens</i>	3.9	5.2	27.4	-	0.1	-	<b>34.8</b>	
<i>Sigmaloipsis schlumbergeri</i>	3.7	4.9	32.3	1.4	2.5	<b>13.3</b>	-	
<i>Saccorhiza ramosa</i>	3.3	4.4	36.7	-	3.0	<b>11.1</b>	0.4	
<i>Rhizammina algaeformis</i>	3.2	4.2	41.0	0.1	2.9	<b>10.7</b>	-	
<i>Cibicides lobatulus</i>	2.9	3.9	44.8	1.1	0.3	0.9	<b>23.1</b>	
<i>Ammolagena clavata</i>	2.8	3.7	48.5	6.4	4.6	-	-	
<i>Melonis pompilioides</i>	2.5	3.4	51.9	4.4	6.1	3.0	-	
<i>Pyrgo sp. div.</i>	2.1	2.8	54.7	4.7	6.1	3.6	1.1	
<i>Hormosina bacillaris</i>	1.7	2.2	56.9	-	3.9	-	-	
<i>Gyroidinoides soldanii</i>	1.6	2.2	59.1	4.4	1.5	1.8	9.6	
<i>Psammosphaera fusca</i>	1.5	2.0	61.1	-	1.8	5.2	0.1	
<i>Heterolepa broeckhiana</i>	1.5	1.9	63.0	7.1	-	-	-	
<i>Tolypammina vagans</i>	1.4	1.9	64.9	-	3.4	-	-	
<i>Paratrochammina challengerii</i>	1.4	1.9	66.8	1.1	0.9	4.9	-	
<i>Cibicides pachyderma</i>	1.4	1.8	68.7	-	-	-	<b>12.4</b>	
<i>Melonis affinis</i>	1.2	1.7	70.3	1.2	3.2	0.4	0.3	
			<b>group</b>	<b>A1</b>	<b>A2</b>	<b>B1</b>	<b>B2</b>	<b>B3</b>
<i>Hoeglundina elegans</i>	6.5	9.4	9.4	<b>32.3</b>	6.8	<b>19.6</b>	<b>14.8</b>	8.3
<i>Rhabdammina abyssorum</i>	4.9	7.1	16.5	0.0	0.1	8.8	6.6	<b>22.0</b>
<i>Cibicides wuellerstorfi</i>	4.0	5.8	22.3	<b>19.7</b>	<b>25.6</b>	5.8	5.4	4.9
<i>Saccorhiza ramosa</i>	3.2	4.6	26.9	-	-	1.3	0.1	<b>10.8</b>
<i>Ammolagena clavata</i>	3.0	4.4	35.8	-	<b>12.8</b>	2.3	<b>10.6</b>	0.3
...								
<i>Tolypammina vagans</i>	1.9	2.8	53.3	-	-	2.1	-	<b>11.3</b>
...								
<i>Heterolepa broeckhiana</i>	1.1	1.6	73.3	<b>14.2</b>	-	-	-	-

All species contributing cumulatively up to 70% are presented. Abundant taxa contributing >10% to the dissimilarity of a cluster are marked in bold. The average overall dissimilarity is 69.5. A secondary SIMPER analysis for clusters A1–2 and B1–3 is presented in a condensed form with the most relevant taxa >10%. It shows the internal characteristics of clusters A (group A1, A2) and B (group B1, B2, B3).

## 4 Results

### 4.1 Sedimentology

#### 4.1.1 Grain Size Distribution

Grain size distribution reveals only small-scale variability within the Iceland Basin CDS (Björn and Gardar Drifts) and large dissimilarities to the Eirik Drift ([Table 2](#)). Sediments from the Björn Drift (3B, 4B, 5B) are characterized by fine silts with a mean grain size of 14.4  $\mu\text{m}$ . Mud/sand ratios cover a range from 39 to 50, with the highest value in sample 5B. In the northern Gardar Drift, sediments are slightly coarser ranging from fine (11B) to medium silt (9K, 12B, 13B). An average grain size of 23.5  $\mu\text{m}$  and comparatively lower mud/sand ratios of 6 (13B) to 36 (12B) are reflecting this. To the south, fine-grained sediments increasingly dominate the detached Gardar Drift reflected in a mean grain size of 8.8  $\mu\text{m}$  and particularly high mud/sand ratios up to 123 (16B). The sediment composition ranges from fine silt (15B) to very fine silt (16B, 18B; [Table 2](#)).

The samples south of Greenland are considerably coarser. Very coarse silt determines the shallower Greenland Margin (27 15B). The samples from the Eirik Drift consist of very fine sand (29 18B) and medium silt (35 25B). Mud/sand ratios range from 0.3 to 1.1 in samples 29 18B and 27 15B and reach 10.2 in the bathymetrically deepest sample 35 25B ([Table 2](#)).

Grain size among samples outside of CDS is medium silt with an average grain size of 21  $\mu\text{m}$  in the Rockall Trough (01 1B) and fine silt with a mean grain size of 19  $\mu\text{m}$  north of the Azores (20B; [Table 2](#)).

#### 4.1.2 Sortable Silt

In the entire data set, sortable silt values cover a range between 17-39  $\mu\text{m}$ , contributing 14-55 % to the total siliciclastic fraction. The linear regression between  $\overline{SS}$  and SS% reveal gradients in flow velocities according to the concept of McCave and Hall (2006; [Figure 2a](#)). Reliability of the  $\overline{SS}$  data is validated by its good correlation with the in situ FSR values ( $r^2=0.68$ , [Figure 2b](#)) determined by Bianchi and McCave (2000).

In the Björn Drift, intermediate values of 21.3-22.8  $\mu\text{m}$  were determined, contributing 42.6 to 43.8 % to the siliciclastic fraction. The highest Sortable Silt values for the Iceland Basin occur in northern Gardar Drift samples and range from 23.9  $\mu\text{m}$  (12B) to 26.2  $\mu\text{m}$  (9K), which covers 46.9-51.4 % of the siliciclastic fraction. In contrast, the southern Gardar Drift shows the lowest  $\overline{SS}$  values over the entire data set with 17  $\mu\text{m}$  (16B) to 20  $\mu\text{m}$  (15B) and very low SS% values (13.7-32.8 %).

In the Eirik Drift of Greenland,  $\overline{SS}$  values range from 26.7  $\mu\text{m}$  (35 25B) to 39.2  $\mu\text{m}$  (29 18B), being significantly higher than those of the Iceland Basin CDS, while the  $\overline{SS}$  proportion at 41.4-55.2 % is comparable to the northern Gardar Drift.

$\overline{SS}$  values of the reference samples 01 1B (25  $\mu\text{m}$ ) and 20B (26.2  $\mu\text{m}$ ) are similar to those from the northern Gardar Drift. However, their  $\overline{SS}$  contribution to the total siliciclastic fraction is lower (29.9-39.9 %) than for the northern Gardar Drift (44.4-51.4 %; [Table 2](#)).

### 4.1.3 Total Organic Carbon Content

The total organic carbon (TOC) content ranges from 0.09 to 0.74 wt.% (Table 2). In the Iceland Basin CDS, all Björn Drift samples and the northern Gardar samples 9K and 11B show values between 0.56-0.72 wt.%. Lower values between 0.09 and 0.39 wt.% are present in the northern Gardar samples 12B, 13B as well as southern Gardar samples 15B, 16B and 18B. The samples from the Eirik Drift range between 0.34 and 0.63 wt.%. Reference samples outside any CDS show a content of 0.30 wt.% in the Rockall Trough (01 1B) and exhibit the highest value of the entire data set of 0.74 wt.% north of the Azores (20B).

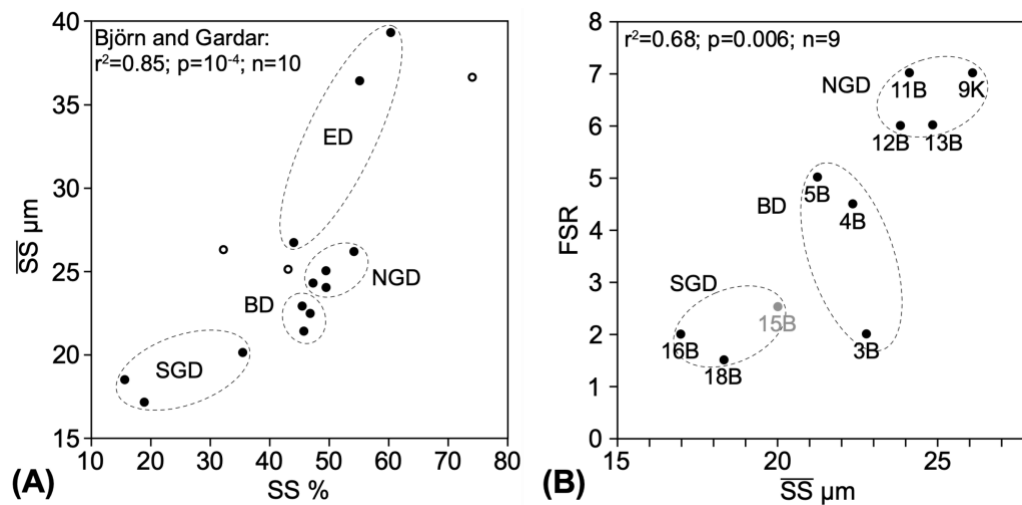


**Figure 2 | (A)** Linear regression between Sortable Silt mean size ( $\overline{SS}$ ) and percentages (SS%) of Northern Atlantic samples indicating flow regimes following the concept of McCave and Hall (2006); circles indicate samples outside a CDS; dots display samples inside a CDS. Abbreviations mean: BD= Björn Drift; ED= Eirik Drift; NGD= Northern Gardar Drift; SGD= Southern Gardar Drift. **(B)** Correlation of flow speed rank (FSR 0-8; McCave and Tucholke, 1986; Bianchi and McCave, 2000) and  $\overline{SS}$  mean size for all NEAPACC samples. The FSR for 15B was not given by Bianchi and McCave (2000) because measurements were not possible caused by high turbidity. A FSR was estimated based on the measurable sample stations. Abbreviations mean: BD= Björn Drift; NGD= Northern Gardar Drift; SGD= Southern Gardar Drift.

## 4.2 Benthic Foraminifera

### 4.2.1 Species Abundances and Assemblages

The foraminiferal fauna  $> 250 \mu\text{m}$  is mainly composed of bathyal epifaunal taxa (Table 3, Appendix 1a). A total of 152 species were identified, of which 53 have an agglutinated, 75 a hyaline and 24 a porcelaneous test wall structure. Tests are generally well preserved. Scanning electron microscope images reveal that taxon-specific predatory bore holes occasionally occur on the tests, particularly on *Hoeglundina elegans* (Figure 3; Culver and Lipps, 2003). The presence of delicate, but well-preserved tests of genera such as *Fissurina* or *Chilostomella* indicates that alteration of assemblage composition due to dissolution effects is thus considered negligible.

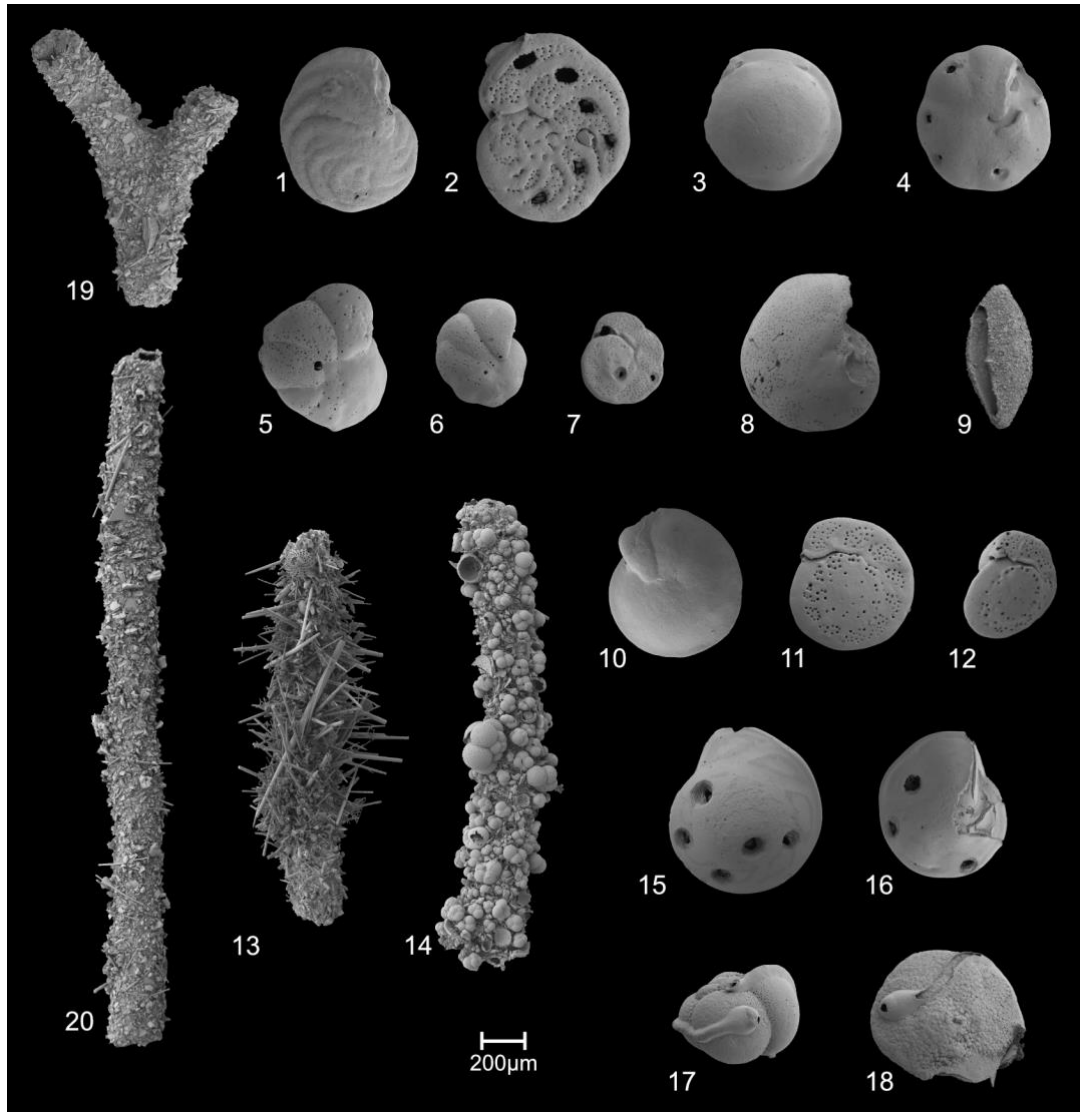


**Figure 3** | Relevant determining taxa: **1** *Cibicoides wuellerstorfi* (Schwager, 1866), umbilical side; **2** *C. wuellerstorfi* (Schwager, 1866), spiral side; **3** *Heterolepa broeckhiana* (Karrer, 1878), spiral side; **4** *H. broeckhiana* (Karrer, 1878), umbilical side; **5** *Cibicides lobatulus* (Walker & Jacob, 1798), umbilical side; **6** *C. lobatulus* (Walker & Jacob, 1798), umbilical side; **7** *Cibicides lobatulus* (Walker & Jacob, 1798), spiral side; **8** *Cibicides refulgens* Montfort, 1808, umbilical side; **9** *Sigmoilopsis schlumbergeri* (Silvestri, 1904), side view; **10** *Cibicoides pachyderma* (Rzehak, 1886), umbilical side; **11** *C. pachyderma* (Rzehak, 1886), spiral side; **12** *C. pachyderma* (Rzehak, 1886), apertural view; **13** *Saccorhiza ramosa* (Brady, 1879), lateral view; **14** *Rhizammina algaeformis* Brady, 1879, lateral view; **15** *Hoeglundina elegans* (d'Orbigny, 1826), spiral side; **16** *H. elegans* (d'Orbigny, 1826), umbilical side; **17** *Ammolagena clavata* (Jones & Parker, 1860), lateral view; **18** *A. clavata* (Jones & Parker, 1860), lateral view; **19** *Rhabdammina abyssorum* Sars in Carpenter, 1869, lateral view; **20** *R. abyssorum* Sars in Carpenter, 1869, lateral view.

Most agglutinated species occur in samples 3B (66 %) and 5B (68 %) in the Björn Drift and 11B (70 %) in the northern Gardar Drift. Most common species of this test type are *Rhabdammina abyssorum*, *Saccorhiza ramosa* and *Ammolagena clavata*. Hyaline foraminifera are most abundant in samples 27 15B (87 %) at the Greenland Margin, and 29 18B (96 %) in the Eirik Drift. *Hoeglundina elegans* and *Cibicoides wuellerstorfi* are the most abundant taxa of this test type. Porcelaneous tests represent a

minor component throughout the data set (3-24 %) with *Sigmoilopsis schlumbergeri* and various *Pyrgo* species being most abundant.

The highest proportion of epifaunal foraminifera was recorded at the Greenland margin contributing 93 % of the total fauna in sample 27 15B, while both Eirik Drift samples 29 18B and 35 25B show proportions < 48 %. Epifaunal taxa determine the fauna in the Iceland Basin samples between 38 % in sample 15B and 69 % in sample 11B and dominate both reference samples 20B (75 %) and 01 1B (52 %).

The cluster analysis (cophenetic correlation coefficient: 0.89) groups the samples into four clusters (A-D), with two clusters subdividing into different groups (A1-2, B1-3; [Figure 4](#)). The SIMPER analysis reveals that 19 taxa contribute to the first cumulative 70 % of the dissimilarities observed in the clusters ([Table 5](#)).

Cluster A (samples 29 18B, 20B) is mainly determined by a *Cibicidoides wuellerstorfi* (23 %)-*Hoeglundina elegans* (20 %) assemblage ([Table 5](#)). Internally, group A1 (29 18B, Eirik Drift) is determined by dominant frequencies of *H. elegans* (32 %) alongside abundant occurrences of *C. wuellerstorfi* (20 %). It is distinguished by abundant *Heterolepa broeckhiana* (14 %), which does not occur in A2. Group A2 (20B, off the Azores), however, is determined by abundant frequencies of *C. wuellerstorfi* (26 %), *Ammolagena clavata* (13 %) and only few occurrences of *H. elegans* (7 %; [Table 5](#)). The absence of *A. clavata* in group A1 contrasts with few occurrences of *H. elegans* and the absence of *H. broeckhiana* in group A2, contributing significantly to the dissimilarity between both groups.

All Gardar Drift samples (9K, 16B, 18B, 12B, 13B, 15B, 11B), the deep Eirik Drift sample (35 25B) and deeper Björn Drift sample (5B) coincide in cluster B, determined by a *Hoeglundina elegans* (16 %) - *Rhabdammina abyssorum* (11 %) assemblage ([Table 5](#)). Cluster B consists of three groups, with group B1 depicting the similarity between Gardar Drift samples 9K, 16B, 18B, and deep Eirik Drift sample 35 25B ([Figure 4](#)). Abundant *H. elegans* occurrences (20 %) with few *Rhabdammina abyssorum* (9 %) and *C. wuellerstorfi* (6 %) frequencies determine group B1. Group B2 is very similar to group B1 with abundant *H. elegans* (15 %) and differs with abundant *A. clavata* populations (11 %; [Table 5](#)). Grouped are samples 12B, 13B and 15B from the central Gardar Drift ([Figure 1](#), [Figure 4](#)). The third group B3 consists of northern Gardar Drift sample 11B and deep Björn Drift sample 5B. B3 differs from B1 and B2 by a mainly agglutinated assemblage of *Rhabdammina abyssorum* (22 %) - *Tolypammina vagans* (11 %) - *Saccorhiza ramosa* (11 %; [Table 5](#)).

Cluster C reflects the similarity of the shallower Björn Drift (3B, 4B) and the Rockall Trough (01 1B), defined by a *Sigmoilopsis schlumbergeri* (13 %) - *Saccorhiza ramosa* (11 %) - *Rhizammina algaeformis* (11 %) assemblage ([Table 5](#)). Few occurrences of *Cibicidoides wuellerstorfi* (9 %) and *Psammosphaera fusca* (5 %) further specify this cluster.

The lowest similarity in faunal composition among the samples is observed for cluster D, composed solely of the shallow Greenland Margin sample (27 15B, [Figure 4](#)). Hyaline attached species *Cibicides*



*refulgens* (34 %) dominates the assemblage with *C. lobatulus* (22 %) and *Cibicidoides pachyderma* (12 %) being abundant (Table 5).

#### 4.2.2 Suspension Feeding Types

Comprising > 50 % of the total fauna, suspension feeders and bottom current associated taxa are dominant in shallow Björn Drift sample 3B, deeper Björn Drift sample 5B, northern Gardar Drift sample 11B and sample 27 15B from the upper slope of Greenland (Table 3). Sample 27 15B (78 %) contains the largest proportions, while the smallest SFT/BCA total values with < 35 % occur in groups B1 and B2 of cluster B (samples 35 25B, 12B, 13B, 15B, 16B, 18B; Table 3, Figure 4).

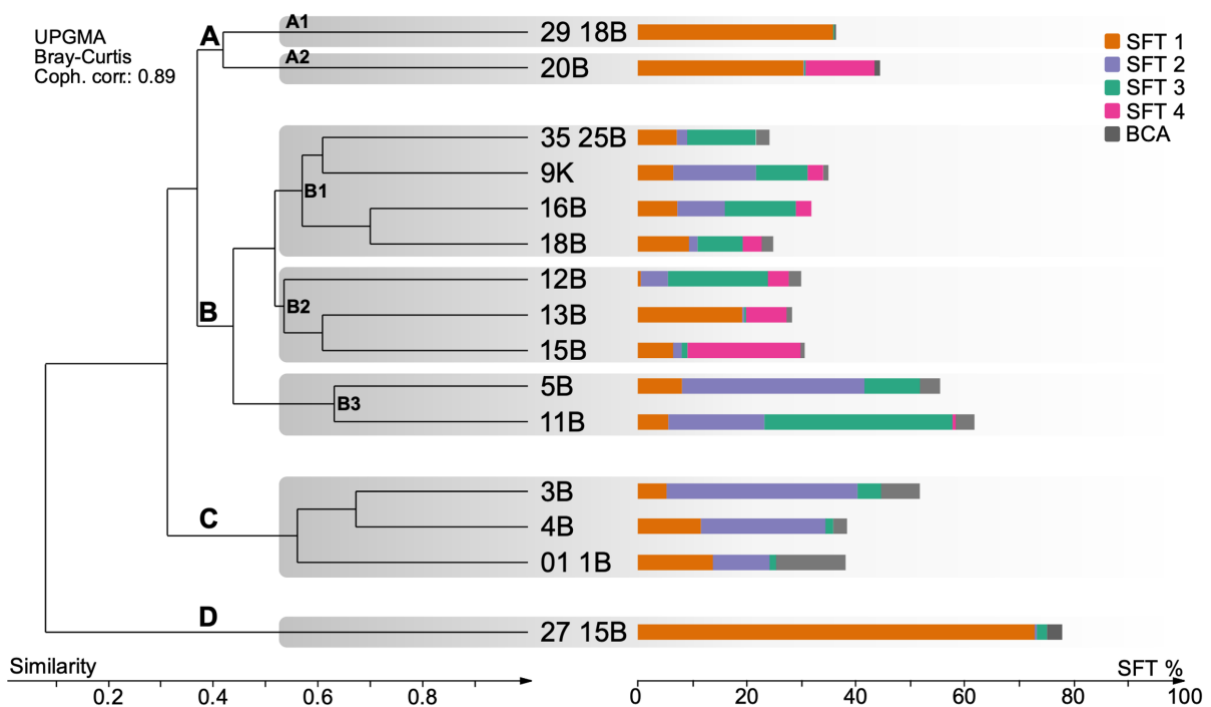


**Figure 4** | Cluster analysis of benthic foraminifera with UPGMA and Bray-Curtis dissimilarity. Four Groups (A-D) could be distinguished. The different SFTs are given in %. **SFT1**: attached epifaunal species; **SFT2**: tubular, branched agglutinated species, capturing food particles with a protoplasmic net; **SFT3**: tubular branched agglutinated species, capable of becoming detritus feeders when environmental conditions change; **SFT4**: encrusted, obligate suspension feeders; **BCA**: Bottom current associated species lacking a suspension-feeding lifestyle but have previously been linked to bottom currents. The remainder are non-SFTs.

SFT1 includes attached epifaunal species, with some settling on elevated substrates sensu Schönfeld (1997, 2002a, 2002b). 16 species belonging to this group have been identified throughout the data, most prominently represented by *Cibicides lobatulus*, *Cibicides refulgens*, *Cibicidoides wuellerstorfi*, *Cibicidoides pachyderma* and *Heterolepa broeckhiana* with highly variable abundances (Table 4). SFT1 is most frequent with 73 % at the Greenland Margin (sample 27 15B), followed by 36 % in the Eirik Drift (sample 29 18B) and 31 % north off the Azores (sample 20B). Internal trends in SFT1 composition south of Greenland are evident with increasing water depth. While *C. refulgens* and *C. lobatulus* predominate in sample 27 15B (768 mbsl), *C. wuellerstorfi* prevails in samples 29 18B (2145 mbsl) and

20B (2878 mbsl, [Table 1](#); [Appendix 1b](#)). In contrast, SFT1 occurrences are much lower in the Iceland Basin CDS occurring between 1-19 %, whereas sample 13B (19 % SFT1) displays an upward deviating exception with *C. wuellerstorfi* as decisive SFT1 taxon. Considering the cluster analysis, particularly clusters A (samples 29 18B and 20B) and D (sample 27 15B) are determined by SFT1 taxa ([Figure 4](#)).

SFT2 comprises tubular and branched agglutinated species, dwelling erect in the sediment, and sometimes interlocking with each other, to capture food particles with a protoplasmic net (Altenbach et al., 1988; Cartwright et al., 1989; Gooday et al., 1992; Linke and Lutze, 1993). Five taxa belonging to SFT2 were identified in the data set, of which *Saccorhiza ramosa* and *Rhizammina algaeformis* were the most common. This suspension feeding type is particularly abundant in the Björn Drift (3B, 4B, 5B) where it determines > 20 % of the total fauna ([Table 3](#)). In contrast, SFT2 taxa account for 5-18 % in the northern Gardar Drift (9K, 11B, 12B) and a maximum of 9 % in the southern Gardar Drift (sample 16B). Iceland Basin samples 13B, 15B and 18B even contain less than 2 % SFT2 taxa ([Table 3](#)). SFT2 was also counted rarely in the Eirik Drift (samples 27 15B, 29 18B, 35 25B) and north of the Azores (sample 20B), being < 2 %. Regarding results of the cluster analysis, cluster C (samples 3B, 4B, 01 1B) is significantly controlled by SFT2 taxa, and group B3 is determined by abundant SFT2 occurrences (5B, 11B; [Figure 4](#)).

Facultative suspension feeders are grouped as SFT3, capable of becoming detritus feeders when environmental conditions change (Linke, 1992; Cedhagen, 1993; Linke and Lutze, 1993; Sen Gupta, 2003). Five associated taxa were identified throughout the data set, of which *Rhabdammina abyssorum* is the main representative. In the Gardar Drift, SFT3 taxa largely contribute to the faunal composition, being even slightly more abundant in the northern drift at 9-34 % (9K, 11B, 12B) than in the southern drift at 8-13 % (16B, 18B). Increased occurrences are also noted in samples 5B from Björn Drift (10 %) and 35 25B from deep Eirik Drift (12 %), while SFT3 does not exceed 5 % in the remaining samples. Abundances of SFT3 thus contribute to the similarity within cluster B, except for samples 13B and 15B ([Figure 4](#)).

Encrusted and obligate suspension feeders are summarized as SFT4 with only *Ammolagena clavata* being present in this data set. This suspension feeding type was recorded exclusively in the Gardar Drift and north off the Azores (9K, 11B, 12B, 13B, 15B, 16B, 18B, 20B). SFT4 particularly defines cluster A, group A2 (sample 20B; 13 %) and cluster B, group B2 (samples 12B, 13B, 15B; 4-21 %), with the highest value in sample 15B (21 %; [Table 3](#)). In the remaining Gardar Drift samples, it does not exceed > 4 % ([Table 3](#)).

Taxa of the BCA group occur sparsely throughout the data set. They are slightly more abundant in the Rockall Trough (sample 01 1B with 13 %), but never exceed 7 % in any other samples.

#### 4.2.3 Assemblages and SFTs distribution

The canonical correspondence analysis (CCA), using scale type 1 of Legendre and Legendre (1998), illustrates the relationship between foraminiferal taxa, explanatory environmental variables, and sample locations ([Figure 5](#)). CCA as a function of distance between the parameters TOC,  $\overline{SS}$ , and water

depth determines > 99 % of the total data set with canonical axes CCA1 (eigenvalue = 0.49, variance = 70.7 %) and CCA2 (eigenvalue = 0.20, variance = 29.3 %).

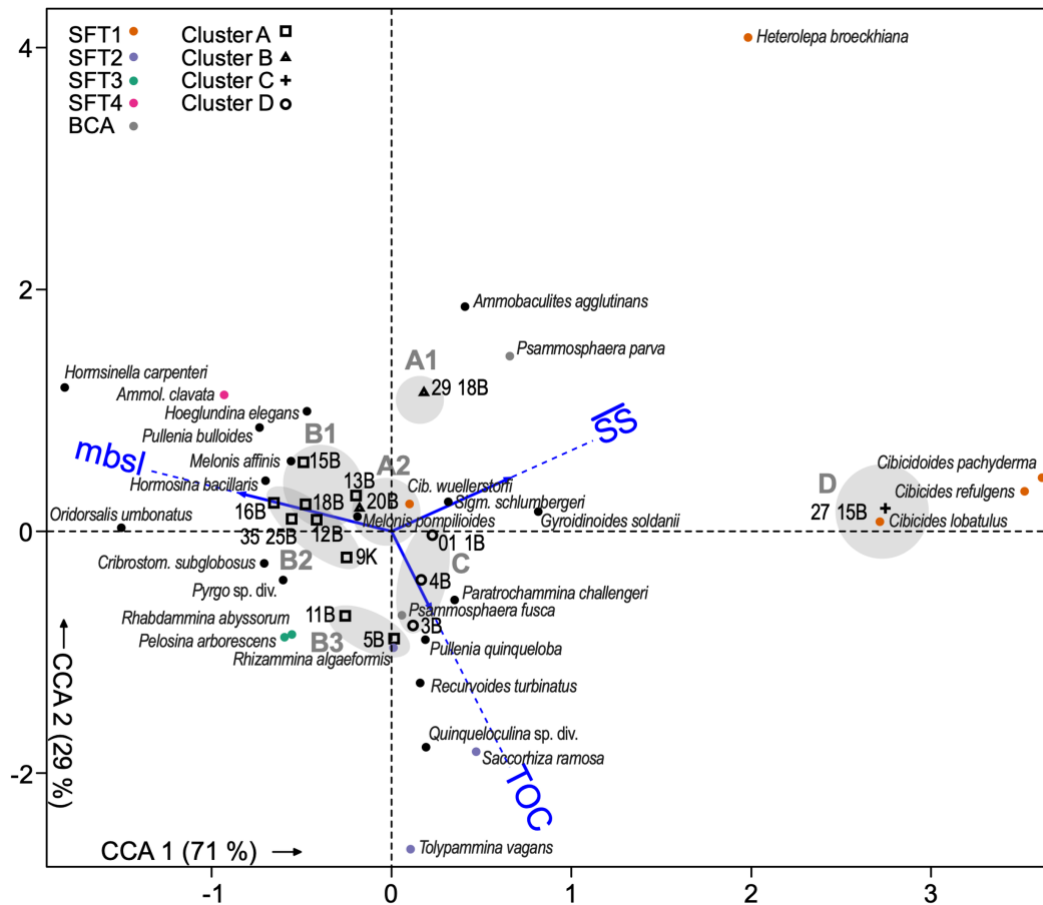


**Figure 5** | Canonical correspondence analysis, scale type 1, with the environmental parameters  $\overline{SS}$ , TOC, and water depth in mbsl. In the statistical analysis, only taxa that occur > 5 % in at least one sample were included.

All environmental parameters are displayed as vectors with a maximum end of 1, with each vector plotting in different segments of the triplot (Figure 5; Appendix 2). Besides differentiating the influence of the environmental parameters in the dataset, the CCA shows that SFT assemblages and clusters can be separated along the axes. SFT1 to SFT4 are partitioned between the four quadrants of the diagram, BCA taxa plot in the positive range of CCA1 (Figure 5). Cluster A is related to the vectors water depth and sortable silt (mbsl, SS), while cluster B plots more closely to the water depth vector on the negative CCA1 axis. Within cluster B, group B3 is closely oriented to cluster C, both of which are near the TOC vector (Figure 5). Cluster D is represented by a single sampling station at the Greenland continental margin. It is clearly demarcated from the remaining data along CCA1 in a positive direction, and plots close to the species *C. lobatulus*, *C. refulgens* and *C. pachyderma* (SFT1, Figure 5).

#### 4.2.4 Abundant Foraminiferal Taxa of Size Fraction 125-250 $\mu\text{m}$

The screening of the size fraction 125-250  $\mu\text{m}$  revealed several abundant taxa which are summarized in [Table 6](#). Sample 27 15B, located on the Greenland Margin, shows increased occurrences of *C. lobatulus* and species of *Cassidulina*, *Hanzawaia* and *Haynesina*. Sample 29 18B from the Eirik Drift contains many species of *Fissurina* and *Gyroidinoides*. Samples 13B, 15B, 16B, and 18B, located primarily along the southern Gardar Drift, display high numbers of *Epistominella exigua*. Sample 13B is the only CDS sample that contains higher abundances of *Melonis affinis*. In the samples of northern Gardar Drift 9K, 11B and 12B, *E. exigua* together with species of *Lagenamina*, *Reophax*, *Chilostomella* and *Haynesina* seem to be predominant. In samples 3B and 4B of the Björn Drift, an increased occurrence of *S. schlumbergeri* is recorded, while sample 5B indicates a strong accumulation of *E. exigua*, as in the Gardar Drift samples. Hyaline shells are most abundant, only few fragments of tubular agglutinated taxa (*Rhizammina algaeformis*, *Rhabdammina abyssorum*) were detected in both Björn and Gardar Drift samples. Infaunal taxa such as *Bulimina*, *Globocassidulina*, *Pullenia*, and *Sigmoilopsis* dominate the 125-250  $\mu\text{m}$  fraction of Rockall Trough sample 01 1B. North of the Azores, an increased occurrence of porcelaneous *Tubinella inornata* is noticed in sample 20B alongside hyaline *E. exigua*, as well as cibicid and bolivinid species.

## 5 Discussion

### 5.1 Patterns of Benthic Foraminiferal Distribution in the High Latitude North Atlantic

In the Atlantic Ocean north of 50°N, typical foraminiferal faunas unaffected by strong bottom currents and outside of CDSs display hyaline-dominated assemblages, while tubular agglutinated species are underrepresented (Belanger and Streeter, 1980; Linke and Lutze, 1993; Rasmussen et al., 2002; Lukashina, 2013; Lukashina and Bashirova, 2015). In the Norwegian-Greenland Sea, *Cibicidoides wuellerstorfi*, *Oridorsalis tener*, *Cribostrum subglobosum*, and *Pyrgo rotalaria* dominate the foraminiferal association > 150  $\mu\text{m}$  in water depths below 1250 m (Belanger and Streeter, 1980; Linke and Lutze, 1993). The region southeast of Reykjanes Ridge, partly influenced by the ISOW, is characterized by a *Hoeglundina elegans-Cibicidoides wuellerstorfi* (reported as *Planulina wuellerstorfi*) assemblage between 2000 and 3800 m water depth within the total sediment bulk (Lukashina, 1988). Rasmussen et al. (2002) report assemblages > 100  $\mu\text{m}$  dominated by *Bolivina pseudopunctata* and *Bulimina exilis* from the Reykjanes Ridge in 1685 m water depth, with *Epistominella exigua* occurring to a lesser extent. From the Iceland Basin east of the Gardar Drift, Lukashina and Bashirova (2015) describe *Melonis affinis* (reported as *M. barleeanum*) and *M. pompilioides* as dominant species in the > 150  $\mu\text{m}$  fraction.

Our new data show that faunal assemblages of the Iceland Basin CDS differ distinctively from typical Atlantic deep-sea faunas. Agglutinated, tubularly branched suspension feeders are documented almost exclusively in association with persistent bottom currents, as in CDS (Linke and Lutze, 1993; Schröder-Adams and van Rooyen, 2010). Quantitative faunal analyses > 250  $\mu\text{m}$  from the Björn and Gardar drifts reveal that agglutinated taxa, and particularly branched tubular species, determine the

data set by up to 70 % (Table 3). Although tubular species have already been reduced (cf. Kurbjewit et al. 2000), an overestimation must still be considered, and their reduction can only be seen as an approximation to the actual species number. Tube-shaped species, such as *Rhabdammina abyssorum* in the Gardar Drift (up to 34 %), and fragile branching species, such as *Saccorhiza ramosa* (11-15 %) and *Rhizammina algaeformis* (7-17 % Appendix 1b) in the Björn Drift, determine faunal patterns in the Iceland Basin CDS. Few occurrences of *S. ramosa* (7 %) and some *R. algaeformis* (3 %, Appendix 1b) also occur in reference sample 01 1B (Rockall Trough), suggesting that the LSW affects both, Rockall Trough and Björn Drift (Figure 4). Frequent occurrences of *R. algaeformis* surrounded by LSW have also been observed by Lintner et al. (2021) in the Rockall Trough between 1000 and 2200 m. The presence of agglutinated taxa susceptible to post-mortem disintegration, especially those with organic-cemented walls such as *Rhizammina algaeformis*, suggest that taphonomic processes did not have a strong impact on test preservation (Cartwright et al., 1989; Kuhnt et al., 2000). This is further supported by aragonitic *Hoeglundina elegans*, occurring as well-preserved translucent tests, thus, according to Gonzales et al. (2017), an intense taphonomically induced dissolution can be excluded.

The absence of infaunal *Bulimina* and *Bolivina* species in all 125-250 µm fractions of CDS samples suggests that they represent distinct faunas compared to typical North Atlantic communities (Table 6). The presence of *Bulimina mexicana* in reference sample 01 1B and *Bolivina subreticulata* in reference sample 20B underscores this assumption, however, both contain > 50 % epifaunal species in the > 250 µm size fraction (Table 3).

**Table 6** | Benthic foraminifera of the 125–250 µm fraction.

	01 1B	27 15B	29 18B	35 25B	3B	4B	5B	9K	11B	12B	13B	15B	16B	18B	20B
<i>Bolivina subreticulata</i>															x
<i>Bulimina mexicana</i>	x														
<i>Cassidulina</i> sp. div.	x	x			x										
<i>Chilostomella</i> sp. div.										x			x		
<i>Cibicides lobatulus</i>		x													x
<i>Cibicoides wuellerstorfi</i>															x
<i>Epistominella exigua</i>							x	x	x	x	x	x	x	x	x
<i>Fissurina</i> sp. div.			x												x
<i>Globocassidulina</i>	x														
<i>Gyroidinoides</i> sp. div.			x												
<i>Hanzawaia boueana</i>		x													
<i>Haynesina germanica</i>		x						x							
<i>Lagenammina</i> sp. div.									x	x			x	x	
<i>Melonis affinis</i>											x				
<i>Pullenia quinqueloba</i>	x														
<i>Reophax</i> sp. div.							x		x						
<i>Sigmoilopsis schlumbergeri</i>	x				x	x									
<i>Tubinella inornata</i>															x

The fraction 125–250 µm was screened for present or absent. Cross means frequently present.

Samples 13B and 15B (Gardar Drift) represent an exception within the CDS, as they contain only small amounts of *R. abyssorum* (0.5-1 %), *S. ramosa* (0-0.3 %) and *R. algaeformis* (0.2-1.4 %, Appendix 1b). This low abundance is more likely to be observed outside the Björn and Gardar drifts, suggesting that both samples represent atypical CDS conditions. Epifaunal species are underrepresented in samples

13B and 15B with < 41 %, compared to the remaining Iceland Basin CDS samples containing > 45 % (Table 3). The epifauna in samples 13B and 15B is determined by *Ammolagena clavata* (8-21 % Appendix 1b), which prefers oligotrophic conditions (Fontanier et al., 2002). *Ammolagena clavata* occurrences from such northern latitudes have only been described by Lintner et al. (2021) from 1008 m water depth in the Rockall Trough, although in very sparse numbers. Its occurrence is attributed to the presence of coarse particles for attachment, but also very fine material, as its outer wall is very smooth (Lindenberg and Auras, 1984; Harloff and Mackensen, 1997).

Sample 13B strongly contributes to the assumption of the lack of a Holocene sedimentary cover on the western flank of the northern Gardar Drifts crest. The foraminiferal association of 13B is consistent with the fauna recorded by Lukashina and Bashirova (2015) from the Iceland Basin during Termination I (*H. elegans*, *C. wuellerstorfi*, *M. affinis* and *M. pompilioides*). A dominant occurrence of *Neogloboquadrina pachyderma* (left coiling) has previously been described by Lukashina (2013) from the MIS 1 in the Iceland Basin. This species was recorded by Bianchi and McCave (2000) exclusively in sample 13B (completely absent from all other stations) along with a strong northward current and coarse lithic grains considered by the authors to be ice-rafted detritus (IRD). Indications of IRD influence could be the increased sand content in sample 13B (14 %) compared to samples 9K, 11B and 12B (3-7 %, Table 2) and is underlined by a weakened deep circulation that prevailed during the last glaciation in the north-eastern Atlantic (Skinner and Shackleton, 2004). This evidence suggests that sample 13B reflects a glacial faunal assemblage which has undergone much less influence from bottom current activity than the younger assemblages of the Gardar Drift samples. Sample 13B is located on the downstream western flank of the crest where strong currents exerted by the ISOW may ablate sediments (Bianchi and McCave, 2000), in contrast to samples 9K, 11B, and 12B on the eastern flank where ISOW sediment loads push against the drift body.

The deep-sea epibenthic species *Epistominella exigua* occurs frequently in the 125-250 µm size fraction of all Gardar samples. This opportunistic species is especially abundant in areas with a high primary production and fresh input of phytodetritus (Smart et al., 1994; Fontanier et al., 2006; Lecroq et al., 2009). It survives very long starvation periods, and lives in larger ranges of organic flux rates compared to other deep-sea foraminifera (Lecroq et al., 2009). Thus, the predominantly abyssal, cosmopolitan, and highly adaptable *E. exigua* encounters optimal living conditions within the thick bottom nepheloid layers of the Gardar Drift (Schönfeld, 1997), where it co-occurs with the facultative and opportunistic *R. abyssorum*.

Clusters A and D underline how strongly the Atlantic samples south of Greenland differ from the CDS samples of the Iceland Basin. Cluster A is characterized by a *C. wuellerstorfi*-*H. elegans* assemblage (Table 5); both taxa are widespread in the deep-sea, and together represent a typical North Atlantic fauna (Lutze and Coulbourn, 1984; Lukashina, 1988; Murray, 2006; Schweizer et al., 2009). Streaming water and oligotrophic conditions characterize the microhabitat of *C. wuellerstorfi* (Lutze and Thiel, 1989), which plots near the SS vector in the CCA (Figure 5). *Hoeglundina elegans* is also known to be oligotrophic (Fontanier et al., 2002; Bhaumik et al., 2014), and both deep-sea taxa are anti-correlated with the vector of TOC in the CCA (Figure 5). This is indicating that high nutrient loads in bottom

waters, as in nepheloid layers within vigorous currents, do not affect the abundances of *C. wuellerstorfi* and *H. elegans*. Within Cluster A the groups A1 and A2, however, differ significantly. In Eirik Drift sample 29 18B the typical North Atlantic assemblage is co-occurring with passive suspension-feeding species *Heterolepa broeckhiana* (14 %, [Appendix 1b](#)). This SFT1 taxon was exclusively detected in the central Eirik Drift sample, showing a distinctive position from all other species in the CCA triplot ([Figure 5](#)). It appears to be rather atypical in regular North Atlantic foraminiferal faunas and is reported in association with fine- to coarse-grained biogenic sands (Langer and Lipps, 2003). It is striking that the sand content is also significantly increased in sample 29 18B (75.5 %), compared to the remaining sample sites (< 50 %; [Table 2](#)). In sample 20B (group A2) the *C. wuellerstorfi*-*H. elegans* assemblage co-occurs with increased numbers of oligotroph *Ammolagena clavata* (Fontanier et al., 2002), and thus emphasises how typical North Atlantic faunas and CDS faunas differ.

Sample 35 25B, taken at the distal Eirik Drift, contains higher amounts of branched agglutinated species (*R. abyssorum* and *Pelosina arborescens* both at 6 %), contrasting sample 29 18B (< 1 %, [Appendix 1b](#)). Their co-occurrence with *H. elegans* (19 %) makes the assemblage of 35 25B resemble the deeper Gardar Drift association.

Apparently, the CDS of the Iceland Basin, especially the Gardar drifts, favour occurrences of *R. abyssorum*. Significantly fewer to no fragments of this taxon were found in reference sample 20B outside contourite drifts and the Rockall Trough sample 01 1B (both < 1 %; [Appendix 1b](#)). While hyaline species dominate the benthic foraminiferal community in the open environments of the Atlantic Ocean north of 50°N, the CDS of the Iceland Basin contain a tubular to branched agglutinated foraminiferal community. This suggests that the persistent bottom currents in the Björn and Gardar Drifts provide optimal habitats for tubular agglutinated suspension feeders (Linke, 1992; Linke and Lutze, 1993).

## 5.2 The Björn/Gardar Drifts: SFTs and their Potential Relation to Bottom Current Strength

SFTs account for an important fraction of the foraminiferal fauna in the Iceland Basin CDS. They reach proportions of at least 30 % and contribute significantly to the subdivision of clusters ([Figure 4](#)). The wealth of previous data on the hydrodynamic conditions on the Björn and Gardar drifts make them ideal study areas for the analysis of benthic foraminifera and the distribution of SFTs along hydrodynamic gradients in increased current regimes. Available data includes current meter measurements and seafloor photographs by Bianchi and McCave (2000) from which they inferred a semi-quantitative flow speed ranking (FSR 0-8, increasing with velocity; McCave and Tucholke, 1986). Our data complements the direct observations with  $\overline{SS}$  values to estimate flow velocity. The good correlation between in situ FSR values and  $\overline{SS}$  data confirms their reliability ([Figure 2a](#)). Together, these data imply distinct latitudinal gradients and bathymetric transitions of the flow regime south of Iceland. The hydrodynamic gradients are reflected in the foraminiferal assemblages, which are very distinctive for each drift ([Figure 6](#), [Table 5](#)). Due to strong indications for the absence of a Holocene sediment cover, sample 13B is not considered in the following discussion.

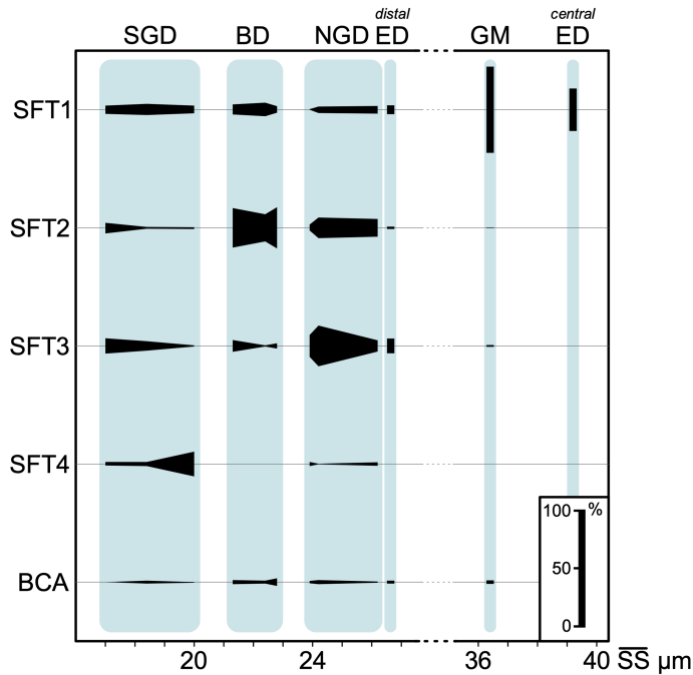


**Figure 6** | Suspension feeding types (SFT) and bottom current associated taxa (BCA) mapped on a Sortable Silt mean size scale ( $\overline{SS}$   $\mu\text{m}$ ), within the ranges of different drift bodies and current affected areas. Abbreviations denote Southern Gardar Drift (SGD), Björn Drift (BD), Northern Gardar Drift (NGD), Eirik Drift (ED) and Greenland Margin (GM). Frequencies at each  $\overline{SS}$  value represent percentages of the total foraminiferal fauna > 250  $\mu\text{m}$ .

### 5.2.1 Björn Drift

The Björn Drift is located along the main paths of the Labrador Sea Water (LSW) and the underlying Iceland Scotland Overflow Water (ISOW). The LSW interacts mainly with the shallower parts of the Björn Drift below 1600 m water depth with current velocities not exceeding  $3.1 \text{ cm s}^{-1}$  (Van Aken and De Boer, 1995; Bianchi and McCave, 2000; Hunter et al., 2007a). In samples 3B and 4B of the Björn Drift, current velocity indicators ( $\text{FSR} < 4.5$ ;  $\overline{SS} < 22.8$ ) and salinity values not exceeding 34.91 indicate that they are bathed by the LSW with no influence of the ISOW (Van Aken and De Boer, 1995; Bianchi and McCave, 2000).

The ISOW increasingly affects the Björn Drift below a depth of 1600 m (Bianchi and McCave, 2000). Björn Drift sample 5B is located at the boundary layer between the LSW and the ISOW, corroborated by increased average flow velocity ( $\text{FSR} = 5$ , [Figure 2b](#)) and salinity (34.93; [Table 1](#)). According to Bianchi and McCave (2000), a higher sediment load has been measured above sampling station 5, indicating stronger bottom nepheloid layers compared to the shallower Björn Drift ([Figure 2b](#)).

In the Björn Drift, taxa of SFT2 are prevalent and determine cluster C (23-35 %), with all other SFTs being present with abundances < 12 % ([Table 3](#), [Table 4](#), [Figure 6](#)). This is well reflected in increased *Saccorhiza ramosa* and *Rhizammina algaeformis* abundances prevailing in samples 3B, 4B and 5B. By embedding sponge spicules into its test, *S. ramosa* spans a protoplasm net which enables sufficient capture of food particles in calmer currents (Altenbach et al., 1988). *Rhizammina algaeformis* grows dichotomously and interlocks with other rhizamminids, to achieve higher stability in the sediment and create enlarged protoplasmic nets (Cartwright et al., 1989). Organic attachments such as sponge spicules or planktonic foraminifera are required by these species for test construction, thus their external morphology strongly depends on the supply of larger particles (Schröder et al., 1988).



Reduced LSW current velocities of only a few centimetres per second provide optimal environments for these delicate agglutinated taxa, dwelling upright in the sediment without becoming unstable due to stronger currents (Altenbach et al., 1988, 1993; de Mello e Sousa et al., 2006; Balestra et al., 2017). Regions with increased contents of suspended organic matter favour occurrences of SFT2 species (Schmiedl et al., 2000). Both species, *S. ramosa* and *R. algaeformis*, plot negatively along CCA2, in a similar region as the TOC vector (Figure 5), indicating a higher input of organic matter at the Björn Drift. The  $\overline{SS}$ -vector on the triplot displays positive CCA2 scores (Figure 5), implying rather reduced flow velocities for the aforementioned species when using the  $\overline{SS}$ -flow speed proxy method exclusively. Only samples 3B and 4B of the shallower Björn Drift appear to be increasingly colonized by *R. algaeformis* (12-17 %), whose abundance is lower in sample 5B (7 %) within the deeper Björn Drift. In sample 5B, meanwhile, an increased SFT3 content is present (10 %), while it remains < 5 % at the shallower Björn Drift (samples 3B, 4B; Table 3). According to de Mello e Sousa et al. (2006), *R. algaeformis* prefers increased mud contents and more importantly a stable substrate. Thus, especially the shallower Björn Drift (samples 3B, 4B), with increased mud/sand ratios of > 38.9 and a reduced flow regime due to the influence of LSW provides an optimal environment for this species. Although the mud/sand ratio is still high in the deeper Björn Drift (sample 5B = 49.5; Table 2), conditions for *R. algaeformis* no longer appear to be ideal at this site. This can be attributed to the increasing influence of ISOW, which is also reflected in the cluster analysis where sample 5B is grouped with the northern Gardar Drift sample 11B (group B3, Figure 4).

Cluster analysis indicates strong similarities in SFT distribution between the shallower Björn Drift (3B, 4B) and the Rockall Plateau (01 1B; Table 3). SFT2 with *S. ramosa* and *R. algaeformis* is abundant at the Rockall Plateau (10 %), however, its proportion is lower compared to the Björn Drift (23-35 %; Table 3). Comparing hydrographic parameters between the two areas reveals similarities in salinity, water temperature, and water depth (ca. 34.9; 3.20-3.25 °C; 1502-1805 m; Table 1). Both areas are influenced by the LSW (Ellett and Martin, 1973; Talley and McCartney, 1982; Bianchi and McCave, 2000; Holliday et al., 2000). The westward flow of the LSW near the Björn Drift is lower at about 3 cm s<sup>-1</sup> than in the Rockall Trough where a maximum of 6 cm s<sup>-1</sup> is possible (Van Aken and De Boer, 1995). Slight differences in flow velocity are supported by the slightly different  $\overline{SS}$  values of samples 3B, 4B (22-23 µm) and 01 1B (25 µm; Table 2).

### 5.2.2 Gardar Drift

The ISOW core runs SW, parallel to the axis of the Reykjanes Ridge, although its direction and intensity can vary locally (Van Aken, 1995; Van Aken and De Boer, 1995; Bianchi and McCave, 2000). The current causes thick bottom nepheloid layers along the Gardar Drift, most prominently in the attached drift north of 58°30'N as well as in the deeper Björn Drift (McCave et al., 1980). A maximum bottom current velocity of 10 cm s<sup>-1</sup> is reached on the eastern flank of the Gardar Drift at depths between 2000 to 2800 m comprising samples 9K, 11B and 12B (Van Aken, 1995; Bianchi and McCave, 2000). This is reflected in increased  $\overline{SS}$  values (> 24.4 µm), high FSRs (6-7; Table 2) and heavy sediment loads in the bottom nepheloid layers at these stations (Bianchi and McCave, 2000).

In the northern attached Gardar Drift, silt/clay ratios (3.9-4.6) and sand contents (2.7-6.9 %) are increased compared to the southern drift (silt/clay: 2.0-3.2; sand: 0.8-2.4 %). This north-south gradient is supported by Bianchi and McCave (2000), who indicate an increased terrigenous silt/clay ratio north of 58°30'N related to the drift's attachment and the proximity to Iceland. In the southern detached Gardar Drift, lower  $\overline{SS}$  values in samples 15B, 16B, and 18B, confirmed by the presence of mudwave fields, support reduced flow speeds in this area (McCave et al., 1980; Manley and Caress, 1994; Bianchi and McCave, 2000). The detached drift is located more distally to Reykjanes Ridge, hence the ISOW, which flows parallel to the ridge, is rather influencing the NW located Björnsson Drift (Bianchi and McCave, 2000). The lower sand contents in samples 15B, 16B, and 18B on the western slope of the detached Gardar Drift illustrate the influence of the topography of large sediment ridges on the flow velocity. Stronger currents are present on the eastern slope of the Gardar Drift, due to Coriolis effects and the location of the slope with respect to the flow direction (McCave et al., 2017).

Foraminiferal distribution patterns across the Gardar Drift are strongly determined by taxa of SFT3 (8-34 %, except for samples 13B and 15B with < 1 %) and SFT4 (1-8 %, in sample 15B up to 21 %; [Appendix 1b](#)), reflected in cluster B ([Figure 6](#)). SFT4 plays a crucial role in cluster B, as species of this type have only been reported in very reduced numbers from such northern latitudes outside the Gardar Drift (*Ammolagena clavata* in Lintner et al., 2021).

The major determinant SFT3 species is *Rhabdammina abyssorum*, which is able to adapt rapidly to changing environmental conditions (Linke, 1992). SFT3 either sustain themselves in increased flow velocities ingesting suspended food particles or feed on detritus when currents are lacking (Gooday et al., 1992; Linke, 1992; Cedhagen, 1993). This provides an advantage over species that are strictly tied to a suspension feeding lifestyle (Linke, 1992; Linke and Lutze, 1993). The adaptability and opportunistic behaviour of SFT3-taxon *R. abyssorum* is beneficial in the Gardar Drift, as the direction and intensity of bottom currents can vary significantly along the ISOW path (Van Aken, 1995; Van Aken and De Boer, 1995; Bianchi and McCave, 2000). As this species may represent varying flow speeds of bottom currents, it explains the opposed position in the CCA triplot in comparison to the  $\overline{SS}$ -vector, when using the latter exclusively as flow speed indicator ([Figure 5](#)). Like hydrographic and sedimentological data, faunal assemblages at the Gardar Drift fall into a northern and southern group, which is also well reflected in the distribution and abundances of SFTs ([Figure 6](#)).

The cluster analysis groups northern Gardar Drift sample 11B with deeper Björn Drift sample 5B (group B3), both defined by high occurrences of SFTs in general (55-62 %, [Table 3](#)) and increased SFT2 (18-33 %) and SFT3 (10-34 %) abundances in particular ([Table 3](#)). This reflects how sample 5B differs from the shallower Björn Drift samples 3B and 4B, which contain only < 5 % SFT3 ([Appendix 1b](#)). This could be attributed to strong bottom nepheloid layers in the northern Drift, which provide high levels of suspended food particles (Bianchi and McCave, 2000). Especially branching agglutinated species are often associated with such layers induced primarily by bottom currents (Altenbach et al., 1988; Schönfeld, 1997).

Assemblages from the southern detached Gardar Drift (15B, 16B, 18B), as well as the crest (9K) and southern rim (12B) of the northern drift show high similarities in the cluster analysis summarized in groups B1 and B2 ([Figure 4](#)). They generally contain lower numbers of SFTs (max. 35 % in sample 9K; [Table 3](#)) and a fauna mainly composed of *R. abyssorum*, *H. elegans*, and *C. wuellerstorfi* ([Table 5](#)). Lower SFT abundances probably reflect southward decreasing flow speeds and the absence of well-developed nepheloid layers (Bianchi and McCave, 2000). Linke and Lutze (1993) point out that *R. abyssorum* colonizes habitats with turbulent circulation patterns and enhanced resuspension as well as areas of local accumulation and deposition of food particles. A reduced supply of food particles is likely in the southern Gardar Drift, reflected in occurrences of oligotrophic taxa including *Hoeglundina elegans* (16 %), *Melonis pompilioides* (6 %), and *Melonis affinis* (3 %; cluster B in [Table 5](#); Lutze and Coulbourn, 1984; Rasmussen and Thomsen, 2017) together with lowest TOC values of the data set in samples 15B, 16B and 18B (0.09-0.34; [Table 2](#)). This is emphasized by the CCA triplot, where samples > 2500 m water depth consistently show negative CCA1 scores and are anticorrelated with the TOC vector ([Figure 5](#)).

Exclusively in the Gardar Drift and north of the Azores (sample 20B), abundances of SFT4 were recorded. They are numerous in groups A2 and B2 of the cluster analysis and present to a lesser extent in the remainder of cluster B ([Figure 4](#)). *Ammolagena clavata*, the only species to be assigned to SFT4, prefers regions with lower bottom currents sensu Kuhnt et al. (2000). The weakened flow regime in sample 15B of the southern Gardar Drift and distinct mud wave fields sensu Bianchi and McCave (2000) explain its occurrence of > 20 %, associated with *Hoeglundina elegans* (23 %; [Appendix 1b](#)). However, the absence of left-coiling *N. pachyderma* contradicts the idea of erosion and a glacial fauna as in sample 13B (compare chapter 5.1). A slow northward flow over sample site 15B, inferred by Bianchi and McCave (2000), appears to significantly affect the fauna. The present-day conditions at this location appear to be much more similar to glacial conditions with reduced bottom currents inferred from sample 13B. This is underlined by the similarity to sample 12B, which is located at the southern outer rim of the northern Gardar Drift. Thus, group B2 reflects a faunal association which prefers rather reduced bottom flow velocities and further suggests that SFT4 prefers regions less strongly affected by currents ([Figure 4](#)).

### 5.2.3 Comparison to Samples from Eirik Drift

Samples 27 15B, 29 18B, and 35 25B were collected south of the Greenland Margin and represent a wide range of water depths and different water masses. Bottom current velocities range from 12-22 cm s<sup>-1</sup> within the DWBC in the Eirik Drift (29 18B, 35 25B; Hunter et al., 2007a) and reach 40 cm s<sup>-1</sup> within the EGC (27 15B; Holliday et al., 2007). The three samples south of the Greenland margin hydrographically deviate strongly from each other, also depicted in the cluster analysis ([Figure 4](#)), and the CCA ([Figure 5](#)), due to large differences in their faunal composition.

A high sand content in sample 27 15B (47.3 %, [Table 2](#)) and erosive high energy conditions postulated by Hunter et al. (2007) are reflected in a particularly high  $\overline{SS}$  value (36.4  $\mu\text{m}$ ; [Table 2](#)). An increased  $\overline{SS}$  size (39.25  $\mu\text{m}$ ) and an extremely high sand content (> 75 %, [Table 2](#)) is also prevalent in the Eirik Drift

sample 29 18B. Sample 27 15B, located on the Greenland Margin, was collected from 768 m water depth, and thus differs significantly from the Björn Drift (1500-1800 m), Gardar Drift (2200-2800 m), and Eirik Drift (max. 3500 m) data sets ([Table 1](#)). The high-energy conditions of this sample are paired with higher temperatures (7.25 °C) and a higher salinity (35.16). However, slightly higher salinity values also prevail in sample 29 18B (34.98, [Table 1](#)).

With its strongly increased epifauna (93 %; [Table 3](#)) sample 27 15B shows the least similarity to the whole data set ([Figure 4](#), [Figure 5](#)). Attached suspension-feeding species of SFT1 contribute > 70 % to the fauna, while remaining SFTs combined show abundances of < 3 % ([Table 3](#)). SFT1 consists mainly of *Cibicides refulgens*, *Cibicides lobatulus*, and *Cibicidoides pachyderma*, all of which are known to be upper to middle slope species (Lutze and Coulbourn, 1984; Schweizer et al., 2009). They are associated with increased bottom current velocities, where they settle on elevated substrates, as evidenced by data from the Mediterranean Outflow Water (MOW) at the Iberian Margin (Schönfeld, 1997, 2002a, 2002b; Hernández-Molina et al., 2014; Sánchez-Leal et al., 2017). Enhanced SFT1 occurrences (36 %; [Table 3](#)) also distinguish sample 29 18B from the other samples (group A1, [Figure 4](#)). Frequent species are *Cibicidoides wuellerstorfi* and *Heterolepa broeckhiana*, together with non-SFT *Hoeglundina elegans*, all known to colonize the lower slope to continental rise (Lutze and Coulbourn, 1984).

In both samples 27 15B and 29 18B branching agglutinated foraminifera are absent. Fentimen et al. (2018, 2020) report similar observations from the downslope Moira Mounds in the northeast Atlantic. The Moira Mounds are influenced by currents between 35-40 cm s<sup>-1</sup> (Fentimen et al., 2020), similar to the Greenland continental margin where EGC affects the foraminiferal community with up to 40 cm s<sup>-1</sup> (Holliday et al., 2007) and slightly higher than DWBC affecting the Eirik Drift with velocities of up to 22 cm s<sup>-1</sup> (Hunter et al., 2007a). This suggests that the increased flow regime with  $\overline{SS}$  values between 36-39  $\mu\text{m}$  (clusters A1, D) does not provide a suitable habitat for SFT2 and SFT3 taxa, and both suspension feeding types are sensitive to flow velocities exceeding 10 cm s<sup>-1</sup> (cf.  $\overline{SS}$  values not exceeding 27  $\mu\text{m}$  in the Iceland Basin; [Figure 6](#)). Although SFT1 is highly abundant in both, clusters A1 (central Eirik Drift) and D (Greenland continental margin), they show the greatest dissimilarities in the cluster analysis. This implies that sandier substrates with strong current velocities are generally dominated by SFT1, however, species composition depends on water depth, temperature, and salinity. An upper to middle slope SFT1 and a deep-basin SFT1 can thus be distinguished (cf. contrasting scores of SFT1 taxa in the CCA, [Figure 5](#)).

Significantly weaker DWBC flows affect sample 35 25B from the deeper, more distal part of Eirik Drift (Hunter et al., 2007a). The  $\overline{SS}$  value (26.7  $\mu\text{m}$ ) and sand content (9 %) of this sample are more consistent with those of the Iceland Basin ([Table 2](#)). In the cluster analysis, sample 35 25B is closely grouped with northern Gardar Drift sample 9K, located at the current-reduced western crest of the drift (contrasting with the current-intensive eastern flank of the northern Gardar Drift; Bianchi and McCave, 2000). Group B1 of the cluster analysis closely relates both samples to samples 16B and 18B, which are determined by greater water depths (2847-3486 m) and a weakened current due to a reduced ISOW (Bianchi and McCave, 2000; Hunter et al., 2007a). The fauna of sample 35 25B is composed of only 24 % SFTs with *Rhabdammina abyssorum* (SFT3) being most abundant. The larger

proportion is composed of non-SFTs such as *H. elegans* and *Melonis pompilioides*. The similarities in setting and faunal composition suggest that these assemblages are typical for distal settings of the studied CDSs.

### 5.3 Comparison to Mid-Latitude Contourite Drifts

The influence of strong bottom currents on the composition of benthic foraminiferal assemblages has been described in several studies from the Iberian Margin (Schönfeld, 1997, 2002a, 2002b; Schönfeld and Zahn, 2000; Diz et al., 2004; Rogerson et al., 2011). There, the Mediterranean Outflow Water (MOW) shapes an extensive CDS through interactions with the continental margin (e.g., Hernández-Molina et al., 2014; de Castro et al., 2021). The mid-latitude Iberian Margin CDS and the herein studied high-latitude CDSs differ markedly in their hydrodynamic and sedimentological parameters. Warm and saline MOW is characterized by an average temperature of 12°C and salinity of 35.5 (Rogerson et al., 2011), contrasting the high-latitude deep waters bathing the Björn, Gardar and Eirik drifts (average temperature 3°C, salinity 34.96-34.98; Hunter et al., 2007b; McCave, 2005; Bianchi and McCave, 2000). Regarding the TOC values of the Iceland Basin CDS and the Eirik Drift (0.09-0.72 %), they agree well with the values along the Iberian Margin (0.2-0.9 %). At the boundary layer just above the MOW, Schönfeld (1997) records a TOC peak (0.9), also reflected in the boundary layer between LSW and ISOW in sample 5B (0.72 %). However, current speeds of the MOW are nearly 300 cm s<sup>-1</sup> in the Strait of Gibraltar, on average 100 cm s<sup>-1</sup> in its upper core, and 15-20 cm s<sup>-1</sup> in distal areas at Cape St. Vincent (e.g., Schönfeld, 2002b; Sánchez-Leal et al., 2017; Sierró et al., 2020). As a result, sandy to silty sediments cover the main path of the MOW, with silt to clayey silt predominating toward its lateral extensions (Schönfeld, 2002a). Thus, hydrological and sedimentological parameters of distal MOW areas (e.g., Cape St. Vincent), resemble those of the Eirik Drift (12-22 cm s<sup>-1</sup>, very fine sand; Hunter et al., 2007a) and the Greenland Continental Margin (40 cm s<sup>-1</sup>, very coarse silt; Holliday et al., 2007). Lower flow regimes and finer grained sediments prevail in the Björn and Gardar drifts (max. 10 cm s<sup>-1</sup>, medium to coarse silt; Van Aken, 1995).

A highly adapted community of benthic foraminiferal species predominantly colonizes elevated substrates within the strong bottom currents of the MOW and was established as the 'epibenthos group' by Schönfeld (1997, 2002a). The 'epibenthos group' (consisting mainly of taxa herein assigned to SFT1 such as *Cibicides lobatulus*, *Discanomalina coronata*, *Hanzawaia concentrica*, *Planulina ariminensis* and *Vulvulina pennatula*) shows abundance maxima on the southern Portuguese Margin at 800-1300 m water depths and prefers high sand concentrations (Schönfeld, 1997; Schönfeld and Zahn, 2000). The 'epibenthos group' is closely tied to areas where the MOW encounters the continental slopes and causes a strong near-bottom current regime. North of 48°N, the MOW current weakens and the epibenthic community changes (Schönfeld and Zahn, 2000; Dorst and Schönfeld, 2013). The 'epibenthos group' is reduced to the co-occurrence of *Cibicides refulgens*, *Cibicides lobatulus*, and *Discanomalina coronata*, which colonize the more distal and attenuated MOW core (Schönfeld, 1997; Schönfeld and Zahn, 2000).

The sedimentological and faunal composition of the distal MOW regime north of 48°N resembles the sample sites south of Greenland (27 15B, 29 18B) with respect to the increased sand content (47.3-75.5 %, [Table 2](#)) and abundant SFT1 taxa (36-71 %, [Table 3](#)). Particularly, the co-occurrence of *Cibicides lobatulus* and *Cibicides refulgens* in the 768 m deep sample at the Greenland Continental Margin (27 15B) is comparable to a distal, attenuated MOW (e.g., Schönfeld, 1997; Schönfeld and Zahn, 2000). As determining SFT1 taxon from central Eirik Drift (29 18B; [Table 5](#)), *Cibicidoides wuellerstorfi*, however, has not been mentioned from MOW areas at all (Schönfeld, 1997, 2002a, 2002b). The deep-water dweller inhabits regions well below the MOW layers (Schweizer et al., 2009).

The fauna from the Iceland Basin (Björn and Gardar drifts) is comparable to the distal areas of the upper and lower MOW core in the Gulf of Cadiz, where tubular agglutinated taxa were recorded. No occurrences, however, were reported from the high velocity layers of the MOW (Schönfeld, 1997, 2002a, 2002b). *Saccorhiza ramosa* and *Rhizammina algaeformis* were only recorded from the deep, distal margins of the MOW, primarily from water depths > 900 m (Schönfeld, 1997, 2002a). The reduced bottom current intensity in the shallower Björn Drift (1500-1600m), highlighted by slightly reduced  $\overline{SS}$  values (21-23  $\mu\text{m}$ ) and FSRs (2-5; [Table 2](#)), suggests that taxa of SFT2 do not tolerate particularly strong current regimes and can rather be correlated with areas of moderate flow velocities (cf. *Saccorhiza ramosa* in Altenbach et al., 1988).

Schönfeld (2002a) describes major occurrences of *R. abyssorum* from the upper MOW core layer and the transition layer above, thus predominantly from distal settings off the Faro Drift. In the northern Gardar Drift, SFT3 taxon *R. abyssorum* primarily colonizes the main path of the ISOW, amidst the strongest current of the drift. However, velocities of the ISOW are much lower than in the core of the MOW and more comparable to its lateral margins.

Overall, the comparison with the Iberian Margin CDS corroborates the hypothesis of chapter 5.2 that tubular agglutinated foraminifera with fragile external morphologies appear to have upper limits for sustained water turbulences. Accordingly, they find optimal habitats in the CDS of the Iceland Basin ([Figure 6](#)).

SFT4 species *Ammolagena clavata* has been recorded as lower slope taxon, that settles primarily in the boundary zones below the MOW core layers at 1000-2000 m depth (Schönfeld, 2002a). This is also reflected in the Iceland Basin, where SFT4 (particularly abundant in groups A2 and B2 of the cluster analysis) represents a distal facies and is related to greater water depths between ca. 2550-2900 m and reduced flow speeds according to the  $\overline{SS}$ -proxy method ( $\overline{SS}$  vector in the CCA; [Figure 5](#)).

## 6 Conclusion

The study of total (stained and unstained) benthic foraminiferal assemblages > 250  $\mu\text{m}$  of the upper 2 cm of sediment from high latitude contourite drift systems (CDS) in the Iceland Basin and along the Greenland Margin reveals variations in meiofaunal distribution along hydrodynamic gradients. Four types of suspension feeding foraminifera (SFT 1-4) are distinguished and related to different

hydrographic regimes. Their distribution depends on bottom current velocity and thus on the sediment composition. The following conclusions are drawn:

- (1) The CDS faunas of the Iceland Basin and south of Greenland differ fundamentally from typical North Atlantic faunas by the dominance of epifaunal taxa. Infaunal species such as *Bolivina*, *Bulimina*, and *Melonis*, which are typical for North Atlantic faunas, are generally underrepresented in the CDS faunas.
- (2) Tubular, agglutinated species (SFTs 2 and 3) dominate the Iceland Basin CDS. High abundances of the fragile *Saccorhiza ramosa* and *Rhizammina algaeformis* (both SFT2) characterize the benthic fauna in the shallower Björn Drift, where low but persistent bottom currents do not exceed  $3.1 \text{ cm s}^{-1}$  (Van Aken and De Boer, 1995). By capturing food particles with their pseudopodial net, these species benefit from the nutrient load carried by the constant bottom flow at the transition between the LSW and ISOW.
- (3) The hydrodynamically more complex setting of the Gardar Drift shows high abundances of facultative suspension feeders and highly adaptable species of SFT3. Bottom current speeds reach maxima of  $10 \text{ cm s}^{-1}$  in the northern Gardar Drift, where *Rhabdammina abyssorum* is clearly dominant over other species. As flow speeds decrease to the south, a *Rhabdammina abyssorum*-*Hoeglundina elegans* assemblage is prevalent.
- (4) Trochospiral, hyaline species of SFT1 characterize the samples off southern Greenland. They show a two-fold distributional pattern. Mean current velocities between  $12\text{-}22 \text{ cm s}^{-1}$  (Hunter et al., 2007b) favour *Cibicidoides wuellerstorfi* and *Heterolepa broeckhiana* in the Eirik Drift, which dominate together with non-SFT-taxon *Hoeglundina elegans*. In shallower, more turbulent bottom waters on the Greenland Margin, however, *Cibicides refulgens*, *Cibicides lobatulus*, and *Cibicidoides pachyderma* dominate the assemblage. The latter assemblage closely resembles associations from the Iberian Margin, where current velocities up to  $100 \text{ cm s}^{-1}$  prevail (Schönfeld, 2002a).
- (5) SFT4 species, only represented by *Ammolagena clavata*, prefer environmental settings less affected by bottom currents (Kuhnt et al., 2000). On the Gardar Drift, they occur in those samples off the main ISOW path, or – where a Holocene sediment cover is missing – reflect glacial conditions with reduced bottom current strength (Bianchi and McCave, 2000; Skinner and Shackleton, 2004).

The considerable differences in faunal composition observed within and between the studied CDS as well as between high and mid-latitude CDSs suggests that foraminifera-based reconstructions of hydrodynamic conditions must rely on well-established regional baseline studies. The present study thus provides an initial framework for the applicability of foraminifera as bottom current indicators in the high latitudes of the Atlantic Ocean.

## Author Contributions

**Anna Saupe** performed the statistical analyses and wrote the manuscript. **Anna Saupe**, Jassin Petersen and Patrick Grunert drafted the concept of the study and contributed to the evaluation of the statistical analyses. **Anna Saupe** and Johanna Schmidt conducted the taxonomic evaluation. André Bahr contributed to the interpretation of sedimentological parameters.

## Acknowledgments

The authors would like to thank Joachim Schönfeld (Geomar, Kiel) for his taxonomic advice and helpful discussions, as well as for providing access to his extensive repertoire of specimens and literature. The RAPID and NEAPACC sample material was kindly provided by Nick McCave and Simon Crowhurst (Cambridge University). We would also like to thank Volker Wennrich (University of Cologne) for his support with the grain size analyses, and Hanna Cieszynski (University of Cologne) for her support with the SEM. Finally, we acknowledge the effort of three anonymous reviewers. This study was financially supported and enabled by the Deutsche Forschungsgemeinschaft (DFG, German Research Foundation) within the project GR52851/1-1.

## Supplementary Material

Supplementary data to this article can be found online at <https://doi.org/10.1016/j.palaeo.2022.111312>.

## References

- Altenbach, A. V., Lutze, G.F., Weinholz, P., 1987. Beobachtungen an Benthos-Foraminiferen (Teilprojekt A3). Berichte aus dem Sonderforschungsbereich 313 (6), pp. 86.
- Altenbach, A. V., Unsöld, G., Walger, E., 1988. The hydrodynamic Environment of *Saccorhiza ramosa* (BRADY). Meyniana 40, 119–132.
- Altenbach, A. V., Heeger, T., Linke, P., Spindler, M., Thies, A., 1993. *Miliolinella subrotunda* (Montagu), a miliolid foraminifer building large detritic tubes for a temporary epibenthic lifestyle. Mar. Micropaleontol. 20, 293–301. [https://doi.org/10.1016/0377-8398\(93\)90038-Y](https://doi.org/10.1016/0377-8398(93)90038-Y)
- Alve, E., Murray, J.W., 1997. High benthic fertility and taphonomy of foraminifera: A case study of the Skagerrak, North Sea. Mar. Micropaleontol. 31, 157–175. [https://doi.org/10.1016/S0377-8398\(97\)00005-4](https://doi.org/10.1016/S0377-8398(97)00005-4)
- Balestra, B., Grunert, P., Ausin, B., Hodell, D., Flores, J.A., Alvarez-Zarikian, C.A., Hernandez-Molina, F.J., Stow, D., Piller, W.E., Paytan, A., 2017. Coccolithophore and benthic foraminifera distribution patterns in the Gulf of Cadiz and Western Iberian Margin during Integrated Ocean Drilling Program (IODP) Expedition 339. J. Mar. Syst. 170, 50–67.



<https://doi.org/10.1016/j.imarsys.2017.01.005>

- Belanger, P.E., Streeter, S.S., 1980. Distribution and ecology of benthic foraminifera in the Norwegian-Greenland Sea. *Mar. Micropaleontol.* 5, 401–428. [https://doi.org/10.1016/0377-8398\(80\)90020-1](https://doi.org/10.1016/0377-8398(80)90020-1)
- Bhaumik, A.K., Gupta, A.K., Clemens, S.C., Mazumder, R., 2014. Functional morphology of *Melonis barleeanum* and *Hoeglundina elegans*: A proxy for water-mass characteristics. *Curr. Sci.* 106, 1133–1140. <https://doi.org/10.18520/cs/v106/i8/1133-1140>
- Bianchi, G.G., McCave, I.N., 1999. Holocene periodicity in North Atlantic climate and deep-ocean flow south of Iceland. *Nature* 397, 515–517. <https://doi.org/10.1038/17362>
- Bianchi, G.G., McCave, I.N., 2000. Hydrography and sedimentation under the deep western boundary current on Björn and Gardar Drifts, Iceland Basin. *Mar. Geol.* 165, 137–169. [https://doi.org/10.1016/S0025-3227\(99\)00139-5](https://doi.org/10.1016/S0025-3227(99)00139-5)
- Bianchi, G.G., Hall, I.R., McCave, I.N., Joseph, L., 1999. Measurement of the sortable silt current speed proxy using the Sedigraph 5100 and Coulter Multisizer II: Precision and accuracy. *Sedimentology* 46, 1001–1014. <https://doi.org/10.1046/j.1365-3091.1999.00256.x>
- Blott, S.J., Pye, K., 2001. Gradistat: A grain size distribution and statistics package for the analysis of unconsolidated sediments. *Earth Surf. Process. Landforms* 26, 1237–1248. <https://doi.org/10.1002/esp.261>
- Cartwright, N.G., Gooday, A.J., Jones, A.R., 1989. The morphology, internal organization, and taxonomic position of *Rhizammina algaeformis* Brady, a large, agglutinated, deep-sea foraminifer. *J. Foraminifer. Res.* 19, 115–125. <https://doi.org/10.2113/gsjfr.19.2.115>
- Cedhagen, T., 1993. Taxonomy and biology of *Pelosina arborescens* with comparative notes on *Astrorhiza limicola* (Foraminiferida). *Ophelia* 37, 143–162. <https://doi.org/10.1080/00785326.1993.10429914>
- Cimerman, F., Langer, M.R., 1991. Mediterranean Foraminifera. Slovenska Akademija Znanosti in Umetnosti. Ljubljana, pp. 118, pl. 93.
- Clarke, R.A., 1984. Transport through the Cape Farewell-Flemish Cap section. *Rapp. Procès-verbaux des Réunion. Int. Counc. Explor. Sea.* 185, 120–130. [https://doi.org/10.1016/0198-0254\(85\)92659-7](https://doi.org/10.1016/0198-0254(85)92659-7)
- Culver, S.J., Lipps, J.H., 2003. Predation on and by Foraminifera, in: Kelley, P.H., Kowalewski, M., Hansen, T.A. (Eds.), *Predator – Prey Interactions in the Fossil Record. Topics in Geobiology*, vol. 20. Springer, Boston, MA, pp. 7–32. [https://doi.org/10.1007/978-1-4615-0161-9\\_2](https://doi.org/10.1007/978-1-4615-0161-9_2)
- de Castro, S., Hernández-Molina, F.J., de Weger, W., Jiménez-Espejo, F.J., Rodríguez-Tovar, F.J., Mena, A., Llave, E., Sierro, F.J., 2021. Contourite characterization and its discrimination from other deep-water deposits in the Gulf of Cadiz contourite depositional system. *Sedimentology* 68, 987–1027. <https://doi.org/10.1111/sed.12813>

- de Mello e Sousa, S.H., Passos, R.F., Fukumoto, M., da Silveira, I.C.A., Figueira, R.C.L., Koutsoukos, E.A.M., de Mahiques, M.M., Rezende, C.E., 2006. Mid-lower bathyal benthic foraminifera of the Campos Basin, Southeastern Brazilian margin: Biotopes and controlling ecological factors. *Mar. Micropaleontol.* 61, 40-57. <https://doi.org/10.1016/j.marmicro.2006.05.003>
- De Stigter, H.C., Jorissen, F.J., Van Der Zwaan, G.J., 1998. Bathymetric distribution and microhabitat partitioning of live (Rose Bengal stained) benthic foraminifera along a shelf to bathyal transect in the southern Adriatic Sea. *J. Foraminifer. Res.* 28, 40–65.
- Diz, P., Guillermo, F., Costas, S., Souto, C., Alejo, I., 2004. Distribution of benthic foraminifera in coarse sediments, Ria de Vigo, NW Iberian Margin. *J. Foraminifer. Res.* 34, 258-275. <https://doi.org/10.2113/34.4.258>
- Dorst, S., Schönfeld, J., 2013. Diversity of benthic foraminifera on the shelf and slope of the ne atlantic: Analysis of datasets. *J. Foraminifer. Res.* 43, 238–254. <https://doi.org/10.2113/gsjfr.43.3.238>
- Dubicka, Z., Zlotnik, M., Borszcz, T., 2015. Test morphology as a function of behavioral strategies - Inferences from benthic foraminifera. *Mar. Micropaleontol.* 116, 38–49. <https://doi.org/10.1016/j.marmicro.2015.01.003>
- Ellett, D.J., Martin, J.H.A., 1973. The physical and chemical oceanography of the Rockall channel. *Deep. Res. Oceanogr. Abstr.* 20. [https://doi.org/10.1016/0011-7471\(73\)90030-2](https://doi.org/10.1016/0011-7471(73)90030-2)
- Fajemila, O.T., Langer, M.R., Lipps, J.H., 2015. Spatial patterns in the distribution, diversity and abundance of benthic foraminifera around Moorea (Society Archipelago, French Polynesia). *PLoS One* 10, 1–25. <https://doi.org/10.1371/journal.pone.0145752>
- Fatela, F., Taborda, R., 2002. Confidence limits of species proportions in microfossil assemblages. *Mar. Micropaleontol.* 45, 169–174. [https://doi.org/10.1016/S0377-8398\(02\)00021-X](https://doi.org/10.1016/S0377-8398(02)00021-X)
- Faugères, J.C., Mézerais, M.L., Stow, D.A.V., 1993. Contourite drift types and their distribution in the North and South Atlantic Ocean basins. *Sediment. Geol.* 82, 189–203. [https://doi.org/10.1016/0037-0738\(93\)90121-K](https://doi.org/10.1016/0037-0738(93)90121-K)
- Faugères, J.C., Stow, D.A.V., Imbert, P., Viana, A., 1999. Seismic features diagnostic of contourite drifts. *Mar. Geol.* 162, 1–38. [https://doi.org/10.1016/S0025-3227\(99\)00068-7](https://doi.org/10.1016/S0025-3227(99)00068-7)
- Fentimen, R., Rüggeberg, A., Lim, A., Kateb, A. El, Foubert, A., Wheeler, A.J., Spezzaferri, S., 2018. Benthic foraminifera in a deep-sea high-energy environment: the Moira Mounds (Porcupine Seabight, SW of Ireland). *Swiss J. Geosci.* 111, 533–544. <https://doi.org/10.1007/s00015-018-0317-4>
- Fentimen, R., Lim, A., Rüggeberg, A., Wheeler, A.J., Rooij, D. Van, 2020. Impact of bottom water currents on benthic foraminiferal assemblages in a cold-water coral environment: The Moira Mounds (NE Atlantic). *Mar. Micropaleontol.* 154, 1–14. <https://doi.org/10.1016/j.marmicro.2019.101799>
- Folk, R.L., Ward, W.C., 1957. Brazos River bar: a study in the significance of grain size parameters. *J.*

- Sediment. Res. 27, 3–26. <https://doi.org/10.1306/74D70646-2B21-11D7-8648000102C1865D>
- Fontanier, C., Jorissen, F.J., Licari, L., Alexandre, A., Anschutz, P., Carbonel, P., 2002. Live benthic foraminiferal faunas from the Bay of Biscay: Faunal density, composition, and microhabitats. Deep. Res. Part I Oceanogr. Res. Pap. 49, 751-785. [https://doi.org/10.1016/S0967-0637\(01\)00078-4](https://doi.org/10.1016/S0967-0637(01)00078-4)
- Fontanier, C., Jorissen, F., Anschutz, P., Chaillou, G., 2006. Seasonal variability of benthic foraminiferal faunas at 1000 m depth in the Bay of Biscay. J. Foraminifer. Res. 36, 61–76. <https://doi.org/10.2113/36.1.61>
- Gili, J.M., Coma, R., 1998. Benthic suspension feeders: Their paramount role in littoral marine food webs. Trends Ecol. Evol. 13, 316-321. [https://doi.org/10.1016/S0169-5347\(98\)01365-2](https://doi.org/10.1016/S0169-5347(98)01365-2)
- Gonzales, M. V., De Almeida, F.K., Costa, K.B., Santarosa, A.C.A., Camillo, E.J., de Quadros, J.P., Toledo, F.A.L., 2017. Help Index: Hoeglundina Elegans Preservation Index For Marine Sediments in the Western South Atlantic. J. Foraminifer. Res. 47, 56–69. <https://doi.org/https://doi.org/10.2113/gsjfr.47.1.56>
- Gooday, A.J., 1986. Meiofaunal foraminiferans from the bathyal Porcupine Seabight (northeast Atlantic): size structure, standing stock, taxonomic composition, species diversity and vertical distribution in the sediment. Deep Sea Res. Part A, Oceanogr. Res. Pap. 33. [https://doi.org/10.1016/0198-0149\(86\)90040-3](https://doi.org/10.1016/0198-0149(86)90040-3)
- Gooday, A.J., 1996. Epifaunal and shallow infaunal foraminiferal communities at three abyssal NE Atlantic sites subject to differing phytodetritus input regimes. Deep. Res. Part I Oceanogr. Res. Pap. 43, 1395–1421. [https://doi.org/10.1016/S0967-0637\(96\)00072-6](https://doi.org/10.1016/S0967-0637(96)00072-6)
- Gooday, A.J., Jorissen, F.J., 2012. Benthic foraminiferal biogeography: Controls on global distribution patterns in deep-water settings. Ann. Rev. Mar. Sci. 4, 237–262. <https://doi.org/10.1146/annurev-marine-120709-142737>
- Gooday, A.J., Levin, L.A., Thomas, C.L., Hecker, B., 1992. The distribution and ecology of *Bathysiphon filiformis* Sars and *B. major* de Folin (Protista, Foraminiferida) on the continental slope off North Carolina. J. Foraminifer. Res. 22, 129–146. <https://doi.org/10.2113/gsjfr.22.2.129>
- Guo, Q., Li, B., Kim, J.K., 2017. Benthic foraminiferal assemblages and bottom water evolution off the Portuguese margin since the Middle Pleistocene. Glob. Planet. Change 150, 94-108. <https://doi.org/10.1016/j.gloplacha.2016.11.004>
- Hammer, Ø., Harper, D.A.T., Ryan, P.D., 2001. Past: Paleontological Statistics Software Package for Education and Data Analysis. Palaeontol. Electron. 4, 1–9.
- Harloff, J., Mackensen, A., 1997. Recent benthic foraminiferal associations and ecology of the Scotia Sea and Argentine Basin. Mar. Micropaleontol. 31, 1–29. [https://doi.org/10.1016/S0377-8398\(96\)00059-X](https://doi.org/10.1016/S0377-8398(96)00059-X)
- Haunold, T.G., 1999. Ecologically controlled distribution of recent Textulariid foraminifera in

- subtropical, carbonate-rich Safaga Bay (Red Sea, Egypt). *Beiträge zur Paläontologie* 24, 69–85.
- Hayward, B.W., Grenfell, H.R., Sabaa, A.T., Neil, H.L., Buzas, M.A., 2010. Recent New Zealand deep-water benthic foraminifera: taxonomy, ecologic distribution, biogeography, and use in paleoenvironmental assessment. GNS Science monograph 26, Lower Hutt, New Zealand.
- Heezen, B.C., Hollister, C., 1964. Deep-sea current evidence from abyssal sediments. *Mar. Geol.* 1, 141–174. [https://doi.org/10.1016/0025-3227\(64\)90012-X](https://doi.org/10.1016/0025-3227(64)90012-X)
- Hernández-Molina, F.J., Stow, D.A.V., Alvarez-Zarikian, C.A., Acton, G., Bahr, A., Balestra, B., Ducassou, E., Flood, R., Flores, J.A., Furota, S., Grunert, P., Hodell, D., Jimenez-Espejo, F., Kim, J.K., Krissek, L., Kuroda, J., Li, B., Llave, E., Lofi, J., Lourens, L., Miller, M., Nanayama, F., Nishida, N., Richter, C., Roque, C., Pereira, H., Sanchez Goñi, M.F., Sierra, F.J., Singh, A.D., Sloss, C., Takashimizu, Y., Tzanova, A., Voelker, A., Williams, T., Xuan, C., 2014. Onset of Mediterranean outflow into the North Atlantic. *Science* 344 (6189), 1244–1250. <https://doi.org/10.1126/science.1251306>
- Holliday, N.P., Pollard, R.T., Read, J.F., Leach, H., 2000. Water mass properties and fluxes in the Rockall Trough, 1975-1998. *Deep. Res. Part I Oceanogr. Res. Pap.* 47, 1303–1332. [https://doi.org/10.1016/S0967-0637\(99\)00109-0](https://doi.org/10.1016/S0967-0637(99)00109-0)
- Holliday, N.P., Meyer, A., Bacon, S., Alderson, S.G., de Cuevas, B., 2007. Retroflexion of part of the east Greenland current at Cape Farewell. *Geophys. Res. Lett.* 34, 1–5. <https://doi.org/10.1029/2006GL029085>
- Hunter, S.E., Wilkinson, D., Louarn, E., McCave, I.N., Rohling, E., Stow, D.A.V., Bacon, S., 2007a. Deep western boundary current dynamics and associated sedimentation on the Eirik Drift, Southern Greenland Margin. *Deep. Res. Part I Oceanogr. Res. Pap.* 54, 2036–2066. <https://doi.org/10.1016/j.dsr.2007.09.007>
- Hunter, S.E., Wilkinson, D., Stanford, J., Stow, D.A.V., Bacon, S., Akhmetzhanov, A.M., Kenyon, N.H., 2007b. The Eirik Drift: A long-term barometer of North Atlantic deepwater flux south of Cape Farewell, Greenland, in: Viana, A.R., Rebesco, M. (Eds.), *Economic and Palaeoceanographic Significance of Contourite Deposits*. Geological Society Special Publication. London, pp. 245–263. <https://doi.org/10.1144/GSL.SP.2007.276.01.12>
- Jones, R.W., 1994. *The Challenger Foraminifera*. Oxford University Press. New York, pp. 149.
- Jorissen, F.J., Fontanier, C., Thomas, E., 2007. Paleoceanographical proxies based on deep-sea benthic foraminiferal assemblage characteristics, in: Hillaire-Marcel, C., de Vernal, A. (Eds.), *Proxies in Late Cenozoic Paleoceanography: Pt. 2: Biological Tracers and Biomarkers*. pp. 263–325. [https://doi.org/10.1016/S1572-5480\(07\)01012-3](https://doi.org/10.1016/S1572-5480(07)01012-3)
- Kaminski, M.A., 1985. Evidence for control of abyssal agglutinated foraminiferal community structure by substrate disturbance: results from the HEBBLE area. *Mar. Geol.* 66, 113–131. [https://doi.org/10.1016/0025-3227\(85\)90025-8](https://doi.org/10.1016/0025-3227(85)90025-8)
- Kaminski, M.A., Cetaan, C.G., Henderson, A.S., 2008. Lectotypes of type species of Agglutinated

- Foraminiferal Genera in the Collections of the Natural History Museum, London. Part 1. Astrorhizina and Saccamminina, in: Kaminski, M.A., Coccioni, R. (Eds.), Proceedings of the Seventh International Workshop on Agglutinated Foraminifera. Grzybowski Foundation Special Publication 13, pp. 63–77.
- Kender, S., Kaminski, M.A., 2017. Modern deep-water agglutinated foraminifera from IODP Expedition 323, Bering Sea: ecological and taxonomic implications. *J. Micropalaeontology* 36, 195–218. <https://doi.org/10.1144/jmpaleo2016-026>
- Knutz, P.C., 2008. Chapter 24 Palaeoceanographic Significance of Contourite Drifts. *Dev. Sedimentol.* 60, 511–535. [https://doi.org/10.1016/S0070-4571\(08\)10024-3](https://doi.org/10.1016/S0070-4571(08)10024-3)
- Kuhlbrodt, T., Griesel, A., Montoya, M., Levermann, A., Hofmann, M., Rahmstorf, S., 2007. On the driving processes of the Atlantic meridional overturning circulation. *Rev. Geophys.* 2, 1–32. <https://doi.org/10.1029/2004RG000166>
- Kuhnt, W., Collins, E., Scott, D.B., 2000. Deep Water Agglutinated Foraminiferal Assemblages across the Gulf Stream: Distribution Patterns and Taphonomy, in: Hart, M.B., Kaminski, M.A., & Smart, C.W. (Eds) 2000. Proceedings of the Fifth International Workshop on Agglutinated Foraminifera. Grzybowski Foundation Special Publication, 7. pp. 261–298.
- Kurbjeweit, F., Schmiedel, G., Schiebel, R., Hemleben, C., Pfannkuche, O., Wallmann, K., Schäfer, P., 2000. Distribution, biomass and diversity of benthic foraminifera in relation to sediment geochemistry in the Arabian Sea. *Deep. Res. Part II Top. Stud. Oceanogr.* 47, 2913–2955. [https://doi.org/10.1016/S0967-0645\(00\)00053-9](https://doi.org/10.1016/S0967-0645(00)00053-9)
- Langer, M.R., Lipps, J.H., 2003. Foraminiferal distribution and diversity, Madang Reef and Lagoon, Papua New Guinea. *Coral Reefs* 22, 143–154. <https://doi.org/10.1007/s00338-003-0298-1>
- Lecroq, B., Gooday, A.J., Pawlowski, J.A.N., 2009. Global genetic homogeneity in the deep-sea foraminiferan *Epistominella exigua* (Rotaliida: Pseudoparrellidae). *Zootaxa* 2096, 23–32. <https://doi.org/10.11646/zootaxa.2096.1.4>
- Lee, A., Ellett, D., 1967. On the water masses of the Northwest Atlantic Ocean. *Deep. Res. Oceanogr. Abstr.* 14, 183–190. [https://doi.org/10.1016/0011-7471\(67\)90004-6](https://doi.org/10.1016/0011-7471(67)90004-6)
- Legendre, L., Legendre, P., 1998. *Numerical Ecology*, Volume 24, 2nd english ed. Elsevier Science. Amsterdam, pp. 852.
- Lindenberg, H.G., Auras, A., 1984. Distribution of arenaceous foraminifera in depth profiles of the Southern Ocean (Kerguelen Plateau area). *Palaeogeogr. Palaeoclimatol. Palaeoecol.* 48, 61–106. [https://doi.org/10.1016/0031-0182\(84\)90092-0](https://doi.org/10.1016/0031-0182(84)90092-0)
- Linke, P., 1992. Metabolic adaptations of deep-sea benthic foraminifera to seasonally varying food input. *Mar. Ecol. Prog. Ser.* 81, 51–63. <https://doi.org/10.3354/meps081051>
- Linke, P., Lutze, G.F., 1993. Microhabitat preferences of benthic foraminifera - a static concept or a dynamic adaptation to optimize food acquisition?. *Mar. Micropaleontol.* 20, 215–234.

[https://doi.org/10.1016/0377-8398\(93\)90034-U](https://doi.org/10.1016/0377-8398(93)90034-U)

- Lintner, B., Lintner, M., Bukenberger, P., Witte, U., Heinz, P., 2021. Living benthic foraminiferal assemblages of a transect in the Rockall Trough (NE Atlantic). *Deep. Res. Part I* 171, 1–19  
<https://doi.org/10.1016/j.dsr.2021.103509>
- Lohmann, G.P., 1978. Abyssal benthonic foraminifera as hydrographic indicators in the western South Atlantic Ocean. *J. Foraminifer. Res.* 8, 6-34. <https://doi.org/10.2113/gsjfr.8.1.6>
- Loubere, P., 1989. Bioturbation and sedimentation rate control of benthic microfossil taxon abundances in surface sediments: A theoretical approach to the analysis of species microhabitats. *Mar. Micropaleontol.* 14, 317–325. [https://doi.org/10.1016/0377-8398\(89\)90016-9](https://doi.org/10.1016/0377-8398(89)90016-9)
- Lukashina, N.P., 1988. Benthic Foraminifera Communities and Water Masses of the North Atlantic and the Norway-Greenland Basin. *Oceanology* 28, 612-617.
- Lukashina, N.P., 2013. Water masses of the northern part of the Iceland Basin in the late Pleistocene. *Oceanology* 53, 99-109. <https://doi.org/10.1134/S0001437013010128>
- Lukashina, N.P., Bashirova, L.D., 2015. Deep water masses in the Iceland Basin during the Last Interglacial (MIS 5e): Evidence from benthic foraminiferal data. *Oceanologia* 57, 212-221. <https://doi.org/10.1016/j.oceano.2014.11.004>
- Lutze, G.F., Altenbach, A. V., 1988. *Rupertina stabilis* (Wallich), a highly adapted, suspension feeding foraminifer. *Meyniana* 40, 55-69. <https://doi.org/10.2312/meyniana.1988.40.55>
- Lutze, G.F., Coulbourn, W.T., 1984. Recent benthic foraminifera from the continental margin of northwest Africa: Community structure and distribution. *Mar. Micropaleontol.* 8, 361-401. [https://doi.org/10.1016/0377-8398\(84\)90002-1](https://doi.org/10.1016/0377-8398(84)90002-1)
- Lutze, G.F., Thiel, H., 1989. Epibenthic foraminifera from elevated microhabitats; *Cibicidoides wuellerstorfi* and *Planulina ariminensis*. *J. Foraminifer. Res.* 19, 153-158. <https://doi.org/10.2113/gsjfr.19.2.153>
- Mackensen, A., 1987. Benthische Foraminiferen auf dem Island-Schottland Rücken: Umwelt-Anzeiger an der Grenze zweier ozeanischer Räume. *Paläontologische Zeitschrift* 61, 149-179. <https://doi.org/10.1007/BF02985902>
- Mackensen, A., Sejrup, H.P., Jansen, E., 1985. The distribution of living benthic foraminifera on the continental slope and rise off southwest Norway. *Mar. Micropaleontol.* 9, 275-306. [https://doi.org/10.1016/0377-8398\(85\)90001-5](https://doi.org/10.1016/0377-8398(85)90001-5)
- Mackensen, A., Schmiedl, G., Harloff, J., Giese, M., 1995. Deep-Sea Foraminifera in the South Atlantic Ocean: Ecology and Assemblage Generation. *Micropaleontology* 41, 342-358. <https://doi.org/10.2307/1485808>
- Manighetti, B., McCave, I.N., 1995. Late glacial and Holocene paleocurrents around Rockall Bank, NE

- Atlantic Ocean. *Paleoceanography* 10, 611-626. <https://doi.org/10.1029/94PA03059>
- Manley, P.L., Caress, D.W., 1994. Mudwaves on the Gardar sediment drift, NE Atlantic. *Paleoceanography* 9, 973-988. <https://doi.org/10.1029/94PA01755>
- McCave, I.N., 1994. R.R.S. Charles Darwin Cruise 88. 25<sup>th</sup> July-15<sup>th</sup> August 1994. Reykjavik to Ponta Delgada. For North East Atlantic Palaeoceanography and Climate Change Community Research Project of NERC. University of Cambridge, Department of Earth Sciences, pp. 45.
- McCave, I.N., 2005. R.R.S. Charles Darwin Cruise 159. 1<sup>st</sup>-30<sup>th</sup> July 2004. Fairlie, Scotland to St. John's, Newfoundland. For the RAPID Climate Change Research Programme of NERC under grant NER/T/S/2002/00436. University of Cambridge, Department of Earth Sciences, pp. 49.
- McCave, I.N., Hall, I.R., 2006. Size sorting in marine muds: Processes, pitfalls, and prospects for paleoflow-speed proxies. *Geochemistry, Geophys. Geosystems* 7, 1-37. <https://doi.org/10.1029/2006GC001284>
- McCave, I.N., Tucholke, B.E., 1986. Deep current-controlled sedimentation in the western North Atlantic. In: Vogt, P.R., Tucholke, B.E. (Eds.). *The Geology of North America. The Western North Atlantic Region, Decade of North American Geology*. Geological Society of America, pp. 451-468. <https://doi.org/10.1130/dnag-gna-m.451>
- McCave, I.N., Lonsdale, P.F., Hollister, C.D., Gardner, W.D., 1980. Sediment transport over the Hatton and Gardar Contourite Drifts. *J. Sediment. Petrol.* 50, 1049-1062. <https://doi.org/10.1306/212F7B76-2B24-11D7-8648000102C1865D>
- McCave, I.N., Manighetti, B., Robinson, S.G., 1995. Sortable silt and fine sediment size/composition slicing: Parameters for palaeocurrent speed and palaeoceanography. *Paleoceanography* 10, 593-610. <https://doi.org/10.1029/94PA03039>
- McCave, I.N., Thornalley, D.J.R., Hall, I.R., 2017. Relation of sortable silt grain-size to deep-sea current speeds: Calibration of the 'Mud Current Meter'. *Deep. Res. Part I Oceanogr. Res. Pap.* 127, 1-12. <https://doi.org/10.1016/j.dsr.2017.07.003>
- Milker, Y., Schmiedl, G., 2012. A taxonomic guide to modern benthic shelf foraminifera of the western Mediterranean Sea. *Palaeontol. Electron.* 15, 1-134. <https://doi.org/10.26879/271>
- Moffa-Sánchez, P., Moreno-Chamarro, E., Reynolds, D.J., Ortega, P., Cunningham, L., Swingedouw, D., Amrhein, D.E., Halfar, J., Jonkers, L., Jungclaus, J.H., Perner, K., Wanamaker, A., Yeager, S., 2019. Variability in the Northern North Atlantic and Arctic Oceans Across the Last Two Millennia: A Review. *Paleoceanogr. Paleoclimatology* 34, 1399-1436. <https://doi.org/10.1029/2018PA003508>
- Müller-Michaelis, A., Uenzelmann-Neben, G., Stein, R., 2013. A revised Early Miocene age for the instigation of the Eirik Drift, offshore southern Greenland: Evidence from high-resolution seismic reflection data. *Mar. Geol.* 340, 1-15. <https://doi.org/10.1016/j.margeo.2013.04.012>
- Müller-Michaelis, A., Uenzelmann-Neben, G., 2014. Development of the Western Boundary

- Undercurrent at Eirik Drift related to changing climate since the early Miocene. *Deep. Res. Part I Oceanogr. Res. Pap.* 93, 21-34. <https://doi.org/10.1016/j.dsr.2014.07.010>
- Murray, J.W., 2006. *Ecology and Applications of Benthic Foraminifera*. Cambridge University Press, Cambridge, pp. 440.
- Paliy, O., Shankar, V., 2016. Application of multivariate statistical techniques in microbial ecology. *Mol. Ecol.* 25, 1032-1057. <https://doi.org/10.1111/mec.13536>
- Parnell-Turner, R., White, N.J., McCave, I.N., Henstock, T.J., Murton, B., Jones, S.M., 2015. Architecture of North Atlantic contourite drifts modified by transient circulation of the Icelandic mantle plume. *Geochemistry Geophys. Geosystems* 16, 3414-3435. <https://doi.org/10.1002/2015GC005947>
- Patterson, R.T., Fishbein, E., 1989. Re-examination of the statistical methods used to determine the number of point counts needed for micropaleontological quantitative research. *J. Paleontol.* 63, 245–248. <https://doi.org/10.1017/S002233600019272>
- Petro, S.M., Pivel, M.A.G., Coimbra, J.C., 2018. Foraminiferal solubility rankings: A contribution to the search for consensus. *J. Foraminifer. Res.* 48, 301-313. <https://doi.org/10.2113/gsjfr.48.4.301>
- Pickart, R.S., 1992. Water mass components of the North Atlantic deep western boundary current. *Deep Sea Res. Part A, Oceanogr. Res. Pap.* 39, 1553-1572. [https://doi.org/10.1016/0198-0149\(92\)90047-W](https://doi.org/10.1016/0198-0149(92)90047-W)
- Ramette, A., 2007. Multivariate analyses in microbial ecology. *FEMS Microbiol. Ecol.* 62, 142-160. <https://doi.org/10.1111/j.1574-6941.2007.00375.x>
- Rasmussen, T.L., Thomsen, E., 2017. Ecology of deep-sea benthic foraminifera in the North Atlantic during the last glaciation: Food or temperature control. *Palaeogeogr. Palaeoclimatol. Palaeoecol.* 472, 15-32. <https://doi.org/10.1016/j.palaeo.2017.02.012>
- Rasmussen, T.L., Thomsen, E., Troelstra, S.R., Kuijpers, A., Prins, M.A., 2002. Millennial-scale glacial variability versus Holocene stability: changes in planktic and benthic foraminifera faunas and ocean circulation in the North Atlantic during the last 60 000 years. *Mar. Micropaleontol.* 47, 143-176. [https://doi.org/10.1016/S0377-8398\(02\)00115-9](https://doi.org/10.1016/S0377-8398(02)00115-9)
- Rebesco, M., Hernández-Molina, F.J., Van Rooij, D., Wählin, A., 2014. Contourites and associated sediments controlled by deep-water circulation processes: State-of-the-art and future considerations. *Mar. Geol.* 352, 111-154. <https://doi.org/10.1016/j.margeo.2014.03.011>
- Rodrigues, A.R., Maluf, J.C.C., Braga, E.D.S., Eichler, B.B., 2010. Recent benthic foraminiferal distribution and related environmental factors in Ezcurra Inlet, King George Island, Antarctica. *Antarct. Sci.* 22, 343-360. <https://doi.org/10.1017/S0954102010000179>
- Rogerson, M., Schönfeld, J., Leng, M.J., 2011. Qualitative and quantitative approaches in palaeohydrography: A case study from core-top parameters in the Gulf of Cadiz. *Mar. Geol.* 280, 150-167. <https://doi.org/10.1016/j.margeo.2010.12.008>



- Ryan, W.B.F., Carbotte, S.M., Coplan, J.O., O'Hara, S., Melkonian, A., Arko, R., Weissel, R.A., Ferrini, V., Goodwillie, A., Nitsche, F., Bonczkowski, J., Zemsky, R., 2009. Global Multi-Resolution Topography synthesis. *Geochemistry, Geophys. Geosystems* 10, 1-9. <https://doi.org/10.1029/2008GC002332>
- Sánchez-Leal, R.F., Bellanco, M.J., Fernández-Salas, L.M., García-Lafuente, J., Gasser-Rubinat, M., González-Pola, C., Hernández-Molina, F.J., Pelegrí, J.L., Peliz, A., Relvas, P., Roque, D., Ruiz-Villarreal, M., Sammartino, S., Sánchez-Garrido, J.C., 2017. The Mediterranean Overflow in the Gulf of Cadiz: A rugged journey. *Sci. Adv.* 3, 1-12. <https://doi.org/10.1126/sciadv.aao0609>
- Sarnthein, M., Winn, K., Jung, S.J.A., Duplessy, J. -C., Labeyrie, L., Erlenkeuser, H., Ganssen, G., 1994. Changes in East Atlantic Deepwater Circulation over the last 30,000 years: Eight time slice reconstructions. *Paleoceanography* 9, 209-267. <https://doi.org/10.1029/93PA03301>
- Sayago-Gil, M., Long, D., Hitchen, K., Díaz-del-Río, V., Fernández-Salas, L.M., Durán-Muñoz, P., 2010. Evidence for current-controlled morphology along the western slope of Hatton Bank (Rockall Plateau, NE Atlantic Ocean). *Geo-Marine Lett.* 30, 99-111. <https://doi.org/10.1007/s00367-009-0163-5>
- Schmiedl, G., Mackensen, A., Müller, P.J., 1997. Recent benthic foraminifera from the eastern South Atlantic Ocean: Dependence on food supply and water masses. *Mar. Micropaleontol.* 32, 249-287. [https://doi.org/10.1016/S0377-8398\(97\)00023-6](https://doi.org/10.1016/S0377-8398(97)00023-6)
- Schmiedl, G., De Bovée, F., Buscail, R., Charrière, B., Hemleben, C., Medernach, L., Picon, P., 2000. Trophic control of benthic foraminiferal abundance and microhabitat in the bathyal Gulf of Lions, western Mediterranean Sea. *Mar. Micropaleontol.* 40, 167-188. [https://doi.org/10.1016/S0377-8398\(00\)00038-4](https://doi.org/10.1016/S0377-8398(00)00038-4)
- Schmitz, W.J., McCartney, M.S., 1993. On the North Atlantic Circulation. *Rev. Geophys.* 31, 29-49. <https://doi.org/10.1029/92RG02583>
- Schönfeld, J., 1997. The impact of the Mediterranean Outflow Water (MOW) on benthic foraminiferal assemblages and surface sediments at the southern Portuguese continental margin, *Mar. Micropaleontol.* 29, 211-236. [https://doi.org/10.1016/S0377-8398\(96\)00050-3](https://doi.org/10.1016/S0377-8398(96)00050-3)
- Schönfeld, J., 2002a. Recent benthic foraminiferal assemblages in deep high-energy environments from the Gulf of Cadiz (Spain). *Mar. Micropaleontol.* 44, 141-162. [https://doi.org/10.1016/S0377-8398\(01\)00039-1](https://doi.org/10.1016/S0377-8398(01)00039-1)
- Schönfeld, J., 2002b. A new benthic foraminiferal proxy for near-bottom current velocities in the Gulf of Cadiz, northeastern Atlantic Ocean. *Deep. Res. I* 49, 1853-1875. [https://doi.org/10.1016/S0967-0637\(02\)00088-2](https://doi.org/10.1016/S0967-0637(02)00088-2)
- Schönfeld, J., 2006. Taxonomy and Distribution of the *Uvigerina Peregrina* Plexus in the Tropical to Northeastern Atlantic. *J. Foraminifer. Res.* 36, 355-367. <https://doi.org/10.2113/gsjfr.36.4.355>
- Schönfeld, J., Zahn, R., 2000. Late Glacial to Holocene history of the Mediterranean Outflow. Evidence

- from benthic foraminiferal assemblages and stable isotopes at the Portuguese margin. *Palaeogeogr. Palaeoclimatol. Palaeoecol.* 159, 85-111. [https://doi.org/10.1016/S0031-0182\(00\)00035-3](https://doi.org/10.1016/S0031-0182(00)00035-3)
- Schönfeld, J., Alve, E., Geslin, E., Jorissen, F., Korsun, S., Spezzaferri, S., Abramovich, S., Almogi-Labin, A., du Chatelet, E.A., Barras, C., Bergamin, L., Bicchi, E., Bouchet, V., Cearreta, A., Di Bella, L., Dijkstra, N., Disaro, S.T., Ferraro, L., Frontalini, F., Gennari, G., Golikova, E., Haynert, K., Hess, S., Husum, K., Martins, V., McGann, M., Oron, S., Romano, E., Sousa, S.M., Tsujimoto, A., 2012. The FOBIMO (FORaminiferal Blo-MONitoring) initiative-Towards a standardised protocol for soft-bottom benthic foraminiferal monitoring studies. *Mar. Micropaleontol.* 94-95, 1-13. <https://doi.org/10.1016/j.marmicro.2012.06.001>
- Schröder-Adams, C.J., van Rooyen, D., 2010. Response of Recent Benthic Foraminiferal Assemblages to Contrasting Environments in Baffin Bay and the Northern Labrador Sea , Northwest Atlantic. *Arctic* 64, 317-341. <https://www.jstor.org/stable/23025731>
- Schröder, C.J., Scott, D.B., Medioli, F.S., Bernstein, B.B., Hessler, R.R., 1988. Larger agglutinated foraminifera: comparison of assemblages from central North Pacific and western North Atlantic (Nares Abyssal Plain). *J. Foraminifer. Res.* 18, 25-41.
- Schröder, C.J., 1988. Subsurface preservation potential of agglutinated foraminifera in the Northwest Atlantic Ocean. *Abhandlungen der Geologischen Bundesanstalt* 41, 325–336.
- Schweizer, M., Pawlowski, J., Kouwenhoven, T., van der Zwaan, B., 2009. Molecular Phylogeny of Common Cibicidids and Related Rotaliida (Foraminifera) Based on Small Subunit Rdna Sequences. *J. Foraminifer. Res.* 39, 300-315. <https://doi.org/10.2113/gsjfr.39.4.300>
- Sejrup, H.-P., Fjaeran, T., Hald, M., Beck, L., Hagen, J., Miljeteig, I., Morvik, I., Norvik, O., 1981. Benthonic foraminifera in surface samples from the Norwegian continental margin between 62°N and 65°N. *J. Foraminifer. Res.* 11, 277-295. <https://doi.org/10.2113/gsjfr.11.4.277>
- Sen Gupta, B.K., ed. 2002. *Modern Foraminifera*. Dordrecht, The Netherlands. Kluwer Academic Publishers, pp. 384.
- Sierro, F.J., Hodell, D.A., Andersen, N., Azibei, L.A., Jimenez-Espejo, F.J., Bahr, A., Flores, J.A., Ausin, B., Rogerson, M., Lozano-Luz, R., Lebreiro, S.M., Hernandez-Molina, F.J., 2020. Mediterranean Overflow Over the Last 250 kyr: Freshwater Forcing From the Tropics to the Ice Sheets. *Paleoceanogr. Paleoclimatology* 35, 1-31. <https://doi.org/10.1029/2020PA003931>
- Singh, A.D., Rai, A.K., Tiwari, M., Naidu, P.D., Verma, K., Chaturvedi, M., Niyogi, A., Pandey, D., 2015. Fluctuations of Mediterranean Outflow Water circulation in the Gulf of Cadiz during MIS 5 to 7: Evidence from benthic foraminiferal assemblage and stable isotope records. *Glob. Planet. Change* 133, 125-140. <https://doi.org/10.1016/j.gloplacha.2015.08.005>
- Skinner, L.C., Shackleton, N.J., 2004. Rapid transient changes in northeast Atlantic deep water ventilation age across Termination I. *Paleoceanography* 19, 1-12.

<https://doi.org/10.1029/2003PA000983>

- Smart, C.W., King, S.C., Gooday, A.J., Murray, J.W., Thomas, E., 1994. A benthic foraminiferal proxy of pulsed organic matter paleofluxes. *Mar. Micropaleontol.* 23, 89-99. [https://doi.org/10.1016/0377-8398\(94\)90002-7](https://doi.org/10.1016/0377-8398(94)90002-7)
- Stow, D. A. V., Holbrook, J.A., 1984. North Atlantic contourites: An overview. *Geol. Soc. Spec. Publ.* 15, 245-256. <https://doi.org/10.1144/GSL.SP.1984.015.01.16>
- Stow, D. A. V., Hernández-Molina, F.J., Alvarez Zarikian, C.A., the Expedition 339 Scientists, 2013. Expedition 339 summary. <https://doi.org/10.2204/iodp.proc.339.101.2013>
- Talley, L.D., McCartney, M.S., 1982. Distribution and Circulation of Labrador Sea Water. *J. Phys. Oceanogr.* 12, 1189-1205. [https://doi.org/10.1175/1520-0485\(1982\)012<1189:DACOLS>2.0.CO;2](https://doi.org/10.1175/1520-0485(1982)012<1189:DACOLS>2.0.CO;2)
- Thornalley, D.J.R., Blaschek, M., Davies, F.J., Praetorius, S., Oppo, D.W., McManus, J.F., Hall, I.R., Kleiven, H., Renssen, H., McCave, I.N., 2013. Long-term variations in iceland-scotland overflow strength during the holocene. *Clim. Past* 9, 2073-2084. <https://doi.org/10.5194/cp-9-2073-2013>
- Thornalley, D.J.R., Oppo, D.W., Ortega, P., Robson, J.I., Brierley, C.M., Davis, R., Hall, I.R., Moffa-Sanchez, P., Rose, N.L., Spooner, P.T., Yashayaev, I., Keigwin, L.D., 2018. Anomalously weak Labrador Sea convection and Atlantic overturning during the past 150 years. *Nature* 556, 227-230. <https://doi.org/10.1038/s41586-018-0007-4>
- Uenzelmann-Neben, G., Gruetzner, J., 2018. Chronology of Greenland Scotland Ridge overflow: What do we really know?. *Mar. Geol.* 406, 109-118. <https://doi.org/10.1016/j.margeo.2018.09.008>
- Van Aken, H.M., 1995. Mean currents and current variability in the iceland basin. *Netherlands J. Sea Res.* 33, 135-145. [https://doi.org/10.1016/0077-7579\(95\)90001-2](https://doi.org/10.1016/0077-7579(95)90001-2)
- Van Aken, H.M., De Boer, C.J., 1995. On the synoptic hydrography of intermediate and deep water masses in the Iceland Basin. *Deep. Res. Part I* 42, 165-189. [https://doi.org/10.1016/0967-0637\(94\)00042-Q](https://doi.org/10.1016/0967-0637(94)00042-Q)
- Van Aken, H.M., Becker, G., 1996. Hydrography and through-flow in the north-eastern North Atlantic Ocean: The NANSEN project. *Prog. Oceanogr.* 38, 297-346. [https://doi.org/10.1016/S0079-6611\(97\)00005-0](https://doi.org/10.1016/S0079-6611(97)00005-0)
- Wildish, D., Kristmanson, D., 1997. *Benthic Suspension Feeders and Flow*. Cambridge University Press, New York, pp. 409.
- Wisshak, M., Rüggeberg, A., 2006. Colonisation and bioerosion of experimental substrates by benthic foraminiferans from euphotic to aphotic depths (Kosterfjord, SW Sweden). *Facies* 52, 1-17. <https://doi.org/10.1007/s10347-005-0033-1>

**Citation:** Saupe, A., Schmidt, J., Petersen, J., Bahr, A., and Grunert, P. (2023): Benthic foraminifera in high latitude contourite drift systems (North Atlantic: Björn, Gardar and Eirik drifts). *Palaeogeography Palaeoclimatology Palaeoecology* 609, 1–18. doi: [10.1016/j.palaeo.2022.111312](https://doi.org/10.1016/j.palaeo.2022.111312)

**Received:** 22 March 2022; **Received in revised form:** 6 September 2022; **Accepted:** 3 November 2022.

**Available online:** 19 November 2022; **Published in print:** 1 January 2023.

**\*Correspondence:** Anna Saupe, [anna.saupe@uni-koeln.de](mailto:anna.saupe@uni-koeln.de)

### 3.3 Biogeographic Patterns in the Atlantic Ocean

Saupe et al. in prep.



# Biogeographic Patterns and Local Adaptations of Benthic Foraminifera in Contourite Drift Systems of the Atlantic Ocean

Anna Saupe <sup>1\*</sup>, Jassin Petersen <sup>1</sup>, and Patrick Grunert <sup>1</sup>

<sup>1</sup> Institute of Geology and Mineralogy, University of Cologne, Cologne, Germany

\*Correspondence: Anna Saupe ([anna.saupe@uni-koeln.de](mailto:anna.saupe@uni-koeln.de))

## Abstract

Contourite drift systems (CDS) - large-scale sediment deposits under the influence of persistent bottom currents - provide optimal habitats for current-adapted foraminiferal assemblages. Several studies previously highlighted the relationship between abundances of certain suspension-feeding benthic foraminifera living on elevated substrates and an increased current activity (e.g., Schönfeld, 1997). This led to the introduction of the elevated epifauna (EEF), which is considered a potential proxy for the reconstruction of bottom currents in the Mediterranean Outflow Water (MOW) of the Northeast Atlantic Basin and particularly in the Gulf of Cadiz.

In this study, biogeographic distribution patterns of benthic foraminifera in CDS are evaluated beyond the Northeast Atlantic Basin and the MOW. Assemblages from low latitude (Campos and Brazil Basins, 11-22°S) and high latitude (Eirik, Björn and Gardar Drifts, 55-62°N) Atlantic regions of increased bottom currents and contourite deposits are assessed, all of which are significantly controlled by the Atlantic Meridional Overturning Circulation (AMOC). Multivariate statistical analysis of data sets from MOW- and AMOC-driven areas revealed a biogeographic divide between benthic foraminiferal assemblages along hydrological and hydrodynamic gradients. A highly diverse EEF in the warm (13°C) and saline (38.4) MOW (with *Cibicides lobatulus*, *Cibicides refulgens* and *Planulina ariminensis* as most abundant species) contrasts with a less diverse or even lacking EEF in cold (max. 4°) and average saline (34.2-34.9) AMOC-driven water masses (mainly *Cibicoides wuellerstorfi*). A sensitivity to water temperature is suggested for the EEF by abundant occurrences in warm pelagic and bottom current-related regions of the AMOC (e.g., Greenland Continental Margin, 6-9°C) comparable to MOW conditions. The exceptionally high EEF diversity along the MOW pathway may be the result of a Mediterranean heritage, i.e., through transported propagules in the strong Mediterranean Outflow. At high latitudes (Björn and Gardar drifts), cold and gentle bottom currents (ISOW, max. 10 cm/s) are reflected in the abundances of tubular agglutinated suspension feeders. Tube-shaped taxa such as *Saccorhiza ramosa*, *Rhizammina algaeformis* and *Rhabdammina abyssorum* might function as potential bottom current indicators in the North Atlantic basins. An ecological niche is occupied by cold-water coral (CWC) mounds, providing a unique elevated habitat for EEF species. CWCs reflect the biogeographic divide by abundant occurrences of *Discanomalina coronata* in MOW surrounded CWCs, in contrast to *Cibicoides wuellerstorfi* occurrences in those surrounded by AMOC. This study demonstrates that local hydrological conditions must be considered as significant factors in addition to the current velocity regarding microfaunal proxy development in the Atlantic Ocean.

**Keywords:** Atlantic Ocean, Bottom Currents, Contourite Drift Systems, Suspension Feeders

## 1. Introduction

Benthic foraminifera are highly adaptable to a wide range of environments, which makes them potentially powerful proxies for the reconstruction of palaeoenvironments (e.g., van der Zwaan et al., 1999; Murray, 2001; Jorissen et al., 2007). Physico-chemical parameters such as oxygen, temperature, and salinity function as limiting factors for abundances of benthic foraminifera species, while the organic matter flux directly influences the population density (e.g., Gooday, 2003; Jorissen et al., 2007). Numerous studies already highlighted the relationship between the abundance of certain benthic species and organic matter flux (e.g., Altenbach, 1988; Mackensen et al., 1995; Harloff and Mackensen, 1997; van der Zwaan et al., 1999; Morigi et al., 2001). Some studies, however, also noted that an increased bottom current activity acts as additional controlling factor on the composition of the epibenthic community (Lutze and Coulbourn, 1984; Lutze and Altenbach, 1988; Lutze and Thiel, 1989; Linke and Lutze, 1993; Schönfeld, 1997, 2002a, 2002b, 2012). These studies found that certain species preferentially settle on elevated substrates within the bottom current, including biogenic objects such as hydroids, sponges, erect tubular foraminiferal tests, or terrigenous particles such as pebbles and gravels (Jorissen et al., 2007). Schönfeld (1997) first introduced this elevated epifauna (EEF)-group and assessed its applicability as a reliable bottom current proxy for the Mediterranean Outflow Water (MOW) in the Northeast Atlantic Basin. The Gulf of Cadiz (Spain) serves as key area for the investigation of EEF, as the MOW contour current strongly influences the composition of foraminiferal assemblages (Schönfeld, 2002a). Sediment drift bodies, such as the Faro Drift in the Gulf of Cadiz, form when near-bottom water masses with high current velocities interact with the seafloor over long periods of time (Rebesco et al., 2014). These contourite deposits provide optimal habitats for the EEF. However, the application of the EEF as a bottom current proxy has so far been limited to the Iberian Margin and has been barely tested outside the SW Iberian Margin (e.g., Schönfeld and Zahn, 2000; Diz et al., 2004). In this study, we aim to assess EEF occurrences beyond the Gulf of Cadiz and consider its applicability as a proxy for bottom currents in the Atlantic Ocean ([Figure 1](#)). Research on the benthic fauna from the low latitudes at the Brazilian continental margin already shows an adapted foraminiferal community in the complex hydrodynamic system of the Campos and Brazil basins (Saupe et al., 2022). Investigations of the high-latitude Iceland Basin (Björn and Gardar drifts) reveal that an adapted foraminiferal community of tubular agglutinated suspension feeders seems to replace the EEF in high-latitude CDSs (Saupe et al., 2023). Possible causes that favour, e.g., occurrences of tubular agglutinated species as competitors to the EEF will be addressed in this article.



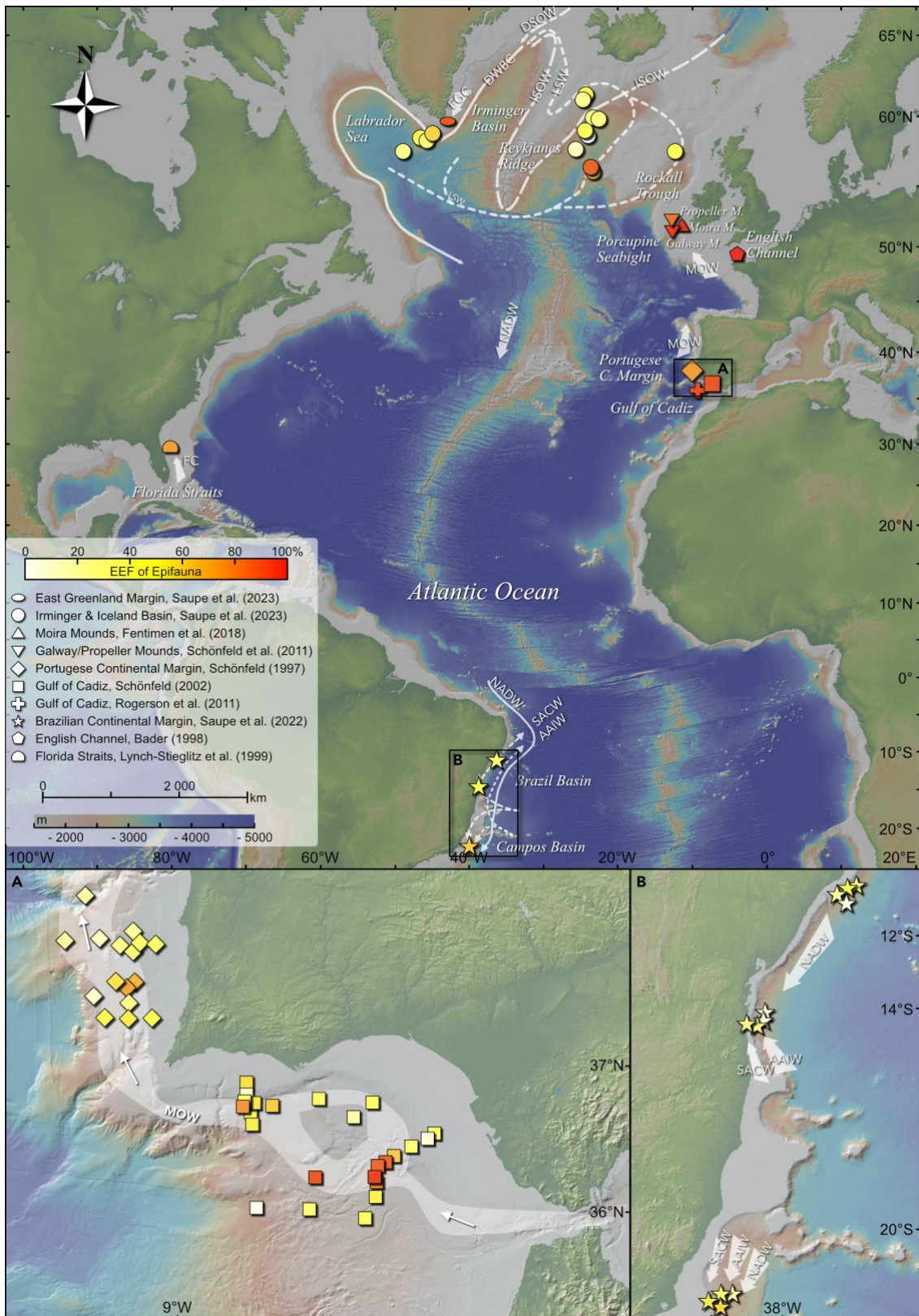


**Figure 1** | Map of the Atlantic Ocean showing stations of multiple studies addressing benthic foraminifera in increased current regimes. Abbreviations mean: AAIW=Antarctic Intermediate Water, DSOW=Denmark Strait Overflow Water, DWBC=Deep Western Boundary Current, EGC=East Greenland Current, FC=Florida Current, ISOW=Iceland Scotland Overflow Water, LSW=Labrador Sea Water, MOW=Mediterranean Outflow Water, NADW=North Atlantic Deep Water, SACW=South Atlantic Central Water. The map was created with GeoMapApp ([www.geomapapp.org](http://www.geomapapp.org)), using the base map of Ryan et al. (2009).

## 2. Oceanographic Setting

The continental slopes of the Atlantic Ocean are characterised by the widespread deposition of extensive contourite drift systems (CDS; Rebesco et al., 2014). CDS formation is driven by complex network of bottom currents of varying intensity which are induced by deep water formation at northern and southern high latitudes of the Atlantic Ocean and at mid latitudes in the Mediterranean Sea (Faugères et al., 1999; Stramma and England, 1999; Kuhlbrodt et al., 2007; Hernández-Molina et al., 2014; Uenzelmann-Neben and Gruetzner, 2018). For this study, sample material from CDSs at different latitudes is compared.

South of Greenland at the upper slope of the Irminger Basin (60°N) down to 800 m water depth, the warm (ca. 6-9° C) and saline (ca. 34.95–35.05) East Greenland Current (EGC) interacts with the ocean floor at current velocities of up to 40 cm/s (Holliday et al., 2007). Underlying North Atlantic Deep Water (NADW) is transported southwards by the Deep Western Boundary Current (DWBC; Stramma and England, 1999), where it affects the Eirik Drift with current velocities of 12-22 cm/s (Hunter et al., 2007). The NADW of the northern hemisphere is a cold deep-water mass with temperatures of < 3°C and a salinity between 34.88 and 34.98 (Stramma and England, 1999; Hunter et al., 2007). To the east, in the Iceland Basin, south-east of Reykjanes Ridge, constant but weak current velocities between 3 and 10 cm/s shape the extensive Björn and Gardar drifts (van Aken, 1995; Bianchi and McCave, 2000). The main water masses influencing the Björn Drift until 1400 m depth are Labrador Sea Water (LSW; 3.4°C and 34.88 *sensu* Bianchi and McCave, 2000) and a mixing layer with subjacent Iceland Scotland Overflow Water (ISOW; Bianchi and McCave, 2000; Holliday et al., 2000; Sayago-Gil et al., 2010). At depths of 2000-3000 m, the Gardar Drift is mainly influenced by cold and comparatively saline ISOW (1.7 °C and 35.0 *sensu* Bianchi and McCave, 2000) entering from the Iceland Scotland Ridge (van Aken and de Boer, 1995; Bianchi and McCave, 2000; Kuhlbrodt et al., 2007). Both Björn and Gardar drifts are characterised by fine to medium silt surface sediments (Saupe et al., 2023)

Rather different conditions prevail in the Northeast Atlantic Basin where the Atlantic Ocean is fed by warm, highly saline Mediterranean Outflow Water (MOW). The MOW enters the Gulf of Cadiz via the Strait of Gibraltar and forms an intermediate water mass which flows from the Gulf of Cadiz (36-37°N) along the Iberian Peninsula and extends into the Norwegian-Greenland Sea (O'Neil Baringer and Price, 1999; Schönfeld and Zahn, 2000; Schönfeld, 2002a; Schönfeld et al., 2011; Hernández-Molina et al., 2014). After leaving the Mediterranean Sea, the MOW divides into an upper (300-800 m) and a lower core (1100 to 1500 m), which are mainly distinguished by temperature differences (Sierro et al., 2020). This comparatively warm water mass shows temperatures between 7°C (lower core) and 13°C (upper core) and an average salinity of 38.4 (Sierro et al., 2020). In Gulf of Cadiz, MOW extends from 600 m to 1500 m water depth, differing from the overlying North Atlantic Central Water (NACW) by its significantly higher temperatures and salinities (O'Neil Baringer and Price, 1999; Schönfeld, 2002a). Due to the narrowing in the Strait of Gibraltar and the rapid sinking when entering the Gulf of Cadiz, the MOW reaches extremely high flow velocities of up to 100 cm/s in its upper core (Schönfeld, 2002a). Its speed decreases continuously from here, and the seafloor is covered by sand and sandy

silt along the main MOW path (Schönfeld, 2002a). Off the Portuguese coast, the MOW interacts with the seafloor at flow speeds around 12 cm/s, with higher velocities on the upper slope and lower velocities in the distal MOW on the lower slope (Schönfeld, 1997). In the northeast Atlantic, offshore of Ireland, the Porcupine Seabight (51-52°N) deep-water basin is affected by northward circulating Eastern North Atlantic Water (ENAW) extending to water depths of 800 m, and underlying MOW extending to about 1100 m depth (White, 2007; Fentimen et al., 2018). The MOW still has rather high temperatures of about 10°C here, but a slightly reduced salinity of nearly 35.48 caused by mixing with the ENAW (White, 2007; Lim et al., 2018). Constant NS oriented bottom currents with velocities between 5 and 15 cm/s have been measured at the eastern margin of the Porcupine Seabight (White, 2007; Schönfeld et al., 2011; Sánchez-Leal et al., 2017; Sierro et al., 2020). Various cold-water coral (CWC) mounds (e.g., Galway, Moira, and Propeller mounds) fringe the region at depths between 550 and 1030 m, with bottom currents reaching peaks between 35 and 40 cm/s (Schönfeld et al., 2011; Fentimen et al., 2018, 2020; Lim et al., 2018).

In the South Atlantic, the Brazilian continental margin spans several physiogeographic provinces, including the Campos (16-22°S) and Brazil basins (5-16°S; Martins and Coutinho, 1981). The seafloor in the Campos Basin is shaped by a pronounced canyon system and channel networks with primarily silty sediments, getting more clayey towards the north in the Brazil Basin (Bahr et al., 2016; Saupe et al., 2022). The region is influenced by several deep-water currents, including the subtropical and tropical South Atlantic Central Water (SACW, until 500 m) and the Antarctic Intermediate Water (AAIW, until 1100 m), both transported northwards by the North Brazil Undercurrent (NBU). The North Atlantic Deep Water (NADW, until 3500 m) reaches the South American continental margins from the north, transported by the DWBC (Peterson and Stramma, 1991; Stramma and England, 1999; da Silveira et al., 2020; Saupe et al., 2022). Flow velocities are highest in the SACW with 50 to 80 cm/s, the AAIW reaches nearly 30 cm/s, and the NADW only 20 cm/s (Viana, 2001; de Mello e Sousa et al., 2006; da Silveira et al., 2020). The SACW is clearly distinguished from the deeper water masses by its higher water temperature of > 10°C (Yamashita et al., 2018; da Silveira et al., 2020). The AAIW has salinities similar to the SACW of nearly 34.8 but is significantly colder with ~4°C (Yamashita et al., 2018; da Silveira et al., 2020). The deep NADW has cooled slightly to c. 1.9 °C on its passage to the south, salinity ranges between 34.6 and 34.9 (de Madron and Weatherly, 1994; Yamashita et al., 2018).

### 3. Material and Methodology

#### 3.1 Sample Material

For this study, abundance data of benthic foraminifera from surface sediments in contourite drift systems or regions of enhanced bottom current activities at different latitudes in the Atlantic Ocean were integrated for statistical analyses. The data set includes published (Schönfeld, 1997, 2002a; Schönfeld et al., 2011; Fentimen et al., 2018; Saupe et al., 2022, 2023) and some unpublished data from the northern North Atlantic ([Table 1](#)). To ensure comparability between studies, only data sets relying on foraminiferal tests > 250 µm were considered. Limitation to this fraction of test sizes

minimizes the potential bias by winnowing and dislocation (Schönfeld, 1997). In total, the statistical analyses comprise 122 samples. Abundance data from Rogerson et al. (2011), covering the same study area as Schönfeld (2002a, b), were not included in the statistical analysis as potential taxonomic inconsistencies could not be resolved. Additional material from the English Channel (Bader, 1998 in Schönfeld, 200b) and the Florida Straits (Lynch-Stieglitz, 1999 in Schönfeld, 2002b), exclusively based on epifaunal species, were assessed for comparison.

**Table 1** | Sample station data.

Reference	Region	Range (Lat)	Range (Long)	Intervals cm	Depth mbsl	Fauna	# stations
Saupe et al. (2023)	N Atlantic, Iceland and Irminger Basin	55–62 °N	12–49 °W	0–2	768–3486	TA	14
<i>New foraminiferal data from IODP material</i>	N Atlantic, Iceland and Irminger Basin	56–61 °N	23–49 °W	0–6	1659–3463	TA	8
Fentimen et al. (2018)	Porcupine Seabight, Moira Mounds	51–52 °N	12 °W	0–1	933–1069	DA	20
Schönfeld et al. (2011)	Porcupine Seabight, Galway & Propeller Mounds	51–52 °N	12–13 °W	0–1	696–982	DA	19
Schönfeld (1997)	Portugese Continental Margin	37–38 °N	9–10 °W	surface	246–3582	DA	23
Schönfeld (2002a)	Gulf of Cadiz	36–37 °N	7–8 °W	0–1	103–1917	DA	25
Saupe et al. (2022)	Brazilian Margin, Campos and Brazil Basin Basin	11–22 °S	36–40 °W	0–1	422–2019	DA	13

Indicated are the datasets used in the cluster analysis with the associated region and geographical range; as well as the applied fauna (Total Assemblage=TA, Dead Assemblage=DA). The sampled intervals and water depths are given as in the original reference.

The data set from the northern North Atlantic comprises 14 samples collected during cruises 88 (NEAPACC) and 159 (RAPID) of the research vessel *Charles Darwin* from the Björn (1502 to 1825 m) and Gardar drifts (2222 to 2879 m) in the Iceland Basin, and the Eirik Drift (2145 and 3486 m) in the Irminger Basin south of Greenland (McCave, 1994, 2005; Saupe et al., 2023). For foraminiferal analysis, surface sediments from NEPACC and RAPID box core or kasten core barrels were recovered from the upper 2 cm (Saupe et al., 2023). Unpublished foraminiferal data from this region were added from core top samples of IODP expedition 303/306 (sites U1305, U1306, U1307, U1314; Channell et al., 2006a, 2006b), DSDP leg 81 (sites 552 and 554; Roberts et al., 1984), and ODP leg 162 (sites 983A and 984B; Jansen and Raymo, 1996). Sediments from IODP and DSDP cores extend to 5 cm depth. The Irminger and Iceland Basin stations cover a geographic range from 55–62°N and 23–49°W.

The two data sets from mounds of cold-water corals in the Porcupine Seabight (51–52°N, 12–13°W) include 20 samples from the Moira Mounds (Fentimen et al., 2018) and 19 samples from the Galway and Propeller Mounds (Schönfeld et al., 2011). In both studies, the top 1 cm of sediment was sampled from box cores at water depths between 696 and 1069 m (Schönfeld et al., 2011; Fentimen et al., 2018).

The CDS along the southwestern Iberian Margin is represented by 23 samples from the Portuguese continental margin (37–38°N, 246–3582 mbsl; Schönfeld, 1997) and samples from 25 stations in the Gulf of Cadiz (34–37 °N; 7–13 °W; 103–1917 mbsl; Schönfeld, 2002b).

Three transects with a total of 13 stations along the Brazilian continental margin were published by Saupe et al. (2022). The benthic foraminiferal community was studied in the top 1 cm of the sediment from the Brazil Basin (8 samples, two transects) between 11 and 14°S and from the Campos Basin (5

samples, one transect) at about 22°S. Bottom-current induced and contour-parallel erosional ridges and contourite deposits on the middle and upper slopes are characteristic for the Brazilian Margin and particularly shape the Campos Basin (Viana, 2001).

### 3.2 Benthic Foraminifera

To ensure taxonomic consistency between the data sets of different authors, a comprehensive taxonomic reference list containing synonyms and spelling differences was compiled ([Table 2](#)).

The majority of included studies relies on dead assemblages (DA; dead/unstained specimens) in their analyses (Schönfeld, 1997, 2002b; Schönfeld et al., 2011; Fentimen et al., 2018; Saupe et al., 2022a), while other material relies on the total assemblages (TA; live+dead/stained+unstained specimens; Saupe et al., 2023, and the new IODP material). Wherever possible, the DA was preferred to ensure a better application to the fossil record. Seasonality effects, as well as species blooms or very sensitive taxa can be excluded in the DA, which more closely resembles fossil assemblages (Schönfeld, 2002b). The TA was only used because of deviating sampling methods that excluded staining with Rose Bengal, thus preventing the distinction between live and dead specimens (Saupe et al., 2023). However, studies by Austin and Evans (2000) and Balestra et al. (2017) show that sediment samples from the Gardar and Björn drifts as well as the Gulf of Cadiz contain very sparse numbers of stained foraminifera compared to the total assemblages, allowing the total assemblage to be compared with dead assemblages.

To verify whether certain adapted species also settle in high currents outside the Gulf of Cadiz, we follow the concept of the elevated epifauna (hereinafter referred to as the EEF) after Schönfeld (1997, 2002a, 2002b; [Table 2](#)).

Tubular species are nearly always fragmented, which makes their quantification problematic. Different approaches of different authors recording the fragments creates further sources of error in the total analysis. To avoid their overrepresentation or a bias between the studies, tubular species are excluded from the statistical analyses, and relative assemblage values were calculated omitting them (e.g., Goineau and Gooday, 2017; Saupe et al., 2022). This involves the following tubular agglutinated species: *Bathysiphon crassatina* (Brady, 1881), *Bathysiphon filiformis* Sars, 1872, *Hyperammina* sp. div., *Rhabdammina abyssorum* Sars in Carpenter, 1869, *Rhabdammina discreta* Brady, 1881, *Rhabdamminella cylindrica* (Brady, 1882), *Rhizammina algaeformis* Brady, 1879 and *Saccorhiza ramosa* (Brady, 1879). In order to avoid neglecting their role in the foraminiferal community, tubular fragments are listed in [Table 3](#) and their presence is assessed qualitatively. For this single aim, agglutinated tubes were calculated as a percentage of the total assemblage.

Table 2 | Taxonomic reference list.

Taxon	given as	in
<i>Ammobaculites agglutinans</i> (d'Orbigny, 1846)		
<i>Ammodiscus tenuis</i> (Brady, 1881)		
<i>Ammoglobigerina globigeriniformis</i> (Parker & Jones, 1865)		
<i>Ammolagena clavata</i> (Jones & Parker, 1860)		
<i>Ammonia beccarii</i> (Linnaeus, 1758)		
<i>Amphicoryna scalaris</i> (Batsch, 1791)		
<i>Astranonion stelligerum</i> (d'Orbigny, 1839)	<i>Astranonion stelligerum</i>	Rogerson et al., (2011)
	<i>Astranonion stellatum</i>	Fentimen et al., (2018)
<i>Bigenerina nodosaria</i> d'Orbigny, 1826		
<i>Bolivina subaenariensis</i> Cushman, 1922		
<i>Bulimina acanthia</i> Costa, 1856		
<i>Bulimina aculeata</i> d'Orbigny, 1826		
<i>Bulimina striata mexicana</i> Cushman, 1922		
* <i>Cibicides lobatulus</i> (Walker & Jacob, 1798)	<i>Lobatula lobatula</i>	Fentimen et al., (2018)
* <i>Cibicides refulgens</i> Montfort, 1808		
<i>Cibicidoides cicatricosus</i> (Schwager, 1866)		
<i>Cibicidoides mundulus</i> (Brady, Parker & Jones, 1888)	<i>Cibicidoides kullenbergi</i>	Schönfeld, (1997, 2002b); Rogerson et al., (2011)
	<i>Cibicides kullenbergi</i>	Fentimen et al., (2018)
	<i>Cibicides pachyderma</i>	Fentimen et al., (2018)
	<i>Cibicidoides pseudoungerianus</i>	Schönfeld, (1997, 2002b)
	<i>Cibicidoides</i> sp.	Schönfeld (2002a)
* <i>Cibicidoides pachyderma</i> (Rzehak, 1886)		Note: According to Schönfeld (2002a) his species <i>Cibicidoides</i> sp. was determined by several authors as <i>Cibicidoides pseudoungerianus</i> (Cushman, 1922), but in Schönfeld's opinion with a more broadly rounded periphery. We group Schönfeld's <i>Cibicidoides</i> sp. and <i>C. pseudoungerianus</i> because of their joint EEF behaviour. <i>Cibicidoides pseudoungerianus</i> is a junior synonym of <i>Cibicidoides pachyderma</i> (Schönfeld, 2002b).
* <i>Cibicidoides</i> aff. <i>pachyderma</i>	<i>Cibicidoides</i> aff. <i>pseudoungerianus</i>	Schönfeld, (2002b)
* <i>Cibicidoides wuellerstorfi</i> (Schwager, 1866)	<i>Planulina wuellerstorfi</i>	Fentimen et al., (2018)
<i>Clavulina mexicana</i> Cushman, 1922		
<i>Cornuloculina inconstans</i> (Brady, 1879)		
<i>Cribrostomoides subglobosus</i> (Cushman, 1910)		
<i>Cyclammina cancellata</i> Brady, 1879	<i>Cyclammina cancelata</i>	Rogerson et al., (2011)
<i>Discammina compressa</i> (Goës, 1882)		
* <i>Discanomalina coronata</i> (Parker & Jones, 1865)	<i>Discanomalina carinata</i>	Rogerson et al., (2011)
* <i>Discanomalina semipunctata</i> (Bailey, 1851)		
<i>Dorothia bradyana</i> Cushman, 1936		
<i>Elphidium crispum</i> (Linnaeus, 1758)		
<i>Elphidium subarcticum</i> Cushman, 1944		
<i>Gaudryina flintii</i> Cushman, 1911		
<i>Globobulimina affinis</i> (d'Orbigny, 1839)		
<i>Globobulimina</i> sp.		Schönfeld, (1997, 2002b); Rogerson et al., (2011)
<i>Globobulimina turgida</i> (Bailey, 1851)		
<i>Globocassidulina subglobosa/crassa</i>	<i>Globocassidulina subglobosa</i>	Schönfeld, (1997)
	<i>Globocassidulina crassa</i>	
	<i>Globocassidulina</i>	Rogerson et al., (2011)
<i>Glomospira charoides</i> (Jones & Parker, 1860)	<i>Usbekistania charoides</i>	Rogerson et al., (2011)
<i>Gyroidina orbicularis</i> d'Orbigny, 1826		
<i>Gyroidina soldanii</i> d'Orbigny, 1826	<i>Gyroidina soldanii</i>	Fentimen et al., (2018)
	<i>Gyroidina neosoldanii</i>	Schönfeld, (1997, 2002b)
	<i>Gyroidinoides soldanii</i>	Saupe et al., (2022)
* <i>Hanzawaia concentrica</i> (Cushman, 1918)		
<i>Heterolepa broeckhiana</i> (Karrer, 1878)		
<i>Hoeglundina elegans</i> (d'Orbigny, 1826)		
<i>Hormosina bacillaris</i> (Brady, 1881)		
<i>Hyalinea balthica</i> (Schröter, 1783)		

...continued

Taxon	given as	in
<i>Karreriella bradyi</i> (Cushman, 1911)	<i>Karreriella bradiana</i>	Rogerson et al., (2011)
<i>Karreriella novangliae</i> (Cushman, 1922)		
<i>Lagenamma laguncula</i> Rhumbler, 1911		
<i>Laticarinina pauperata</i> (Parker & Jones, 1865)	<i>Laticoryna pauperata</i>	Rogerson et al., (2011)
<i>Lenticulina rotulata</i> (Lamarck, 1804)		
<i>Martinottiella communis</i> (d'Orbigny, 1846)	<i>Martinottiella communis</i>	Rogerson et al., (2011)
<i>Melonis affinis</i> (Reuss, 1851)	<i>Nonion barleeanum</i>	Rogerson et al., (2011)
	<i>Melonis barleeanum</i>	Fentimen et al., (2018); Schönfeld, (1997, 2002b)
<i>Melonis pompilioides</i> (Fichtel & Moll, 1798)	<i>Nonion soldanii</i>	Rogerson et al., (2011)
<i>Miliolinella subrotunda</i> (Montagu, 1803)		
<i>Nonion asterizans</i> (Fichtel & Moll, 1798)		
<i>Oridorsalis umbonatus</i> (Reuss, 1851)		
<i>Paratrochammina challengerii</i> Brönnimann & Whittaker, 1988		
* <i>Planulina ariminensis</i> d'Orbigny, 1826		
<i>Psammatodendron arborescens</i> Norman in Brady, 1881		
<i>Psammosphaera fusca</i> Schulze, 1875		
<i>Psammosphaera parva</i> Flint, 1899		
<i>Pullenia bulloides</i> (d'Orbigny, 1846)		
<i>Pullenia quinqueloba</i> (Reuss, 1851)		
<i>Pyrgo murrhina</i> (Schwager, 1866)		
<i>Pyrgo</i> sp.		Saupe et al., (2022, 2023)
<i>Quinqueloculina seminulum</i> (Linnaeus, 1758)	<i>Quinqueloculina semilunaris</i>	Fentimen et al., (2018)
	<i>Quinqueloculina seminula</i>	Saupe et al., (2022)
<i>Reophax bilocularis</i> Flint, 1899		
<i>Reophax</i> aff. <i>diffflugiformis</i>		Schönfeld, (2002b)
<i>Reophax scorpiurus</i> Montfort, 1808		
* <i>Saccamina sphaerica</i> Brady, 1871	<i>Saccamina sphaerica</i>	Fentimen et al., (2018)
<i>Sigmoilopsis schlumbergeri</i> (Silvestri, 1904)		
<i>Sigmoilopsis woodi</i> Atkinson, 1968		
<i>Siphonina tubulosa</i> Cushman, 1924		
<i>Sphaeroidina bulloides</i> d'Orbigny in Deshayes, 1828		
<i>Spiroplectinella subhaeringensis</i> (Grzybowski, 1896)		
<i>Textularia hystrix</i> Jones, 1994	<i>Dorothia rudis</i>	Bader, (1998) in Schönfeld, (2002b)
<i>Tolypamma vagans</i> (Brady, 1879)		
<i>Trifarina fornasinii</i> (Selli, 1948)		
<i>Triloculina tricarinata</i> d'Orbigny, 1826		
<i>Trochammina globigeriniformis</i> (Parker & Jones, 1865)		
<i>Uvigerina auberiana</i> d'Orbigny, 1839		
<i>Uvigerina celtica</i> Schönfeld, 2006	<i>Uvigerina</i> sp. 221	Schönfeld, (1997, 2002b)
<i>Uvigerina elongatastriata</i> (Colom, 1952)		
<i>Uvigerina mediterranea</i> Hofker, 1932		
<i>Uvigerina peregrina</i> Cushman, 1923		
<i>Uvigerina peregrina parva</i> Lutze, 1986		
* <i>Vulvulina pennatula</i> (Batsch, 1791)	<i>Valvulina pennulata</i>	Rogerson et al., (2011)

Listed are all taxa that were used for the cluster analysis in [Figure 2](#) (i.e., those that occur > 5% in at least one sample). If a species was named differently in the original published data set, the alternative name and author are given. Species marked with an asterisk are assigned to the Elevated Epifauna (EEF) according to Lutze and Thiel (1989), Linke and Lutze (1993), and Schönfeld (1997, 2002a, 2002b).

### 3.3 Multivariate Statistics

For the hierarchical Q-mode cluster analysis (HCA; UPGMA algorithm, Bray-Curtis similarity index), the software package Past 4.02 (Hammer et al., 2001) was used. The HCA algorithm groups similar assemblages into groups to simplify the evaluation of large data sets via graphical outcome (Ramette 2007). The HCA is based solely on species names from the taxonomic reference list. Only samples with at least 100 specimens were selected for the analysis to ensure statistical reliability (Fatela and Taborda, 2002). This resulted in 106 samples that remained for performing the HCA. In order to obtain the closest concordance between different data sets, the compiled data set was reduced to those species that occur to at least 5 % in a sample. The contribution of each species to the dissimilarity of each cluster is determined by a similarity percentage analysis (=SIMPER analysis, Bray-Curtis similarity index). This allows the identification of the species which are most relevant for the observed similarity/dissimilarity patterns between clusters.

## 4. Results

### 4.1 Assemblage Composition and Distribution

New foraminiferal records (> 250 µm) from eight IODP core tops (DSDP sites 552 and 554, ODP sites 983A and 984B, IODP 303 sites U1305, U1306 and U1307, and IODP 306 site U1314) complement the North Atlantic data set in the Irminger (58-59°N, 46-49°W) and Iceland basins (56-61°N, 23-28°W). A total of 84 species were identified, of which five species are assigned to the delicate agglutinated tubular suspension feeders (*Hyperammia* sp., *Rhabdammina abyssorum*, *Rhabdamminella cylindrica*, *Rhizammina algaeformis* and *Saccorhiza ramosa*). Most tubular fragments originate from the deeper Björn Drift in the Iceland Basin (37 % in ODP sample 983A), while the Irminger Basin samples contain a maximum of 12 % (IODP sample 303-U1307). Excluding fragile tubular taxa, agglutinated species are most abundant in IODP 303 site U1307 (29 %, Eirik Drift, Irminger Basin) and in ODP site 983A (35 %, Björn Drift, Iceland Basin), with *Ammolagena clavata* and *Recurvoides turbinatus* being the most abundant species. Hyaline taxa dominate the assemblages with a maximum of 88 % in DSDP site 554 (Gardar Drift, Iceland Basin) and a maximum of 82 % in IODP 303 site U1305 (Eirik Drift, Irminger Basin). *Cibicidoides wuellerstorfi* and *Hoeglundina elegans* are major contributors to the assemblages. Porcellanous tests are rather underrepresented (4-11 %), mainly consisting of various species of *Pyrgo* and occurrences of *Sigmoilopsis schlumbergeri*. The epifaunal proportion of the total assemblages ranges from 27 % (Irminger Basin, IODP 303 site U1306) to 56 % (Iceland Basin, DSDP site 554).

Integrated HCA of all data sets results in 9 clusters of samples (cophenetic correlation 0.8507), which can be combined into two groups A (clusters 1-3) and B (clusters 4-9; [Figure 2](#)). A SIMPER analysis shows that 11 species contribute to the first cumulative 50 % of dissimilarity between clusters ([Table 4](#)).



**Table 3 |** Proportion of tubular fragments, epifauna and EEF within the epifauna.

Cluster	Sample	Sample reference	Tubular Fragments %	Epifauna % of total	EEF % of Epifauna	major EEF species
cluster 1	M39029-3	1_01	11.2	61.6	2.5	<i>Cib. pachyderma</i> (5%),
	SO75 9KG	1_02	8.0	21.2	36.4	
	SO83 1GK	1_03	17.9	46.4	15.7	
	SO75 30KG	1_04	7.7	60.3	44.3	
cluster 2	N-11B	2_01	69.4	47.5	20.8	<i>Cib. wuellerstorfi</i> (12%)
	N-5B	2_02	56.2	61.5	19.3	
	R-35 25B	2_03	20.4	28.3	18.8	
	N-15B	2_04	7.6	44.5	10.4	
	N-12B	2_05	47.8	25.5	-	
	N-13B	2_06	1.9	42.9	31.9	
	N-9K	2_07	36.4	37.3	21.4	
	IODP-U1307	2_08	12.1	50.7	33.0	
	IODP-U1306	2_09	4.2	26.6	23.0	
	DSDP site 554	2_10	1.0	56.1	69.9	
	DSDP site 552	2_11	7.7	48.4	49.3	
	R-29 18B	2_12	0.1	48.0	45.1	
	cluster 3	M125-77	3_01	5.0	35.8	
M125-72		3_02	5.2	53.6	4.5	
M125-95		3_03	28.3	20.9	4.3	
M125-29		3_04	30.6	47.5	12.3	
M125-102		3_05	51.1	31.7	20.0	
M125-93		3_06	5.7	29.1	15.8	
M125-78		3_07	6.3	38.3	26.7	
M125-25		3_08	9.0	58.2	24.4	
M125-24		3_09	11.1	66.1	40.5	
M125-34		3_10	2.5	59.4	43.8	
N-4B		3_11	48.2	41.6	36.2	
R-01 1B		3_12	27.4	48.1	31.8	
M125-107		3_13	10.4	33.6	30.1	
M125-80		4_01	1.8	70.7	47.0	<i>C. pachyderma</i> (19%), <i>Pl. ariminensis</i> (13%)
cluster 5	M39006-1	5_01	0.3	38.2	14.1	<i>C. lobatulus</i> (3%)
	M39005-3	5_02	0.8	31.4	26.8	
	M39024-2	5_03	-	23.2	42.4	
cluster 6	GeoB 6718-1	6_01	0.9	45.6	26.1	<i>S. sphaerica</i> (9%)
	M39004-1	6_02	17.1	53.9	74.5	
	M39002-2	6_03	16.3	44.1	24.4	
	SO75 25KG	6_04	12.0	31.4	16.7	
	PO200/10-4-1	6_05	33.1	33.9	35.9	
cluster 7	M39021-5	7_01	5.7	43.0	52.8	<i>Pl. ariminensis</i> (5%), <i>Cib. pachyderma</i> (5%)
	M39021-3	7_02	5.2	56.7	50.4	
	M39022-1	7_03	21.9	56.0	44.8	
	M39016-1	7_04	2.6	44.1	32.8	
	M39008-4	7_05	7.3	42.7	45.0	
	M39017-5	7_06	-	46.5	22.2	
	M39020-1	7_07	4.4	47.1	50.0	
	M39023-3	7_08	1.0	36.9	42.1	
	M39028-3	7_09	0.4	32.2	52.1	
	M39018-1	7_10	0.6	34.0	27.3	
	M39009-1	7_11	-	32.8	78.1	
	M39007-1	7_12	-	35.2	32.6	
	M39027-1	7_13	0.5	33.7	50.8	
	M39025-1	7_14	-	16.3	34.8	
	GeoB 9220-2	7_15	-	63.2	82.8	
	GeoB 8074-1	7_16	2.0	40.5	61.3	
	GeoB 8039-1	7_17	0.4	53.8	71.8	
	GeoB 6721-1	7_18	0.3	43.5	75.9	
	GeoB 9246-3	7_19	0.6	59.1	80.4	
	GeoB 8073-1	7_20	0.6	12.9	21.7	
	GeoB 8059-1	7_21	0.1	23.1	66.0	
	GeoB 6708-1	7_22	0.2	31.4	66.1	
	GeoB 9245-1	7_23	0.3	15.9	61.5	
	GIK15809	7_24	1.4	35.9	38.7	
	M39003-1	7_25	1.5	29.6	44.1	
	SO75 37VL	7_26	9.7	20.7	52.0	
	SO75 15KG	7_27	10.3	43.4	54.7	
	PO200/10-3-1	7_28	10.8	30.4	61.6	
	SO75 11KG	7_29	2.3	38.7	64.6	
	SO75 13KG	7_30	0.9	39.0	65.2	
	SO83 9GK	7_31	8.2	19.4	48.6	
	PO200/10-5-1	7_32	1.9	37.4	50.0	
SO75 7VL	7_33	0.3	29.8	66.1		
SO83 10GK	7_34	1.0	55.0	53.8		
SO83 11GK	7_35	-	15.7	30.6		
PO200/10-1-1	7_36	-	21.2	38.3		
cluster 8	GeoB 9205-1	8_01	1.2	61.3	71.7	<i>Disc. coronata</i> (24%)
	GeoB 9204-1	8_02	0.6	72.1	71.8	
	GeoB 9206-1	8_03	1.2	82.0	83.0	
	PO316-525	8_04	-	80.1	89.1	
	GeoB 9209-2	8_05	-	75.6	84.7	
	GeoB 9218-1	8_06	1.3	88.6	81.4	
	GeoB 9219-1	8_07	-	91.8	88.0	
	GeoB 8047-1	8_08	0.3	76.8	59.9	
	BC22	8_09	-	48.6	44.4	
	BC14	8_10	-	51.7	31.3	
	BC35	8_11	0.7	83.1	56.7	
	BC26	8_12	0.9	81.7	59.3	
	BC28	8_13	-	82.2	51.6	
	BC25	8_14	0.5	83.4	55.0	
	BC24	8_15	5.7	77.7	53.5	
	BC34	8_16	2.6	76.9	76.1	
	BC23	8_17	-	88.2	88.4	
	BC31	8_18	1.3	60.9	44.2	
	BC32	8_19	1.5	70.2	46.6	
	BC21	8_20	-	73.6	51.4	
	BC33	8_21	0.3	58.3	28.9	
	BC5	8_22	1.4	68.0	44.5	
	BC4	8_23	-	57.2	37.7	
	BC36	8_24	-	70.8	19.7	
	BC17	8_25	-	68.7	9.3	
	BC20	8_26	-	66.2	21.5	
	BC10	8_27	-	67.6	28.7	
BC1	8_28	-	65.4	24.5		
cluster 9	M39010-2	9_01	-	57.9	69.7	<i>C. lobatulus</i> (21%), <i>C. refulgens</i> (10%)
	M39012-1	9_02	-	48.8	64.4	
	M39011-1	9_03	-	57.2	75.3	
	R-27 15B	9_04	5.1	93.3	78.8	

The proportions of tubular fragments refer to an extended assemblage (100% including tub. fragments). The proportion of epifauna refers to the normal assemblage without tub. fragments, as used in the HCA. The EEF is plotted as a proportion of the total epifauna. The major EEF species refer to the EEF-SIMPER analysis (table 5), with all bold species accounting for > 10%.

Group A is mainly composed of samples between 23° and 49°W, including stations from the North Atlantic Irminger and Iceland basins and stations from the South Atlantic Brazil and Campos basins. The SIMPER analysis reveals that group A is determined by an assemblage with common occurrences of *Hoeglundina elegans* (11 %) and *Cibicidoides wuellerstorfi* (9 %), and the absence of *Uvigerina mediterranea* (Table 4). Only four stations east of 23°W are assigned to group A, all of which belong to cluster 1 and are located at the Iberian Peninsula: one station from the distal MOW in the Gulf of Cadiz and three stations from the Portuguese continental margin. The assemblage of cluster 1 is largely determined by abundant occurrences of *Uvigerina peregrina* (16 %) with common occurrences of *Hoeglundina elegans* (7 %), *Cibicidoides pachyderma* (6 %), and *Bulimina striata mexicana* (7 %). Tubular agglutinated taxa account for 8-18 % in the samples of cluster 1 (Table 3, Figure 2). Clusters 2 and 3 cover sample stations located west of 23°W. Cluster 2 groups all stations from the Gardar Drift and the Eirik Drift, being distinguished by an assemblage of abundant *Hoeglundina elegans* (21 %) and *Cibicidoides wuellerstorfi* (12 %) with common occurrences of *Melonis pompilioides* (8 %). Cluster 3 comprises NADW and AAIW samples from the Brazilian continental margin and two samples from the North Atlantic (Björn Drift and Rockall Trough). Common occurrences of *Cibicidoides wuellerstorfi* (8 %) and *Sigmoilopsis schlumbergeri* (6 %) characterise the assemblage of cluster 3. Maximum values of up to 70 % of tubular agglutinated species were determined in the samples of cluster 2 and of up to 51 % in the samples of cluster 3 (Table 3, Figure 2).

Group B mainly comprises samples further east between 7° and 13° W, along the pathway of MOW, with two exceptions, originating from the Brazilian (14°S, 39°W) and the Greenland continental margin (60°N, 43°W). Group B is determined by an assemblage of abundant *Uvigerina mediterranea* (14 %) and occasionally high abundances of *Discanomalina coronata* (10%) and *Cibicidoides mundulus* (8 %; Table 4). Within this group, cluster 4 represents an outlier, comprising only a single sample from the SACW layer of the Brazilian continental margin. Cluster 4 shows a unique composition with high abundances of *Cibicidoides pachyderma* (19 %), and *Planulina ariminensis* (13 %), as well as few *Siphonina tubulosa* (8 %), *Gyroidina soldanii* (8 %), and *Spiroplectinella subhaeringensis* (7 %). Agglutinated tubular species occur with only 2 % (Table 3, Figure 2). Three samples from the Gulf of Cadiz, located nearest to the shelf, are grouped as cluster 5. An assemblage of abundant *Hyalinea balthica* (16 %), *Ammonia beccarii* (12 %) and *Nonion asterizans* (12 %) defines this cluster; agglutinated tubular species are rare with > 1 % (Table 3, Figure 2). Cluster 6 consists mainly of sample stations located in the Gulf of Cadiz distally to the Strait of Gibraltar, and one station from the Portuguese continental margin and from the Propeller Mound in the Porcupine Seabight, respectively. An assemblage of abundant *Bulimina striata mexicana* (12 %), and common *Saccamina sphaerica* (9 %), *Uvigerina peregrina parva* (8 %), *Melonis affinis* (7 %) and *Uvigerina mediterranea* (5 %) determines cluster 6. On average 16 % tubular agglutinated fragments are present in the samples of cluster 6 (Table 3, Figure 2). Cluster 7 is the most comprehensive cluster, comprising 36 stations

located in the Gulf of Cadiz, the Propeller Mound (Porcupine Seabight) and the Portuguese continental margin. The assemblage of cluster 7 is significantly determined by *Uvigerina mediterranea* (25 %). Tubular suspension feeders are rare in cluster 7, accounting on average for 4 % of the total assemblage (Table 3, Figure 2). Cluster 8 consists entirely of samples from the Porcupine Seabight (Galway and Moira Mounds) accounting for 28 stations. These samples are clustered together based on high

**Table 4** | Assemblage distribution via SIMPER analysis.

	Av. dissim.	Contrib. %	Cumul. %	cluster								
				1	2	3	4	5	6	7	8	9
<i>Uvigerina mediterranea</i>	8.6	10.1	10.1	-	-	-	-	3.1	5.2	<b>25.0</b>	5.6	0.7
<i>Discanomalina coronata</i>	7.3	8.6	18.7	-	-	<0.1	-	-	0.1	1.8	<b>24.3</b>	1.2
<i>Cibicidoides mundulus</i>	6.2	7.3	26.0	4.9	0.4	1.6	-	-	-	0.2	<b>20.7</b>	-
<i>Hoeglundina elegans</i>	4.1	4.8	30.8	7.2	<b>20.6</b>	3.5	3.8	-	1.1	2.0	2.3	1.0
<i>Cibicidoides wuellerstorfi</i>	3.4	4.0	34.8	1.1	<b>11.5</b>	8.4	-	-	0.9	2.1	1.2	0.4
<i>Sigmoilopsis schlumbergeri</i>	2.9	3.4	38.2	1.9	3.5	6.2	1.4	1.2	0.2	2.2	6.9	0.3
<i>Cibicides lobatulus</i>	2.6	3.0	41.3	0.2	1.1	0.7	-	2.9	0.3	2.3	4.2	<b>21.4</b>
<i>Cibicidoides pachyderma</i>	2.4	2.9	44.1	5.5	-	0.2	<b>19.1</b>	0.9	0.7	4.8	0.9	5.0
<i>Planulina ariminensis</i>	2.2	2.6	46.7	-	-	0.4	<b>12.9</b>	-	0.2	4.9	3.0	1.1
<i>Cibicides refulgens</i>	2.1	2.5	49.2	-	0.2	0.2	-	0.5	-	0.6	5.6	9.9
<i>Melonis affinis</i>	2.0	2.3	51.5	-	3.8	<0.1	-	1.8	6.5	3.0	3.4	1.8
<i>Bulimina striata mexicana</i>	1.9	2.3	53.8	6.6	-	0.2	1.4	-	11.7	2.6	<0.1	0.2
<i>Hyalinea balthica</i>	1.9	2.2	56.0	-	-	-	-	<b>16.1</b>	4.3	3.2	0.3	0.9
<i>Uvigerina peregrina</i>	1.8	2.1	58.1	<b>16.4</b>	-	4.4	-	-	0.1	-	0.8	-
<i>Uvigerina peregrina parva</i>	1.6	1.9	60.0	0.6	<0.1	0.8	0.2	-	7.5	3.3	0.1	-
<i>Uvigerina celtica</i>	1.6	1.8	61.8	-	<0.1	0.1	-	9.3	1.8	3.3	<0.1	0.2
...												
<i>Melonis pompilioides</i>	1.3	1.5	65.0	-	7.9	0.8	-	-	-	-	-	-
<i>Amphicoryna scalaris</i>	1.2	1.4	66.3	-	-	-	-	7.9	0.3	2.6	<0.1	-
<i>Saccammina sphaerica</i>	1.1	1.3	67.7	4.0	0.3	0.5	-	<0.1	9.2	0.5	0.5	-
...												
<i>Gyroidina soldanii</i>	1.0	1.2	70.0	0.3	1.7	0.7	7.6	0.4	1.2	1.5	1.5	2.9
...												
<i>Ammonia beccarii</i>	0.8	0.9	74.1	-	-	-	-	<b>11.6</b>	-	0.3	<0.1	4.3
...												
<i>Cibicidoides aff. pachyderma</i>	0.7	0.8	79.3	-	-	-	-	0.6	-	1.2	-	5.2
...												
<i>Elphidium crispum</i>	0.5	0.6	86.3	-	-	-	-	0.7	-	0.2	<0.1	8.0
<i>Nonion asterizans</i>	0.5	0.6	86.9	-	-	-	-	<b>11.5</b>	-	0.1	-	0.3
...												
<i>Discanomalina semipunctata</i>	0.5	0.6	88.1	-	-	<0.1	-	-	-	0.2	0.1	6.8
...												
<i>Siphonina tubulosa</i>	0.2	0.2	98.1	-	-	0.3	8.4	-	-	-	-	-
...												
<i>Spiroplectinella subhaeringensis</i>	0.1	0.1	99.9	-	-	<0.1	6.6	-	-	-	-	-
				<b>group A</b>				<b>group B</b>				
<i>Uvigerina mediterranea</i>	8.8	9.8	9.8	-				<b>14.2</b>				
<i>Hoeglundina elegans</i>	6.0	6.7	16.5	<b>11.1</b>				2.0				
<i>Discanomalina coronata</i>	6.0	6.7	23.2	<0.1				9.8				
<i>Cibicidoides mundulus</i>	5.0	5.6	28.8	1.5				7.6				
<i>Cibicidoides wuellerstorfi</i>	4.9	5.5	34.3	8.7				1.5				

Similarity Percentage analysis (SIMPER, Bray-Curtis similarity index; overall average dissimilarity=85.15) based on clusters 1-9 and groups A (clusters 1-3) and B (clusters 4-9). Displayed are only taxa that determine a cluster by at least 5 %. Species that make up more than 10 % are highlighted in bold.

abundances of *Discanomalina coronata* (24 %) and *Cibicidoides mundulus* (21 %) as well as common occurrences of *Sigmoilopsis schlumbergeri* (7 %), *Cibicides refulgens* (6 %) and *Uvigerina mediterranea* (6 %). In this cluster, agglutinated tubular suspension feeders are also rare, averaging 1 % (Table 3, Figure 2). Cluster 9 is composed of samples from the central MOW in the Gulf of Cadiz and one sample from the Greenland continental margin. An assemblage of *Cibicides lobatulus* (21 %), *Cibicides*

*refulgens* (10 %) and *Elphidium crispum* (8 %) is characteristic for this cluster (Table 4). Agglutinated tubular species are absent in the samples except for the Greenland continental margin where they account for 5 % (Table 3, Figure 2).

#### 4.2 Epifauna and the Elevated Epifauna (EEF) Group

The EEF – a group of highly adapted benthic foraminifera settling primarily on elevated substrates in enhanced bottom currents (Schönfeld, 1997, 2002a, 2002b) – is expressed as the proportion of the total epifauna. In the data sets of our study, the following EEF species according to Lutze and Altenbach (1988), Lutze and Thiel, (1989), Linke and Lutze (1993) and Schönfeld (1997, 2002b, 2002a) have been identified: *Cibicides lobatulus* (Walker & Jacob, 1798), *Cibicides refulgens* Montfort, 1808, *Cibicoides pachyderma* (Rzehak, 1886), *Cibicoides wuellerstorfi* (Schwager, 1866), *Discanomalina coronata* (Parker & Jones, 1865), *Discanomalina semipunctata* (Bailey, 1851), *Hanzawaia concentrica* (Cushman, 1918), *Planulina ariminensis* d'Orbigny, 1826, *Saccammina sphaerica* Brady, 1871 and *Vulvulina pennatula* (Batsch, 1791) (Table 2). HCA-group A contains EEF values of 0 to 70 %, while group B contains values between 9 and 89 % (Table 3). Maximum EEF values of 70% are present in cluster 2 of group A and in cluster 8 of group B (89 %), respectively. Median values of clusters 1-9 show a weak trend from 25 % to 70 % with increasing cluster numbers (Figure 2). A SIMPER analysis, based on EEF taxa only, reveals that the most abundant species of group A are *Cibicoides wuellerstorfi* and *Cibicoides pachyderma*, while most abundant species of group B are *Discanomalina coronata*, *Cibicides lobatulus*, *Planulina ariminensis*, *Cibicoides pachyderma*, *Cibicides refulgens*, *Saccammina sphaerica* and *Discanomalina semipunctata* (occurrences of > 10 %; Table 5).

## 5. Discussion

### 5.1 Benthic Foraminiferal Distribution Patterns

While biogeographic distributions of benthic deep-sea foraminifera in many regions are primarily determined by the availability of food and oxygen, our data set indicates that areas of intensified bottom currents constitute a more complex setting. Organic matter suspended and advected by intensified bottom currents offer an additional food source for epibenthic organisms and generally favours abundances of suspension feeders (Wildish and Kristmanson, 1997; Gili and Coma, 1998). For micro- and meiobenthic suspension feeders such as foraminifera, exploitation of this food source results in adaptations of test morphology, tiering and motility (see suspension feeding types in Saupe et al., 2023). Elongated, tube-shaped tests allow extension into the current, however, they are fragile and probably cannot withstand high bottom current velocities > 15-20 cm/s. In contrast, suspension feeders with trochospiral, planoconvex tests increasingly occupy elevated substrates to exploit bottom currents as a food source. Attached to the substrate by organic or inorganic cements, they withstand dislocation by the bottom current. Most EEF species belong to the latter group. Depending on flow velocities, one or the other strategy will be favoured (Schönfeld, 1997; Saupe et al., 2023).

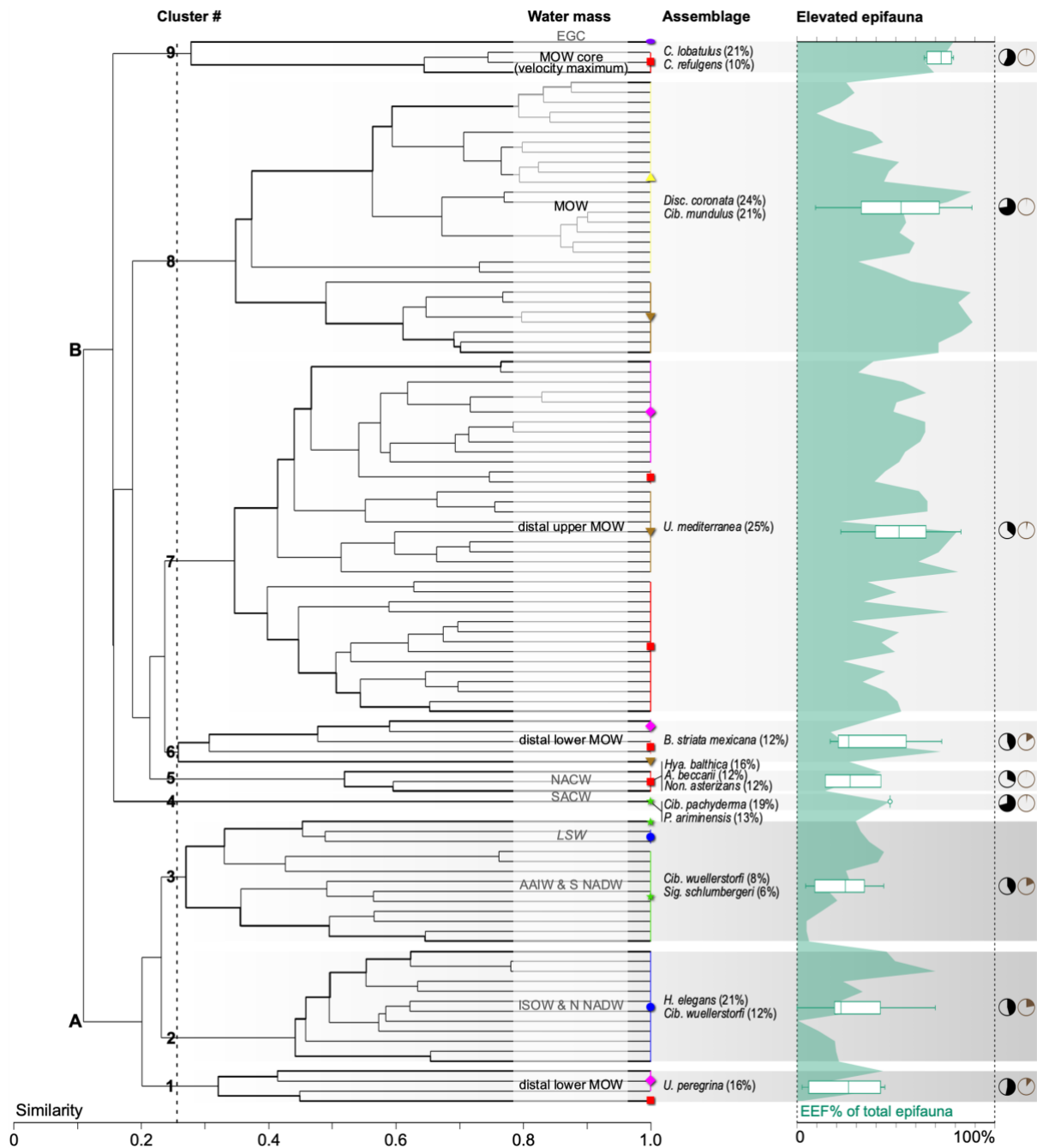


**Figure 2 |** Hierarchical cluster analysis (HCA) for benthic foraminiferal communities from Atlantic Ocean CDS and current regimes. The assemblages are based on the SIMPER analysis (Table 4). The elevated epifauna (EEF) is shown as relative proportion of the epifauna, and the boxplots summarise the respective cluster. Black pie charts show the amount of epifauna% of the total counts (without tubular taxa), brown pie charts show the amount of tubular agglutinated taxa, integrated in the total counts. Abbreviations mean: AAIW=Antarctic Intermediate Water, EGC=East Greenland Current, ISOW=Iceland Scotland Overflow Water, LSW=Labrador Sea Water, MOW=Mediterranean Outflow Water, NADW=North Atlantic Deep Water, SACW=South Atlantic Central Water. The symbols show the publication and location of the following data sets: North Atlantic, Greenland Continental Margin (purple ellipsis, Saupe et al., 2023); North Atlantic, Björn, Gardar, Eirik Drift (blue circle, Saupe et al., 2023); Porcupine Seabight, Moira Mounds (yellow triangle tip up, Fentimen et al., 2018); Porcupine Seabight, Galway & Propeller Mounds (brown triangle tip down, Schönfeld et al., 2011); Portugese Continental Margin (pink diamond, Schönfeld, 1997); Gulf of Cadiz (red square, Schönfeld, 2002a); Brazilian Continental Margin (green star, Saupe et al., 2022).

The integrated data sets suggest that Atlantic CDS assemblages influenced by AMOC-driven water masses differ in species composition and abundance of suspension feeding types particularly from CDS assemblages in the Northeast Atlantic basin controlled by the MOW (Figure 2). This biogeographic divide corresponds to distinct differences in physico-chemical properties (e.g., temperature, salinity) between AMOC- and MOW-driven water masses and suggests that these factors in addition to flow velocity must be considered.

#### 5.1.1 Benthic Foraminifera in AMOC-driven Water Masses

Increased occurrences of *Hoeglundina elegans* and *Cibicoides wuellerstorfi* prevail in Atlantic assemblages within AMOC-driven water masses (Table 4, group A). Both are cosmopolitan oligotrophic species that are widespread in the deep-sea, with *C. wuellerstorfi* preferring microhabitats with streaming water (Lutze and Thiel, 1989; Fontanier et al., 2002; Bhaumik et al., 2014). The aragonitic *Hoeglundina elegans* dwells at the sediment-water interface and preferably inhabits the outer shelf and slopes down to water depths of 4000 m (Rosenthal et al., 2006).

In the Iceland Basin (N Atlantic), agglutinated, tubular species (e.g., *Saccorhiza* spp., *Rhabdammina* spp.) are abundant in the Björn and Gardar drifts and thus differ from surrounding North Atlantic faunas, which are dominated by hyaline species (Austin and Evans, 2000; Saupe et al., 2023). Erect, delicate suspension feeders such as *Saccorhiza ramosa* and *Rhizammina algaeformis* favour moderate current intensities of maximum 3 cm/s in the Björn Drift (Linke and Lutze, 1993; van Aken and de Boer, 1995; Saupe et al., 2023). In the Gardar Drift, the ISOW largely controls the bottom current intensity, allowing the flow speed reach up to 10 cm/s and favouring adaptive and more stable erect species such as *Rhabdammina abyssorum* (Bianchi and McCave, 2000; Saupe et al., 2023). In the Eirik Drift within the Irminger Basin, the DWBC causes comparatively higher flow velocities of up to 22 cm/s (Hunter et al., 2007), in which attached species such as *Cibicoides wuellerstorfi* and *Heterolepa broeckhiana* thrive well, and tubular agglutinated species are decreased (Saupe et al., 2023). Excluding fragile tubular agglutinated taxa (Figure 2), the assemblages in the Irminger and Iceland basins are determined by abundant *H. elegans* and *C. wuellerstorfi* with few *Melonis pompilioides* and thus more closely resemble a typical North Atlantic assemblage of oligotrophic deep water species outside CDSs (Table 4, cluster 2; e.g., Lutze and Thiel, 1989; Schmiedl et al., 1997; Bhaumik et al., 2014; Rasmussen and Thomsen, 2017; Gooday, 2019). This suggests that ISOW-affected CDS faunas in the northern Atlantic are mainly distinguished by the presence of agglutinated tubular and delicate suspension feeders (Table 3, cluster 2 and 3, Saupe et al., 2023).

In the South Atlantic Campos and Brazil basins, increased bottom flow velocities and a pronounced canyon system result in the lateral transport of organic matter (Viana, 2001; Viana et al., 2002; de Mello e Sousa et al., 2006; Bahr et al., 2020). In this environment, opportunistic *C. wuellerstorfi* coexists with endobenthic *Sigmoilopsis schlumbergeri*, which thrives well in the gently streaming waters, preferring a moderate lateral food supply (De and Gupta, 2010; Rasmussen and Thomsen, 2017). Their occurrences in the southern sample stations along the Brazilian continental margin coincide with lower concentrations of organic matter in the surface substrates (de Mello e Sousa et

al., 2006; Gaye et al., 2018; Saupe et al., 2022). Flow velocities within AAIW and NADW between 20 and 30 cm/s are comparable to the Eirik Drift in the Irminger Basin, likewise characterised by occurrences of *Cibicidoides wuellerstorfi*. In the Atlantic Ocean, this deep-sea species finds its ideal living conditions in moderate to increased current speeds, and a comparatively cooler environment with temperatures < 4°C (Lutze and Thiel, 1989; Schweizer et al., 2009; Burkett et al., 2016). This makes *Cibicidoides wuellerstorfi* one of the most common species in cold AMOC-driven water masses, e.g., affected by AAIW and cold NADW (Figure 2, cluster 2 and 3).

In contrast, the warmer SACW layers at the Brazilian margin with enhanced flow velocities of up to 80 cm/s, contain a *Cibicidoides pachyderma*–*Planulina ariminensis* assemblage, while *C. wuellerstorfi* is completely absent (Table 4, cluster 4). This might be related to the clearly increased temperatures of ~10°C (sensu Yamashita et al., 2018) which is preferred by oligotrophic *C. pachyderma* (Schweizer et al., 2009; da Silveira et al., 2020). Together with the increased bottom current intensity of the SACW layer these environments favour species such as *C. pachyderma* and *Planulina ariminensis*, which can withstand the streaming water by attaching themselves to hard substrates and capturing suspended food particles from the current (Altenbach et al., 1987; Lutze and Thiel, 1989; Schönfeld and Zahn, 2000; Schönfeld, 2002b; Rüggeberg et al., 2007).

#### 5.1.2 Benthic Foraminifera in MOW-controlled Environments

In the northeast Atlantic, MOW generates a highly unique environment for benthic organisms on its path northwards from the Gulf of Cadiz and along the Iberian Peninsula. Foraminiferal assemblages are largely determined by *Uvigerina mediterranea* and *Discanomalina coronata* (Table 4, group B). *Uvigerina mediterranea* responds to high organic flux rates and is very reactive to phytodetritus (Gooday, 2003; Fontanier et al., 2006), while attached *Discanomalina coronata* preferably inhabits CWC mounds (e.g., Schönfeld et al., 2011; Fentimen et al., 2018, 2020).

The distal areas of the upper and lower MOW core are characterised by attenuated flow speed intensities (Schönfeld, 2002a). In the Gulf of Cadiz and the Iberian Peninsula, *Uvigerina mediterranea* occurs mainly on the upper slope, where it prefers the up to 13°C warm and saline layers of the distal upper MOW core and appears to be by far the most abundant taxon (25 %; Schönfeld, 1997). Co-occurrences of few to rare *Planulina ariminensis* and *Cibicidoides pachyderma* (5 % each; Table 4, cluster 7) emphasise a moderate to intense current pattern with 10-15 cm/s in distal upper MOW core settings (Schönfeld, 2002a) and up to 20-30 cm/s in isolated eddies (Schönfeld, 1997). The endemic occurrence of *U. mediterranea* in the Mediterranean Sea and the NE Atlantic basin indicates a Mediterranean heritage that is carried by the MOW. This could be caused by the strong currents of the Mediterranean outflow, which favour the dispersal of propagules migrating from the warm and saline Mediterranean to the MOW areas (Schönfeld, 2002b; Alve and Goldstein, 2014).

At the base of the lower MOW core, lateral advection of organic matter causes strongly enhanced flux rates (Schönfeld, 1997; Schönfeld and Zahn, 2000). This is accompanied by a comparatively weaker current (5-10 cm/s) in the distal lower MOW core (Schönfeld, 2002a). A positive correlation of *Bulimina striata mexicana* with high flux rates leads to an increased occurrence of this species in the

fine-grained, organic-rich sediments distal to the lower MOW core in the Gulf of Cadiz ([Figure 2](#), cluster 6; Schmiel et al., 2000). Similarly, organic matter fluxes favour an increased occurrence of *Uvigerina peregrina* in the distal parts of the lower MOW core layer beyond the flow speed maxima on the Portuguese continental margin ([Figure 2](#), cluster 1; Schönfeld and Zahn, 2000). Thus, two *Uvigerina* assemblages (a *U. mediterranea* assemblage in the distal upper core versus a *B. striata-U. peregrina* assemblage in the distal lower core) exist at the outer rims of the MOW, both benefiting from high flux rates. Since there is only negligible difference in salinity between the upper and lower MOW, the different assemblages seem to be largely driven by distinct temperature differences (Sierra et al., 2020). However, occurrences of both, *U. mediterranea* and *U. peregrina*, are also recorded in the warmer Mediterranean, mainly in relation to the quality of organic matter (Schmiel et al., 2000; Fontanier et al., 2008). Schönfeld and Altenbach (2005) therefore propose that the nature of organic matter reaching the seafloor (fresh phytodetritus vs. algal remains) influences which *Uvigerina* species is prevalent.

In proximal areas of MOW, after it has passed the Strait of Gibraltar and flows contour-parallel to the slope, flow speed maxima of up to 100 cm/s can be reached (Schönfeld, 2002a). In this strongly increased current regime an assemblage of abundant *Cibicides lobatulus* and few *Cibicides refulgens* and *Discanomalina semipunctata* occurs ([Table 4](#), cluster 9), which all belong to the elevated epifauna (EEF; [Table 2](#)). Such extreme habitats provide an ecological niche for these opportunistic species to capture nutrients from the streaming water (Schönfeld, 1997). Few occurrences of shelf-associated species such as *Elphidium crispum* and *Ammonia beccarii* ([Table 4](#), cluster 9) indicate downslope transport and redeposition from the continental shelf (Schönfeld, 2002b). Such shelf-associated species are generally abundant in the NACW above the MOW, where the shelf to upper bathyal species *Hyalinea balthica* co-occurs with typical shelf-associated species such as *Ammonia beccarii* and *Nonion asterizans* ([Table 4](#), cluster 5; Schönfeld et al., 2011).

### 5.1.3 Cold-Water Corals

In the Porcupine Seabight, the MOW (and overlying ENAW) encounters clusters of carbonate mounds, largely consisting of the framework of live and dead cold-water corals (CWC; White, 2007). These large provinces of coral banks co-occur with current-driven deposits (van Rooij et al., 2007; Hebbeln et al., 2016). By virtue of their scaffolds, the CWC reefs thus provide an optimal habitat for attached species dwelling elevated above the seafloor in a constant current environment (Schönfeld et al., 2011; Fentimen et al., 2018, 2020). The CWC framework favours an assemblage with abundant occurrences of *Discanomalina coronata* and *Cibicidoides mundulus* ([Table 4](#), cluster 8). However, the habitats of *D. coronata* and *C. mundulus* differ within the CWC mound structure. *Discanomalina coronata* preferentially colonises the elevated areas of the coral scaffolds to benefit from circulating water and suspended entrained nutrients (Schönfeld, 1997; Schönfeld et al., 2011). Living CWCs are preferred by *D. coronata* over dead ones, as the current within an active CWC mound reaches its maximum speed there (Margreth et al., 2009; Schönfeld et al., 2011; Fentimen et al., 2018). Using active mounds as an ecological niche *D. coronata* mainly settles at living CWC species *Desmophyllum pertusum* (previously



*Lophelia pertusa*) and is thus proposed as an index taxon for living coral mounds (Margreth et al., 2009). *Cibicidoides mundulus*, however, prefers to inhabit the off-mound facies, where sediments with sand-grain-sized components predominate and current speed is comparatively reduced (Margreth et al., 2009; Fentimen et al., 2018). The oligotrophic and physico-chemically stable environment prevailing in the off-mound facies provides an ideal habitat for passive suspension feeders such as *C. mundulus* (Margreth et al., 2009).

Although CWC mounds also occur on the Brazilian continental margin, the Campos Basin CWC assemblages and the Porcupine Seabight CWC assemblages strongly differ in their faunal composition. CWC mounds in the Campos Basin are bathed by 4°C AAIW and provide an elevated habitat for *Cibicidoides wuellerstorfi* which benefits from food particles transported within the current (Lutze and Thiel, 1989). Occurrences of epi- to slightly infaunal *Sigmoilopsis schlumbergeri* are typical for the sandwave facies, which are located on the mound flank, close to the living coral facies (Margreth et al., 2009; Fentimen et al., 2018, 2020). Negligible numbers of *Discanomalina* suggest that the AAIW does not provide favourable conditions for this species. Although CWC species *Desmophyllum pertusum* is also framework-building in the cold AAIW layers of the Campos Basin (Raddatz et al., 2020), a coexistence with *D. coronata* seems to be restricted to the warmer and more saline MOW. Thus, the unique foraminiferal assemblage of active CWC mounds in the Porcupine Seabight appears to be caused by the distinctive combination of warm (10°C) and saline (35.48) MOW (White, 2007; Lim et al., 2018).

## 5.2 Biogeographic Distribution of the EEF

A relationship between elevated epibenthic species (elevated epifauna, EEF) and bottom current strength has been reported by several authors for the Northeast Atlantic basin and MOW-related areas (Mackensen et al., 1985; Altenbach et al., 1987; Lutze and Altenbach, 1988; Lutze and Thiel, 1989; Linke and Lutze, 1993; Schönfeld, 1997, 2002a, 2002b; Schönfeld and Zahn, 2000; Rasmussen et al., 2002; Diz et al., 2004; Jorissen et al., 2007; Rogerson et al., 2011). The composition of EEF species is related to their hydrodynamic environment, e.g., the physico-chemical composition of the surrounding water mass and their position in relation to the main current and thus the velocity maxima (Figure 3; Schönfeld, 2002b). In general, the EEF is less abundant and less diverse in the abyssal areas of AMOC-driven water masses compared to MOW-driven environments, even under continuous bottom currents, such as in the Björn and Gardar drifts (Figure 1, Figure 2; e.g., Austin and Evans, 2000; Saupe et al., 2023).

In abyssal Atlantic waters, EEF is largely determined by opportunistic *Cibicidoides wuellerstorfi*, which is well adapted to < 4°C cold environments, e.g., AAIW and southern NADW at the Brazilian Margin, or northern NADW in the North Atlantic Eirik Drift (Table 5, cluster 2 and 3). Other EEF species are very rare or even lacking. Within the ISOW, however, which largely shapes the Björn and Gardar drifts, even *Cibicidoides wuellerstorfi* occurrences are very low or it is absent (Saupe et al., 2023). Slightly increased salinities at about 35.0, compared to other AMOC-driven water masses, might affect the foraminiferal community in the Iceland basin CDS's (Bianchi and McCave, 2000). Together with the

limited flow velocities of maximum 10 cm/s, this environment seems hardly beneficial for EEF taxa ([Figure 1](#)); however, it provides an optimal habitat for tubular agglutinated species (see section 5.3; [Table 3](#), cluster 2; Austin and Evans, 2000; Saupe et al., 2023).

**Table 5** | EEF distribution via SIMPER analysis.

EEF Taxon	Av. dissim	Contrib. %	Cumul. %	cluster									ECh	FStr	GoC-R
				1	2	3	4	5	6	7	8	9			
<i>Discanomalina coronata</i>	15.2	18.0	18.0	-	-	<0.1	-	-	0.1	1.8	<b>24.3</b>	1.2	-	-	0.6
<i>Cibicides lobatulus</i>	15.0	17.8	35.8	0.2	1.1	0.7	-	2.9	0.3	2.3	4.2	<b>21.4</b>	32.9	1.1	<b>6.3</b>
<i>Cibicoides wuellerstorfi</i>	14.0	16.6	52.5	1.1	<b>11.5</b>	<b>8.4</b>	-	-	0.9	2.1	1.2	0.4	-	-	0.8
<i>Planulina ariminensis</i>	10.7	12.7	65.2	-	-	0.4	<b>12.9</b>	-	0.2	4.9	3.0	1.1	0.2	-	3.2
<i>Cibicoides pachyderma</i>	8.0	9.4	74.6	<b>5.5</b>	-	0.2	<b>19.1</b>	0.9	0.7	4.8	0.9	5.0	-	-	-
<i>Cibicides refulgens</i>	5.2	6.1	80.8	-	0.2	0.2	-	0.5	-	0.6	<b>5.6</b>	<b>9.9</b>	0.3	-	0.1
<i>Saccammina sphaerica</i>	3.9	4.7	85.4	4.0	0.3	0.5	-	0.1	<b>9.2</b>	0.5	0.5	-	-	-	-
<i>Textularia pseudogramen</i>	3.4	4.1	89.5	-	-	<0.1	-	2.0	-	0.3	-	0.7	2.6	-	1.9
<i>Vulvulina pennatula</i>	1.9	2.3	91.8	-	-	-	0.6	-	2.1	0.7	0.3	-	-	-	0.2
<i>Eponides repandus</i>	1.8	2.2	94.0	-	-	-	-	-	-	-	-	-	25.9	-	-
<i>Hanzawaia concentrica</i>	1.5	1.8	95.8	-	-	-	-	-	1.1	1.1	-	-	-	-	-
<i>Discanomalina semipunctata</i>	1.0	1.2	97.0	-	-	<0.1	-	-	-	0.2	0.1	<b>6.8</b>	-	-	-
<i>Hanzawaia rhodiensis</i>	0.7	0.8	97.9	-	-	-	-	1.5	<0.1	0.3	-	-	-	-	-
<i>Ammodiscus anguillae</i>	0.6	0.8	98.6	-	-	0.4	-	-	0.9	<0.1	-	-	-	-	<0.1
<i>Rosalina anomala</i>	0.4	0.5	99.1	-	-	-	-	-	-	<0.1	<0.1	0.7	3.9	-	-
<i>Tritaxis fusca</i>	0.4	0.5	99.6	-	<0.1	<0.1	0.2	-	0.6	<0.1	0.2	-	-	-	-
<i>Placopsilina confusa</i>	0.1	0.2	99.8	-	<0.1	-	0.2	-	<0.1	<0.1	0.1	-	-	-	-
<i>Hanzawaia strattoni</i>	0.1	0.1	99.9	-	-	-	-	-	-	-	-	-	-	0.9	-
<i>Rupertina stabilis</i>	0.1	0.1	100.0	-	0.1	-	-	-	-	-	-	<0.1	-	-	-
<i>Gavelinopsis translucens</i>	0.0	0.0	100.0	-	-	-	-	-	-	<0.1	-	-	-	-	-

Similarity Percentage analysis (SIMPER, Bray-Curtis similarity index; overall average dissimilarity=82.52) for elevated epifauna (EEF) species, based on clusters 1-9 and additional stations from the English Channel (ECh; Bader, 1998 in Schönfeld, 2002b), the Florida Straits (FStr; Lynch-Stieglitz et al., 1999 in Schönfeld, 2002b), and the Gulf of Cadiz (GoC-R; Rogerson et al., 2011). Species that make up more than 5 % are highlighted in bold.

In the distal settings and boundary layers of the lower MOW core, EEF occurrences are also very low and homogeneous, mainly consisting of *Cibicoides pachyderma* and *Saccammina sphaerica* ([Table 5](#), cluster 1 and 6; Schönfeld, 1997). *Cibicoides pachyderma* occurs attached to hydroids, but according to Altenbach et al. (1987) only slightly above the seafloor. Schönfeld (2002a, 2002b) reports that *S. sphaerica* prefers elevated substrates up to a maximum of 2.8 cm, even if higher substrates are available. Both species require high organic matter flux rates as they occur from lateral advection at the MOW's base (and where they also favour a *Bulimina striata-Uvigerina peregrina* assemblage; Schönfeld and Zahn, 2000; Gooday, 2003; Fontanier et al., 2008). *Cibicoides pachyderma* inhabits the relatively strong flowing SACW layer on the Brazilian continental margin ([Table 5](#), cluster 4) and thus appears to be more robust to stronger currents than *S. sphaerica*. In the Atlantic Ocean, *S. sphaerica* occurs at abyssal depths with gentle bottom currents (e.g., Kuhnt et al., 2000; Schröder-Adams and van Rooyen, 2010; Lintner et al., 2021; Saupe et al., 2023). However, within the North Atlantic CDS (Björn and Gardar Drift) it also contributes little to the main assemblage (Saupe et al., 2023).

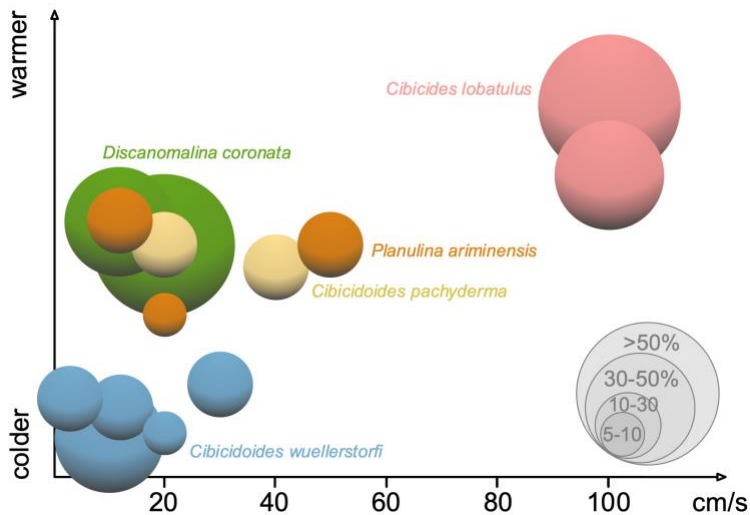


**Figure 3** | Distribution of the five most important EEF taxa in current regimes of the Atlantic Ocean, based on the data of this study.

Diverse and abundant occurrences of EEF taxa seem to be mainly restricted to warm and saline water masses like the MOW (Figure 2, group B). Within the MOWs velocity core maximum in the Gulf of Cadiz and at the Iberian Peninsula *Cibicides lobatulus* is the most significant EEF taxon (Table 5, cluster 9). Together with *Cibicides refulgens*, it is considered as indicator for the high velocity core of the MOW (García-Gallardo et al., 2017), however it also occurs in high numbers within NACW in the English Channel and EGC south of Greenland (Figure 2). In the English Channel, environmental conditions (8-16°C, 34.9-35.5 psu; Bader, 2001) are comparable to the proximal Gulf of Cadiz (7-13°C, 38.4 psu; Schönfeld, 2002b). Near-bottom currents can reach 100-200 cm/s, with pebbles, gravels and stocks of e.g., hydrozoans providing elevated habitats (Bader, 2001; Schönfeld, 2002b). Beyond the Northeast Atlantic Basin, *C. lobatulus* occurs in mesopelagic areas such as the Florida Straits within the Florida Current (Lynch-Stieglitz et al., 1999; Schönfeld, 2002b), or south of Greenland within the EGC (Saupe et al., 2023), where it contributes to a high proportion of EEF (Figure 1). However, it should be noted that the proportion of epifauna in the Florida Straits is very low, so that the contribution of the EEF to the total assemblage is marginal (Table 5). According to Schönfeld et al. (2011), conditions in the Florida Straits (7-10°, 34.6 psu, bottom flow speeds of 9-11 cm/s) are rather comparable to a distal Gulf of Cadiz. The shallow EGC offers favourable conditions for *C. lobatulus* because of its warm (6-9°C), saline (~35.0) and intense bottom flow (40 cm/s; Holliday et al., 2007; Hunter et al., 2007). Due to its particularly large pores on its flattened and attached face, *C. lobatulus* secures its attachment to elevated substrates via organic outgrowths, even in strongly increased currents (Dubicka et al., 2015). It attaches itself with the protoplasm rather than with carbonate cement, allowing it to retain some mobility (Burkett et al., 2020). Its occurrence is limited to the shelf and the upper slope within the comparatively warmer water mass layers (e.g., Sejrup et al., 1981; Lutze and Coulbourn, 1984; Mackensen et al., 1985; Schweizer et al., 2009; Dorst and Schönfeld, 2013). Consequently, *C. lobatulus* further inhabits the on-mound facies of CWC mounds, surrounded by warm and saline MOW (Rüggeberg et al., 2007). Within the CWC mounds surrounded by distinctly colder AAIW in the Campos Basin of the Brazilian margin, this EEF species is absent (e.g., de Mello e Sousa et al., 2006; Saupe et al., 2022).

In the distal upper MOW core, *Planulina ariminensis* largely determines the EEF's composition ([Table 3](#), cluster 7). By comparison, at the Brazilian continental margin, *P. ariminensis* is recorded from the warmer SACW layer only, while it is lacking in the colder and deeper layers ([Table 4](#), cluster 4; Saupe et al., 2022). Its occurrences are also described as typical for the upper zone (< 1000 m) from other regions such as the central North Atlantic or the continental margin of northwest Africa (e.g., Lutze and Coulbourn, 1984; Hermelin and Scott, 1985). Moreover, *P. ariminensis* prefers the elevated substrates of the dead coral facies in CWC mounds, which are characterised by continuous currents and fine-grained sediments such as mud and silt (Margreth et al., 2009). In the Propeller Mound (Porcupine Seabight), where current maxima do not exceed 40 m/s, it also occurs in the on-mound facies (Rüggeberg et al., 2007; Schönfeld et al., 2011), but is rare to absent in the velocity maxima of the MOW in the Gulf of Cadiz and the Portuguese continental margin. The CWC mounds surrounded by the MOW are largely populated by EEF species *Discaenoma coronata*, which also determines the total assemblage ([Table 4](#), cluster 8). This illustrates that the CWC mounds of the Porcupine Seabight surrounded by the warm and saline MOW result in a specific setting that seems unique for this region (Rüggeberg et al., 2007; Raddatz et al., 2011; Schönfeld et al., 2011; Fentimen et al., 2018, 2020).

### 5.3 Agglutinated Tubular Species as Indicators of Bottom Currents

Agglutinated tubular taxa such as *Saccorhiza ramosa*, *Rhizammina algaeformis* and *Rhabdammina abyssorum* are common in our data set in cold (1.7-4°C) AMOC-driven water masses ([Figure 2](#), [Table 3](#)), preferring weak (~3 cm/s for *Saccorhiza* and *Rhizammina*) to intermediate (~10 cm/s for *Rhabdammina*) flow velocities (Altenbach et al., 1988, 1993; Saupe et al., 2023). Their delicate tubular tests make them susceptible to destruction by strong bottom currents and thus they only occur in the very distal areas of the MOW (Schönfeld, 1997). Schönfeld (1997, 2002a) reports few to abundant occurrences of *Saccorhiza* tubes from Iberian Peninsula within the mixing layer of MOW and NADW, indicating that agglutinated tubular species prefer calm currents and average salinities, e.g., compared to normal northern and southern NADW ([Figure 2](#), [Table 3](#), cluster 6). As such, their occurrences in surface sediments may generally serve as indicators of comparably weak bottom currents (Saupe et al., 2023). However, fragmentation of tubular agglutinated tests results in potentially significant overestimations of their contribution to the foraminiferal assemblages. Their quantitative interpretation in both, the recent and fossil record, has thus to be carefully considered, e.g., through reduction by a certain factor (Kurbjeweit et al., 2000; Saupe et al., 2023) or separate investigation of calcareous and agglutinated tests in the assemblage. Yet, if carefully considered, the qualitative or semi-quantitative assessment of their presence and/or absence may give a good indication of relative bottom current intensity.

The overall preservation potential of tubular agglutinated taxa in the fossil record differs considerably and may affect their flow speed proxy assessment. Several studies have demonstrated a high preservation potential for firmly cemented tests of *Saccorhiza* and *Rhabdammina* (Schröder, 1988; Kuhnt et al., 2000; Grunert et al., 2015). We thus expect their representation in the fossil record to resemble their original contribution closely. In contrast, the fragile, loosely cemented tests of

*Rhizammina* are prone to quick and complete post-mortem disintegration and show a low preservation potential (Schröder, 1988). Fossil assemblages from the study areas will thus likely miss most or all remains of *Rhizammina* (if organic linings are not considered; Kuhnt et al., 2000). However, tubes of better preservable *Saccorhiza ramosa*, which largely occur in the same environments as *Rhizammina*, potentially remain in the fossil record (Schröder, 1988; Saupe et al., 2023).

## 6. Conclusion

The compilation and assessment of benthic foraminifera > 250 µm in enhanced current regimes and contourite drift systems of the Atlantic Ocean reveal a biogeographic divide between assemblages in AMOC-driven water masses and MOW-controlled areas. One of the major contributors to this divide lies in substantial temperature and salinity differences between both areas. The warm (13°C) and saline (38.4) MOW favours a diverse benthic foraminiferal fauna determined mainly by *Cibicides lobatulus*, *Cibicidoides mundulus*, *Discanomalina coronata*, *Uvigerina mediterranea*, and *Uvigerina peregrina*. Cold (1.7-4°C) and less saline (34.2-34.9) water masses of the AMOC (e.g., northern and southern NADW) rather favour a *Hoeglundina elegans*-*Cibicidoides wuellerstorfi* assemblage. It further appears, that the biogeographic delimitation of the MOW can be related to a Mediterranean heritage, e.g., reflected in the endemic occurrence of *U. mediterranea* in the Mediterranean and in MOW areas, or the specific adaptation of *Discanomalina coronata* to MOW surrounded CWC mounds. It suggests that the strong bottom currents of the Mediterranean Outflow e.g., favours the dispersal of propagules typical for warm and saline Mediterranean water into MOW areas (Schönfeld, 2002b; Alve and Goldstein, 2014). All these environmental factors combined create a unique habitat for a distinct foraminiferal association.

The vigorous bottom current velocities of the MOW (up to 100 cm/s) favour a diverse elevated epifauna (EEF), led by *Cibicides lobatulus*, *C. refulgens* and *Planulina ariminensis* in the proximal MOW core (Schönfeld, 1997, 2002a, 2002b) and led by *Discanomalina coronata* in the on-mound facies of CWCs (Schönfeld et al., 2011; Fentimen et al., 2018). Occurrences of *C. lobatulus*, *C. refulgens* or *Cibicidoides pachyderma* in regions such as the English Channel (8-16°, 100-200 cm/s, NACW) or the southern continental margin of Greenland (6-9°, 40 cm/s, EGC) emphasises a temperature sensitivity of typical EEF species and suggests that the EEF proxy method can be applied outside the MOW when warm, pelagic areas are considered. Finally, in the cold and deep AMOC-driven water masses (e.g., northern and southern NADW, AAIW) with currents of up to 40 cm/s, only *Cibicidoides wuellerstorfi* finds a suitable habitat, while other EEF taxa are lacking.

Reduced, yet variable bottom flow velocities in AMOC-driven sites are reflected in abundance differences between hyaline attached species and tubular suspension feeders (Saupe et al., 2023). In the Björn and Gardar drifts (Iceland basin), which are mainly controlled by the ISOW, deep-water EEF taxon *C. wuellerstorfi* is significantly reduced or completely absent. Instead, tubular agglutinated species such as *Saccorhiza ramosa*, *Rhizammina algaeformis* and *Rhabdammina abyssorum* control the assemblages (Saupe et al., 2023). These tubular, fragile suspension feeders prefer cold waters

(max. 4°C) and gentle flow velocities (max. 10 cm/s) and might serve as indicators for weak bottom currents in the North Atlantic basins.

Cold water coral (CWC) mounds, bathed by the MOW, form an exception regarding EEF occurrences (e.g., Porcupine Seabight). *Discanomalina coronata* (on-mound facies) and *Cibicidoides mundulus* (off-mound facies) largely determine the assemblages in the Porcupine Seabight (Schönfeld et al., 2011; Fentimen et al., 2018). This contrasts with CWC mounds, e.g., on the Brazilian continental margin, bathed by cold AAIW, where an assemblage of *Cibicidoides wuellerstorfi* and *Sigmoilopsis schlumbergeri* prevails, while *Discanomalina* is completely absent. Since species-specific dependencies on certain CWC taxa can be excluded (e.g., Margreth et al., 2009; Raddatz et al., 2020), a Mediterranean heritage also seems to be reflected in the MOW-surrounded CWCs.

The initial results of the assessment and evaluation of a EEF bottom current proxy beyond the Iberian Margin suggest that local hydrological conditions (temperature, salinity), in addition to hydrodynamic properties (bottom flow speeds), play a major role in proxy development. Furthermore, a Mediterranean heritage at MOW-related areas must be considered as site-specific impact factor, thus a strong heterogeneous EEF seems to be restricted to the northeast Atlantic basin.

## Acknowledgements

The authors would like to thank Joachim Schönfeld (Geomar, Kiel, Germany), who provided his data sets from the Gulf of Cadiz and was always available for discussions. Further acknowledgements go to Robin Fentimen (École normale supérieure de Lyon, France), who also made his data from the Porcupine Seabight available. This study was financially supported by the Deutsche Forschungsgemeinschaft (DFG, project number GR52851-1).

## References

- Altenbach, A.V., 1988. Deep-sea foraminifera and flux rates of organic carbon. *Revue de Paléobiologie Special 2*, 719–720.
- Altenbach, A.V., Heeger, T., Linke, P., Spindler, M., Thies, A., 1993. *Miliolinella subrotunda* (Montagu), a miliolid foraminifer building large detritic tubes for a temporary epibenthic lifestyle. *Mar Micropaleontol* 20, 293–301. [https://doi.org/10.1016/0377-8398\(93\)90038-Y](https://doi.org/10.1016/0377-8398(93)90038-Y)
- Altenbach, A.V., Lutze, G.F., Weinholz, P., 1987. Beobachtungen an Benthos-Foraminiferen (Teilprojekt A3), Berichte aus dem Sonderforschungsbereich 313, Universität Kiel.
- Altenbach, A.V., Unsöld, G., Walger, E., 1988. The hydrodynamic Environment of *Saccorhiza ramosa* (BRADY). *Meyniana* 40, 119–132.
- Alve, E., Goldstein, S.T., 2014. The Propagule Method as an Experimental Tool in Foraminiferal Ecology, in: Kitazato, H., Bernhard, J.M. (Eds.), *Approaches to Study Living Foraminifera: Collection*,

- Maintenance and Experimentation. Springer, Japan, pp. 1–12. [https://doi.org/10.1007/978-4-431-54388-6\\_1](https://doi.org/10.1007/978-4-431-54388-6_1)
- Austin, W.E.N., Evans, J.R., 2000. NE Atlantic benthic foraminifera: modern distribution patterns and palaeoecological significance, *Journal of the Geological Society*.
- Bader, B., 2001. Modern Bryomol-Sediments in a Cool-Water, High-Energy Setting: The Inner Shelf off Northern Brittany. *Facies* 81–104. <https://doi.org/10.1007/bf02668169>
- Bahr, A., Doubrawa, M., Titschack, J., Austermann, G., Koutsodendris, A., Nürnberg, D., Luiza Albuquerque, A., Friedrich, O., Raddatz, J., 2020. Monsoonal forcing of cold-water coral growth off southeastern Brazil during the past 160 kyr. *Biogeosciences* 17, 5883–5908. <https://doi.org/10.5194/bg-17-5883-2020>
- Bahr, A., Spadano Albuquerque, A.L., Ardenghi, N., Batenburg, S.J., Bayer, M., Catunda, M.C., Conforti, A., Dias, B., Ramos, R.D., Egger, L.M., Evers, F., Fischer, T., Hatsukano, K., Hennrich, B., Hoffmann, J., Jivcov, S., Kusch, S., Munz, P., Niedermeyer, E., Osborne, A., Raddatz, J., Raeke, A.W., Reissig, S., Sebastian, U., Taniguchi, N., Martins Venancio, I., Voigt, S., Wachholz, A., 2016. METEOR-Berichte: South American Hydrological Balance and Paleoceanography during the Late Pleistocene and Holocene (SAMBA) - Cruise No. M125. [https://doi.org/10.2312/cr\\_m125](https://doi.org/10.2312/cr_m125)
- Balestra, B., Grunert, P., Ausin, B., Hodell, D., Flores, J.A., Alvarez-Zarikian, C.A., Hernandez-Molina, F.J., Stow, D., Piller, W.E., Paytan, A., 2017. Coccolithophore and benthic foraminifera distribution patterns in the Gulf of Cadiz and Western Iberian Margin during Integrated Ocean Drilling Program (IODP) Expedition 339. *Journal of Marine Systems* 170, 50–67. <https://doi.org/10.1016/j.jmarsys.2017.01.005>
- Bhaumik, A.K., Gupta, A.K., Clemens, S.C., Mazumder, R., 2014. Functional morphology of *Melonis barleeanum* and *Hoeglundina elegans*: A proxy for water-mass characteristics. *Curr Sci* 106, 1133–1140. <https://doi.org/10.18520/cs/v106/i8/1133-1140>
- Bianchi, G.G., McCave, I.N., 2000. Hydrography and sedimentation under the deep western boundary current on Björn and Gardar Drifts, Iceland Basin. *Mar Geol* 165, 137–169. [https://doi.org/10.1016/S0025-3227\(99\)00139-5](https://doi.org/10.1016/S0025-3227(99)00139-5)
- Burkett, A., Rathburn, A., Pratt, R.B., Holzmann, M., 2020. Insights into the ecology of epibenthic calcareous foraminifera from a colonization study at 4000 m (Station M) in the NE Pacific Ocean. *Deep-Sea Research Part II*. <https://doi.org/10.1016/j.dsr2.2019.104709>
- Burkett, A.M., Rathburn, A.E., Elena Pérez, M., Levin, L.A., Martin, J.B., 2016. Colonization of over a thousand *Cibicides wuellerstorfi* (foraminifera: Schwager, 1866) on artificial substrates in seep and adjacent off-seep locations in dysoxic, deep-sea environments. *Deep Sea Res 1 Oceanogr Res Pap* 117, 39–50. <https://doi.org/10.1016/j.dsr.2016.08.011>

- Channell, J.E.T., Kanamatsu, T., Sato, T., Stein, R., Alvarez Zarikian, C.A., Malone, M.J., Scientists, the E. 303/306, 2006a. Expedition 303 summary. Proceedings of the IODP, 303/306 303. <https://doi.org/10.2204/iodp.proc.303306.101.2006>
- Channell, J.E.T., Kanamatsu, T., Sato, T., Stein, R., Alvarez Zarikian, C.A., Malone, M.J., Scientists, the E. 303/306, 2006b. Expedition 306 summary. Proceedings of the IODP, 303/306 303, 1–29. <https://doi.org/10.2204/iodp.proc.303306.109.2006>
- da Silveira, I.C.A., Napolitano, D.C., Farias, I.U., 2020. Water Masses and Oceanic Circulation of the Brazilian Continental Margin and Adjacent Abyssal Plain 7–36. [https://doi.org/10.1007/978-3-030-53222-2\\_2](https://doi.org/10.1007/978-3-030-53222-2_2)
- de Madron, X.D., Weatherly, G., 1994. Circulation, transport and bottom boundary layers of the deep currents in the Brazil Basin. *J Mar Res* 52, 583–638. <https://doi.org/10.1357/0022240943076975>
- de Mello e Sousa, S.H., Passos, R.F., Fukumoto, M., da Silveira, I.C.A., Figueira, R.C.L., Koutsoukos, E.A.M., de Mahiques, M.M., Rezende, C.E., 2006. Mid-lower bathyal benthic foraminifera of the Campos Basin, Southeastern Brazilian margin: Biotopes and controlling ecological factors. *Mar Micropaleontol* 61, 40–57. <https://doi.org/10.1016/j.marmicro.2006.05.003>
- De, S., Gupta, A.K., 2010. Deep-sea faunal provinces and their inferred environments in the Indian Ocean based on distribution of Recent benthic foraminifera. *Palaeogeogr Palaeoclimatol Palaeoecol* 291, 429–442. <https://doi.org/10.1016/j.palaeo.2010.03.012>
- Diz, P., Guillermo, F., Costas, S., Souto, C., Alejo, I., 2004. Distribution of benthic foraminifera in coarse sediments, Ria de Vigo, NW Iberian Margin. *The Journal of Foraminiferal Research* 34, 258–275. <https://doi.org/10.2113/34.4.258>
- Dorst, S., Schönfeld, J., 2013. Diversity of benthic foraminifera on the shelf and slope of the ne atlantic: Analysis of datasets. *J Foraminifer Res* 43, 238–254. <https://doi.org/10.2113/gsjfr.43.3.238>
- Dubicka, Z., Zlotnik, M., Borszcz, T., 2015. Marine Micropaleontology Test morphology as a function of behavioral strategies — Inferences from benthic foraminifera. *Mar Micropaleontol* 116, 38–49. <https://doi.org/10.1016/j.marmicro.2015.01.003>
- Fatela, F., Taborda, R., 2002. Confidence limits of species proportions in microfossil assemblages. *Mar Micropaleontol* 45, 169–174. [https://doi.org/10.1016/S0377-8398\(02\)00021-X](https://doi.org/10.1016/S0377-8398(02)00021-X)
- Fentimen, R., Lim, A., Rüggeberg, A., Wheeler, A.J., Rooij, D. van, 2020. Impact of bottom water currents on benthic foraminiferal assemblages in a cold-water coral environment: The Moira Mounds (NE Atlantic). *Mar Micropaleontol* 154, 1–14. <https://doi.org/10.1016/j.marmicro.2019.101799>
- Fentimen, R., Rüggeberg, A., Lim, A., Kateb, A. el, Foubert, A., Wheeler, A.J., Spezzaferri, S., 2018. Benthic foraminifera in a deep-sea high-energy environment: the Moira Mounds (Porcupine Seabight, SW of Ireland). *Swiss J Geosci* 111, 533–544. <https://doi.org/10.1007/s00015-018-0317-4>



- Fontanier, C., Jorissen, F.J., Anschutz, P., Chaillou, G., 2006. Seasonal variability of benthic foraminiferal faunas at 1000 m depth in the Bay of Biscay. *J Foraminifer Res* 36, 61–76. <https://doi.org/10.2113/36.1.61>
- Fontanier, C., Jorissen, F.J., Lansard, B., Mouret, A., Buscail, R., Schmidt, S., Kerhervé, P., Buron, F., Zaragosi, S., Hunault, G., Ernoult, E., Artero, C., Anschutz, P., Rabouille, C., 2008. Live foraminifera from the open slope between Grand Rhône and Petit Rhône Canyons (Gulf of Lions, NW Mediterranean). *Deep Sea Res 1 Oceanogr Res Pap* 55, 1532–1553. <https://doi.org/10.1016/j.dsr.2008.07.003>
- Fontanier, C., Jorissen, F.J., Licari, L., Alexandre, A., Anschutz, P., Carbonel, P., 2002. Live benthic foraminiferal faunas from the Bay of Biscay: Faunal density, composition, and microhabitats. *Deep Sea Res 1 Oceanogr Res Pap* 49, 751–785. [https://doi.org/10.1016/S0967-0637\(01\)00078-4](https://doi.org/10.1016/S0967-0637(01)00078-4)
- García-Gallardo, Á., Grunert, P., van der Schee, M., Sierro, F.J., Jiménez-Espejo, F.J., Alvarez Zarikian, C.A., Piller, W.E., 2017. Benthic foraminifera-based reconstruction of the first Mediterranean-Atlantic exchange in the early Pliocene Gulf of Cadiz. *Palaeogeogr Palaeoclimatol Palaeoecol* 472, 93–107. <https://doi.org/10.1016/j.palaeo.2017.02.009>
- Gaye, B., Böll, A., Segschneider, J., Burdanowitz, N., Emeis, K.C., Ramaswamy, V., Lahajnar, N., Lückge, A., Rixen, T., 2018. Glacial-interglacial changes and Holocene variations in Arabian Sea denitrification. *Biogeosciences* 15, 507–527. <https://doi.org/10.5194/bg-15-507-2018>
- Gili, J.M., Coma, R., 1998. Benthic suspension feeders: Their paramount role in littoral marine food webs. *Trends Ecol Evol* 13, 316–321. [https://doi.org/10.1016/S0169-5347\(98\)01365-2](https://doi.org/10.1016/S0169-5347(98)01365-2)
- Goineau, A., Gooday, A.J., 2017. Novel benthic foraminifera are abundant and diverse in an area of the abyssal equatorial Pacific licensed for polymetallic nodule exploration. *Sci Rep* 7, 1–15. <https://doi.org/10.1038/srep45288>
- Gooday, A.J., 2014. Deep-sea benthic foraminifera, in: Cochran, J.K., Bokuniewicz, H.J., Yager, P.L. (Eds.), *Encyclopedia of Ocean Sciences*. Elsevier, pp. 684–705. <https://doi.org/10.1016/B978-0-12-409548-9.09071-0>
- Gooday, A.J., 2003. Benthic foraminifera (protista) as tools in deep-water palaeoceanography: Environmental influences on faunal characteristics. *Adv Mar Biol* 46, 1–90. [https://doi.org/10.1016/S0065-2881\(03\)46002-1](https://doi.org/10.1016/S0065-2881(03)46002-1)
- Grunert, P., Skinner, L., Hodell, D.A., Piller, W.E., 2015. A micropalaeontological perspective on export productivity, oxygenation and temperature in NE Atlantic deep-waters across Terminations I and II. *Glob Planet Change* 131, 174–191. <https://doi.org/10.1016/j.gloplacha.2015.06.002>
- Hammer, Ø., Harper, D.A.T., Ryan, P.D., 2001. Past: Paleontological Statistics Software Package for Education and Data Analysis. *Palaeontologia Electronica* 4, 9.

- Harloff, J., Mackensen, A., 1997. Recent benthic foraminiferal associations and ecology of the Scotia Sea and Argentine Basin. *Mar Micropaleontol* 31, 1–29. [https://doi.org/10.1016/S0377-8398\(96\)00059-X](https://doi.org/10.1016/S0377-8398(96)00059-X)
- Hebbeln, D., van Rooij, D., Wienberg, C., 2016. Good neighbours shaped by vigorous currents: Cold-water coral mounds and contourites in the North Atlantic. *Mar Geol* 378, 171–185. <https://doi.org/10.1016/j.margeo.2016.01.014>
- Hermelin, J.O.R., Scott, D.B., 1985. Recent benthic foraminifera from the central North Atlantic. *Micropaleontology* 31, 199–220.
- Holliday, N.P., Meyer, A., Bacon, S., Alderson, S.G., de Cuevas, B., 2007. Retroflexion of part of the east Greenland current at Cape Farewell. *Geophys Res Lett* 34, 1–5. <https://doi.org/10.1029/2006GL029085>
- Holliday, N.P., Pollard, R.T., Read, J.F., Leach, H., 2000. Water mass properties and fluxes in the Rockall Trough, 1975–1998. *Deep Sea Res 1 Oceanogr Res Pap* 47, 1303–1332. [https://doi.org/10.1016/S0967-0637\(99\)00109-0](https://doi.org/10.1016/S0967-0637(99)00109-0)
- Hunter, S.E., Wilkinson, D., Louarn, E., McCave, I.N., Rohling, E., Stow, D.A.V., Bacon, S., 2007. Deep western boundary current dynamics and associated sedimentation on the Eirik Drift, Southern Greenland Margin. *Deep Sea Res 1 Oceanogr Res Pap* 54, 2036–2066. <https://doi.org/10.1016/j.dsr.2007.09.007>
- Jansen, E., Raymo, M.E., 1996. Leg 162: New Frontiers on Past Climates. Proceedings of the Ocean Drilling Program, Initial Reports 162, 5–20. <https://doi.org/10.2973/odp.proc.ir.162.101.1996>
- Jorissen, F.J., Fontanier, C., Thomas, E., 2007. Paleoceanographical proxies based on deep-sea benthic foraminiferal assemblage characteristics, in: Hillaire-Marcel, C., de Vernal, A. (Eds.), *Proxies in Late Cenozoic Paleoceanography: Pt. 2: Biological Tracers and Biomarkers*. pp. 263–325. [https://doi.org/10.1016/S1572-5480\(07\)01012-3](https://doi.org/10.1016/S1572-5480(07)01012-3)
- Kuhlbrodt, T., Griesel, A., Montoya, M., Levermann, A., Hofmann, M., Rahmstorf, S., 2007. On the driving processes of the Atlantic meridional overturning circulation. *Reviews of Geophysics* 2, 1–32. <https://doi.org/10.1029/2004RG000166.1.INTRODUCTION>
- Kuhnt, W., Collins, E., Scott, D.B., 2000. Deep Water Agglutinated Foraminiferal Assemblages across the Gulf Stream: Distribution Patterns and Taphonomy, in: Hart, M.B., Kaminski, M.A., & Smart, C.W. (Eds) 2000. *Proceedings of the Fifth International Workshop on Agglutinated Foraminifera*. Grzybowski Foundation Special Publication, 7. pp. 261–298.
- Kurbjeweit, F., Schmiedl, G., Schiebel, R., Hemleben, C., Pfannkuche, O., Wallmann, K., Schäfer, P., 2000. Distribution, biomass and diversity of benthic foraminifera in relation to sediment geochemistry in the Arabian Sea. *Deep Sea Res 2 Top Stud Oceanogr* 47, 2913–2955. [https://doi.org/10.1016/S0967-0645\(00\)00053-9](https://doi.org/10.1016/S0967-0645(00)00053-9)

- Lim, A., Huvenne, V.A.I., Vertino, A., Spezzaferri, S., Wheeler, A.J., 2018. New insights on coral mound development from groundtruthed high-resolution ROV-mounted multibeam imaging. *Mar Geol* 401, 225–237. <https://doi.org/https://doi.org/10.1016/j.margeo.2018.06.006>
- Linke, P., Lutze, G.F., 1993. Microhabitat preferences of benthic foraminifera – a static concept or a dynamic adaptation to optimize food acquisition? *Mar Micropaleontol* 20, 215–234. [https://doi.org/doi.org/10.1016/0377-8398\(93\)90034-U](https://doi.org/doi.org/10.1016/0377-8398(93)90034-U)
- Lintner, B., Lintner, M., Bukenberg, P., Witte, U., Heinz, P., 2021. Living benthic foraminiferal assemblages of a transect in the Rockall Trough (NE Atlantic). *Deep-Sea Research Part I* 171, 1–19. <https://doi.org/10.1016/j.dsr.2021.103509>
- Lutze, G.F., Altenbach, A.V., 1988. *Rupertina stabilis* (Wallich), a highly adapted, suspension feeding foraminifer. *Meyniana* 40, 55–69. <https://doi.org/10.2312/meyniana.1988.40.55>
- Lutze, G.F., Coulbourn, W.T., 1984. Recent benthic foraminifera from the continental margin of northwest Africa: Community structure and distribution. *Mar Micropaleontol* 8, 361–401. [https://doi.org/10.1016/0377-8398\(84\)90002-1](https://doi.org/10.1016/0377-8398(84)90002-1)
- Lutze, G.F., Thiel, H., 1989. Epibenthic foraminifera from elevated microhabitats; *Cibicidoides wuellerstorfi* and *Planulina ariminensis*. *The Journal of Foraminiferal Research* 19, 153–158. <https://doi.org/10.2113/gsjfr.19.2.153>
- Lynch-Stieglitz, J., Curry, W.B., Slowey, N., 1999. A geostrophic transport estimate for the Florida Current from the oxygen isotope composition of benthic foraminifera. *Paleoceanogr Paleoclimatol* 14, 360–373. <https://doi.org/10.1029/1999PA900001>
- Mackensen, A., Schmiedl, G., Harloff, J., Giese, M., 1995. Deep-Sea Foraminifera in the South Atlantic Ocean: Ecology and Assemblage Generation. *Micropaleontology* 41, 342–358. <https://doi.org/10.2307/1485808>
- Mackensen, A., Sejrup, H.P., Jansen, E., 1985. The distribution of living benthic foraminifera on the continental slope and rise off southwest Norway. *Mar Micropaleontol* 9, 275–306. [https://doi.org/https://doi.org/10.1016/0377-8398\(85\)90001-5](https://doi.org/https://doi.org/10.1016/0377-8398(85)90001-5)
- Margreth, S., Rüggeberg, A., Spezzaferri, S., 2009. Benthic foraminifera as bioindicator for cold-water coral reef ecosystems along the Irish margin. *Deep Sea Res 1 Oceanogr Res Pap* 56, 2216–2234. <https://doi.org/10.1016/j.dsr.2009.07.009>
- Martins, L.R., Coutinho, P.N., 1981. The Brazilian continental margin. *Earth Science Reviews* 17, 87–107. [https://doi.org/10.1016/0012-8252\(81\)90007-6](https://doi.org/10.1016/0012-8252(81)90007-6)
- Morigi, C., Jorissen, F.J., Gervais, A., Guichard, S., Borsetti, A.M., 2001. Benthic foraminiferal faunas in surface sediments off NW Africa: Relationship with organic flux to the ocean floor. *J Foraminifer Res* 31, 350–368. <https://doi.org/10.2113/0310350>
- Murray, J.W., 2001. The niche of benthic foraminifera, critical thresholds and proxies. *Mar Micropaleontol* 41, 1–7. [https://doi.org/10.1016/S0377-8398\(00\)00057-8](https://doi.org/10.1016/S0377-8398(00)00057-8)

- O'Neil Baringer, M., Price, J.F., 1999. A review of the physical oceanography of the Mediterranean outflow. *Mar Geol* 155, 63–82.
- Peterson, R.G., Stramma, L., 1991. Upper-level circulation in the South Atlantic Ocean. *Prog Oceanogr* 26, 1–73. [https://doi.org/10.1016/0079-6611\(91\)90006-8](https://doi.org/10.1016/0079-6611(91)90006-8)
- Raddatz, J., Rüggeberg, A., Margreth, S., Dullo, W.C., 2011. Paleoenvironmental reconstruction of Challenger Mound initiation in the Porcupine Seabight, NE Atlantic. *Mar Geol* 282, 79–90. <https://doi.org/10.1016/j.margeo.2010.10.019>
- Raddatz, J., Titschack, J., Frank, N., Freiwald, A., Conforti, A., Osborne, A., Skornitzke, S., Stiller, W., Rüggeberg, A., Voigt, S., Albuquerque, A.L.S., Vertino, A., Schröder-Ritzrau, A., Bahr, A., 2020. *Solenosmilia variabilis*-bearing cold-water coral mounds off Brazil. *Coral Reefs* 39, 69–83. <https://doi.org/10.1007/s00338-019-01882-w>
- Rasmussen, T.L., Thomsen, E., 2017. Ecology of deep-sea benthic foraminifera in the North Atlantic during the last glaciation: Food or temperature control. *Palaeogeogr Palaeoclimatol Palaeoecol* 472, 15–32. <https://doi.org/10.1016/j.palaeo.2017.02.012>
- Rasmussen, T.L., Thomsen, E., Troelstra, S.R., Kuijpers, A., Prins, M.A., 2002. Millennial-scale glacial variability versus Holocene stability: changes in planktic and benthic foraminifera faunas and ocean circulation in the North Atlantic during the last 60 000 years. *Mar Micropaleontol* 47, 143–176. [https://doi.org/https://doi.org/10.1016/S0377-8398\(02\)00115-9](https://doi.org/https://doi.org/10.1016/S0377-8398(02)00115-9)
- Rebesco, M., Hernández-Molina, F.J., van Rooij, D., Wåhlin, A., 2014. Contourites and associated sediments controlled by deep-water circulation processes: State-of-the-art and future considerations. *Mar Geol* 352, 111–154. <https://doi.org/10.1016/j.margeo.2014.03.011>
- Roberts, D.G., Backman, J., Morton, A.C., Keene, J.B., 1984. Introduction and Explanatory Notes, Leg 81, Deep Sea Drilling Project. Initial Reports of the Deep Sea Drilling Project 81, 5–28. <https://doi.org/10.2973/dsdp.proc.81.101.1984>
- Rogerson, M., Schönfeld, J., Leng, M.J., 2011. Qualitative and quantitative approaches in palaeohydrography: A case study from core-top parameters in the Gulf of Cadiz. *Mar Geol* 280, 150–167. <https://doi.org/10.1016/j.margeo.2010.12.008>
- Rosenthal, Y., Lear, C.H., Oppo, D.W., Linsley, B.K., 2006. Temperature and carbonate ion effects on Mg/Ca and Sr/Ca ratios in benthic foraminifera: Aragonitic species *Hoeglundina elegans*. *Paleoceanography* 21, 1–14. <https://doi.org/10.1029/2005PA001158>
- Rüggeberg, A., Dullo, C., Dorschel, B., Hebbeln, D., 2007. Environmental changes and growth history of a cold-water carbonate mound (Propeller Mound, Porcupine Seabight). *International Journal of Earth Sciences* 96, 57–72. <https://doi.org/10.1007/s00531-005-0504-1>
- Sánchez-Leal, R.F., Bellanco, M.J., Fernández-Salas, L.M., García-Lafuente, J., Gasser-Rubinat, M., González-Pola, C., Hernández-Molina, F.J., Pelegrí, J.L., Peliz, A., Relvas, P., Roque, D., Ruiz-

- Villarreal, M., Sammartino, S., Sánchez-Garrido, J.C., 2017. The Mediterranean Overflow in the Gulf of Cadiz: A rugged journey. *Sci Adv* 3, 1–12. <https://doi.org/10.1126/sciadv.aao0609>
- Saupe, A., Schmidt, J., Petersen, J., Bahr, A., Dias, B.B., Albuquerque, A.L.S., Díaz Ramos, R.A., Grunert, P., 2022. Controlling Parameters of Benthic Deep-Sea Foraminiferal Biogeography at the Brazilian Continental Margin (11–22°S). *Front Mar Sci* 9, 1–17. <https://doi.org/10.3389/fmars.2022.901224>
- Saupe, A., Schmidt, J., Petersen, J., Bahr, A., Grunert, P., 2023. Benthic foraminifera in high latitude contourite drift systems (North Atlantic: Björn, Gardar and Eirik drifts). *Palaeogeogr Palaeoclimatol Palaeoecol* 609, 1–18. <https://doi.org/10.1016/j.palaeo.2022.111312>
- Sayago-Gil, M., Long, D., Hitchen, K., Díaz-del-Río, V., Fernández-Salas, L.M., Durán-Muñoz, P., 2010. Evidence for current-controlled morphology along the western slope of Hatton Bank (Rockall Plateau, NE Atlantic Ocean). *Geo-Marine Letters* 30, 99–111. <https://doi.org/10.1007/s00367-009-0163-5>
- Schmiedl, G., de Bovée, F., Buscail, R., Charrière, B., Hemleben, C., Medernach, L., Picon, P., 2000. Trophic control of benthic foraminiferal abundance and microhabitat in the bathyal Gulf of Lions, western Mediterranean Sea. *Mar Micropaleontol* 40, 167–188. [https://doi.org/10.1016/S0377-8398\(00\)00038-4](https://doi.org/10.1016/S0377-8398(00)00038-4)
- Schmiedl, G., Mackensen, A., Müller, P.J., 1997. Recent benthic foraminifera from the eastern South Atlantic Ocean: Dependence on food supply and water masses. *Mar Micropaleontol* 32, 249–287. [https://doi.org/10.1016/S0377-8398\(97\)00023-6](https://doi.org/10.1016/S0377-8398(97)00023-6)
- Schönfeld, J., 2012. History and development of methods in Recent benthic foraminiferal studies. *J Micropalaeontol* 31, 53–72. <https://doi.org/10.1144/0262-821x11-008>
- Schönfeld, J., 2002a. Recent benthic foraminiferal assemblages in deep high-energy environments from the Gulf of Cadiz (Spain). *Mar Micropaleontol* 44, 141–162. [https://doi.org/10.1016/S0377-8398\(01\)00039-1](https://doi.org/10.1016/S0377-8398(01)00039-1)
- Schönfeld, J., 2002b. A new benthic foraminiferal proxy for near-bottom current velocities in the Gulf of Cadiz, northeastern Atlantic Ocean. *Deep-Sea Research I* 49, 1853–1875. [https://doi.org/https://doi.org/10.1016/S0967-0637\(02\)00088-2](https://doi.org/https://doi.org/10.1016/S0967-0637(02)00088-2)
- Schönfeld, J., 1997. The impact of the Mediterranean Outflow Water (MOW) on benthic foraminiferal assemblages and surface sediments at the southern Portuguese continental margin. *Mar Micropaleontol* 29, 21–236. [https://doi.org/https://doi.org/10.1016/S0377-8398\(96\)00050-3](https://doi.org/https://doi.org/10.1016/S0377-8398(96)00050-3)
- Schönfeld, J., Altenbach, A.V., 2005. Late Glacial to Recent distribution pattern of deep-water *Uvigerina* species in the north-eastern Atlantic. *Mar Micropaleontol* 57, 1–24. <https://doi.org/10.1016/j.marmicro.2005.05.004>

- Schönfeld, J., Dullo, W.C., Pfannkuche, O., Freiwald, A., Rüggeberg, A., Schmidt, S., Weston, J., 2011. Recent benthic foraminiferal assemblages from cold-water coral mounds in the Porcupine Seabight. *Facies* 57, 187–213. <https://doi.org/10.1007/s10347-010-0234-0>
- Schönfeld, J., Zahn, R., 2000. Late Glacial to Holocene history of the Mediterranean Outflow. Evidence from benthic foraminiferal assemblages and stable isotopes at the Portuguese margin. *Palaeogeogr Palaeoclimatol Palaeoecol* 159, 85–111. [https://doi.org/https://doi.org/10.1016/S0031-0182\(00\)00035-3](https://doi.org/https://doi.org/10.1016/S0031-0182(00)00035-3)
- Schröder, C.J., 1988. Subsurface preservation of agglutinated foraminifera in the Northwest Atlantic Ocean. *Abhandlungen der Geologischen Bundesanstalt* 41, 325–336.
- Schröder-Adams, C.J., van Rooyen, D., 2010. Response of Recent Benthic Foraminiferal Assemblages to Contrasting Environments in Baffin Bay and the Northern Labrador Sea , Northwest Atlantic. *Arctic* 64, 317–341. <https://doi.org/https://www.jstor.org/stable/23025731>
- Schweizer, M., Pawlowski, J., Kouwenhoven, T., van der Zwaan, B., 2009. Molecular Phylogeny of Common Cibicidids and Related Rotaliida (Foraminifera) Based on Small Subunit Rdna Sequences. *The Journal of Foraminiferal Research* 39, 300–315. <https://doi.org/10.2113/gsjfr.39.4.300>
- Sejrup, H.-P., Fjaeran, T., Hald, M., Beck, L., Hagen, J., Miljeteig, I., Morvik, I., Norvik, O., 1981. Benthonic foraminifera in surface samples from the Norwegian continental margin between 62°N and 65°N. *The Journal of Foraminiferal Research* 11, 277–295. <https://doi.org/10.2113/gsjfr.11.4.277>
- Sierro, F.J., Hodell, D.A., Andersen, N., Azibeiro, L.A., Jimenez-Espejo, F.J., Bahr, A., Flores, J.A., Ausin, B., Rogerson, M., Lozano-Luz, R., Lebreiro, S.M., Hernandez-Molina, F.J., 2020. Mediterranean Overflow Over the Last 250 kyr: Freshwater Forcing From the Tropics to the Ice Sheets. *Paleoceanogr Paleoclimatol* 35, 1–31. <https://doi.org/10.1029/2020PA003931>
- Stramma, L., England, M., 1999. On the water masses and mean circulation of the South Atlantic Ocean. *Geophysical Research* 104, 20,863–20,883. <https://doi.org/doi.org/10.1029/1999JC900139>
- van Aken, H.M., 1995. Mean Currents and Current Variability in the Iceland Basin. *Netherlands Journal of Sea Research* 33, 135–145. [https://doi.org/10.1016/0077-7579\(95\)90001-2](https://doi.org/10.1016/0077-7579(95)90001-2)
- van Aken, H.M., de Boer, C.J., 1995. On the synoptic hydrography of intermediate and deep water masses in the Iceland Basin. *Deep-Sea Research Part I* 42, 165–189. [https://doi.org/10.1016/0967-0637\(94\)00042-Q](https://doi.org/10.1016/0967-0637(94)00042-Q)
- van der Zwaan, G.J., Duijnste, I.A.P., den Dulk, M., Ernst, S.R., Jannink, N.T., Kouwenhoven, T.J., 1999. Benthic foraminifers: proxies or problems? *Earth Sci Rev* 46, 213–236. [https://doi.org/10.1016/s0012-8252\(99\)00011-2](https://doi.org/10.1016/s0012-8252(99)00011-2)

- van Rooij, D., Blamart, D., Kozachenko, M., Henriët, J.-P., 2007. Small mounded contourite drifts associated with deep-water coral banks, Porcupine Seabight, NE Atlantic Ocean. Geological Society, London, Special Publications 276, 225–244.
- Viana, A.R., 2001. Seismic expression of shallow- to deep-water contourites along the south-eastern Brazilian margin. *Marine Geophysical Research* 22, 509–521. <https://doi.org/10.1023/A:1016307918182>
- Viana, A.R., Almeida Jr., W. de, Almeida, C.W., 2002. Upper slope sands: late Quaternary shallow-water sandy contourites of Campos Basin, SW Atlantic Margin. Geological Society, London, Memoirs 22, 261–270. <https://doi.org/doi.org/10.1144/GSL.MEM.2002.022.01.19>
- White, M., 2007. Benthic dynamics at the carbonate mound regions of the Porcupine Sea Bight continental margin. *International Journal of Earth Sciences* 96, 1–9. <https://doi.org/10.1007/s00531-006-0099-1>
- Wildish, D., Kristmanson, D., 1997. *Benthic Suspension Feeders and Flow*. Cambridge University Press, New York.
- Yamashita, C., Mello e Sousa, S.H. de, Vicente, T.M., Martins, M.V., Nagai, R.H., Frontalini, F., Godoi, S.S., Napolitano, D., Burone, L., Carreira, R., Figueira, R.C.L., Taniguchi, N.K., Rezende, C.E. de, Koutsoukos, E.A.M., 2018. Environmental controls on the distribution of living (stained) benthic foraminifera on the continental slope in the Campos Basin area (SW Atlantic). *Journal of Marine Systems* 181, 37–52. <https://doi.org/10.1016/j.jmarsys.2018.01.010>





## 4. Summary and Conclusions

The complex current system of the Atlantic Ocean, controlled by the AMOC, is a key player within global ocean-climate dynamics (Kuhlbrodt et al., 2007; Eldevik and Nilsen, 2013). Understanding biological and ecological factors within extensive drift systems, shaped by vigorous bottom currents, is of particular relevance for palaeoceanographic and paleoclimatic reconstructions from biogenic proxy methods (Rebesco et al., 2014).

By assessing and interpreting benthic foraminiferal communities > 250 µm from surface sediment samples in contourite drift systems (CDS) of the Atlantic Ocean, this thesis demonstrates that faunal assemblages in cold (< 4°C) and averaging saline (34.2-34.9) deep AMOC-driven water masses differ strongly from assemblages in warm (up to 13 °C) and saline (up to 38.4) MOW-controlled areas of the Northeast Atlantic Basin. Suspended organic matter, flow velocity, substrate properties, temperature and salinity determine biogeographic patterns of distinct groups of benthic foraminifera adapted to CDSs.

New microfaunal data from the Brazilian continental margin between 11 and 22°S indicate that the benthic fauna is largely controlled by temperature variations, substrate properties and hydrodynamic conditions, as well as the availability of organic matter. Branched canyons and complex channel systems with locally enhanced bottom currents favour BCF taxa in the Campos Basin, as reflected in a dominant *Globocassidulina subglobosa/crassa* assemblage (Bahr et al., 2016; Saupe et al., 2022). In the Brazil Basin, which is characterised by a higher nutrient supply and more stable substrates, bolivinids tend to be more abundant. At the lower slope in the cold (1.9-4°C), streaming (20-30 cm/s) waters of AAIW and NADW, the elevated epibenthic species *Cibicidoides wuellerstorfi* occurs in the assemblages. In the much warmer (> 10°C) and faster flowing (50-80 cm/s) SACW at the upper slope, occurrences of *Cibicidoides pachyderma* are recorded, although this species selects its elevated habitat only slightly above the seafloor (Altenbach et al., 1987). Generally, there is little diversity of the EEF at the Brazilian continental margin.

Analyses of the high latitudes of the North Atlantic revealed variations in the distribution of benthic foraminifera in an oligotrophic setting along hydrologic and hydrodynamic gradients. The assemblages from CDSs of the Iceland Basin are determined by tubular agglutinated suspension feeders. In the Björn Drift, where cold and persistent bottom currents do not exceed 3 cm/s (van Aken and de Boer, 1995), high abundances of fragile tubes of *Saccorhiza ramosa* and *Rhizammina algaeformis* occur. They use their pseudopodial network to capture food particles entrained in the constant bottom flow of LSW and its mixing layer with underlain ISOW. However, occurrences of *Rhabdammina abyssorum* - a tubular facultative suspension feeder - determine the assemblages in the hydrodynamically more complex Gardar Drift. The ISOW shapes this drift body at maximum flow speeds of 10 cm/s (Bianchi and McCave, 2000). Current velocities at the Eirik Drift (Irminger Basin, south of Greenland) are even higher, reaching about 22 cm/s (Hunter et al., 2007). Tubular suspension feeders are largely absent, but *Cibicidoides wuellerstorfi*, similar to the Brazilian continental margin, colonises the deep NADW

layers. While the EEF remains poorly diverse at the Eirik Drift, its abundances are slightly increased at the upper slope of the Greenland continental margin, within the much warmer (6-9°C) and intense (40 cm/s) East Greenland Current (Holliday et al., 2007). *Cibicides refulgens*, *Cibicides lobatulus*, and *Cibicoides pachyderma* determine the assemblage and resemble associations from the MOW at the Iberian margin (where bottom flow velocities can exceed 100 cm/s, Schönfeld, 2002a).

The hydrological and hydrodynamic properties of the warm and saline MOW, particularly favour a highly diverse EEF. Occurrences of EEF species in regions outside the Northeast Atlantic Basin, e.g., on the southern continental margin of Greenland (EGC), suggest that these species tend to prefer warmer water masses, strongly increased current velocities and coarser grain sizes. However, their diversity is comparably increased in MOW assemblages. This may be related to a Mediterranean heritage carried by the MOW. The strong bottom currents of the Mediterranean outflow seem to favour the dispersal of propagules transporting them far into the Northeast Atlantic Basin (Schönfeld, 2002b; Alve and Goldstein, 2014). Indications for this include the endemic occurrence of *Uvigerina mediterranea*, or the specific adaptation of *Discanomalina coronata* to MOW surrounded CWC mounds. Thus, in the more pelagic and warmer AMOC-driven water masses (e.g., Greenland continental margin), less EEF species can spread. Whereas cold and abyssal AMOC-driven water masses (e.g., northern and southern NADW, AAIW, ISOW) are generally more suitable habitats for cosmopolitan deep-water species such as *Cibicoides wuellerstorfi*, whereas other EEF taxa are largely absent.

The applicability of the EEF as a potential bottom current proxy requires local consideration and appears to be largely restricted to the Northeast Atlantic Basin and continental margins affected by strongly intensified bottom currents. In the deeper AMOC-driven CDSs, agglutinated tubular suspension feeders replace EEF taxa and potentially provide indicators for reconstructing weak bottom currents (Saupe et al., 2023). However, fragmentation of tubular agglutinated tests results in potentially significant overestimations of their contribution to the foraminiferal assemblages. Their quantitative interpretation in both, the recent and fossil record, has thus to be carefully considered.

This study provides a first baseline for the assessment of benthic foraminifera as indicators of bottom current intensity within Atlantic water mass dynamics. Further research is needed for a better understanding of local ecological controls on benthic foraminiferal distribution in individual Atlantic CDSs. Studies on the taphonomy of tubular agglutinated foraminifera are needed to assess opportunities and limitations of their application of bottom current indicators in the fossil record.

---

## 5. References

- Altenbach, A.V., 1988. Deep-sea foraminifera and flux rates of organic carbon. *Revue de Paléobiologie Special 2*, 719–720.
- Altenbach, A.V., Heeger, T., Linke, P., Spindler, M., Thies, A., 1993. *Miliolinella subrotunda* (Montagu), a miliolid foraminifer building large detritic tubes for a temporary epibenthic lifestyle. *Mar Micropaleontol* 20, 293–301. [https://doi.org/10.1016/0377-8398\(93\)90038-Y](https://doi.org/10.1016/0377-8398(93)90038-Y)
- Altenbach, A.V., Lutze, G.F., Weinholz, P., 1987. Beobachtungen an Benthos-Foraminiferen (Teilprojekt A3), Berichte aus dem Sonderforschungsbereich 313, Universität Kiel.
- Alve, E., Goldstein, S.T., 2014. The Propagule Method as an Experimental Tool in Foraminiferal Ecology, in: Kitazato, H., Bernhard, J.M. (Eds.), *Approaches to Study Living Foraminifera: Collection, Maintenance and Experimentation*. Springer, Japan, pp. 1–12. [https://doi.org/10.1007/978-4-431-54388-6\\_1](https://doi.org/10.1007/978-4-431-54388-6_1)
- Bahr, A., Jiménez-Espejo, F.J., Kolasinac, N., Grunert, P., Hernández-Molina, F.J., Röhl, U., Voelker, A.H.L., Escutia, C., Stow, D.A.V., Hodell, D., Alvarez-Zarikian, C.A., 2014. Deciphering bottom current velocity and paleoclimate signals from contourite deposits in the Gulf of Cádiz during the last 140 kyr: An inorganic geochemical approach. *Geochemistry, Geophysics, Geosystems* 15, 3145–3160. <https://doi.org/10.1002/2014GC005356>
- Bahr, A., Spadano Albuquerque, A.L., Ardenghi, N., Batenburg, S.J., Bayer, M., Catunda, M.C., Conforti, A., Dias, B., Ramos, R.D., Egger, L.M., Evers, F., Fischer, T., Hatsukano, K., Henrich, B., Hoffmann, J., Jivcov, S., Kusch, S., Munz, P., Niedermeyer, E., Osborne, A., Raddatz, J., Raeke, A.W., Reissig, S., Sebastian, U., Taniguchi, N., Martins Venancio, I., Voigt, S., Wachholz, A., 2016. METEOR-Berichte: South American Hydrological Balance and Paleoceanography during the Late Pleistocene and Holocene (SAMBA) - Cruise No. M125. [https://doi.org/10.2312/cr\\_m125](https://doi.org/10.2312/cr_m125)
- Bianchi, G.G., Hall, I.R., McCave, I.N., Joseph, L., 1999. Measurement of the sortable silt current speed proxy using the Sedigraph 5100 and Coulter Multisizer II: Precision and accuracy. *Sedimentology* 46, 1001–1014. <https://doi.org/10.1046/j.1365-3091.1999.00256.x>
- Bianchi, G.G., McCave, I.N., 2000. Hydrography and sedimentation under the deep western boundary current on Björn and Gardar Drifts, Iceland Basin. *Mar Geol* 165, 137–169. [https://doi.org/10.1016/S0025-3227\(99\)00139-5](https://doi.org/10.1016/S0025-3227(99)00139-5)
- Cimerman, F., Langer, M.R., 1991. Mediterranean Foraminifera. Slovenska Akademija Znanosti in Umetnosti, Ljubljana.
- da Silveira, I.C.A., Napolitano, D.C., Farias, I.U., 2020. Water Masses and Oceanic Circulation of the Brazilian Continental Margin and Adjacent Abyssal Plain 7–36. [https://doi.org/10.1007/978-3-030-53222-2\\_2](https://doi.org/10.1007/978-3-030-53222-2_2)

- de Castro, S., Hernández-Molina, F.J., de Weger, W., Jiménez-Espejo, F.J., Rodríguez-Tovar, F.J., Mena, A., Llave, E., Sierro, F.J., 2021. Contourite characterization and its discrimination from other deep-water deposits in the Gulf of Cadiz contourite depositional system. *Sedimentology* 68, 987–1027. <https://doi.org/10.1111/sed.12813>
- de Madron, X.D., Weatherly, G., 1994. Circulation, transport and bottom boundary layers of the deep currents in the Brazil Basin. *J Mar Res* 52, 583–638. <https://doi.org/10.1357/0022240943076975>
- Dickson, R.R., Brown, J., 1994. The production of North Atlantic Deep Water: sources, rates, and pathways. *J Geophys Res* 99, 12319–12341. <https://doi.org/10.1029/94jc00530>
- Diz, P., Guillermo, F., Costas, S., Souto, C., Alejo, I., 2004. Distribution of benthic foraminifera in coarse sediments, Ria de Vigo, NW Iberian Margin. *The Journal of Foraminiferal Research* 34, 258–275. <https://doi.org/10.2113/34.4.258>
- Eldevik, T., Nilsen, J.E.Ø., 2013. The arctic-atlantic thermohaline circulation. *J Clim* 26, 8698–8705. <https://doi.org/10.1175/JCLI-D-13-00305.1>
- Faugères, J.-C., Gonthier, E., Stow, D.A.V., 1984. Contourite drift molded by deep Mediterranean outflow. *Geology* 12, 296–300.
- Faugères, J.-C., Mézerais, M.L., Stow, D.A.V., 1993. Contourite drift types and their distribution in the North and South Atlantic Ocean basins. *Sediment Geol* 82, 189–203. [https://doi.org/10.1016/0037-0738\(93\)90121-K](https://doi.org/10.1016/0037-0738(93)90121-K)
- Faugères, J.-C., Mulder, T., 2011. Chapter 3 - Contour Currents and Contourite Drifts. *Developments in Sedimentology Deep-Sea S*, 149–214. [https://doi.org/10.1016/S0070-4571\(11\)63003-3](https://doi.org/10.1016/S0070-4571(11)63003-3)
- Faugères, J.-C., Stow, D.A.V., Imbert, P., Viana, A.R., 1999. Seismic features diagnostic of contourite drifts. *Mar Geol* 162, 1–38. [https://doi.org/10.1016/S0025-3227\(99\)00068-7](https://doi.org/10.1016/S0025-3227(99)00068-7)
- Fentimen, R., Rüggeberg, A., Lim, A., Kateb, A. el, Foubert, A., Wheeler, A.J., Spezzaferri, S., 2018. Benthic foraminifera in a deep-sea high-energy environment: the Moira Mounds (Porcupine Seabight, SW of Ireland). *Swiss J Geosci* 111, 533–544. <https://doi.org/10.1007/s00015-018-0317-4>
- Fraile-Nuez, E., MacHín, F., Vélez-Belchí, P., López-Laatzén, F., Borges, R., Benítez-Barrios, V., Hernández-Guerra, A., 2010. Nine years of mass transport data in the eastern boundary of the North Atlantic Subtropical Gyre. *J Geophys Res Oceans* 115. <https://doi.org/10.1029/2010JC006161>
- García-Gallardo, Á., Grunert, P., Piller, W.E., 2016. New insights on “elevated epifauna” as proxies for Mediterranean Outflow Water (MOW) reconstruction in the Gulf of Cadiz, EGU - Geophysical Research Abstracts.
- García-Gallardo, Á., Grunert, P., van der Schee, M., Sierro, F.J., Jiménez-Espejo, F.J., Alvarez Zarikian, C.A., Piller, W.E., 2017. Benthic foraminifera-based reconstruction of the first Mediterranean-

- Atlantic exchange in the early Pliocene Gulf of Cadiz. *Palaeogeogr Palaeoclimatol Palaeoecol* 472, 93–107. <https://doi.org/10.1016/j.palaeo.2017.02.009>
- Gooday, A.J., 2014. Deep-sea benthic foraminifera, in: Cochran, J.K., Bokuniewicz, H.J., Yager, P.L. (Eds.), *Encyclopedia of Ocean Sciences*. Elsevier, pp. 684–705. <https://doi.org/10.1016/B978-0-12-409548-9.09071-0>
- Gooday, A.J., 2003. Benthic foraminifera (protista) as tools in deep-water palaeoceanography: Environmental influences on faunal characteristics. *Adv Mar Biol* 46, 1–90. [https://doi.org/10.1016/S0065-2881\(03\)46002-1](https://doi.org/10.1016/S0065-2881(03)46002-1)
- Gooday, A.J., Jorissen, F.J., 2012. Benthic foraminiferal biogeography: Controls on global distribution patterns in deep-water settings. *Ann Rev Mar Sci* 4, 237–262. <https://doi.org/10.1146/annurev-marine-120709-142737>
- Hammer, Ø., Harper, D.A.T., Ryan, P.D., 2001. Past: Paleontological Statistics Software Package for Education and Data Analysis. *Palaeontologia Electronica* 4, 9.
- Harloff, J., Mackensen, A., 1997. Recent benthic foraminiferal associations and ecology of the Scotia Sea and Argentine Basin. *Mar Micropaleontol* 31, 1–29. [https://doi.org/10.1016/S0377-8398\(96\)00059-X](https://doi.org/10.1016/S0377-8398(96)00059-X)
- Hernández-Molina, F.J., Stow, D.A.V., Alvarez-Zarikian, C.A., Acton, G., Bahr, A., Balestra, B., Ducassou, E., Flood, R., Flores, J.A., Furota, S., Grunert, P., Hodell, D., Jimenez-Espejo, F., Kim, J.K., Krissek, L., Kuroda, J., Li, B., Llave, E., Lofi, J., Lourens, L., Miller, M., Nanayama, F., Nishida, N., Richter, C., Roque, C., Pereira, H., Sanchez Goñi, M.F., Sierro, F.J., Singh, A.D., Sloss, C., Takashimizu, Y., Tzanova, A., Voelker, A.H.L., Williams, T., Xuan, C., 2014. Onset of Mediterranean outflow into the North Atlantic. *Science* (1979) 344, 1244–1250. <https://doi.org/10.1126/science.1251306>
- Hodell, D.A., Minth, E.K., Curtis, J.H., McCave, I.N., Hall, I.R., Channell, J.E.T., Xuan, C., 2009. Surface and deep-water hydrography on Gardar Drift (Iceland Basin) during the last interglacial period. *Earth Planet Sci Lett* 288, 10–19. <https://doi.org/10.1016/j.epsl.2009.08.040>
- Holliday, N.P., Meyer, A., Bacon, S., Alderson, S.G., de Cuevas, B., 2007. Retroflexion of part of the east Greenland current at Cape Farewell. *Geophys Res Lett* 34, 1–5. <https://doi.org/10.1029/2006GL029085>
- Hunter, S.E., Wilkinson, D., Louarn, E., McCave, I.N., Rohling, E., Stow, D.A.V., Bacon, S., 2007a. Deep western boundary current dynamics and associated sedimentation on the Eirik Drift, Southern Greenland Margin. *Deep Sea Res 1 Oceanogr Res Pap* 54, 2036–2066. <https://doi.org/10.1016/j.dsr.2007.09.007>
- Hunter, S.E., Wilkinson, D., Stanford, J., Stow, D.A.V., Bacon, S., Akhmetzhanov, A.M., Kenyon, N.H., 2007b. The Eirik Drift: A long-term barometer of North Atlantic deepwater flux south of Cape Farewell, Greenland, in: Viana, A.R., Rebesco, M. (Eds.), *Economic and Palaeoceanographic*

- Significance of Contourite Deposits. Geological Society Special Publication. London, pp. 245–263. <https://doi.org/10.1144/GSL.SP.2007.276.01.12>
- Jones, R.W., 1994. The Challenger Foraminifera. Oxford University Press Inc., New York.
- Jorissen, F.J., de Stigter, H.C., Widmark, J.G.V., 1995. A conceptual model explaining benthic foraminiferal microhabitats. *Mar Micropaleontol* 26, 3–15. [https://doi.org/10.1016/0377-8398\(95\)00047-X](https://doi.org/10.1016/0377-8398(95)00047-X)
- Jorissen, F.J., Fontanier, C., Thomas, E., 2007. Paleoceanographical proxies based on deep-sea benthic foraminiferal assemblage characteristics, in: Hillaire-Marcel, C., de Vernal, A. (Eds.), *Proxies in Late Cenozoic Paleoceanography: Pt. 2: Biological Tracers and Biomarkers*. pp. 263–325. [https://doi.org/10.1016/S1572-5480\(07\)01012-3](https://doi.org/10.1016/S1572-5480(07)01012-3)
- Kaminski, M.A., Cetaan, C.G., Henderson, A.S., 2008. Lectotypes of type species of Agglutinated Foraminiferal Genera in the Collections of the Natural History Museum, London. Part 1. Astrorhizina and Saccamminina, in: Kaminski, M.A., Coccioni, R. (Eds.), *Proceedings of the Seventh International Workshop on Agglutinated Foraminifera*. Grzybowski Foundation Special Publication, pp. 63–77.
- Knutz, P.C., 2008. Chapter 24 Palaeoceanographic Significance of Contourite Drifts. *Developments in Sedimentology* 60, 511–535. [https://doi.org/10.1016/S0070-4571\(08\)10024-3](https://doi.org/10.1016/S0070-4571(08)10024-3)
- Kuhlbrodt, T., Griesel, A., Montoya, M., Levermann, A., Hofmann, M., Rahmstorf, S., 2007. On the driving processes of the Atlantic meridional overturning circulation. *Reviews of Geophysics* 2, 1–32. <https://doi.org/10.1029/2004RG000166.1.INTRODUCTION>
- Kuhnt, W., Collins, E., Scott, D.B., 2000. Deep Water Agglutinated Foraminiferal Assemblages across the Gulf Stream: Distribution Patterns and Taphonomy, in: Hart, M.B., Kaminski, M.A., & Smart, C.W. (Eds) 2000. *Proceedings of the Fifth International Workshop on Agglutinated Foraminifera*. Grzybowski Foundation Special Publication, 7. pp. 261–298.
- Lim, A., Huvenne, V.A.I., Vertino, A., Spezzaferri, S., Wheeler, A.J., 2018. New insights on coral mound development from groundtruthed high-resolution ROV-mounted multibeam imaging. *Mar Geol* 401, 225–237. <https://doi.org/https://doi.org/10.1016/j.margeo.2018.06.006>
- Linke, P., Lutze, G.F., 1993. Microhabitat preferences of benthic foraminifera – a static concept or a dynamic adaptation to optimize food acquisition? *Mar Micropaleontol* 20, 215–234. [https://doi.org/doi.org/10.1016/0377-8398\(93\)90034-U](https://doi.org/doi.org/10.1016/0377-8398(93)90034-U)
- Loeblich, A.R., Tappan, H., 1988. *Foraminiferal Genera*, New York.
- Lohmann, G.P., 1978. Abyssal benthonic foraminifera as hydrographic indicators in the western South Atlantic Ocean. *The Journal of Foraminiferal Research* 8, 6–34. <https://doi.org/10.2113/gsjfr.8.1.6>
- Lutze, G.F., Altenbach, A.V., 1988. *Rupertina stabilis* (Wallich), a highly adapted, suspension feeding foraminifer. *Meyniana* 40, 55–69. <https://doi.org/10.2312/meyniana.1988.40.55>

- Lutze, G.F., Coulbourn, W.T., 1984. Recent benthic foraminifera from the continental margin of northwest Africa: Community structure and distribution. *Mar Micropaleontol* 8, 361–401. [https://doi.org/10.1016/0377-8398\(84\)90002-1](https://doi.org/10.1016/0377-8398(84)90002-1)
- Lutze, G.F., Thiel, H., 1989. Epibenthic foraminifera from elevated microhabitats; *Cibicidoides wuellerstorfi* and *Planulina ariminensis*. *The Journal of Foraminiferal Research* 19, 153–158. <https://doi.org/10.2113/gsjfr.19.2.153>
- Mackensen, A., Schmiedl, G., Harloff, J., Giese, M., 1995. Deep-Sea Foraminifera in the South Atlantic Ocean: Ecology and Assemblage Generation. *Micropaleontology* 41, 342–358. <https://doi.org/10.2307/1485808>
- McCave, I.N., 2005. R.R.S. Charles Darwin Cruise 159.
- McCave, I.N., 1994. R.R.S. Charles Darwin Cruise 88.
- McCave, I.N., Hall, I.R., 2006. Size sorting in marine muds: Processes, pitfalls, and prospects for paleoflow-speed proxies. *Geochemistry, Geophysics, Geosystems* 7, 1–37. <https://doi.org/10.1029/2006GC001284>
- McCave, I.N., Manighetti, B., Robinson, S.G., 1995. Sortable silt and fine sediment size/composition slicing: Parameters for palaeocurrent speed and palaeoceanography. *Paleoceanography* 10, 593–610. <https://doi.org/10.1029/94PA03039>
- Milker, Y., Schmiedl, G., 2012. A taxonomic guide to modern benthic shelf foraminifera of the western Mediterranean Sea. *Palaeontologia Electronica* 15, 1–134. <https://doi.org/10.26879/271>
- Morigi, C., Jorissen, F.J., Gervais, A., Guichard, S., Borsetti, A.M., 2001. Benthic foraminiferal faunas in surface sediments off NW Africa: Relationship with organic flux to the ocean floor. *J Foraminifer Res* 31, 350–368. <https://doi.org/10.2113/0310350>
- Mulder, T., Voisset, M., Lecroart, P., le Drezen, E., Gonthier, E., Hanquiez, V., Faugères, J.-C., Habgood, E., Hernandez-Molina, F.J., Estrada, F., Llave-Barranco, E., Poirier, D., Gorini, C., Fuchey, Y., Voelker, A.H.L., Freitas, P., Sanchez, F.L., Fernandez, L.M., Kenyon, N.H., Morel, J., 2003. The Gulf of Cadiz: An unstable giant contouritic levee. *Geo-Marine Letters* 23, 7–18. <https://doi.org/10.1007/s00367-003-0119-0>
- Müller-Michaelis, A., Uenzelmann-Neben, G., 2014. Development of the Western Boundary Undercurrent at Eirik Drift related to changing climate since the early Miocene. *Deep Sea Res 1 Oceanogr Res Pap* 93, 21–34. <https://doi.org/10.1016/j.dsr.2014.07.010>
- Murray, J.W., 2006. *Ecology and Applications of Benthic Foraminifera*. Cambridge University Press, Cambridge, p. 440.
- Murray, J.W., 2001. The niche of benthic foraminifera, critical thresholds and proxies. *Mar Micropaleontol* 41, 1–7. [https://doi.org/10.1016/S0377-8398\(00\)00057-8](https://doi.org/10.1016/S0377-8398(00)00057-8)

- Peterson, R.G., Stramma, L., 1991. Upper-level circulation in the South Atlantic Ocean. *Prog Oceanogr* 26, 1–73. [https://doi.org/10.1016/0079-6611\(91\)90006-8](https://doi.org/10.1016/0079-6611(91)90006-8)
- Rasmussen, T.L., Thomsen, E., Troelstra, S.R., Kuijpers, A., Prins, M.A., 2002. Millennial-scale glacial variability versus Holocene stability: changes in planktic and benthic foraminifera faunas and ocean circulation in the North Atlantic during the last 60 000 years. *Mar Micropaleontol* 47, 143–176. [https://doi.org/https://doi.org/10.1016/S0377-8398\(02\)00115-9](https://doi.org/https://doi.org/10.1016/S0377-8398(02)00115-9)
- Rebesco, M., Hernández-Molina, F.J., van Rooij, D., Wåhlin, A., 2014. Contourites and associated sediments controlled by deep-water circulation processes: State-of-the-art and future considerations. *Mar Geol* 352, 111–154. <https://doi.org/10.1016/j.margeo.2014.03.011>
- Rüggeberg, A., Dullo, C., Dorschel, B., Hebbeln, D., 2007. Environmental changes and growth history of a cold-water carbonate mound (Propeller Mound, Porcupine Seabight). *International Journal of Earth Sciences* 96, 57–72. <https://doi.org/10.1007/s00531-005-0504-1>
- Sánchez-Leal, R.F., Bellanco, M.J., Fernández-Salas, L.M., García-Lafuente, J., Gasser-Rubinat, M., González-Pola, C., Hernández-Molina, F.J., Pelegrí, J.L., Peliz, A., Relvas, P., Roque, D., Ruiz-Villarreal, M., Sammartino, S., Sánchez-Garrido, J.C., 2017. The Mediterranean Overflow in the Gulf of Cadiz: A rugged journey. *Sci Adv* 3, 1–12. <https://doi.org/10.1126/sciadv.aao0609>
- Sarnthein, M., Winn, K., Jung, S.J.A., Duplessy, J.-C., Labeyrie, L., Erlenkeuser, H., Ganssen, G., 1994. Changes in East Atlantic Deepwater Circulation over the last 30,000 years: Eight time slice reconstructions. *Paleoceanography* 9, 209–267. <https://doi.org/10.1029/93PA03301>
- Saupe, A., Schmidt, J., Petersen, J., Bahr, A., Dias, B.B., Albuquerque, A.L.S., Díaz Ramos, R.A., Grunert, P., 2022. Controlling Parameters of Benthic Deep-Sea Foraminiferal Biogeography at the Brazilian Continental Margin (11–22°S). *Front Mar Sci* 9, 1–17. <https://doi.org/10.3389/fmars.2022.901224>
- Saupe, A., Schmidt, J., Petersen, J., Bahr, A., Grunert, P., 2023. Benthic foraminifera in high latitude contourite drift systems (North Atlantic: Björn, Gardar and Eirik drifts). *Palaeogeogr Palaeoclimatol Palaeoecol* 609, 1–18. <https://doi.org/10.1016/j.palaeo.2022.111312>
- Schönfeld, J., 2006. Taxonomy and Distribution of the *Uvigerina peregrina plexus* in the Tropical To Northeastern Atlantic. *The Journal of Foraminiferal Research* 36, 355–367. <https://doi.org/10.2113/gsjfr.36.4.355>
- Schönfeld, J., 2002a. Recent benthic foraminiferal assemblages in deep high-energy environments from the Gulf of Cadiz (Spain). *Mar Micropaleontol* 44, 141–162. [https://doi.org/10.1016/S0377-8398\(01\)00039-1](https://doi.org/10.1016/S0377-8398(01)00039-1)
- Schönfeld, J., 2002b. A new benthic foraminiferal proxy for near-bottom current velocities in the Gulf of Cadiz, northeastern Atlantic Ocean. *Deep-Sea Research I* 49, 1853–1875. [https://doi.org/https://doi.org/10.1016/S0967-0637\(02\)00088-2](https://doi.org/https://doi.org/10.1016/S0967-0637(02)00088-2)



- Schönfeld, J., 1997. The impact of the Mediterranean Outflow Water (MOW) on benthic foraminiferal assemblages and surface sediments at the southern Portuguese continental margin. *Mar Micropaleontol* 29, 21–236. [https://doi.org/https://doi.org/10.1016/S0377-8398\(96\)00050-3](https://doi.org/https://doi.org/10.1016/S0377-8398(96)00050-3)
- Schönfeld, J., Dullo, W.C., Pfannkuche, O., Freiwald, A., Rüggeberg, A., Schmidt, S., Weston, J., 2011. Recent benthic foraminiferal assemblages from cold-water coral mounds in the Porcupine Seabight. *Facies* 57, 187–213. <https://doi.org/10.1007/s10347-010-0234-0>
- Schönfeld, J., Zahn, R., 2000. Late Glacial to Holocene history of the Mediterranean Outflow. Evidence from benthic foraminiferal assemblages and stable isotopes at the Portuguese margin. *Palaeogeogr Palaeoclimatol Palaeoecol* 159, 85–111. [https://doi.org/https://doi.org/10.1016/S0031-0182\(00\)00035-3](https://doi.org/https://doi.org/10.1016/S0031-0182(00)00035-3)
- Schott, F.A., Dengler, M., Zantopp, R., Stramma, L., Fischer, J., Brandt, P., 2005. The Shallow and Deep Western Boundary Circulation of the South Atlantic at 5°–11°S. *Journal of Physical Oceanography* 35, 2031–2053. <https://doi.org/10.1175/JPO2813.1>
- Sejrup, H.-P., Fjaeran, T., Hald, M., Beck, L., Hagen, J., Miljeteig, I., Morvik, I., Norvik, O., 1981. Benthonic foraminifera in surface samples from the Norwegian continental margin between 62°N and 65°N. *The Journal of Foraminiferal Research* 11, 277–295. <https://doi.org/10.2113/gsjfr.11.4.277>
- Sierro, F.J., Hodell, D.A., Andersen, N., Azibei, L.A., Jimenez-Espejo, F.J., Bahr, A., Flores, J.A., Ausin, B., Rogerson, M., Lozano-Luz, R., Lebreiro, S.M., Hernandez-Molina, F.J., 2020. Mediterranean Overflow Over the Last 250 kyr: Freshwater Forcing from the Tropics to the Ice Sheets. *Paleoceanogr Paleoclimatol* 35, 1–31. <https://doi.org/10.1029/2020PA003931>
- Singh, A.D., Rai, A.K., Tiwari, M., Naidu, P.D., Verma, K., Chaturvedi, M., Niyogi, A., Pandey, D., 2015. Fluctuations of Mediterranean Outflow Water circulation in the Gulf of Cadiz during MIS 5 to 7: Evidence from benthic foraminiferal assemblage and stable isotope records. *Glob Planet Change* 133, 125–140. <https://doi.org/10.1016/j.gloplacha.2015.08.005>
- Stramma, L., England, M., 1999. On the water masses and mean circulation of the South Atlantic Ocean. *Geophysical Research* 104, 20,863–20,883. <https://doi.org/doi.org/10.1029/1999JC900139>
- Toucanne, S., Mulder, T., Schönfeld, J., Hanquiez, V., Gonthier, E., Duprat, J., Cremer, M., Zaragosi, S., 2007. Contourites of the Gulf of Cadiz: A high-resolution record of the paleocirculation of the Mediterranean outflow water during the last 50,000 years. *Palaeogeogr Palaeoclimatol Palaeoecol* 246, 354–366. <https://doi.org/10.1016/j.palaeo.2006.10.007>
- Uenzelmann-Neben, G., Gruetzner, J., 2018. Chronology of Greenland Scotland Ridge overflow: What do we really know? *Mar Geol* 406, 109–118. <https://doi.org/10.1016/j.margeo.2018.09.008>

- van Aken, H.M., de Boer, C.J., 1995. On the synoptic hydrography of intermediate and deep water masses in the Iceland Basin. *Deep-Sea Research Part I* 42, 165–189.  
[https://doi.org/10.1016/0967-0637\(94\)00042-Q](https://doi.org/10.1016/0967-0637(94)00042-Q)
- van der Zwaan, G.J., Duijnste, I.A.P., den Dulk, M., Ernst, S.R., Jannink, N.T., Kouwenhoven, T.J., 1999. Benthic foraminifers: proxies or problems? *Earth Sci Rev* 46, 213–236.  
[https://doi.org/10.1016/s0012-8252\(99\)00011-2](https://doi.org/10.1016/s0012-8252(99)00011-2)
- Viana, A.R., 2001. Seismic expression of shallow- to deep-water contourites along the south-eastern Brazilian margin. *Marine Geophysical Research* 22, 509–521.  
<https://doi.org/10.1023/A:1016307918182>
- Wildish, D., Kristmanson, D., 1997. *Benthic Suspension Feeders and Flow*. Cambridge University Press, New York, p. 409.
- Yamashita, C., Mello e Sousa, S.H. de, Vicente, T.M., Martins, M.V., Nagai, R.H., Frontalini, F., Godoi, S.S., Napolitano, D., Burone, L., Carreira, R., Figueira, R.C.L., Taniguchi, N.K., Rezende, C.E. de, Koutsoukos, E.A.M., 2018. Environmental controls on the distribution of living (stained) benthic foraminifera on the continental slope in the Campos Basin area (SW Atlantic). *Journal of Marine Systems* 181, 37–52. <https://doi.org/10.1016/j.imarsys.2018.01.010>

## 6. Acknowledgements

First and foremost, I am very grateful to my supervisor, Prof. Dr. Patrick Grunert, who came up with the idea and impetus for this work. His mentoring, ideas, and encouragement, as well as his invaluable patience have been crucial to the success of this work.

Many thanks go to the members of my examination committee. Dr. Jassin Petersen always had an open ear for all my questions, which he answered with his priceless calmness and composure. Prof. Dr. Gerhard Schmiedl (University of Hamburg) spent his valuable time and effort to read and evaluate this thesis. Prof. Dr. Hartmut Arndt accepted the chairmanship of the examination committee.

I appreciate the excellent cooperation with my co-authors, and especially want to thank Dr. André Bahr for his guidance and support throughout my PhD.

Dr. Joachim Schönfeld (GEOMAR, Kiel) is warmly thanked for his expertise and helpful comments during this project. The insights into his vast collection of benthic foraminifera, and his valuable advice on taxonomic problems, were a great help to me.

I further thank my teammate Johanna Schmidt for the wonderful time we spent together in our office, but also at exciting and valuable conferences and training events. I thank Hanna Cieszynski for her efforts at the SEM, but I especially appreciate that she always made sure all members of our working group were well supplied with Polish cuisine. The student assistants Marie Scheel and Konstantinos Ztoupis of the MicPal group should be mentioned, as they assisted me tirelessly in counting countless foraminifera.

Finally, I am extremely grateful to my husband Felix Saupe and to my family, who have always supported me over the last few years and without whom this endeavour would not have been possible.



# Curriculum Vitae

## Anna Saupe

Date of birth: 10 February 1990  
Place of birth: Rostock, Germany  
Nationality: german

### Academic Career

2018-present PhD student, University of Cologne  
07/2018 Master's degree (M.Sc.) in Geosciences, University of Münster  
2015-2018 Master studies in Geosciences, University of Münster  
2014-2015 Master studies in Geosciences, University of Bochum  
09/2014 Bachelor's degree (B.Sc.) in Geosciences, University of Münster  
2010-2014 Bachelor studies in Geosciences, University of Münster  
06/2009 Allgemeine Hochschulreife (Abitur), Kaiser-Friedrich-Ufer Gymnasium, Hamburg

### Academic Experience & Related Employment

2022-2023 Staff member of the Environmental Analysis Laboratory  
University of Münster, Institute of Geology and Palaeontology  
2022 Head of the Palaeontological & Sedimentological Laboratory  
University of Münster, Institute of Geology and Palaeontology  
2018-2022 Research Assistant  
in the project: *Benthic foraminifera as proxies in Contourite Drift Systems*  
University of Cologne, Institute of Geology and Mineralogy  
2017-2018 Self-employed palaeontologist  
on behalf of the Geological Survey (Geologischer Dienst) NRW  
2017-2018 Student Assistant  
University of Münster, Institute of Geology and Palaeontology

### Extracurricular Education

2020 Shipboard Scientist  
on expedition AL534/2: *Transport and Fate of Marine Microplastics* (FS Alkor, GEOMAR)  
2019 ISF Summerschool: *12<sup>th</sup> International School on Foraminifera*  
University of Urbino, Italy  
2019 ECORD Training Course: *Virtual Drillship Experience*  
MARUM and IODP Core Repository (BCR), University of Bremen  
2016 Erasmus programme: *Master Sciences de la Terre et des planètes, environnement*  
Université Blaise Pascal, Clermont-Ferrand, France

  
Köln, den 5. März 2023



## Erklärung zur Dissertation

gemäß der Promotionsordnung vom 12. März 2020

„Hiermit versichere ich an Eides statt, dass ich die vorliegende Dissertation selbstständig und ohne die Benutzung anderer als der angegebenen Hilfsmittel und Literatur angefertigt habe. Alle Stellen, die wörtlich oder sinngemäß aus veröffentlichten und nicht veröffentlichten Werken dem Wortlaut oder dem Sinn nach entnommen wurden, sind als solche kenntlich gemacht. Ich versichere an Eides statt, dass diese Dissertation noch keiner anderen Fakultät oder Universität zur Prüfung vorgelegen hat; dass sie - abgesehen von unten angegebenen Teilpublikationen und eingebundenen Artikeln und Manuskripten - noch nicht veröffentlicht worden ist sowie, dass ich eine Veröffentlichung der Dissertation vor Abschluss der Promotion nicht ohne Genehmigung des Promotionsausschusses vornehmen werde. Die Bestimmungen dieser Ordnung sind mir bekannt. Darüber hinaus erkläre ich hiermit, dass ich die Ordnung zur Sicherung guter wissenschaftlicher Praxis und zum Umgang mit wissenschaftlichem Fehlverhalten der Universität zu Köln gelesen und sie bei der Durchführung der Dissertation zugrundeliegenden Arbeiten und der schriftlich verfassten Dissertation beachtet habe und verpflichte mich hiermit, die dort genannten Vorgaben bei allen wissenschaftlichen Tätigkeiten zu beachten und umzusetzen. Ich versichere, dass die eingereichte elektronische Fassung der eingereichten Druckfassung vollständig entspricht.“

Teilpublikationen:

**Saupe, A.**, Schmidt, J., Petersen, J., Bahr, A., Dias, B. B., Albuquerque, A. L. S., Díaz Ramos, R. A., and Grunert, P. (2022): Controlling Parameters of Benthic Deep-Sea Foraminiferal Biogeography at the Brazilian Continental Margin (11-22°S). *Front. Mar. Sci.* 9:901224. doi: [10.3389/fmars.2022.901224](https://doi.org/10.3389/fmars.2022.901224)

**Saupe, A.**, Schmidt, J., Petersen, J., Bahr, A., and Grunert, P. (2023): Benthic foraminifera in high latitude contourite drift systems (North Atlantic: Björn, Gardar and Eirik drifts). *Palaeogeography Palaeoclimatology Palaeoecology* 609, 1–18. doi: [10.1016/j.palaeo.2022.111312](https://doi.org/10.1016/j.palaeo.2022.111312)



Köln, den 5. März 2023